NEW ELECTROCHROMIC SYSTEMS: MULTICOLORED, SEMI-SOLID AND EASY-TO-MAKE

YOLANDA ALESANCO MENDIVE

Doctoral thesis 2017

eman ta zabal zazu

Universidad del País Vasco

Euskal Herriko Unibertsitatea

Ph.D Thesis

New Electrochromic Systems: Multicolored, Semi-Solid and Easy-to-Make

Yolanda Alesanco Mendive

Directed by
Ana Viñuales Martínez (IK4-CIDETEC)
David Mecerreyes Molero (POLYMAT-EHU/UPV)

Donostia-San Sebastián 2017

TABLE OF CONTENTS

CHAPTER 1

INTRODUCTION

1.1. Introduction

Contemporary man generally spends about 90% of his time indoors (i.e., vehicles and buildings), and as a consequence, increasing efforts and energy are being focused on maintaining the indoor environment in both comfortable and healthy levels. [1]

One attractive and suitable approach to adjust the indoor environment according to the needs is to modulate it in a reversible way. Nowadays this is to some extent possible by integrating the so-called chromogenic technologies into daily use items (e.g. glazing in buildings, automobiles, planes and certain types of electronic displays),[2] due to their ability to change their optical properties in a response to different external stimuli, including light (photochromism),[3] temperature (thermochromism),[4] or external voltage (electrochromism,[5] electrophoretic suspended particles,[6] and polymer dispersed liquid crystals (PDLCs)[7] among others). Amongst the chromogenic technologies, electrochromism has attracted significant attention attributable to the some recognized strengths over other technologies. Thus, the electrochromic technology allows the control of switching by the user, not directly possible by means of thermochromism or photochromism.[8] On the other hand, in comparison to liquid crystals technology, electrochromism offers not only greater optical contrast regardless of the back lighting and of the visual angle,[9] but also adjustable memory.[9a] More than 900 patents filed in the US between 1975 and 2000 on that field,[9a] and more than two thousand papers published in the previous decade reporting new electrochromic (EC) systems and its properties[10] endorse the interest sustained by electrochromism.

1.2. Electrochromism: fundaments and applications

1.2.1. Fundamentals

Although the term "Electrochromism" was first assigned in 1961 by Platt in analogy to "thermochromism" and "photochromism",[11] the first electrochemical change of color dates back to 1930, when Kobosew and Nekrassow observed the electrochemical reduction of a bulk tungsten oxide.[12]

As it is already known, electrochromism describes the property which exhibits some materials to change their color reversibly by means of redox reaction induced by an appropriate external voltage. Even though this term may include the modulation of other regions of the electromagnetic spectrum (i.e., near-infrared and microwave regions),[13] it will be restricted herein to the visible range.

The electroactive species can gain or release an electron, being therefore reduced or oxidized, respectively, when induced by an appropriate external voltage. The different redox forms will exhibit different spectroscopic transitions between the ground and excited states. Therefore, each redox form will require certain energy for electron promotion between two energy levels (energy gap), absorbing photons from different part of the electromagnetic spectrum, resulting in a color change when the absorption occurs in the visible region.[14]

1.2.2. Applications

EC materials have aroused great interest in the last decades because of their utility for the development of displays[15] (e.g., electronic paper)[16] and smart systems for the automotive and building industries (i.e., rearview mirrors,[17] helmet visors,[2] smart windows,[18]and climate adaptive building shell (CABS)).[19]

As the EC systems may enable users to adjust at will the light transmission according to the needs, they have been effectively used for energy-saving purposes in the case of EC windows,[19-20] thus providing light and thermal comfort, while enhancing the aesthetics which also translates into visual comfort of the occupants. Although some commercial examples of smart windows which provide different intermediate tint levels have been fabricated (e.g., by View Inc. and Sage Electrochromics Inc. US)[21] their extended commercialization was limited by long-term stability issues,[9a] since lifetime over 20 years and around 100 000 cycles are required for this application.[22] In this regard, the EC windows developed by SageGlass are the only ones that successfully pass the standard test ASTM-E-2141-06.

EC antiglare rear-view-mirrors, on the contrary, reached successfully the market and are still being widely commercialized by most major brands of vehicles. The latter require fast commutation times (i.e., ≤ 5s) and operating temperatures between +10 and +40°C for indoor mirrors, but less ambitious number of cycles (i.e., 10 000 – 100 000).[22] These EC rear-view-mirrors are being mainly produced by the companies Gentex[17b, 23] and Donnelly,[24] showing in both cases bluish colored states which require a constant electric supply to maintain the coloration.

Other EC systems which may provide visual comfort translated into safety concerns for the wearer or driver are the smart sunglasses and variable-tint visor helmets for motorcycle, described in a prototype stage.[25]

EC displays could have a broad applicability as informative panels and sings (e.g., airports, railway stations, shops and city squares and so on)[22] due to their well-known advantages in comparison to other technologies such as not requiring back lighting and their easy view from any angle (paper-like or painted surface appearance).[9]

The vast majority of the examples given above exhibit one or different tint levels of the same bluish coloration in their colored sate. Aiming to expand

the potential of the electrochromic technology, large amount of inquiry has been conducted in the last years on generating full-color electrochromic devices (ECDs)[26] and on diversifying the colors of the EC materials including more neutral colorations (i. e., gray or black). The latter provide exceptional aesthetic properties as they adapt better to any chromaticity surroundings easing their implementation, and exhibit light-filtering properties as they absorb in the most of the visible range. However, the achievement of high performance EC materials which offer colorless-to-gray/black electrochromism by themselves,[13] and the fabrication of ECDs which provide multicolored behavior while maintaining simple device architecture still remain a strategic challenge.

1.3. Types of electrochromic materials:

A simple method developed by IBM[27] but still in use,[13-14] classifies the EC materials in terms of the phases they exhibit before and after the electrochromic reaction, being thus divided into 3 different types.[13, 27] In the so-called type I and III, the electrochromic materials remain in solution and as solid film, respectively, at all times during the electrochromic process, therefore, no phase change is observed during the redox process. On the contrary, type II electrochromes remain dissolved in their colorless forms, but form a solid phase in their colored form.

Alternatively, depending on the chemical nature of the EC materials, they can be broadly divided into two different groups, organics and inorganics, each of them exhibiting its core strengths and weakness. On the one hand, inorganic EC materials offer high optical contrast and are quite stable against UV radiation, but the commutation times between the bleached and colored states are usually slow,[28] the synthesis and deposition process require high temperatures and pressures, and the diversity of provided colors is limited. The organic EC materials, on the contrary, are easier to deposit, may provide a wide variety of colors and offer comparatively

fast response times (i.e., in the range of seconds), but as a weakness they are less stable not only against the UV, but also against temperature and overpotentials.

1.3.1. Inorganic EC materials

There is extensive literature describing the inorganic electrochromic materials,[29] but the most reported materials comprise the **metal oxides**[30] and the **Prussian Blue** (PB) systems.[31] Some **metal oxides** exhibit cathodic EC behavior, thus displaying the most colored estate after being reduced (e. g., WO_3, MoO_3, V_2O_5, Nb_2O_5 and TiO_2), whereas others reveal anodic EC behavior, wherein the colored state is observed after oxidation process (e.g., $Ir(OH)_3$ and $(Ni(OH)_2$).[13] The change of color produced in WO_3,[13] one of the most studied EC materials, and in TiO_2,[32] employed not only for its EC properties, but also considered one of the most important semiconductor electrode materials,[32] can be represented as follows.

$$W^{VI}O_3 + x(M^+ + e^-) \longrightarrow M_xW^{VI}_{(1-x)}W^{V}_{x}O_3$$

$$TiO_2 + x(M^+ + e^-) \longrightarrow M_xTiO_2$$

Both EC materials change from initial colorless state, to blue coloration by intercalation of ion, usually Li^+, into their lattice upon sufficiently negative applied potentials, caused by intervalence charge-transfer optical transitions (IVCT).[13] As ions must be intercalated/deintercalated into the bulk of metal oxide film, the commutation times are consequently restricted by the pace of diffusion of the ions into the compact metal oxide framework, taking even minutes to be completed.[28] This weakness is minimized when employing thin film layers of metal oxide, but in return, the coloration levels achieved are very low. Consequently, a tradeoff between suitable switching times but low coloration levels (thin films) and between high colorations but slow switching times (thick films) must be made. [9a]

Nevertheless, metal oxides have been employed in some applications wherein switching times in the range of minutes can be sufficient,[22] as in EC windows (e.g., the ones developed by Sage Electrochromics Inc. and View Inc.[21]).

Other inorganic material widely studied for its EC properties is the Iron (III) hexacyanoferrate (II) compound, known as **Prussian Blue** (PB) whose blue color arises from the intervalence charge-transfer between the mixed-balance iron oxidation states.[13] Although the partial electrochemical oxidation of the PB may lead to a green colored product (Prussian Green), the colorless state obtained by its total electrochemical reduction has been more studied with EC purposes. In the latter, the iron atoms exhibit a single oxidation state (II) and consequently the blue color disappears, being it known as Prussian white or Everitt salt.

$[Fe^{+3}Fe^{+2}(CN)_6]^-$ (Prussian Blue) + $e^- \longrightarrow [Fe^{+2}Fe^{+2}(CN)_6]^{-2}$ (Prussian white)

1.3.2. Organic EC materials

Although a variety of organic molecules exhibit EC behavior, conducting polymers and viologens are the most studied organic EC systems.

1.3.2.1. Conducting polymers

The EC properties of the conducting polymer (e. g. polypyrrole,[33] polyaniline,[34] or polythiophene and its derivatives[35] among others) have been studied for over 35 years. They exhibit electronic conjugation due to the delocalized π-electron band structures in their oxidized state wherein their positive change carriers are balanced by the counter ions (p-doped). Upon reduction, they lose their conjugation leading to electrically insulating form while egressing counteranions (undoped neutral form) or integrating cations (n-doping).[13, 35] The electrochromic properties of the conducting polymers arise from the bandgap (E_g) magnitude between the highest-occupied π-electron band and the lowest unoccupied band of

the undoped form.[13] In a recent times, a huge variety of new conjugated polymers have been reported as promising multi-electrochromic materials through their band gap control by structural modification.[36] Although some of them provided more than one colored state including in some cases the gray hue in their neutral state,[37] partially doped state,[38] or full-doped oxidized state,[39] their lack of a sufficiently colorless bleached state and slow response time in comparison to several single-molecular materials such as viologens,[26b] are noticeably their major weakness.

1.3.2.2. Viologens

A widely studied class of organic electrochromic compounds are the 1,1'-disubstituted 4,4'-bipyridilium salts, commonly known as "**viologens**" following the proposition made by Michaelis and Hill, [40] or "paraquat" according to trade name of the herbicide developed by the ICI brand.[41]

The suitability of the viologens is known for some time now because of the many advantages they offer over other EC materials. Apart from those mentioned above that are common to organic EC materials (i.e., their easy deposition process and the wide variety of colors they may offer), they exhibit mainly colorless off state, high extinction coefficients in the reduced state which lead to high coloration intensities [16] and excellent optical contrasts[42], short commutation times even of milliseconds,[43] low redox potential,[44] and high solubility in most common solvents[45] due to their non-macromolecular condition which may ease the device fabrication as explained below.

The cathodic electrochromic behavior of the viologens and their well-known three common redox forms are as follows: i) the dication ($bipm^{2+}$), which is the most stable, ii) the radical-cation ($bipm^{+\bullet}$), formed by one electron reduction of the dication, and iii) the neutral state (di-reduced form, $bipm^{0}$), obtained by two electron reduction of the dication. The latter has been proven to be very unstable[46] and can react with the dication

leading to radical-cation upon comproportionation.[47] Thus, the mainly colorless dication and highly colored radical-cation forms, are commonly the ones exploited in electrochromic devices.[46]

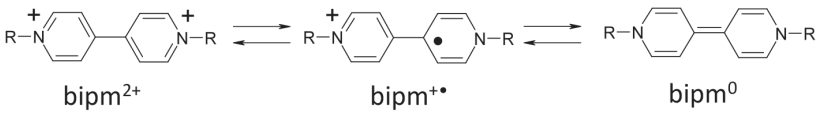

Figure 1.1: different redox forms of the viologens: dication ($bipm^{2+}$), radical-cation ($bipm^{+\bullet}$) and neutral state ($bipm^{0}$).

One significant advantage of the bipyridilium derivatives is their ability to be synthetically tunable achieving different coloration in their reduced form by simply modification of the substituents on the nitrogen atoms (-R in the Figure 1).[46] Thus, although the exhibited coloration may also depend on the solvent,[46] simple alkyl groups provide blue/violet radical cations, while aryl groups generally lead to green coloration.

The nature of the substituent will also determine other parameters such as the potential required to form the radical-cation[48] and the extinction coefficients, among others. The latter are solvent dependent[49] and usually range from 1 to 4 x 10^{-4} $M^{-1}cm^{-1}$ for the radical-cations,[50] (i.e., 1 - 2 x 10^{-4} $M^{-1}cm^{-1}$ for N,N'-dialkylviologens), but can reach values even above 5 x 10^{-4} $M^{-1}cm^{-1}$ for N,N'-diarylviologens in organic solvents.[9a] The solubility of the radical cation also depends on the nature of the viologen. Thus, aqueous solutions comprising 1,1'-dimethyl-4,4'-bipyridilium, termed as methyl viologen, have been classified as a type I,[48] while other 1,1'-alkyl-substituted viologens of longer chains (i.e., heptyl or benzyl viologens)[9a, 46] and 1,1'-aryl-substituted viologens have been confirmed to belong to type-II, while being equally tested in aqueous media.[51]

A simplified view of the intense coloration exhibited by the radical-cations is explained by the optical charge transfer (CT) between the formally +1

and formally zero-charge nitrogens. Accordingly, the color intensity of the di-reduced form (bipm^0, diamagnetic)[52] may be expected to be and has been reported to be low since no internal transition or optical CT appears to be accessible in the range of visible wavelengths.[48] However, it is assumed that the positive charge in the case of the radical-cation is not localized on N but it is delocalized over the ring instead, being probably better viewed as a "intramolecular photo-effected electronic excitation".[48]

It is worth to mention that the most widespread application of EC systems, which corresponds to the antiglare rear-view-mirrors mainly produced by the companies Donnelly[24] and Gentex[17b, 23] is based on viologens. The latter technology has been also implemented in the aeronautical sector marketed by PPG Aerospace under the brand name "Alteos™ Interactive Window System",[53] the world's first EC window shades for commercial aircraft (Boing 787 Dreamliner).

Due to the more advantages and possibilities they offer, and with the aim of exploring them with more detail, the EC systems developed and described herein are based on viologens.

1.4. Electrochromic devices: components and types.

A great deal of research has been conducted in the field of ECDs since the first sandwich type ECD described by Deb in 1969,[54] approach by which the switching time of a thin film of WO_3 was dropped from 30 minutes to less than one minute while the electric field was being applied across it. In the last decades, different structures have been proposed, to ensure the controlled color change upon applying convenient potential and to meet the requirements for commercial applications to boost market entry. The latter include high level of coloration and transmittance changes, high white-erase efficiency or reversibility, high color efficiencies, fast switching speeds between the colored and bleached states, good cyclability and long durability or life time, along with competitive price. Additionally, high

transparency at bleached state is also crucial in the case of non-reflective ECDs, and good memory effect may be required for certain applications. The definition employed herein for some of these parameters along with the method employed to estimate them are explained in the following chapter.

Despite the diverse device architectures developed, the vast majority of the existing ECDs comprise at least two electrode substrates separated by the electrolyte, along with the EC material and in most systems also a redox mediator. The latter refers to an electroactive material, usually non-electrochromic, which can gain electrons while the EC materials are releasing them and vice versa. The electrode substrates that will be employed as working and counter electrodes (WE and CE, respectively) comprise a metallic conductor or a semiconductor deposited as thin film on glass or plastic substrate.[14] The most reported studies in the last 20 years in the field of ECDs are based on commercially available fluorine-doped tin oxide (FTO) coated glass substrates and tin-doped indium oxide (ITO) coated glass or plastic (PET) substrates. The electrolytes, on the contrary, have been and are still being widely studied nowadays, due to the crucial role they play in different fields, not only in ECDs[55] as will be shown below, but also in lithium batteries,[56] and solar cells.[57]

1.4.1. Electrolytes in ECDs: requirements and a brief overview

The development of competitive electrolytes is crucial to achieve high-performance ECDs. The electrolyte maintains the working and counter electrode separated from each other, while ensuring the ionic transport between them to balance the charges which arises from the redox processes. To this end, a model electrolyte of any ECD has to exhibit high ionic conductivity (i.e., between $1e^{-4}$ and $1e^{-3}$ S cm^{-1}),[58] ideal zero electronic conductivity[22], high thermal (i.e., up to +60 °C)[58a] and electrochemical stability,[13, 59] and high transmission in the visible region.[58b]

In addition, other desirable requirements have also been reported such as certain stickiness and adhesion[22, 59] to provide good interaction with the electrode and/or electrochromic layer, and elasticity[22] to relieve mechanical stress which may arise from the manipulation or from thermal variations, therefore extending the durability of the ECDs.

Traditionally, electrolytes for ECDs are based on organic polar solvents of high dielectric constant and low viscosity to ease the ion migration,[9a] wherein the electroactive components can be dissolved.[60] Despite their extended use, liquid electrolytes are not exempted from several disadvantages, such as risk of solvent leaking[61] and presence of bubbles, low chemical stability, or a complicated industrialization due to solvent-related safety issues.[22, 62]

Several efforts towards the development of solid or semi-solid electrolytes have been proposed in the literature throughout the last 20 years. First attempts comprises solvent free polymer electrolytes[63] and polymer-solvent systems[64] but due to their low ionic conductivity (i.e., $1e^{-5}$ S cm^{-1}) [63] they were not suitable for ECDs. The polymer-salt-solvent systems,[58a] based on lithium salts and polymeric matrix to achieve more solid-like mechanical properties (i.e., PMMA, [58-59, 62a, 65] PVC, [58a, 62c, 62d] PEO, [58a, 62b, 66] PAN[67]), dispersed in a conventional solvent (i.e., PC, EC, γ-butyrolactone), lead to ionic conductivities up to 4.8 10^{-3} S cm^{-1}. However, gelation times between 3[62, 66a] and 5 [58a] days were required and the quality of gelation and durability worsened with the amount of the salt.[58a] On the contrary, other gelatin based electrolytes composed of animal protein-derived gels in an aqueous media with[68] and without the addition of salts,[69] or in organic solvents[70], exhibited fast gelation an ionic conductivity values between 1.5 10^{-5} - 3 10^{-3} S cm^{-1}, although the presence of bubbles was difficult to avoid due to the rapid gelation process.

In other approaches, taking advantage of the exceptional properties of the ionic liquids (ILs) they have replaced the current solvent in the electrolytes[71]

in combination with conventional polymers (i.e., PVA) and salts,[72] or in combination with gelatin which offer mechanical flexibility in the so-called "Ion jelly",[73] achieving ionic conductivities (ic) up to 10^{-4} S cm^{-1}. The subsequent approach based on synthesizing new functional polymers through polymerization of ionic liquid monomers (PILs),[55a, 71a, 74] in most cases employing ILs as liquid solvent,[55a, 71a] lead to ionic conductivities strongly depended on the IL content, reaching values as high as 10^{-2} S cm^{-1} for more liquid electrolytes with high content of IL.[55a]

Apart from the most explored strategies cited above, other innovative approaches have been reported aimed to obtain solid electrolytes such as the ones based on organically modified silanes termed as "Ormolyte" (ic = 10^{-4} S cm^{-1}),[75] a tetralayered electrolyte obtained by layer-by-layer (ic = 10^{-5} S cm^{-1}),[76] or other solid electrolytes obtained by irreversible chemical cross-linked polymers cured by UV-radiation[8, 77] or thermal treatments,[71b] before[77a, 77c] or after being assembled.[8]

Despite the big efforts carried out aimed to achieve the ideal electrolyte, the performance of the ECDs based on solid electrolytes is still poorer than that observed with liquid electrolytes and the development of electrolytes which ensure good interfacing with the electrodes and/or the EC layer is crucial to achieve high-performance ECDs.[76]

1.4.2. Types of ECDs

ECDs with different degrees of complexity and architectures have been proposed, from the simplest configuration wherein the EC layer plays simultaneously the role of the electrode conducting material (e.g., poly[3,4-(ethylenedioxy)thiophene] (PEDOT)),[66b] to some interdigitated electrodes in which the counter and working electrodes are supported on the same substrate.[78] However, the most employed device architectures are those exhibiting sandwich configurations explained below, which will also be employed in the present thesis.

1.4.2.1. All-in-one ECDs

The term all-in-one,[71b] describes the symmetric device architecture (Figure 1.2) wherein the EC material and the redox mediator are dissolved into liquid[60] or semi-solid[10, 47] electrolyte and the resulting EC mixture is sandwiched between two electrode substrates in a very simple configuration(glass/TCO/EC mixture/TCO/glass). Therefore, this design is restricted to EC materials which are soluble in the electrolytic media, among which viologens may be included.

As the chromophores are distributed all over the electrolytic layer, this device configuration may offer high levels of coloration, providing that the chromophore exhibits high solubility in the electrolyte. However, the switching times between the bleached and colored states are usually poor as the pace of diffusion of the chromophores towards the electrode limits its rate of coloration.

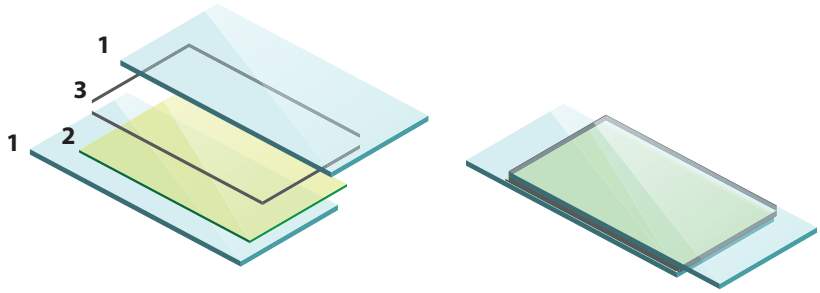

Figure 1.2: Confifuration of all-in-one ECD and components: 1) TCO/glass; 2) EC mixture; 3) spacers.

Additional side reactions or processes have been associated with viologen-based ECDs employing this kind of configuration such as comproportionation,[71b, 79] dimerization[71b, 80] and recrystallization[81] associated in some cases with a poor reversibility and ciclability[74] along with an aging of the ECD.[82] In this regard, although the dimerization, also called "pimerization"[83] can sometimes be desirable as demonstrated

by the attempts to stabilize the dimers,[84] the comproportionation and the crystallization are effects to be avoided. Several texts pointed out that the first reduced form (radical-cations) of some viologens (type II), tends to agglomerate on the surface of the working electrode forming a deposit[8, 71b] whose subsequent reorganization may lead to a crystallization,[71b, 82] and irreversible bleaching process. Moreover, in this kind of configuration wherein the viologens are dissolved in the EC mixture, the comproportionation is more likely to occur since the encounter between the dications and neutral molecules is very probable.

In this regard, a strategy to avoid the above mentioned weaknesses is the employment of ECDs wherein the chromophores are attached on the surface of the electrode substrates.

1.4.2.2. Layered ECDs

This kind of asymmetric ECD in which the chromophore is deposited or attached to the working electrode has been widely reported for different EC materials displaying different degree of complexity.

Some reported systems comprised inorganic metal oxide films deposited on one of the electrodes as chromogenic materials, such as WO_3, V_2O_5, TiO_2,[85] ATO,[86] or combinations of them,[78] while the other electrode was coated with a convenient intrinsic electron donating material which also exhibit the ability to store the required charge to provide the device with "memory effect" in open circuit.

Other device architectures combine the excellent properties of some of these inorganic materials, usually sintered TiO_2 films, while avoiding the above-mentioned drawbacks of these inorganic materials when used as chromophors, and employed them just as a donor support wherein other chromophores were anchored. This strategy first reported by Marguerettaz et al,[87] employed by Cinnsealach et al. in EC devices some years later,[61, 88] including variants patented by NTERA Ltd under the tradename

NanoCrhomics[16] was based on a TiO_2 nanoscrystaline films coated with chemically absorbed viologen molecules,[16, 50, 61, 88-89] (although other chromophores have also been studied).[90] This approach have proven to provide competitive coloration levels and extraordinary fast switching times of 1-3 seconds [61, 91] or even lower.[90a] It is worth noting that nanocrystalline TiO_2 is regarded as the most suitable semiconductor for this application because of its high transparency in the visible light range, high surface area, semiconductor behavior with fast electron transfer through the conduction band and high affinity toward certain ligands)[56a, 92]

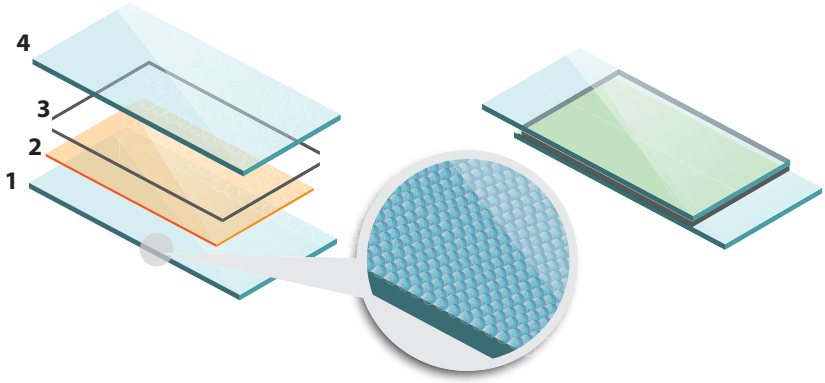

Figure 1.3: Confifuration of layered ECD and components: 1) TCO/glass provided with nanostrucured layer; 2) electrolyte; 3) spacers; 4) TCO/glass.

Besides transparent ECDs based on sintered films of small-size nanoparticles of anatase TiO_2 deposited on the electrode, reflective displays have also been developed either by integrating an additional white reflective layer in the device[9a, 16] or using intrinsically reflective support layer (e.g., composed by TiO_2 particles of appropriate size[89c] or by polymeric microspheres conveniently functionalized[93]).

To attach the viologens to the TiO_2 nanocrystals, diverse anchoring groups have been studied such as salicylic acid,[85, 87, 91, 94], and carboxylic acids[94-95] including benzoic acid,[91] or the most widely employed phosphonic acid [16, 50, 61, 88-89] because of its proven stronger chemisorption in comparison to

the others reported,[91] even considered irreversible toward nanocrystalline TiO_2-coated electrodes.[88] Specifically, the most employed moiety is the ethyl phosphonic acid, [16, 56a, 61, 89b, 89c, 90a, 92] even though its grafting process entails times as large as 24h[56a, 61, 89b, 89c, 90a] to ensure full attachment of the viologen and therefore suitable levels of coloration. Apart from the time consumption, these procedures may damage some electrode substrates (i.e., ITO) due to the acid conditions to which it is exposed, habitually 20 mM water solution of viologen functionalized with two phosphonic acid pendants, [61, 89c, 90a, 92] reaching pH values between 1 – 2. Therefore, the development of viologens which exhibit chemisorption as strong as the latter, but with more rapid binding process towards nanostructured layer and consequently lower grafting times, are necessary to accomplish EC systems compatible with plastic substrates (i.e., ITO/PET) and with any fabrication process required for up-scaling (e.g., coating or printing technology such as dip-coating or ink-jet including roll-to-roll processing, among others).

Going one step further, the other electrode substrate may also comprise additional chromophore with complementary EC behavior to obtain simultaneously the coloration of both chromophores upon applying appropriate external voltage. Some reported examples of these "dual-type " ECDs include cathodically coloring layers such as WO_3[1, 96] or viologen-coated TiO_2 films[89a, 89b, 90a, 91], with anodically coloring materials including PB,[91, 96] or SnO_2-coated with phenothiazine derivative,[89a, 90a] among others.

Taking advantage of these approaches along with their combination with different, and regularly more complex, device architectures, great deal of research have been conducted to overcome the limitations of the EC materials such as the limited palette of colors (especially the small amount of EC systems which exhibit neutral tones such as gray or black with colorless off state) or multicolor or even multielectrochromism. Following the "color mixing" approach, two,[97] three,[98] or even four[99] EC materials of different

colored states have been combined to obtain "colorless-to-gray/black" ECDs using diverse device architectures including blends,[98] multilayered devices [97b, 97c, 99]or even multielectrodes. [97a] Equally, multilayered,[36b, 99-100] multielectrode, [97a, 101] or patterned-based device configurations[36b, 36d, 50] (e.g. pixel structure)[50] used to integrate EC materials of different hues in the same ECD,[36c, 60a, 100] have to some extent expanded the provided colorations of ECDs, although their color versatility may be significantly limited by the single coloration of the monoelectrochromic materials generally used. [102] Nevertheless, apart from the complexity of these systems, they are habitually accompanied by some operational problems such as the loss of transparency caused by the larger number of layers and/or electrodes, along with the increment of the electrical resistivity in the multilayered electrodes which can limit the size of the ECDs and the response time. Therefore, the development of ECDs with a simple device architecture avoiding the large number of layers while easing the fabrication process, but without leaving up their performance including the variety of colors together with neutral tones, is necessary to expand the potential applicability of the electrochromic technology.

In summary, despite the significant effort expended in the last 30 years in the field of electrochromism, there are some improvable aspects in the EC technology, which will be the object of study in this thesis.

1.5. Objectives and outline of the thesis

In the light of the concerns stated throughout these pages, the purpose of this thesis is to make a significant contribution in the field of electrochromic materials and devices, addressing some weaknesses detected and expanding the potential of the electrochromic technology. The main objectives are listed below.

- Synthetizing viologens provided with suitable anchoring groups which offer strong chemisorption towards nanostructured layers and rapid binding process compatible with plastic substrates (i.e., ITO/PET).

- Developing a new semi-solid electrolyte which combines the advantages of both liquid and solid electrolytes, but avoiding the weaknesses of them and enabling the fabrication of high-performance ECDs.

- Developing ECDs which exhibit colorless-to-neutral color (i.e., gray and black) switching with simple device architecture and competitive performance.

- Developing ECDs which provide more than one colored state including multielectrochromic systems with simple fabrication process and configuration.

To achieve these aims, certain new asymmetric and symmetric viologens have been synthesized, both functionalized with a suitable anchoring group which allow their integration in layered ECDs and without any anchoring moiety to be tested in all-in-one configuration. Additionally, a new semi-solid polyelectrolyte has been developed and different ECD architectures comprising the new electrolyte and the new viologens as well as conventional ones have been tested.

The work is presented according to the following outline:

In chapter 2, the techniques and methods employed in the following chapters to estimate some important parameters of the electrochromic devices are established.

In chapter 3, the first proof of concept of new bonding moiety which provides strong chemisorption of the viologens towards nanostructured TiO_2 layers and rapid binding process compatible with plastic substrates

(i.e., ITO/PET) is reported. Its successful integration in plastic ECDs is also demonstrated.

Chapter 4 displays the development of a new semi-solid polyelectrolyte based on a non-Newtonian viscoelastic fluid, which combines the advantages of both liquid and solid electrolytes, while enabling the easy fabrication of high-performance ECDs in terms of transmittance change, switching times and cyclability.

Once this two limiting factors have been addressed (i.e., the electrolyte and the grafting process of some viologens while using layered ECDs), the following chapters are focused on diversifying the colors of the EC materials including more neutral colorations as well as multicoloration. Thus, the chapters 5, 6 and 7 deal with the achievement of ECDs which provide colorless-to-gray/black colored states with competitive performance, using different approaches and device configurations. More specifically:

In chapter 5 new asymmetric viologens are synthesized and successfully incorporated in all-in-one ECDs achieving gray colored states.

In chapters 6 and 7, on the contrary, the neutral colorations are achieved using layered electrodes, entailing the use of the viologens provided with anchoring group. Different strategies have been followed. In particular, the chapter 6 is focused on color mixing approach using symmetric viologens of different nature wherein the simple layered configuration is preserved, whereas the chapter 7 includes the design and synthesis of new asymmetric viologens also anchored on the nanostructured layer.

In chapter 8, a new concept of multielectrochromic systems is demonstrated using very simple device architecture and easy fabrication process. Additionally, the proof of concept of new ECDs based on simple zoning design each of which offers the possibility of displaying different multiswitchable colors independently, is also demonstrated.

Finally, chapter 9 summarizes the most relevant achievements developed in the present thesis and how they can contribute to expanding the potential of the electrochromic technology.

1.6. References

[1] C. G. Granqvist, A. Azens, P. Heszler, L. B. Kish, L. Österlund, *Sol. Energy Mater. Sol. Cells* **2007**, *91*, 355-365.

[2] C. M. Lampert, *Materials Today* **2004**, *7*, 28-35.

[3] R. A. Evans, T. L. Hanley, M. A. Skidmore, T. P. Davis, G. K. Such, L. H. Yee, G. E. Ball, D. A. Lewis, *Nat Mater* **2005**, *4*, 249-253.

[4] A. Seeboth, D. Lötzsch, *Thermochromic and Thermotropic Materials*, Pan Stanford Publishing, **2013**.

[5] C.-G. Granqvist, *Nat Mater* **2006**, *5*, 89-90.

[6] J. A. Check, A. Joseph, *Vol. US5463492*, Research Frontiers Incorporated (Woodbury, NY) **1995**.

[7] P. S. Drzaic, *Liquid Crystal Dispersions*, World Scientific, **1995**.

[8] H.-C. Lu, S.-Y. Kao, T.-H. Chang, C.-W. Kung, K.-C. Ho, *Sol. Energy Mater. Sol. Cells* **2016**, *147*, 75-84.

[9] a) P. Bonhôte, E. Gogniat, F. Campus, L. Walder, M. Grätzel, *Displays* **1999**, *20*, 137-144; b) D. A. A. de Mello, M. R. S. Oliveira, L. C. S. de Oliveira, S. C. de Oliveira, *Sol. Energy Mater. Sol. Cells* **2012**, *103*, 17-24.

[10] C.-W. Hu, K.-M. Lee, K.-C. Chen, L.-C. Chang, K.-Y. Shen, S.-C. Lai, T.-H. Kuo, C.-Y. Hsu, L.-M. Huang, R. Vittal, K.-C. Ho, *Sol. Energy Mater. Sol. Cells* **2012**, *99*, 135-140.

[11] J. R. Platt, *The Journal of Chemical Physics* **1961**, *34*, 862-863.

[12] P. M. S. Monk, R. J. Mortimer, D. R. Rosseinsky, *Electrochromism and Electrochromic Devices: a brief history of electrochromism*, Cambridge University Press, United States of America **2007**.

[13] R. J. Mortimer, *Annu. Rev. Mater. Res.* **2011**, *41*, 241-268.

[14] P. M. S. Monk, R. J. Mortimer, D. R. Rosseinsky, *Electrochromism and Electrochromic Devices: introduction to electrochromism*, Cambridge University Press, United States of America **2007**.

[15] R. J. Mortimer, A. L. Dyer, J. R. Reynolds, *Displays* **2006**, *27*, 2-18.

[16] U. Bach, D. Corr, D. Lupo, F. Pichot, M. Ryan, *Adv. Mater.* **2002**, *14*, 845-848.

[17] a) W. L. Tonar, H. J. Byker, K. E. Siegrist, J. S. Anderson, K. L. Ash, Gentex Corporation, **1999**; b) H. J. Byker, (Ed.: C. Gentex), US4902108, **1990**.

[18] a) D. T. Gillaspie, R. C. Tenent, A. C. Dillon, *Journal of Materials Chemistry* **2010**, *20*, 9585-9592; b) A. Llordes, G. Garcia, J. Gazquez, D. J. Milliron, *Nature* **2013**, *500*, 323-326.

[19] R. C. G. M. Loonen, M. Trčka, D. Cóstola, J. L. M. Hensen, *Renewable Sustainable Energy Rev.* **2013**, *25*, 483-493.

[20] a) A. Piccolo, *Energy and Buildings* **2010**, *42*, 1409-1417; b) E. S. Lee, D. L. DiBartolomeo, S. E. Selkowitz, *Energy and Buildings* **2006**, *38*, 30-44; c) R. Baetens, B. P. Jelle, A. Gustavsen, *Sol. Energy Mater. Sol. Cells* **2010**, *94*, 87-105.

[21] a) *Vol. Nov. 23, 2016*, http://sageglass.com; b) http://viewglass.com.

[22] Å. Stefan, *J. New Mater. Electrochem. Syst.* **2001**, *4*, 173-179.

[23] H. J. Byker, (Ed.: G. Corporation), 5128799, **1992**.

[24] D. V. Varaprasad, H. Habibi, I. A. Mccabe, N. R. Lynam, M. Zhao, C. A. Dornan, (Ed.: D. Corporation), WO1995030495 A1, **1995**.

[25] a) C. Ma, M. Taya, C. Xu, *Polymer Engineering & Science* **2008**, *48*, 2224-2228; b) D. Barrios Puerto, Universidad Carlos III de Madrid **2012**; c) R. Vergaz Benito, J. M. Sánchez-Pena, C. Vázquez, D. Mecerreyes, J. A. Pomposo, *Mundo Electrónico* **2004**, *350*, 60-64.

[26] a) A. L. Dyer, E. J. Thompson, J. R. Reynolds, *ACS Appl. Mater. Interfaces* **2011**, *3*, 1787-1795; b) R. H. Bulloch, J. A. Kerszulis, A. L. Dyer, J. R. Reynolds, *ACS Appl. Mater. Interfaces* **2015**, *7*, 1406-1412.

[27] I. F. Chang, B. L. Gilbert, T. I. Sun, *J. Electrochem. Soc.* **1975**, *122*, 955-962.

[28] P. Monk, Roger Mortimer,, D. Rosseinsky., *Electrochromism and Electrochromic Devices*, Cambridge University Press, **2007**.

[29] C. G. Granqvist, in *Handbook of Inorganic Electrochromic Materials*, Elsevier Science B.V., Amsterdam, **1995**.

[30] P. M. S. Monk, R. J. Mortimer, D. R. Rosseinsky, in *Electrochromism*, Wiley-VCH Verlag GmbH, **2007**, pp. 59-92.

[31] P. M. S. Monk, R. J. Mortimer, D. R. Rosseinsky, in *Electrochromism*, Wiley-VCH Verlag GmbH, **2007**, pp. 101-119.

[32] N. N. Dinh, N. T. T. Oanh, P. D. Long, M. C. Bernard, A. Hugot-Le Goff, *Thin Solid Films* **2003**, *423*, 70-76.

[33] F. Garnier, G. Tourillon, M. Gazard, J. C. Dubois, *Journal of Electroanalytical Chemistry and Interfacial Electrochemistry* **1983**, *148*, 299-303.

[34] A. F. Diaz, J. A. Logan, *Journal of Electroanalytical Chemistry and Interfacial Electrochemistry* **1980**, *111*, 111-114.

[35] R. J. Mortimer, *Electrochim. Acta* **1999**, *44*, 2971-2981.

[36] a) A. A. Argun, A. Cirpan, J. R. Reynolds, *Adv. Mater.* **2003**, *15*, 1338-1341; b) A. A. Argun, P.-H. Aubert, B. C. Thompson, I. Schwendeman, C. L. Gaupp, J. Hwang, N. J. Pinto, D. B. Tanner, A. G. MacDiarmid, J. R. Reynolds, *Chem. Mater.* **2004**, *16*, 4401-4412; c) H. C. Ko, S. Kim, H. Lee, B. Moon, *Advanced Functional Materials* **2005**, *15*, 905-909; d) J. A. Kerszulis, K. E. Johnson, M. Kuepfert, D. Khoshabo, A. L. Dyer, J. R. Reynolds, *J. Mater. Chem. C* **2015**, *3*, 3211-3218.

[37] a) G. Wang, X. Fu, J. Huang, L. Wu, Q. Du, *Electrochim. Acta* **2010**, *55*, 6933-6940; b) D. Chao, X. Jia, H. Liu, L. He, L. Cui, C. Wang, E. B. Berda, *J. Polym. Sci., Part A: Polym. Chem.* **2011**, *49*, 1605-1614; c) Y. A. Udum, C. G. Hızlıateş, Y. Ergün, L. Toppare, *Thin Solid Films* **2015**, *595, Part A*, 61-67; d) K. Lin, Y. Zhao, S. Ming, H. Liu, S. Zhen, J. Xu, B. Lu, *J. Polym. Sci., Part A: Polym. Chem.* **2016**, *54*, 1468-1478; e) W. T. Neo, C. M. Cho, Z. Shi, S.-J. Chua, J. Xu, *J. Mater. Chem. C* **2016**, *4*, 28-32.

[38] a) G. Xu, J. Zhao, J. Liu, C. Cui, Y. Hou, Y. Kong, *J. Electrochem. Soc.* **2013**, *160*, G149-G155; b) T. Yi-Jie, C. Hai-Feng, Z. Wen-Wei, Z. Zhao-Yang, *J. Appl. Polym. Sci.* **2013**, *127*, 636-642; c) W. Yang, J. Zhao, C. Cui, Y. Kong, X. Zhang, P. Li, *J. Solid State Electrochem.* **2012**, *16*, 3805-3815.

[39] a) S. Cogal, M. Kiristi, K. Ocakoglu, L. Oksuz, A. U. Oksuz, *Mater. Sci. Semicond. Process.* **2015**, *31*, 551-560; b) E. N. Esmer, S. Tarkuc, Y. A. Udum, L. Toppare, *Mater. Chem. Phys.* **2011**, *131*, 519-524; c) B. Kim, J. Kim, E. Kim, *Macromolecules* **2011**, *44*, 8791-8797; d) B. Yigitsoy, S. M. A. Karim, A. Balan, D. Baran, L. Toppare, *Synth. Met.* **2010**, *160*, 2534-2539; e) H. Zhao, Y. Wei, J. Zhao, M. Wang, *Electrochim. Acta* **2014**, *146*, 231-241.

[40] L. Michaelis, E. S. Hill, *The Journal of General Physiology* **1933**, *16*, 859-873.

[41] N. W. Drewe, P. E. Giffard, A. C. Waters, *Vol. US3920443 A*, Ici Ltd, **1975**.

[42] a) B. Kok, H. J. Rurainski, O. V. H. Owens, *Biochimica et Biophysica Acta (BBA) - Biophysics including Photosynthesis* **1965**, *109*, 347-356; b) P. A. Trudiatger, *Anal. Biochem.* **1970**, *36*, 222-225.

[43] C. J. Schoot, J. J. Ponjee, H. T. v. Dam, R. A. v. Doorn, P. T. Bolwijn, *Applied Physics Letters* **1973**, *23*, 64-65.

[44] C. L. Bird, A. T. Kuhn, *Chem. Soc. Rev.* **1981**, *10*, 49-82.

[45] P. M. S. Monk, *J. Electroanal. Chem.* **1997**, *432*, 175-179.

[46] P. M. S. Monk, *The viologens: physicochemical properties, synthesis, and applications of the salts of 4,4'-bipyridine*, Wiley, **1998**.

[47] S. Cospito, B. C. De Simone, A. Beneduci, D. Imbardelli, G. Chidichimo, *Mater. Chem. Phys.* **2013**, *140*, 431-434.

[48] P. M. S. Monk, R. J. Mortimer, D. R. Rosseinsky, *Electrochromism and Electrochromic Devices: the viologens*, Cambridge University Press, United States of America **2007**.

[49] T. Watanabe, K. Honda, *The Journal of Physical Chemistry* **1982**, *86*, 2617-2619.

[50] M. Möller, S. Asaftei, D. Corr, M. Ryan, L. Walder, *Adv. Mater.* **2004**, *16*, 1558-1562.

[51] a) D. R. Rosseinsky, P. M. S. Monk, *Sol. Energy Mater. Sol. Cells* **1992**, *25*, 201-210; b) D. R. Rosseinsky, P. M. S. Monk, R. A. Hann, *Electrochim. Acta* **1990**, *35*, 1113-1123.

[52] E. Müller, K. A. Bruhn, *Chem. Ber.* **1953**, *86*, 1122-1132.

[53] *Vol. Febr. 17, 2017*, http://www.ppgaerospace.com/getdoc/18dce3cb-180e-45a1-ba7b-2bc1770143cc/Alteos.aspx.

[54] S. K. Deb, *Appl. Opt.* **1969**, *8*, 192-195.

[55] a) R. Marcilla, F. Alcaide, H. Sardon, J. A. Pomposo, C. Pozo-Gonzalo, D. Mecerreyes, *Electrochemistry Communications* **2006**, *8*, 482-488; b) Y. Zhu, M. T. Otley, F. A. Alamer, A. Kumar, X. Zhang, D. M. D. Mamangun, M. Li, B. G. Arden, G. A. Sotzing, *Organic Electronics* **2014**, *15*, 1378-1386.

[56] a) Y. J. Kim, H. K. Jeong, J. K. Seo, S. Y. Chai, Y. S. Kim, G. I. Lim, M. H. Cho, I.-M. Lee, Y. S. Choi, W. I. Lee, *Journal of Nanoscience and Nanotechnology* **2007**, *7*, 4106-4110; b) A.-L. Pont, R. Marcilla, I. De Meatza, H. Grande, D. Mecerreyes, *Journal of Power Sources* **2009**, *188*, 558-563.

[57] E. Azaceta, R. Marcilla, A. Sanchez-Diaz, E. Palomares, D. Mecerreyes, *Electrochim. Acta* **2010**, *56*, 42-46.

[58] a) M. Kucharski, T. Lukaszewicz, P. Mrozek, *Opto-Electronics Review* **2004**, *12*, 175-180 ; b) S. S. Sekhon, Deepa, S. A. Agnihotry, *Solid State Ionics* **2000**, *136–137*, 1189-1192.

[59] S. A. Agnihotry, Nidhi, Pradeep, S. S. Sekhon, *Solid State Ionics* **2000**, *136–137*, 573-576.

[60] a) C. Pozo-Gonzalo, M. Salsamendi, A. Viñuales, J. A. Pomposo, H.-J. Grande, *Sol. Energy Mater. Sol. Cells* **2009**, *93*, 2093-2097; b) C. P. Gonzalo, R. M. Garcia, M. S. Telleria, J. A. P. Alonso, H. J. G. Telleria, **2011**; c) G. C. Pozo, G. R. Marcilla, T. M. Salsamendi, A. J. A. POMPOSO, T. H. J. GRANDE, **2012**.

[61] R. Cinnsealach, G. Boschloo, S. Nagaraja Rao, D. Fitzmaurice, *Sol. Energy Mater. Sol. Cells* **1998**, *55*, 215-223.

[62] a) L. Su, Z. Xiao, Z. Lu, *Mater. Chem. Phys.* **1998**, *52*, 180-183; b) L. Su, H. Wang, Z. Lu, *Mater. Chem. Phys.* **1998**, *56*, 266-270; c) S. Lianyong, W. Hong, L. Zuhong,

Supramolecular Science **1998**, *5*, 657-659; d) L. Su, Z. Xiao, Z. Lu, *Thin Solid Films* **1998**, *320*, 285-289.

[63] M. Armand, *Solid State Ionics* **1983**, *9–10, Part 2*, 745-754.

[64] M.-C. Bernard, A. Hugot-Le Goff, W. Zeng, *Synth. Met.* **1997**, *85*, 1347-1348.

[65] S. A. Agnihotry, P. Pradeep, S. S. Sekhon, *Electrochim. Acta* **1999**, *44*, 3121-3126.

[66] a) S. Lianyong, F. Jinghuai, L. Zuhong, *Jpn. J. Appl. Phys.* **1997**, *36*, 5747-5750; b) D. Mecerreyes, R. Marcilla, E. Ochoteco, H. Grande, J. A. Pomposo, R. Vergaz, J. M. Sánchez Pena, *Electrochim. Acta* **2004**, *49*, 3555-3559.

[67] S. S. Sekhon, N. Arora, S. A. Agnihotry, *Solid State Ionics* **2000**, *136–137*, 1201-1204.

[68] M. M. Silva, P. C. Barbosa, L. C. Rodrigues, A. Gonçalves, C. Costa, E. Fortunato, *Optical Materials* **2010**, *32*, 719-722.

[69] S. C. de Oliveira, L. C. de Morais, A. A. da Silva Curvelo, R. M. Torresib, *J. Electrochem. Soc.* **2003**, *150*, E578-E583.

[70] a) C. O. Avellaneda, D. F. Vieira, A. Al-Kahlout, E. R. Leite, A. Pawlicka, M. A. Aegerter, *Electrochim. Acta* **2007**, *53*, 1648-1654; b) C. O. Avellaneda, D. F. Vieira, A. Al-Kahlout, S. Heusing, E. R. Leite, A. Pawlicka, M. A. Aegerter, *Sol. Energy Mater. Sol. Cells* **2008**, *92*, 228-233.

[71] a) Q. Du, X. Fu, S. Liu, L. Niu, *Polymer International* **2012**, *61*, 222-227; b) S.-Y. Kao, C.-W. Kung, H.-W. Chen, C.-W. Hu, K.-C. Ho, *Sol. Energy Mater. Sol. Cells* **2016**, *145, Part 1*, 61-68.

[72] a) Y.-S. Ye, J. Rick, B.-J. Hwang, *Journal of Materials Chemistry A* **2013**, *1*, 2719-2743; b) A. L. Saroj, R. K. Singh, *Journal of Physics and Chemistry of Solids* **2012**, *73*, 162-168.

[73] P. Vidinha, N. M. T. Lourenco, C. Pinheiro, A. R. Bras, T. Carvalho, T. Santos-Silva, A. Mukhopadhyay, M. J. Romao, J. Parola, M. Dionisio, J. M. S. Cabral, C. A. M. Afonso, S. Barreiros, *Chemical Communications* **2008**, 5842-5844.

[74] H.-C. Lu, S.-Y. Kao, H.-F. Yu, T.-H. Chang, C.-W. Kung, K.-C. Ho, *ACS Appl. Mater. Interfaces* **2016**, *8*, 30351-30361.

[75] a) C. O. Avellaneda, K. Dahmouche, L. O. S. Bulhões, A. Pawlicka, *Journal of Sol-Gel Science and Technology* **2000**, *19*, 447-451; b) B. Munro, P. Conrad, S. Krämer, H. Schmidt, P. Zapp, *Sol. Energy Mater. Sol. Cells* **1998**, *54*, 131-137; c) B. Orel, U. Opara Krašovec, U. Lavrenčič Štangar, P. Judeinstein, *Journal of Sol-Gel Science and Technology* **1998**, *11*, 87-104.

[76] C. A. Nguyen, A. A. Argun, P. T. Hammond, X. Lu, P. S. Lee, *Chem. Mater.* **2011**, *23*, 2142-2149.

[77] a) T.-H. Chang, C.-W. Hu, R. Vittal, K.-C. Ho, *Sol. Energy Mater. Sol. Cells* **2014**, *126*, 213-218; b) A. M. Soutar, D. R. Rosseinsky, W. Freeman, X. Zhang, X. How, H. Jiang, X. Zeng, X. Miao, *Sol. Energy Mater. Sol. Cells* **2012**, *100*, 268-270; c) G. Chidichimo, B. C. De Simone, D. Imbardelli, M. De Benedittis, M. Barberio, L. Ricciardi, A. Beneduci, *The Journal of Physical Chemistry C* **2014**, *118*, 13484-13492.

[78] J. Liu, J. P. Coleman, *Materials Science and Engineering: A* **2000**, *286*, 144-148.

[79] P. M. S. Monk, R. D. Fairweather, M. D. Ingram, J. A. Duffy, *Journal of the Chemical Society, Perkin Transactions 2* **1992**, 2039-2041.

[80] K. Wadhwa, S. Nuryyeva, A. C. Fahrenbach, M. Elhabiri, C. Platas-Iglesias, A. Trabolsi, *J. Mater. Chem. C* **2013**, *1*, 2302-2307.

[81] P. M. S. Monk, R. J. Mortimer, D. R. Rosseinsky, in *Electrochromism*, Wiley-VCH Verlag GmbH, **2007**, pp. 124-142.

[82] A. Bewick, A. C. Lowe, C. W. Wederell, *Electrochim. Acta* **1983**, *28*, 1899-1902.

[83] W. Geuder, S. Hünig, A. Suchy, *Tetrahedron* **1986**, *42*, 1665-1677.

[84] a) W. S. Jeon, H.-J. Kim, C. Lee, K. Kim, *Chemical Communications* **2002**, 1828-1829; b) P. A. Quintela, A. E. Kaifer, *Langmuir* **1987**, *3*, 769-773; c) J. W. Park, N. H. Choi, J. H. Kim, *The Journal of Physical Chemistry* **1996**, *100*, 769-774.

[85] A. Hagfeldt, N. Vlachopoulos, M. Grätzel, *J. Electrochem. Soc.* **1994**, *141*, L82-L84.

[86] a) J. P. Coleman, A. T. Lynch, P. Madhukar, J. H. Wagenknecht, *Sol. Energy Mater. Sol. Cells* **1999**, *56*, 375-394; b) J. P. Coleman, J. J. Freeman, P. Madhukar, J. H. Wagenknecht, *Displays* **1999**, *20*, 145-154.

[87] X. Marguerettaz, R. O'Neill, D. Fitzmaurice, *J. Am. Chem. Soc.* **1994**, *116*, 2629-2630.

[88] R. Cinnsealach, G. Boschloo, S. Nagaraja Rao, D. Fitzmaurice, *Sol. Energy Mater. Sol. Cells* **1999**, *57*, 107-125.

[89] a) N. Vlachopoulos, J. Nissfolk, M. Möller, A. Briançon, D. Corr, C. Grave, N. Leyland, R. Mesmer, F. Pichot, M. Ryan, G. Boschloo, A. Hagfeldt, *Electrochim. Acta* **2008**, *53*, 4065-4071; b) H. J. Kim, J. K. Seo, Y. J. Kim, H. K. Jeong, G. I. Lim, Y. S. Choi, W. I. Lee, *Sol. Energy Mater. Sol. Cells* **2009**, *93*, 2108-2112; c) S. Bhandari, M. Deepa, A. K. Srivastava, S. T. Lakshmikumar, RamaKant, *Solid State Ionics* **2009**, *180*, 41-49; d) P. Pechy, F. P. Rotzinger, M. K. Nazeeruddin, O. Kohle, S. M. Zakeeruddin, R. Humphry-Baker, M. Gratzel, *Journal of the Chemical Society, Chemical Communications* **1995**, 65-66; e) S. M. Zakeeruddin, M. K. Nazeeruddin, P. Pechy, F. P. Rotzinger, R. Humphry-Baker, K. Kalyanasundaram, M. Grätzel, V. Shklover, T. Haibach, *Inorganic Chemistry* **1997**, *36*, 5937-5946.

[90] a) D. Cummins, G. Boschloo, M. Ryan, D. Corr, S. N. Rao, D. Fitzmaurice, *J. Phys. Chem. B* **2000**, *104*, 11449-11459; b) P. Bonhôte, E. Gogniat, M. Grätzel, P. V. Ashrit, *Thin Solid Films* **1999**, *350*, 269-275.

[91] F. Campus, P. Bonhôte, M. Grätzel, S. Heinen, L. Walder, *Sol. Energy Mater. Sol. Cells* **1999**, *56*, 281-297.

[92] S. Y. Choi, M. Mamak, N. Coombs, N. Chopra, G. A. Ozin, *Nano Letters* **2004**, *4*, 1231-1235.

[93] a) J.-H. Ryu, D.-O. Shin, K.-D. Suh, *J. Polym. Sci., Part A: Polym. Chem.* **2005**, *43*, 6562-6572; b) J.-H. Ryu, M.-S. Park, K.-D. Suh, *Colloid Polym. Sci.* **2007**, *285*, 1675-1681.

[94] A. Hagfeldt, L. Walder, M. Graetzel, *Vol. 2531*, **1995**, pp. 60-69.

[95] a) M. K. Nazeeruddin, P. Liska, J. Moser, N. Vlachopoulos, M. Grätzel, *Helv. Chim. Acta* **1990**, *73*, 1788-1803; b) A. Hagfeldt, N. Vlachopoulos, S. Gilbert, M. Graetzel, *Vol. 2255* (Eds.: V. Wittwer, C. G. Granqvist, C. M. Lampert), **1994**, pp. 297-304.

[96] K.-C. Ho, *Sol. Energy Mater. Sol. Cells* **1999**, *56*, 271-280.

[97] a) E. Unur, P. M. Beaujuge, S. Ellinger, J.-H. Jung, J. R. Reynolds, *Chem. Mater.* **2009**, *21*, 5145-5153; b) C. S. Ah, J. Song, S. M. Cho, T.-Y. Kim, H. N. Kim, J. Y. Oh, H. Y. Chu, H. Ryu, *Bull. Korean Chem. Soc.* **2015**, *36*, 548-552; c) D. Weng, Y. Shi, J. Zheng, C. Xu, *Organic Electronics* **2016**, *34*, 139-145.

[98] P.-Y. Chen, C.-S. Chen, T.-H. Yeh, *J. Appl. Polym. Sci.* **2014**, *131*, 40485.

[99] H. Shin, Y. Kim, T. Bhuvana, J. Lee, X. Yang, C. Park, E. Kim, *ACS Appl. Mater. Interfaces* **2012**, *4*, 185-191.

[100] B. Xu, L. Xu, G. Gao, Y. Yang, W. Guo, S. Liu, Z. Sun, *Electrochim. Acta* **2009**, *54*, 2246-2252.

[101] Y.-M. Zhang, X. Wang, W. Zhang, W. Li, X. Fang, B. Yang, M. Li, S. X.-A. Zhang, *Light Sci Appl* **2015**, *4*, e249.

[102] G. Bar, N. Larina, L. Grinis, V. Lokshin, R. Gvishi, I. Kiryuschev, A. Zaban, V. Khodorkovsky, *Sol. Energy Mater. Sol. Cells* **2012**, *99*, 123-128.

CHAPTER 2

FUNDAMENTALS, CORE MATERIALS AND GENERAL PROCEDURES

2.1. Introduction

The type of materials employed in the electrochromic devices (ECDs) will determine their resultant performance. The subsequent assessment of the electrochromic behavior of the ECDs is crucial to identify their core strengths and weakness and to evaluate their potential applicability. To this end, some parameters are habitually employed aimed to quantify the response of the ECDs.

This chapter aims, firstly, to introduce the type of core materials developed in this thesis, secondly to set the requirements to be met by a competitive ECD along with the definition employed herein for each parameter, and finally, to explain the method selected in the following chapters to estimate these parameters and developed colorations.

A brief description of the light absorption and optical characterization fundamentals is included. The methods and instruments which are common to all chapters such as the procedures for the fabrication of the ECDs are described in this chapter, whereas other procedures and instruments used in each specific chapter will be described in the corresponding sections.

2.2. Core materials

The most relevant constituents of the ECDs are the EC material and the electrolyte. The core materials developed in this thesis and employed in the following chapters are introduced in this section. The strategies and fundamentals regarding these components are explained below.

2.2.1. EC materials: symmetric and asymmetric viologens

As pointed out in the previous chapter, the electrochromic (EC) systems developed and described in this thesis are based on 1,1'-disubstituted 4,4'-bipyridilium salts, commonly known as "viologens". Among the advantages of this widely studied class of cathodic electrochromic compounds, their ability to be synthetically tunable may be considered one of their key strengths. Thus, the properties of the molecule can be adjusted by varying the nature of the substituents on the nitrogen atoms of the molecule (-R1 and –R2 in the Figure 2.1).[1]

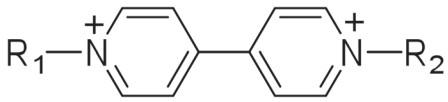

Figure 2.1: General structure of the viologens.

The most broadly studied viologen molecules are those which comprise the same substituent bonded to both nitrogen atoms of the bipyridine. Hence, this kind of molecules wherein both R_1 and R_2 substituents correspond to the same moiety are referred to as symmetric viologens. The colors provided by these symmetric viologens in their first reduced form have been well studied. Thus, although the exhibited coloration may also depend on the solvent, simple alkyl groups provide blue/violet colored state, aryl groups generally lead to green coloration, while some carbazole groups have been reported to show red colored state.

On the other hand, the viologen molecule may comprise different substituents bonded to its nitrogen atoms. In those cases wherein R_1 and R_2 are different from each other the resulting molecule is termed herein asymmetric viologen. When both substituents exhibit similar chemical nature no significant changes are expected in the provided coloration. Thus, reported asymmetric viologens based on 1-alkyl-1'-alkyl substituent

of varying lengths or/and ramification[2], exhibited similar blue/purple colored state, yet different redox potentials and/or response times.

Moreover, the substituents not only determine the color and other properties of viologen, but also may provide the molecule with a convenient functional group. Thus, when the viologens are incorporated adsorbed on the electrode surface in layered-electrode configuration, at least one of the substituents must comprise an adequate anchoring group. In this regard, other reports involving asymmetric viologens employed the asymmetry just as a strategy to provide the viologen with a suitable anchoring group in one of the substituents,[3] being the other substituent exempted from it.

The research work developed in this thesis, include the design and synthesis of new symmetric and asymmetric viologens. The asymmetry has been explored in the present work aiming at achieving new colorations and specially focused on the neutral-color (gray/black) electrochromism, since it remains a challenge not fully scientifically resolved yet, as detected by Prof. R. J. Mortimer.[4]

Two types of viologens have been synthesized in the present thesis:

- Functionalized with a suitable anchoring group to allow their integration in layered ECDs through chemical adsorption

- without any anchoring moiety to be tested in all-in-one configuration.

Detailed information regarding the synthesis of these viologens along with their characterization is described in the corresponding chapters.

2.2.2. Electrolytic matrix: PVA-borax gels

The development of new semi-solid electrolyte which combines the advantages of both liquid and solid electrolytes, but avoiding the weaknesses of them is crucial to expand the potential of the electrochromic technology.

An interesting approach to achieve this goal may be the use of electrolyte mixtures which could be cured by dynamic covalent chemistries, exhibiting rheological behavior about midway between the solid and liquid materials, hence non-Newtonian behavior.

Unlike the Newtonian fluids whose viscosity is independent of shear rate, the non-Newtonian fluids may exhibit a wide range of viscosities depending on the shear rate.[5] Thus, the non-Newtonian behavior shown by shear-thickening (dilatant) or by shear-thinning fluids (pseudoplastic) is evidenced by the increase or decrease of their viscosity with the shear rate, respectively. Additionally, none of them exhibit lineal proportional behavior between shear stress and shear rate, contrary to that observed for the Newtonian fluids.[6] Other non-Newtonian behavior is observed in the viscoelastic fluids, which show both viscous and elastic features under deformation, thus in-between both liquid and solid materials.

A well-known non-Newtonian fluid is the so-called Slime developed by Maki Papavasiliou of the Mattel Materials Laboratory,[7] described as a reversible cross-linking gel obtained by the addition of borax to Guar gum. This material used as a component of diverse toys (i.e., Master of the Universe Slime, Nickelodeon Green Slime)[7b] exhibited quite attractive properties, behaving like a liquid under low stress (can flow and stretch) but conversely, behaving more like a solid under high stress.[7b, 8]

Similar non-Newtonian character has been observed for different polyhydroxy polymers (e.g., poly(glyceryl methacrylate[9]) including some polysaccharides (i.e., O-(2,3-dihydroxypropyl)cellulose[10] or Galactomannan[9b]) in the presence of borax. Among them, one of the most widely reported polyhydroxy polymers and the one employed in the present thesis has been the poly(vinyl alcohol) (PVA), whose gelation with borax was described by David Weill in 1981 and proven to form a Slime-type material.

The gelation process of the PVA with borax occurs immediately[5, 11] as also reported for other hydroxylated species with borate ions.[12] Moreover, due to its ability to flow, the bubbles which may be formed as a result of the rapid gelation process disappear if the gel is allowed to settle for a few minutes, therefore achieving completely bubble-free material.

These PVA-borax gel obtained by complexation of hydroxyl groups of the PVA chain with borate ions, have been reported to be non-Newtonian[6-8] shear thickening[6, 7b, 8, 9b] and viscoelastic fluid.[5, 9b, 13]

The mechanism of crosslinking reaction known as "di-diol" complexation is believed to occur in two successive reactions formed between two diol units and one borate ion. In the first stage borate anion reacts with a diol unit on a polymer leading to monodiol complexation (monocomplexation) and in a second stage, the monodiol reacts with a second diol unit forming the didiol (dicomplexation[9a, 12b, 14] or cross-linking reaction[6, 15]).

Despite the efforts focused on elucidating the mechanism of the alcohol-borax complexation, this concern seems to be unsettled.[5] Some authors assumed that borate esters were being formed,[6, 12a, 15] other reports ascribed the dynamic equilibrium to the cooperative effect of a large number of hydrogen bonding interactions only,[8, 16] whereas some reports suggested the contribution of both borate ester and hydrogen bonding[15b] as an additional stabilizing factor.[17]

Wide variety of PVA and conditions have been proven to form a Slime-type material. Thus, PVA of different molecular weights (ranging from 15 000 to 120 000,[5, 8, 14b, 15b, 15c, 16b, 18]), different concentrations of both PVA and borax (usually from 1.5 to 8 wt% [5-6, 7b, 8, 13, 15b, 16b, 18-19]), and in different volumetric ratios of PVA:borax solutions, (usually between 10:1 and 1:1 [7b, 16b, 18a, 19-20]), have been reported.

The PVA-borax gels employed in this thesis as polyelectrolyte were obtained from a highly hydrolyzed (aprox. 99%) PVA of 61 000 molecular weight, and

borax (sodium tetraborate decahydrate 99.5%) purchased from Aldrich, using the general procedure described below.

2.2.2.1 General procedure to prepare PVA-borax gel materials

A 4% solution of PVA was prepared by placing 4 g of PVA and 96 mL of distilled water in an appropriate flask equipped with mechanical stirrer. A silicon oil bath was employed to heat the dissolution to 90 ^{0}C, until the complete dissolution of the polymer was achieved. Separately, 4% solution of borax was prepared. Once the solutions were obtained, all gels were prepared according to the following procedure. To a 4% solution of PVA, required amount of electroactive components (i.e., redox pair and viologen when necessary) were added. The resulting mixture was stirred until homogeneous solution was obtained. Then, this solution was mixed with a 4% borax aqueous solution in a 4:1 volumetric ratio by vigorous stirring with a spatula, until a gel was formed. The formulations were left to settle on its own until completely bubble-free materials were obtained.

The assessment of thus obtained PVA-borax gel as polyelectrolyte is described in the chapter 4. Additionally, detailed information regarding the types and concentrations of electroactive materials employed in each chapter is described in the corresponding section.

2.3. Principles of light absorption and optical characterization

2.3.1. Light absorption

The observed coloration in any material is the result of the interaction of the moiety which imparts a color, so-called chromophore, with the light. White light comprises the wavelength (λ) associate to all the colors, and when a chromophore absorbs photons from a part of the electromagnetic spectrum, the observed color is the one corresponding to the non-absorbed

wavelengths, termed "complementary color".[21] This absorption may be attributed to the intervalence charge transfer (IVCT) between different oxidation states of the same element available in the moiety (internal redox process), or to internal electronic excitation of moderate energy. The energy gap (E),[4] is related to the wavelength of the light absorbed according to the Planck relation (Equation 2.1, wherein "h" and "c" correspond to the Planck constant and the speed of the light in vacuo, respectively).

$$E = h\nu = \frac{hc}{\lambda} \qquad \text{(Eq. 2.1)}$$

Although all the organic compounds may absorb electromagnetic radiation as a result of the excitation of their valence electrons to higher energy levels, only some of these electronic transitions take place within the visible region (380-780 nm). The latter transitions habitually involve nonbonding electrons (n) and π electrons of the bonding (π) and antibonding (π*) molecular orbitals of the chromophore moiety, being n → π* or π → π* electronic transitions mostly positioned in the range of 200 – 700 nm.

As the electroactive species exhibit different spectroscopic transitions between the ground and excited state in each redox form, they will absorb different zone of the electromagnetic spectrum at each form.

2.3.2. Optical characterization

The optical characterization is habitually carried out using UV-vis spectrophotometer. One of the most important optical parameter is the transmittance, usually expressed as percentage of incident light at a given wavelength that is transmitted through the sample (Eq. 2.2 wherein I_0 corresponds to the intensity of incident light and I to the intensity of the light transmitted though the sample).

$$\%T_\lambda = \frac{I}{I_0}\, x\, 100 \qquad \text{(Eq. 2.2)}$$

The absorbance, also used when measuring optical responses, is described as the minus logarithm of the transmittance.

The measurement procedure employed in the following chapters, consist of a UV-vis spectrophotometer connected to potentiostat as a direct current source which allows the acquisition of the transmittance with and without applying any appropriate external voltage, thus obtaining the transmittance at colored and bleached state ($\%T_c$ and $\%T_b$, respectively). It is worth to note that the bleached state of EC systems based on viologens corresponds to the off state since no potential is required; however, it is not necessarily true for EC systems based on other EC materials which may need any external voltage to reach the colorless state.

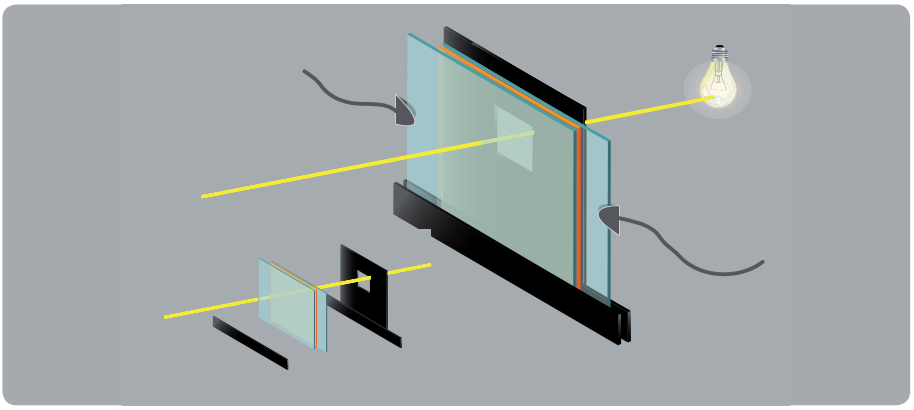

Fihure 2.2. Schematic illustration of the measurement procedure.

2.4. Assessment of the electrochromic performance

When developing new ECDs is important to assess its electrochromic behavior. Some important requirements which one competitive ECD must meet include high level of coloration, fast switching times between the colored and bleached states, high color efficiencies, high white-erase efficiency or reversibility, good redox cyclability and high transparency

at bleached state in the case of non-reflective ECDs. Additionally, the quantification of the colors developed at each redox state is also crucial to achieve an accuracy comparison between different colored states or between different EC materials. The definition of the key parameters employed to evaluate the electrochromic behavior in this thesis are listed below.

2.4.1. Performance parameters

- Level of coloration: the level of coloration of one ECD gives an idea about the degree of darkening of the device at colored state. The parameter employed in the present thesis to assess this feature has been the transmittance change (Δ%T) defined as the difference between the percentage of transmittance at bleached state ($\%T_b$) and the percentage of transmittance at colored state ($\%T_c$) at a certain wavelength (Eq. 2.3), usually the maximum contrast wavelength (λ_{max}). The measurement procedure consists in recording the percentage of transmittance (%T) of ECDs as a function of the wavelength at off state and at suitable voltage to achieve the colored state.

  To ensure that the system has reached the maximum colored state, the devices are exposed to the same voltage during 40 s (i.e, significantly longer than coloring time) before recording the transmittance at colored state

$$\Delta\%T = \%T_b - \%T_c \qquad \text{(Eq. 2.3)}$$

  Other parameter also employed to quantify the level of coloration is the contrast ratio, defined as the percentage of transmittance at bleached state divided by the percentage of transmittance at colored state (Eq. 2.4).

$$Contrast\ ratio = \frac{\%T_b}{\%T_c} \qquad \text{(Eq. 2.4)}$$

- Switching times: the response times or switching times of the ECD are defined as the time required to change between the bleached and the colored state. Usually the change is defined as a certain percentage of the total Δ%T, however, no universal agreement exists and different percentages have been established (i.e., 60%,[22] 65%,[23] 70%,[24] 80%,[25] 90%[26] or even 95%[27]). The criteria chosen herein has been the time required to reach the 90% of the total Δ%T for the colored (t_c) and bleached steps (t_b).

  The measurement procedure consists in registering the transmittance changes at a certain wavelength, usually λ_{max} detected in the UV-vis spectra, *versus* time while square-wave potential-steps between bleached and colored state are being applied.

  It is worth to mention that the transmittance change can equally be calculated from the $\%T_b$ and $\%T_c$ obtained by this procedure, providing that the λ_{max} is known beforehand.

- Color efficiencies: the color efficiency (CE or η) is a measure of power efficiency or a quantification of the electrochemically formed color and is expressed in $cm^2\ C^{-1}$. It is defined as the change in optical density (ΔOD) during the redox process at a given wavelength divided by injected/ejected charge as a function of the electrode area (Q_d), by means of the following expressions (Eq. 2.5 – 2.7 where Q = injected/ejected charge (in C) for the colored and bleached processes and A = device area (in cm^2).[28]

$$\eta = CE = \frac{\Delta OD}{Q_d} \qquad \text{(Eq. 2.5)}$$

Being

$$\Delta OD = \log \frac{T_b}{T_c} \qquad \text{(Eq. 2.6)}$$

$$Q_d = \frac{Q}{A} \qquad \text{(Eq. 2.7)}$$

The measurement process is usually carried out simultaneously with the switching times determination since the injected/ejected charge is calculated from the chronoamperometry registered while square-wave potential-steps between bleached and colored state are being applied (Integrated area for the required switching time).

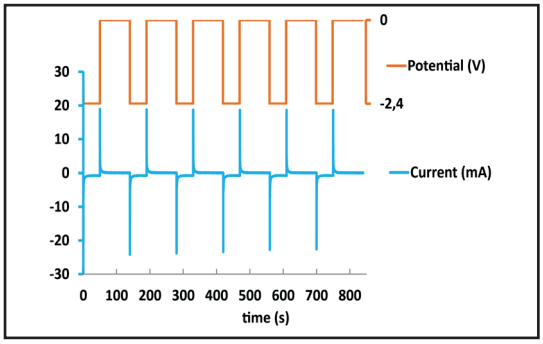

Figure 2.3. Color efficiency and switching time simultaneous measurement procedure.

- Write-erase efficiency: this parameter which asses the reversibility of the coloration and bleaching process is defined as the percentage of the formed coloration which can be reversibly bleached electrochemically. ECDs must exhibit white-erase efficiencies of about 100%.[21]
- Cyclability: An experimental procedure to estimate the durability of one ECD consist in measuring the number of write-erase cycles (i.e. registering %T *vs* time at the λ_{max}) to which one ECD can be exposed without showing significant signs of degradation, although a 50% deterioration may be tolerable in some applications (e.g., displays).[21] This parameter termed as "cycle life" must include cycles of equal or greater duration than the switching time, even though it is not always meet in all procedures reported in the literature.

2.4.2. Quantification of color

One important parameter while talking about the electrochromic properties of any EC systems is the developed coloration during the redox process. The description of a color or the comparison of different colored states is relatively difficult due to the subjective nature of the color.[29]

The objective measure of color absorption provided by the spectra of visible region, does not offer a clear intuition into the influence on the human eye subjective perception. Colorimetry, on the contrary, measures the human eye's sensitivity to light across the visible region while providing a more accurate way to describe color.[30]

Any color can be defined and quantified using the three attributes which are the hue (wavelength associated with the color), the saturation (relative levels of white and/or black) and luminance (the brightness of the color or how light or dark a color is). These three attributes must be described numerically in a given color system.[29]

For accurate calculation CIE (Commission Internationale de l'Eclairage) has established several color spaces expressed in terms of XYZ tristimulus concept, based on the three-component theory of color vision (blue, green and red).[29] Some of the most commonly used color spaces are the CIE 1931 xyY and the CIE 1976 $L^*a^*b^*$ (also known as CIELAB).

- CIE 1931 xyY

Based on X, Y and Z tristimulus values (from 0 to 100), x and y color coordinates of the CIE 1931 xyY color space also named 2º Standard Observer, are calculated using the following expressions (Eq. 2.8 and 2.9) while Y component corresponds to the brightness or luminance of the color (luminance of the sample / luminance of the background or perfect transmitter), usually expressed as a percentage.[29]

$$x = \frac{X}{X+Y+Z} \quad \text{(Eq. 2.8)}$$

$$y = \frac{Y}{X+Y+Z} \quad \text{(Eq. 2.9)}$$

When using this color space, x represents the red-to-blue ratio of the signal whereas y measures the green-to-blue ratio.[30] Color coordinates $x = y = 0.33$ are considered to correspond to perfect neutral color which translates into white when Y = 100, gray when Y = 50 and black when Y = 0.[31]

- CIE 1976 $L^*a^*b^*$

The main advantage of $L^*a^*b^*$ color space is that equal perceived color differences are represented by equal distances on the graph, thus, allowing the accurate representation and calculation of color differences. These color coordinates are calculated correlating the triestimulus values of the sample (X, Y and Z) with the tristimulus values of a perfect reflecting diffuser (Xn, Yn and Zn standard illuminant[30]) through the following expressions (Eq. 2.10 – 2.12).

$$L^* = 116 \times \left(\frac{Y}{Y_n}\right)^{1/3} - 16 \quad \text{(Eq. 2.10)}$$

$$a^* = 500 \times \left[\left(\frac{X}{X_n}\right)^{1/3} - \left(\frac{Y}{Y_n}\right)^{1/3}\right] \quad \text{(Eq. 2.11)}$$

$$b^* = 200 \times \left[\left(\frac{Y}{Y_n}\right)^{1/3} - \left(\frac{Z}{Z_n}\right)^{1/3}\right] \quad \text{(Eq. 2.12)}$$

CIE 1976 color space represents the relation between green (- a^*) and red (+ a^*), and between blue (- b^*) and yellow (+ b^*), while L^* value indicates the lightness. The values of a^* and b^* increase with the saturation of color, whereas the 0, 0 value corresponds to an ideal achromatic sample (i.e., neutral colors such as gray or black).

Although color is a three-dimensional phenomenon, color spaces are usually represented graphically separated into two attributes, chromaticity and luminance, in such a way that can be more easily visualized in a two-dimensional space.[29] Thus, chromaticity which represents the hue and saturation are represented in a two-dimensional space, while the luminance which describes the brightness of the color is set at a fixed value (e.g., xy chromaticity diagrams).

The color of the ECDs developed herein has been evaluated through $L^*a^*b^*$ (1976) and xyY (1931) color coordinates obtained by both spectrophotometric and colorimetric method following the procedures described in section 2.6.

2.5. Fabrication of ECDs

Despite the wide variety of device architectures reported in the last decades, the vast majority of ECDs used so far exhibit two-electrode configuration, that is to say one working electrode (WE) and one counter electrode (CE). The main drawback of this device configuration is that it does not allow a consistent electrochemical characterization due to the lack of a reference electrode (RE). With the aim of overcoming this weakness, a new configuration of three-electrode ECD has been designed in this thesis to correlate the electrochemical behavior with the provided colorations. Thus, this three-electrode configuration provided with a pseudoreference electrode enables the in situ spectroelectrochemical study of the EC systems reported herein. It is worth noting that unlike the little reported three-electrode ECDs which were based on stacked electrodes and separating insulating layers,[32] the three-electrode ECD architectures developed herein do not require additional insulating layers, avoiding in this way the unwanted loss of transparency and significant changes in the device thickness which the former may cause.

The fabrication process followed for the device assembly of both two-electrode and three-electrode device configurations is described below.

2.5.1. Two-electrode (2-E) ECD fabrication:

In the 2-E configuration, the device comprise one WE substrate connected to the WE wire of the potentiostat, whereas the CE of the ECD is connected to the reference and counter electrodes' wires of the potentiostat shorted together. This 2-E device configuration has been used in both all-in-one and layered ECDs as explained below.

- All-in-one ECDs in 2-E configuration

  When using all-in-one device configuration (Figure 1.2 shown in chapter 1) with *gel EC mixtures*, the EC gel was spread on the FTO or ITO-coated side of one of the substrates provided with a 220 μm thick and 1-2 mm wide double-side adhesive tape frame used as spacer placed along the whole perimeter. Then it was covered with the other electrode substrate, applying a light pressure, and both electrodes were clipped using paper clip clamps. The EC gel flows and adapts to the shape of the substrates, providing uniform films with excellent contact to both electrodes. Interestingly, if the gel was left to settle on its own for a few minutes before covering with the second electrode, a completely bubble-free device could be obtained.

  In the case of *liquid EC mixtures* employed for comparison purposes or in optimization stages, the electrochromic formulations were introduced in a previously assembled functional cell by surface capillarity. To this end, two electrode substrates (i.e., FTO/glass, ITO/glass or ITO/PET) were joined through a doubled-side adhesive tape (220 μm thick and 1-2 mm wide) placed along the whole perimeter, but leaving two small openings (1 mm wide) placed in opposite corners. After introducing the liquid EC mixture into the internal

spacing of the sandwich structure by surface capillarity, the holes were sealed with transparent silicone (Loctite 595).

- Layered ECDs in 2-E configuration

  When using layered electrodes (Figure 1.3 shown in chapter 1), commercially available titanium dioxide dispersion (transparent Ti-Nanoxide T from Solaronix), was spread on FTO-coated side of one of the substrates using a doctor-blade method with a suitable applicator (from 12 to 200 μm groove depths). The substrate was previously masked by a Scotch tape covering the area reserved for the electrical connection. Following drying at room temperature for 30 min and at 90 ºC for 1h, the films were sintered at 450 ºC for 3h using a heating rate of 10 ºC/min, and the resulting transparent nanostrutured TiO_2 films were conveniently modified by anchoring the viologen as it will be descried in the corresponding chapters. Afterward, 220 μm thick and 1-2 mm wide double-side adhesive tape was placed around the perimeter of the viologen-modified TiO_2 film, and the following steps required for device assembling were similar to those indicated for all-in-one device configuration, but replacing the EC mixtures (i.e., gel or liquid EC mixture) by the electrolyte exempted from any EC materials instead (i.e., gel or liquid electrolyte).

2.5.2. Three-electrode (3-E) ECD fabrication:

This device architecture incorporates Ag/Ag^+ redox couple based pseudo-reference electrode deposited on one discrete area of the WE substrate, but insulated from it by laser scribing of the TCO layer. Equally, this 3-E device configuration can be employed in both all-in-one and layered ECDs, and using gel and liquid EC mixtures or electrolytes.

- All-in-one ECDs in 3-E configuration

  The ECDs were prepared as follows: 5 cm x 2.5 cm FTO or ITO-coated glass substrate was electrically insulated by laser scribing into two sections, having an approximate active area of 5 cm x 2 cm and 5 cm x 0.5 cm. AgCl ink, purchased from Acheson (Electrodag PF-410), was employed to draw a layer on the 5 cm x 0.5 cm section which was employed as pseudo-reference electrode after being dried at 90 °C (RE). The wider section of the same substrate was employed as a working electrode (WE), while other FTO orITO-coated glass substrate (without any laser treatment) was used as counter electrode (CE). Afterward, 220 μm thick and 1-2 mm wide double-side adhesive tape was placed around the perimeter of the WE-RE substrate and the following steps required for device assembling were similar to those indicated for 2-E electrochromic devices.

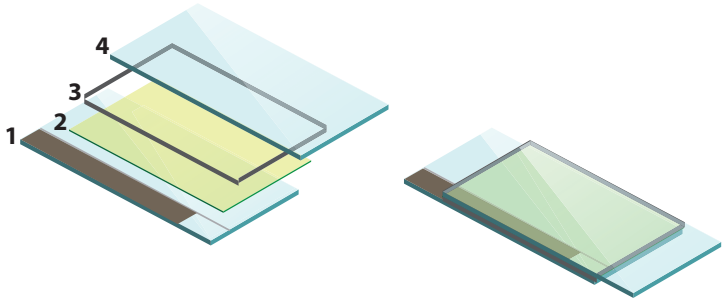

Figure 2.4. Schematic illustration of all-in-one ECDs in 3-E configuration and components: 1) pseudoreference electrode on TCO/glass; 2) EC mixture; 3) spacers; 4) TCO/glass.

- Layered ECDs in 3-E configuration

  The ECDs were prepared as follows: 5 cm x 3 cm FTO or ITO-coated glass substrate was electrically insulated into two sections of 5 cm x 2.5 cm and 5 cm x 0.5 cm approximately, through laser scribing. The substrate was masked by a Scotch tape covering the area reserved for the electrical connection and the whole small area

of 5 cm x 0.5 cm of the substrate. Commercially available titanium dioxide dispersion (transparent Ti-Nanoxide T from Solaronix) was then spread by doctor-blade technique using a wire wound rod of 100 μm groove depth. After drying at room temperature for 30 min and at 90 °C for 1h, the films were sintered at 450 °C for 3h using a heating rate of 10 °C/min. Transparent nanostrutured TiO_2 films deposited on the wider section of the substrates employed as a WEs, were conveniently modified by anchoring the viologen. Afterward, AgCl layer was drawn on the 5 cm x 0.5 cm section using AgCl ink (Electrodag PF-410 from Acheson) and dried at 50 °C for at least 5 h, before being used as a pseudo-reference electrode. Further steps of the assembling procedure were analogous to those described for the 2-E ECDs.

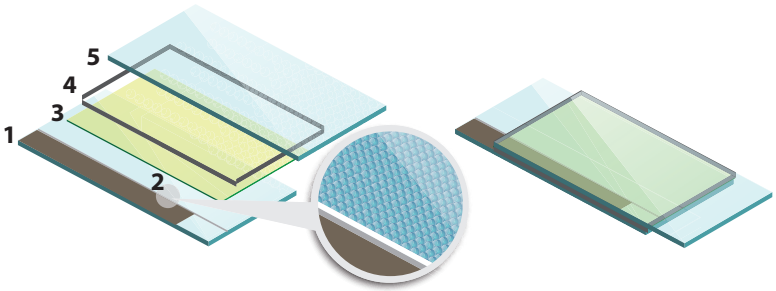

Figure 2.5. Schematic illustration of layered ECDs in 3-E configuration and components: 1) pseudoreference electrode on TCO/glass; 2) nanostructured layer on TCO/glass; 3) electrolyte ; 4) spacers; 5) TCO/glass.

2.6. Methods and instruments

The instrumental employed to characteriz The ^{1}H, ^{13}C and ^{31}P NMR spectra were measured by means of a Bruker 500MHz spectrometer in D_2O, DMSO-*d6* or $CDCl_3$ using tetramethylsilane as internal reference.

- Fourier transform infrared spectra (FT-IR) of the pure solids were obtained by Attenuated Total Reflectance (ATR) technique with a 4100LE FTIR from Jasco.
- Anion content was determined by Ion Chromatography system (IC) from Metrohm (2.850.2030 model), provided by 850 professional IC2 conductivity detector. The column (Metrosep A sup 7 250/4.0) was thermostated at 40 ºC and sodium carbonate anhydrous (0.382 g L^{-1}; 0.7 mL min^{-1}; 9.84 MPa) was employed as eluent.
- Elemental analysis of C, H and N was carried out with LECO CHNS microanalyzer by subjecting the sample to combustion at 1100ºC under oxygen atmosphere.

Equipment required for the fabrication of layered electrodes and ECDs is indicated below.

- Nanostructured TiO_2 films were obtained by doctor-blade technique using 1137 equipment from Sheen provided with wire wound rods and quadrangular applicators of different groove depths (from 12 to 200 μm).
- The sintering treatments were carried out in a Carbolite CWF 11/23 chamber furnace.
- FTO and ITO-etching was made by laser scribing with a Rofin Powerline E-Air 25 at 1064 nm and 25W, using a frequency of 20 kHz and a speed of 150 mm/s for the former and a frequency of 10 kHz and a speed of 700 mm/s for the latter.
- ECDs used for cycling performance were sealed with colorless UV-curing adhesive (NOA from Norland Products Inc) covering the active area with a black mask using a TECHNIGRAF AKTIPRINT T/A 40-2 UV-curing tunnel.

The electrodes and nanostructured layers were analyzed by the following techniques.

- Micrographs of the bare electrodes were taken through a Leica DM4000M optical microscope fitted with a Leica camera DFC420C (Leica Microsystems).
- The thicknesses of the nanostructured films were examined in cross-sectional view using a ULTRA plus ZEISS field emission scanning electron microscope (FESEM) in collaboration with Eneko Azaceta (IK4-CIDETEC).
- Powder X-ray diffraction measurements were performed in a 2Θ range from 10 to 7 using a Bruker D8 advance diffractometer with CuKα radiation (λ = 1.5406 Å), in collaboration with Ivet Kosta (IK4-CIDETEC). The crystalline phases of TiO_2 were identified by using the NIST M&A collection code A 50867 ST1243 (pattern 03-065-5714).

Gel formulations developed herein were studied using the following equipments.

- Rheological testing was carried out in a TA instruments AR2000ex rheometer using a 20 mm plate-plate geometry, in collaboration with Alaitz Ruiz de Luzuriaga (IK4-CIDETEC). A 5% strain step was applied and storage and loss modulus (G´and G´´, Pa) were monitored at room temperature.
- Conductivity values were monitored in a Crison CM35+ conductimeter over a temperature ramp from 20 to 90 ºC.

The assessment of the ECDs was evaluated by the techniques and instrumental indicated below.

- UV-Vis spectra obtained in transmission/absorption mode and the transmittance changes registered at a certain wavelength vs time

were acquired on a Jasco V-570 spectrophotometer using air as the background. The measurements were obtained using a films holder accessory for solid samples, while the devices were connected to Biologic MPG potentiostat-galvanostat as a direct current source.

- The chronoamperometric and cyclic voltammetric (30 mV/s) studies were carried out using Biologic MPG potentiostat-galvanostat.
- Cyclability assays were equally performed with a Biologic MPG potentiostat-galvanostat with ECDs previously sealed.
- Color of the ECDs developed herein has been evaluated through $L^*a^*b^*$ (1976) and xyY (1931) color coordinates obtained by spectrophotometric method developed by R. J. Mortimer and T. S. Varley.[30, 33] Thus, absorbance/transmittance-wavelength data from visible region spectra is taken as input and using a Microsoft® Excel® spreadsheet luminance and chromaticity coordinates are obtained as output.[30] To this end, a computer spreadsheet employs the so-called color matching functions (numerical data describing the chromatic responses of the three types of cone in the human eye) to calculate the tristimulus values of the sample X, Y and Z, and these data are transformed by the microcomputer to values of color coordinates.[30]

  When employing colorimetric method for comparative purposes, the $L^*a^*b^*$ color coordinates were acquired using a spectroradiometer Konika Minolta CS-1000A, employing in both cases a D65 illumination source.

  Color swatches representing the color interpretation of the registered color coordinates included to ease their elucidation were acquired from the $L^*a^*b^*$ color coordinates through a color converter website.[34]

- The photographs of the ECDs were acquired using Canon IXUS 105 camera without the employment of flash, using a focal distance of 5

mm, maximum opening of 3 and exposition time between 30-50 s^{-1}, while the ECDs were being lit with fluorescent light source (Phillips TL-D 80 18W/840).

2.7. References

[1] P. M. S. Monk, *The viologens: physicochemical properties, synthesis, and applications of the salts of 4,4'-bipyridine*, Wiley, **1998**.

[2] C. L. Bird, A. T. Kuhn, *Chem. Soc. Rev.* **1981**, *10*, 49-82.

[3] a) J.-H. Ryu, Y.-H. Lee, K.-D. Suh, *J. Appl. Polym. Sci.* **2008**, *107*, 102-108; b) J.-H. Ryu, J.-H. Lee, S.-J. Han, K.-D. Suh, *Colloids and Surfaces A: Physicochemical and Engineering Aspects* **2008**, *315*, 31-37.

[4] R. J. Mortimer, *Annu. Rev. Mater. Res.* **2011**, *41*, 241-268.

[5] V. de Zea Bermudez, P. P. de Almeida, J. F. Seita, *J. Chem. Educ.* **1998**, *75*, 1410.

[6] G. A. Hurst, M. Bella, C. G. Salzmann, *J. Chem. Educ.* **2015**, *92*, 940-945.

[7] a) D. A. Katz, *J. Chem. Educ.* **1994**, *71*, 891; b) D. A. Katz., *Vol. Jan. 18, 2017*, http://www.chymist.com/PVA%20Slime.pdf, **2005**.

[8] *Vol. Jan. 18, 2017*, RSC Advancing the Chemical Sciences, http://www.rsc.org/learn-chemistry/resource/res00000756/.

[9] a) E. Pezron, L. Leibler, A. Ricard, F. Lafuma, R. Audebert, *Macromolecules* **1989**, *22*, 1169-1174; b)T. Inoue, K. Osaki, *Rheologica Acta* **1993**, *32*, 550-555.

[10] T. Sato, Y. Tsujii, T. Fukuda, T. Miyamoto, *Macromolecules* **1992**, *25*, 5970-5973.

[11] H. Ochiai, S. Fukushima, M. Fujikawa, H. Yamamura, *Polym J* **1976**, *8*, 131-133.

[12] a) G. Wulff, *Pure Appl. Chem.* **1982**, *54*, 2093-2102; b) G. Keita, A. Ricard, R. Audebert, E. Pezron, L. Leibler, *Polymer* **1995**, *36*, 49-54.

[13] A. Koike, N. Nemoto, T. Inoue, K. Osaki, *Macromolecules* **1995**, *28*, 2339-2344.

[14] a) C. Y. Chen, J. Y. Guo, T. L. Yu, S. C. Wu, *Journal of Polymer Research* **1998**, *5*, 67-76; b) H. Ochiai, Y. Fujino, Y. Tadokoro, I. Murakami, *Polym J* **1982**, *14*, 423-426.

[15] a) H. Kurokawa, M. Shibayama, T. Ishimaru, S. Nomura, W.-l. Wu, *Polymer* **1992**, *33*, 2182-2188; b) H.-L. Lin, Y.-F. Liu, T. L. Yu, W.-H. Liu, S.-P. Rwei, *Polymer* **2005**, *46*, 5541-5549; c) E. T. Wise, S. G. Weber, *Macromolecules* **1995**, *28*, 8321-8327.

[16] a) R. F. Nickerson, *J. Appl. Polym. Sci.* **1971**, *15*, 111-116; b) E. Z. Casassa, A. M. Sarquis, C. H. Van Dyke, *J. Chem. Educ.* **1986**, *63*, 57.

[17] M. Van Duin, J. A. Peters, A. P. G. Kieboom, H. Van Bekkum, *Tetrahedron* **1985**, *41*, 3411-3421.

[18] a) K. W. McLaughlin, N. K. Wyffels, A. B. Jentz, M. V. Keenan, *J. Chem. Educ.* **1997**, *74*, 97; b) R. K. Schultz, R. R. Myers, *Macromolecules* **1969**, *2*, 281-285.

[19] *Vol. Jan. 18, 2017*, https://projects.ncsu.edu/project/chemistrydemos/Organic/Slime.pdf.

[20] G. G. Stroebel, J. A. Whitesell, R. M. Kriegel, *J. Chem. Educ.* **1993**, *70*, 893.

[21] P. M. S. Monk, R. J. Mortimer, D. R. Rosseinsky, *Electrochromism and Electrochromic Devices: introduction to electrochromism*, Cambridge University Press, United States of America **2007**.

[22] N. Garino, S. Zanarini, S. Bodoardo, J. R. Nair, S. Pereira, L. Pereira, R. Martins, E. Fortunato, N. Penazzi, *International Journal of Electrochemistry* **2013**, *2013*, 10.

[23] a) R. Cinnsealach, G. Boschloo, S. Nagaraja Rao, D. Fitzmaurice, *Sol. Energy Mater. Sol. Cells* **1998**, *55*, 215-223; b) D. Cummins, G. Boschloo, M. Ryan, D. Corr, S. N. Rao, D. Fitzmaurice, *J. Phys. Chem. B* **2000**, *104*, 11449-11459; c) J.-H. Ryu, D.-O. Shin, K.-D. Suh, *J. Polym. Sci., Part A: Polym. Chem.* **2005**, *43*, 6562-6572; d) S. Y. Choi, M. Mamak, N. Coombs, N. Chopra, G. A. Ozin, *Nano Letters* **2004**, *4*, 1231-1235.

[24] H. Shin, Y. Kim, T. Bhuvana, J. Lee, X. Yang, C. Park, E. Kim, *ACS Appl. Mater. Interfaces* **2012**, *4*, 185-191.

[25] C. S. Ah, J. Song, S. M. Cho, T.-Y. Kim, H. N. Kim, J. Y. Oh, H. Y. Chu, H. Ryu, *Bull. Korean Chem. Soc.* **2015**, *36*, 548-552.

[26] a) W. H. Nguyen, C. J. Barile, M. D. McGehee, *The Journal of Physical Chemistry C* **2016**, *120*, 26336-26341; b) D. Weng, Y. Shi, J. Zheng, C. Xu, *Organic Electronics* **2016**, *34*, 139-145.

[27] a) E. Unur, P. M. Beaujuge, S. Ellinger, J.-H. Jung, J. R. Reynolds, *Chem. Mater.* **2009**, *21*, 5145-5153; b) B. Hu, X. Lv, J. Sun, G. Bian, M. Ouyang, Z. Fu, P. Wang, C. Zhang, *Organic Electronics* **2013**, *14*, 1521-1530.

[28] a) K. Bange, T. Gambke, *Adv. Mater.* **1990**, *2*, 10-16; b) S. A. Sapp, G. A. Sotzing, J. R. Reynolds, *Chem. Mater.* **1998**, *10*, 2101-2108; c) B. B. Çarbaş, A. Kivrak, A. M. Önal, *Electrochim. Acta* **2011**, *58*, 223-230.

[29] P. M. S. Monk, R. J. Mortimer, D. R. Rosseinsky, *Electrochromism and Electrochromic Devices: Optical effects and quantification of colour*, Cambridge University Press, United States of America **2007**.

[30] R. J. Mortimer, T. S. Varley, *Displays* **2011**, *32*, 35-44.

[31] D. Barrios Puerto, Universidad Carlos III de Madrid **2012**.

[32] a) S. Taunier, C. Guery, J. M. Tarascon, *Electrochim. Acta* **1999**, *44*, 3219-3225; b) C. Xu, L. Liu, S. E. Legenski, D. Ning, M. Taya, *J. Mater. Res.* **2004**, *19*, 2072-2080; cD) . A. A. de Mello, M. R. S. Oliveira, L. C. S. de Oliveira, S. C. de Oliveira, *Sol. Energy Mater. Sol. Cells* **2012**, *103*, 17-24; d) S. C. de Oliveira, L. C. de Morais, A. A. da Silva Curvelo, R. M. Torresib, *J. Electrochem. Soc.* **2003**, *150*, E578-E583.

[33] R. J. Mortimer, T. S. Varley, *Sol. Energy Mater. Sol. Cells* **2012**, *99*, 213-220.

[34] *Vol. January 5, 2017*, http://www.workwithcolor.com/color-converter-01.htm.

CHAPTER 3

PLASTIC ELECTROCHROMIC DEVICES BASED ON VIOLOGEN-MODIFIED TiO_2 FILMS PREPARED AT LOW TEMPERATURE

3.1. Introduction

A great deal of research has been conducted in the last decades on generating ECDs of diverse architectures which may meet the requirements for commercial applications to boost market entry. To expand the potential applicability of the EC technology, new systems compatible with the maximum type of transparent materials (i.e., plastic or glass), adaptable to any surface (i.e., flexible) and suitable for up-scaling production may play a crucial role in the implementation of new EC products. However, the development of high-performance ECDs using flexible plastic substrates exhibits some incompatibilities which remain to be overcome.

As explained in the chapter 1, the viologens can be incorporated in ECDs either dissolved in the electrolyte (all-in-one configuration),[1] or adsorbed on the electrode surface (layered configuration). Following the latter approach, when a monolayer of viologen is adsorbed on the surface of a flat conducting substrate, the resulting color change is very weak, hence not sufficient for practical applications.[2] This limitation can be overcome by adsorbing the viologen molecules on the surface of nanostructured metal oxide electrodes in order to get a high electro-chromophore loading due to the large surface area of the nanoparticles building up the film. Among the wide number of metal oxides used to prepare nanostructured electrodes (typically wide bandgap, n-type semiconductors), nanocrystalline TiO_2 electrodes are especially suitable due to a series of intrinsic properties such as high transparency in the visible light range, ultra-fast electron transfer through the conduction band, large surface area and strong binding affinity towards certain organic groups enabling surface modification.[3]

Several electrochromic device architectures employing viologen-modified nanostructured TiO_2 on SnO_2-based transparent conductive oxide (TCO) electrodes have been described in the literature.[4] The conduction band position of TiO_2 is higher than that of the TCOs and slightly lower than the first reduction potential of the viologens.[3b] This leads to a fast interfacial electron transfer between the TiO_2 nanoparticles and the viologen, and consequently an efficient reduction of the viologens upon negative polarization of the nanostructured TiO_2 electrode, resulting in a deep coloration. Being the electro-chromophore adsorbed at the surface of the nanostructured TiO_2 film, the rate of reduction of the viologen is not limited by its rate of diffusion towards the electrode as occurring in EC systems based on viologens dissolved in the electrolyte (all-in-one configuration). Consequently, this type of electrochromic devices is characterized by a fast transition between the bleached and colored states (i.e., 1-3 seconds [4b, 4j] or even lower[5]) as well as low power consumption.[5]

To attach the viologens to the TiO_2 nanocrystals, viologens provided with diverse anchoring groups have been studied such as carboxylic acids[6] including benzoic acid[4j] or salicylic acid,[4j, 6a, 7] or the most widely employed phosphonic acid.[4a-i] The latter has been proven to provide stronger chemisorption in comparison to the others reported,[4j] even considered irreversible toward nanocrystalline TiO_2-coated electrodes. [4a] However, anchoring moiety most widely employed when using it, the ethylphosphonic acid, entails grafting times as large as 24h[3b, 4b, 4f, 4g, 5] to ensure full attachment of the viologen and therefore suitable levels of coloration. Apart from the huge time consumption which hinders the industrialization, these procedures may damage some electrode substrates (i.e., ITO) due to the acid conditions to which it is exposed, habitually 20 mmol L^{-1} water solution of viologen functionalized with two phosphonic acid pendants, [3c, 4b, 4g, 5] reaching pH values between 1 – 2. Therefore, the development of viologens which exhibit chemisorption as strong as

the latter, but with more rapid binding process towards nanostructured layer and consequently lower grafting times, are necessary to accomplish EC systems compatible with plastic substrates (i.e., ITO/PET) and with any fabrication process required for up-scaling (e.g., coating or printing technology such as dip-coating or ink-jet including roll-to-roll processing, among others).

On the other hand, the preparation of the nanocrystalline electrodes usually involves thermal sintering treatments (above 400 ºC) [3b, 4a-c, 4f, 5] in order to ensure sufficient ohmic contact between the TiO_2 nanoparticles, and an open porous network with extremely high specific surface which allows the adsorption of great amount of electro-chromophores. However, this sintering process is not compatible with many substrates including plastics, limiting the use of this technology to thermally stable substrates such as glass. Some low-temperature approaches reported based on nanostructured TiO_2 (i.e., chemical[8] or UV-sintering[9]) or on alternative supporting materials (e.g. polymeric microspheres[10]) showed some limitations such as complexity, poor switching and/or lack of transparency, not allowing their use in applications that require high transparency such as smart windows, lenses or mirrors. Therefore, the finding of transparent nanostructured layers processed at low temperature suitable for anchoring functionalized viologens is also required.

3.1.1. Objective

The main goal of the research study described in this chapter was to synthetize new viologen conveniently functionalized with an anchoring moiety specifically designed to offer fast grafting onto the TiO_2 surface avoiding delamination of the TCO on plastic substrates while providing colorless-to-blue switching.

The compatibility of this viologen with transparent nanostructured TiO_2 films prepared at low temperature and its successful integration in flexible

plastic electrochromic devices (ECDs) was also a challenge. To this end, the finding of suitable nanostructured TiO_2 films processed at low temperature avoiding sintering stage while exhibiting adequate high surface area to ensure the bonding of the viologen was also a requisite.

The optimization of the plastic device performance involved the study of different parameters such as the thickness of the nanostructured layer, the grafting conditions of the viologen, the composition of the electrolyte (i.e., content of redox pair) or even their incorporation in dual-type ECDs.

Going a step further, the viability of scaling-up the preparation of the viologen-TiO_2 films on ITO/PET and their subsequent incorporation in ECDs was also crucial to demonstrate the suitability of the present technology for the production of large-area (i.e., 40 cm x 30 cm) plastic ECDs.

3.2. Material and methods

3.2.1. Materials

4,4'-dipyridyl (98%), diethyl 2-bromoethylphosphonate (97%), *a*,*a*'-dichloro-p-xylene (98%), triethyl phosphite (98%), lithium perchlorate trihydrate and hydroquinone (HQ) (≥ 99%) were provided by Aldrich. All these reagents were used without further purification. HCl (37%) and organic solvents (toluene, hexane, chloroform, 2-propanol, acetone, ethanol) were purchased from Scharlab and used as received, while g-butyrolactone was purchased from Acros Organics and degassed by bubbling Ar for 15 min prior to use. Ultra-pure silica gel (40-60 μm, 60A) was supplied by Acros Organics. Devices were fabricated on FTO/glass electrode substrates (Pilkington TEC glass™ providing a sheet resistance of 12-14 Ohm/sq.) and on ITO coated-PET films (EASTMAN OC50 providing a sheet resistance of 50 Ohm/sq.). The substrates were rinsed

subsequently with water, acetone and 2-propanol and dried with nitrogen stream prior to use.

3.2.1.1. Synthesis and characterization of viologens

Synthesis of Bis(2-phosphonoethyl)-4,4'-bipyridilium dichloride ***[Et-PO_3H_2-Vio]***

Viologen **[Et-PO_3H_2-Vio]** was synthesized following the procedure described in the literature.[4b] 85% yield. ^{1}H NMR (D_2O, δ, ppm): 9.17 (d, 4H, *J* 6.89 Hz), 8.55 (d, 4H, *J* 6.73 Hz), 4.90 (m, 4H, $2CH_2N$), 2.43 (m, 4H, $2CH_2P$). ^{31}P NMR (D_2O, δ, ppm): 17.86. IR (bulk ATR): v (cm^{-1}) = 3018 (C-H), 2695-2400 (PO-H st), 2380-2135 (PO-H comb), 1631, 1552 (C=C, C=N), 1223-1172 (P=O st), 1093, 992, 966, 931 (P-OH st), 814 (*o*-phenylene H).

Synthesis of Bis(phosphonomethyl-4-benzyl)-4,4'-bipyridilium dichloride ***[Bn-PO_3H_2-Vio]***

Synthesis of diethyl(4-chloromethyl)benzylphosphonate **[I]**. Derivative **[I]** was obtained according to the method described in the literature.[11] Briefly, to a boiling solution of 5.3 g (0.03 mol) of a,a'-dichloro-p-xylene in 3 ml of toluene, 1.7 ml (0.01 mol) of triethyl phosphite was added dropwise within 1-1.5 h, stirring the reaction mixture at reflux for additional 0.5 h. The reaction mixture was evaporated under vacuum and the residue was chromatographed on column with 160 g of silica gel using as eluents hexane and hexane:chloroform (4:1, 2:1 and 1:1) to isolate the a,a'-dichloro-p-xylene and then a mixture of chloroform and 3% of 2-propanol to isolate 2.3 g of diethyl(4-chloromethyl)benzylphosphonate **[I]** (85% yield). ^{1}H NMR ($CDCl_3$, δ, ppm): 7.32 (m, 4H, C_6H_4), 4.57 (s, 2H, CH_2Cl), 4.02 (m, 4H, $2CH_2$), 3.14 (d, 2H, $2CH_2P$, *J* 21.7 Hz), 1.24 (t, 6H, $2CH_3$, *J* 7.05) (Figure 3.1).

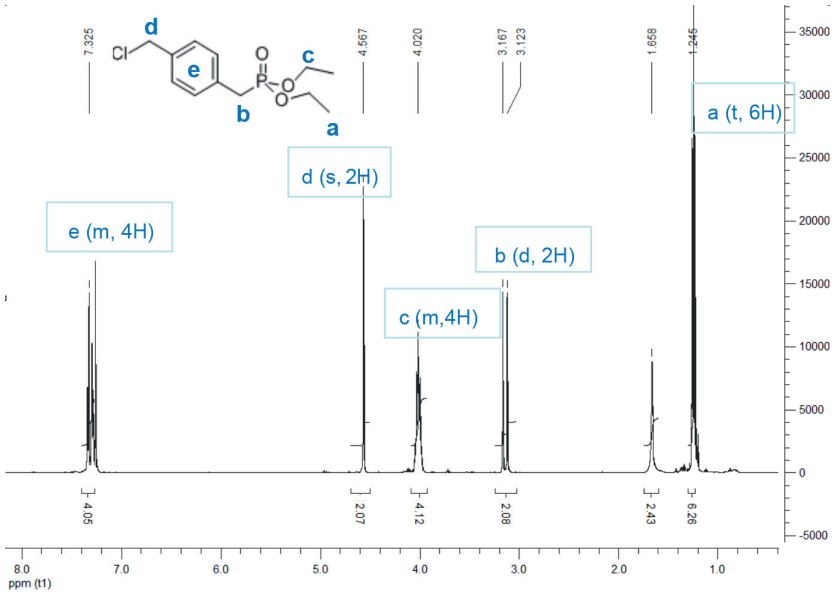

Figure 3.1: ^{1}H NMR spectra of intermediate diethyl(4-chloromethyl) benzylphosphonate **[I]**.

Synthesis of Bis(phosphonomethyl-4-benzyl)-4,4'-bipyridilium dichloride ***[Bn-PO$_3$H$_2$-Vio]***

To a stirred solution of 4,4'-dipyridyl (0.95 g, 0.006 mol) in ethanol, 3.74 g (0.013 mol) of **[I]** was added. The resulting solution was refluxed for 72 h and then allowed to cool. After addition of concentrated HCl, the mixture was refluxed for further 24 h. The reaction mixture was then concentrated and 2-propanol was added dropwise, stirred on ice for an hour and filtered. The solid was washed with 2-propanol and dried to give the bis(phosphonomethyl-4-benzyl)-4,4'-bipyridilium dichloride **[Bn-PO$_3$H$_2$-Vio]** (94% yield). Elemental analysis data: Anal. Calcd for $C_{26}H_{28}N_2O_6P_2Cl_2$: C, 52.27; H, 4.72; N, 4.69. Found: C, 49.80; H, 5.26; N,

4.83. ^{1}H NMR (D_2O, δ, ppm): 9.14 (d, 4H, J = 6.87 Hz), 8.50 (d, 4H, J = 6.84 Hz), 7.45 (m, 8H, $2C_6H_4$), 5.90 (s, 4H, $2CH_2N$) and 3.06 (d, 4H, $2CH_2P$, J = 20.8 Hz) (Figure 3.2). ^{13}C NMR (D_2O, δ, ppm): 152.96, 148.04, 140.45, 133.33, 132.51, 132.17, 129.64, 67.33 and 38.48 (Figure 3.3). ^{31}P NMR (D_2O, δ, ppm): 19.31 (Figure 3.4). IR (bulk ATR): v (cm^{-1}) = 3040 (C-H), 2800-2603 (PO-H st), 2263-2200 (PO-H comb), 1631, 1558 (C=C, C=N), 1207, 1150 (P=O st), 913 (P-OH st) and 830 (*o*-phenylene H).

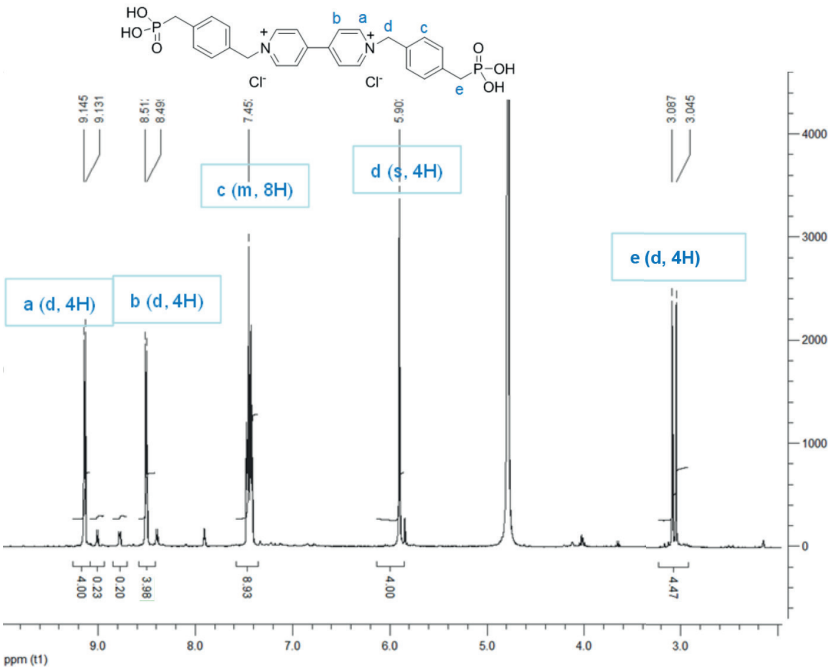

Figure 3.2. ^{1}H NMR spectra of **[Bn-PO_3H_2-Vio]**.

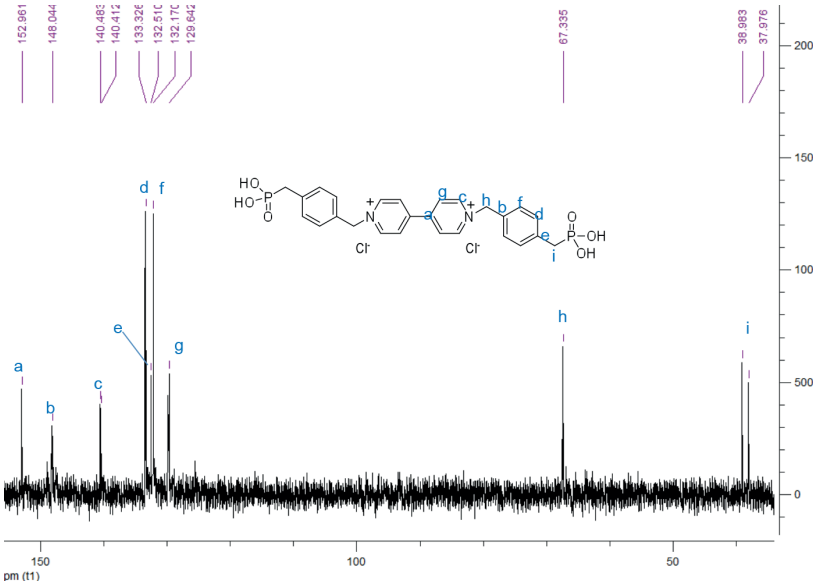

Figure 3.3: ^{13}C NMR spectra of [**Bn-PO$_3$H$_2$-Vio**].

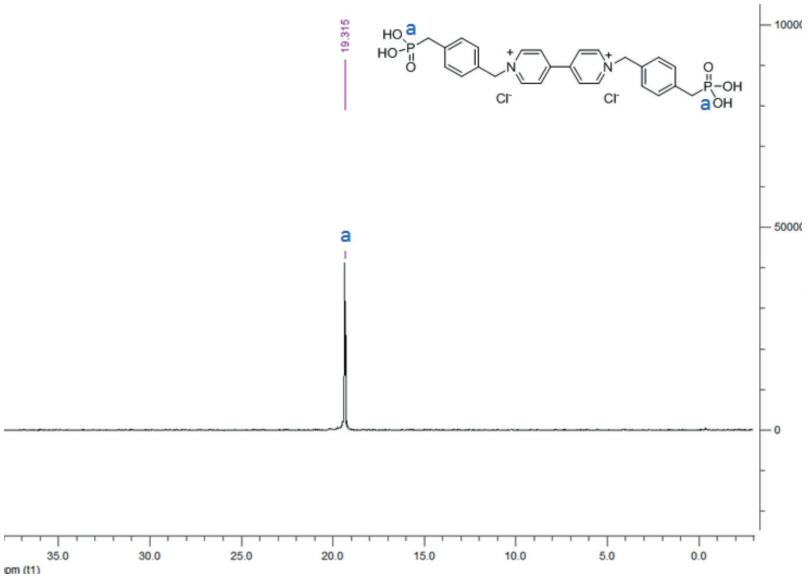

Figure 3.4: ^{31}P NMR spectra of [**Bn-PO$_3$H$_2$-Vio**].

3.2.2. Methods

3.2.2.1. Preparation of transparent, nanostructured TiO_2 electrodes

The nanostructured TiO_2 films processed at low temperature (i.e., ≤ 120 ºC) were provided by Fraunhofer Institute for Silicate Research (ISC). Small-size (i.e., 2.5 cm x 5 cm) films were obtained by dip-coating on FTO/glass and ITO/PET (using withdrawal rates from 4 to 30 cm/min (whereas large-scale TiO_2 films (40 cm x 30 cm) were obtained by slot-die coating technique with a roll-to-roll pilot coater on ITO/PET (using web speed of 0.5 m/min and dispersion feed from 3 to 12 ml/ min). The dispersions employed to this end (6 - 12 wt% of TiO_2 crystalline anatase phase) were equally formulated by Fraunhofer ISC according to previously reported sol-gel hydrothermal method,[12] while the size of the primary nanoparticles and thus the mesoporous structure of the electrode films were tailored by varying the autoclaving times and temperatures.

3.2.2.2. Preparation of viologen-modified TiO_2 electrodes

The surface of the particle-derived TiO_2 films was modified in IK4-CIDETEC by grafting the viologen according to the following procedure. The TiO_2-coated FTO/glass substrates (5 cm x 2.5 cm) were placed in a vessel containing a 20 mmol L^{-1} solution of bis(2-phosphonoethyl)-4,4'-bipyridilium dichloride **[Et-PO_3H_2-Vio]** in water. After 48 h, the resulting viologen-modified TiO_2/FTO/glass electrodes were removed from the vessel, subsequently rinsed with water and ethanol and then dried overnight at 50 ºC under vacuum. The same procedure was followed for the modification with bis(phosphonomethyl-4-benzyl)-4,4'-bipyridilium dichloride **[Bn-PO_3H_2-Vio]** with the concentration of the solution being 5 mmol L^{-1} and the immersion time 20 h.

Small-area (5 cm x 2.5 cm) TiO_2-coated ITO/PET substrates were attached to glass substrates by adhesive tape, with the TiO_2 film outwards-faced, and then placed in a vessel containing 5 mmol L^{-1} solution of **[Bn-PO_3H_2-Vio]**, following the same procedure described above, but with variable immersion times (0.25, 0.5, 1, 3, 5 and 20 h).

Large-area (40 cm x 30 cm) TiO_2-coated ITO/PET substrates were placed for 30 min in a suitable vessel containing 2.5 L of 5 mmol L^{-1} **[Bn-PO_3H_2-Vio]** water-solution. The solution was then removed from the vessel and the film subsequently washed with water and ethanol and dried at 60°C overnight.

3.2.2.3. Preparation of Prussian Blue-coated ITO/PET electrodes

Prussian Blue (PB) coated ITO/PET substrates used as counter electrode in the "dual-type" ECDs were provided by Fraunhofer ISC and obtained by electrodeposition from $K_3Fe(CN)_6$ and $FeCl_3$ 6 H_2O water solutions on ITO/PET (WE) using carbon as a CE and Calomel as a RE. The final electrodes provided a charge capacities between 2.0 and 3.5 mC cm^{-2}.

3.2.2.4. Composition of electrolytes

Liquid electrolyte consisted of $LiClO_4$ (0.2 mol L^{-1}) and suitable contents of hydroquinone redox promoter (from 0 to 0.0075 mol L^{-1}) in g-butyrolactone.

Solid electrolyte employed in the large-scale ECDs provided by IREQ – Institute de Recherche d'Hydro-Québec was based on an irreversible cross-linked polymer cured by UV-radiation after the assembly process. The latter consisted of 4 branches pre-polymer with cross-mixed poly(ethylene-propylene)oxide chains having terminal acrylate groups, lithium bis(trifluoromethylsulfonyl)imide salt (LiTFSI) and a commercial photo-initiator.

3.2.2.5. Fabrication of electrochromic devices

Functional cells (5 cm x 2.5 cm) comprising a viologen-modified TiO_2-layer deposited on FTO/glass or ITO/PET (working electrode) and a bare electrode (FTO/glass or ITO/PET substrates, respectively employed as counter electrode), were assembled as described in the chapter 2 section 2.5.1. for two-electrode ECD using liquid electrolyte.

In a second approach wherein PB-coated ITO/PET substrates were employed as counter electrodes in the "dual-type" ECDs, assembly process was similar to that mentioned above, using hydroquinone-free electrolyte, instead.

The large-area devices comprising viologen-modified TiO_2-coated ITO/PET (WE), PB-coated ITO/PET (CE), and solid electrolyte were assembled by IREQ with a homemade laminator rubber roller followed by sealing of the thus obtained ECDs with an adhesive tape along the whole perimeter.

3.3. Results and discussion

Mesoporous TiO_2 films deposited on both rigid FTO/glass and flexible ITO/PET substrates entailing a low temperature heat treatment (max. 120 °C) were provided by Fraunhofer ISC. These films of anatase crystalline structure as confirmed in published work,[13] exhibited high transparency (i.e., $\%T_{\lambda = 600nm}$ = 85 – 90 %).

To assess the suitability of these low-temperature processed nanostructured TiO_2 layers for anchoring functionalized viologens, bis(2-phosphonoethyl)-4,4'-bipyridilium dichloride **[Et-PO_3H_2-Vio]** was employed as the first electro-chromophore due to its proven compatibility with sintered nanostructured TiO_2 on FTO/glass (400 – 450 °C).[3b, 3c, 4b, 4c, 4f, 4g, 5] Equally, the ECDs reported herein based on nanostructured TiO_2 films deposited on FTO/glass substrates and subsequently modified with **[Et-PO_3H_2-Vio]** showed good EC performance in spite of being obtained by low-temperature

processes. The latter, exhibited a colorless-to-blue switching (at 1.5 V), attributable to the one-electron reduction of the colorless dicationic form leading to a radical-cationic form ($bipm^{+\bullet}$), with a transmittance change above 46% (Figure 3.5).

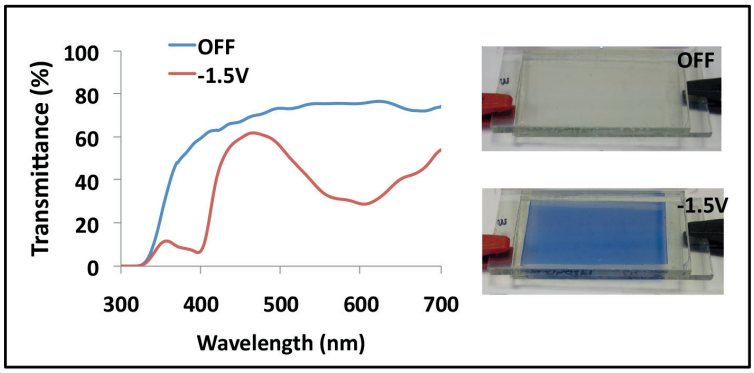

Figure 3.5: Transmittance spectra and pictures in the bleached (OFF) and colored (-1.5 V) states of an electrochromic device based on **[Et-PO_3H_2-Vio]**-modified TiO_2 electrodes on FTO/glass cured at 120 °C.

Contrariwise, no switching was observed for ECDs based on **[Et-PO_3H_2-Vio]** -TiO_2 electrodes applied on ITO/PET substrates. The failure was attributed to electrode damage occurring during the modification step with **[Et-PO_3H_2-Vio]**. The relatively high viologen concentration (20 mmol L^{-1}) and long immersion time (at least 24 h) required to ensure complete grafting of the **[Et-PO_3H_2-Vio]** on the nanostructured TiO_2 surface, caused delamination of the ITO layer, presumably because of the acidic nature of the viologen solution (i.e., pH values between 1 – 2).

Interestingly, SEM images of an ITO/PET substrate taken after immersion in the **[Et-PO_3H_2-Vio]** solution for 24 h confirmed that the delamination had taken place in spatially limited circular structures (Figure 3.6).

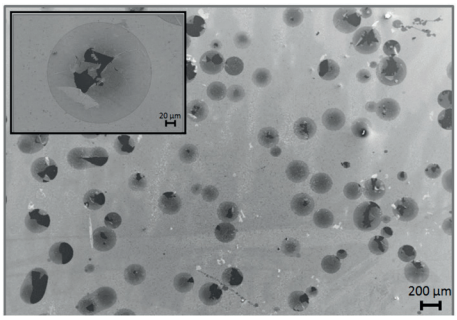

Figure 3.6. SEM images of delaminated ITO on PET substrate after 24 h of immersion in a **[Et-PO_3H_2-Vio]** solution.

SEM/EDX investigations revealed a wt% ratio of In_2O_3/SnO_2 in the range of 2/1 to 3/1 within the damaged circles and of 9/1 outside them, indicating that the acid-sensitive In_2O_3 could be being dissolved by the acidic viologen solution leaving In-depleted non-functional areas.

This issue unveiled the already expected need to synthesize an alternative viologen which provide a faster anchoring rate. In this regard, it could be expected that the presence of aryl groups in the adjacent carbons of the phosphonic acid group could stabilize the less stable resonance forms of the phosphonic acid group with formal charge, thus with higher affinity towards the attachment to the TiO_2 surface, easing therefore the anchoring. Consequently, a new viologen (**[Bn-PO_3H_2-Vio]**) containing aryl groups linked to the bipyridine moiety through a methylene group in order to ensure blue coloration was synthesized (Figure 3.7).

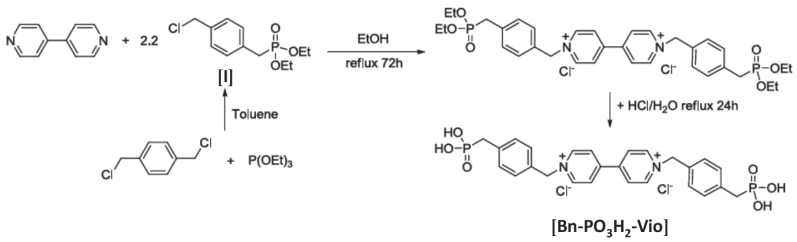

Figure 3.7. Synthetic route for viologen **[Bn-PO_3H_2-Vio]**.

The compatibility of new viologen **[Bn-PO_3H_2-Vio]** with ITO/PET was tested by immersing ITO/PET substrates in 5 mmol L^{-1} aqueous solution of **[Bn-PO_3H_2-Vio]**, being this concentration the maximum water solubility of the latter, for different periods of time, specifically 5 h, 10 h, 15 h and 24 h.

In a similar manner, ITO/PET films were also immersed in a 20 mmol L^{-1} aqueous solution of **[Et-PO_3H_2-Vio]** for similar periods for comparative purposes. It is noteworthy that using **[Et-PO_3H_2-Vio]** concentrations lower than 20 mmol L^{-1} would entail very long grafting times (well above 48 h) and for this reason the concentration was maintained at 20 mmol L^{-1}. Figure 3.8 depicts the optical micrographs of the ITO/PET films after different immersion times in the viologen solutions. It can clearly be seen that ITO/PET withstood the immersion conditions in the case of **[Bn-PO_3H_2-Vio]**, showing no damage even after 24 h of immersion, while only 10 h in **[Et-PO_3H_2-Vio]** solution caused ITO delamination.

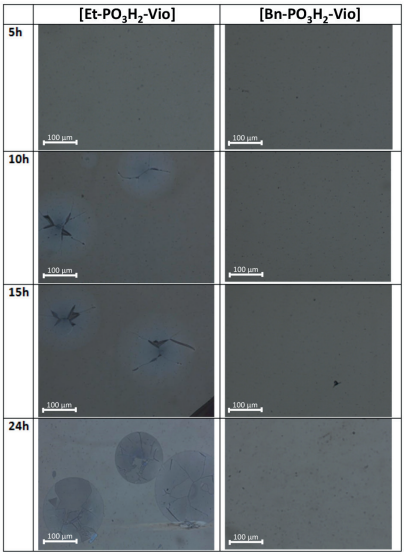

Figure 3.8. Optical micrographs of ITO/PET substrates after different immersion times in **[Et-PO_3H_2-Vio]** and **[Bn-PO_3H_2-Vio]** solutions.

These results revealed the higher compatibility of **[Bn-PO_3H_2-Vio]** with ITO/PET substrate electrodes than **[Et-PO_3H_2-Vio]**. Next, TiO_2 films were modified with **[Bn-PO_3H_2-Vio]** and the composition of these films was evaluated in order to assess the presence of the viologen on treated TiO_2 layers.

3.3.1. Characterization of viologen [Bn-PO_3H_2-Vio]-modified TiO_2 films

TiO_2-coated FTO/glass substrates were immersed in a 5 mmol L^{-1} aqueous solution of **[Bn-PO_3H_2-Vio]** for 5 h, and the presence of **[Bn-PO_3H_2-Vio]** viologen moieties on / in nanostructured TiO_2 layers was confirmed through both EDX and XPS spectroscopic techniques.

Energy-dispersive X-ray (EDX) spectroscopy was performed in Fraunhofer ISC from EDAX equipped with a Sapphire Si(Li) detecting unit. The presence of phosphorus (P) and chlorine (Cl) on the surface of a viologen-modified TiO_2 film was proven by this technique unlike that observed for an unmodified TiO_2 film (Figure 3.9), therefore proving the presence of viologen moieties available in the former but not in the latter.

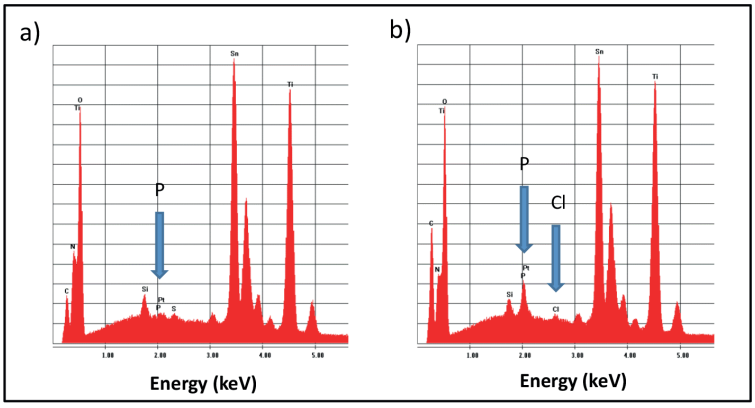

Figure 3.9. EDX study of unmodified (A) and **[Bn-PO_3H_2-Vio]**-modified TiO_2 films (B) on FTO/glass.

On the other hand, the availability of viologen strutures on TiO_2 surface sites inside the porous network was investigated by determining the elemental composition of a viologen-modified TiO_2 film by X-ray photoelectron spectroscopy XPS. These measurements were also performed in Fraunhofer ISC using the Surface Sciences Instruments (SSI) M-Probe model 2730. The depth-profile of Ti, Sn, O, C, N, and P within the approximately 600 nm thick TiO_2 film and the glass substrates (FTO/glass) is shown in the Figure 3.10. A narrow interface between the TiO_2 film and the FTO layer was apparent, where the atomic percentage of Ti and Sn abruptly decreased and increased, respectively. The transition from the FTO film to the glass substrate was equally detected by a decreasing percentage of Sn.

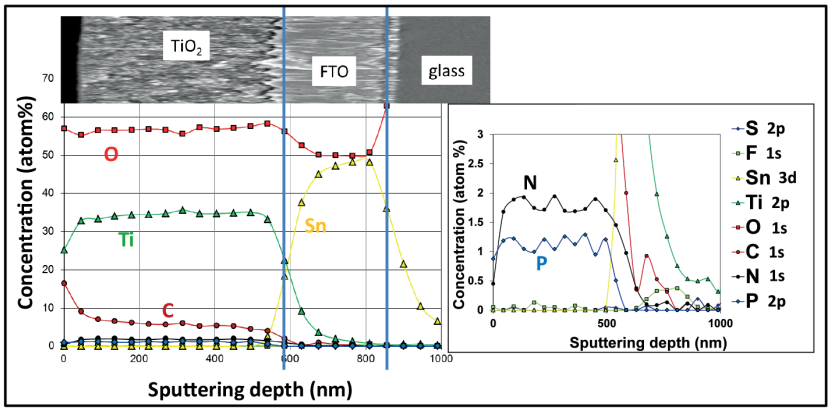

Figure 3.10. Elemental composition of a **[Bn-PO_3H_2-Vio]**-modified TiO_2 film on FTO/glass by XPS depth-profiling. Zoom of the atomic percentage of N and P (inset).

Carbon (C) representing viologen moieties anchored to the particles surface and organic residues was detected as well. The higher atomic percentage of C detected on the very surface of the film is probably due to contamination of the sample during handling at ambient conditions ("adventitious carbon"). Nitrogen (N) and phosphorus (P) solely representing viologen structures were detected to a small extent throughout the entire TiO_2 film, with the

concentration abruptly decreasing towards the TiO_2-FTO interface (Figure 3.10 (inset)). This result suggests the migration of viologen molecules into the pore network of the TiO_2 film throughout its entire thickness, showing that **[Bn-PO_3H_2-Vio]** may represent an alternative to the well-known **[Et-PO_3H_2-Vio]** to provide intense blue coloration, being much more compatible with the use of ITO/PET substrates.

3.3.2. Proof of concept of plastic ECDs based on [Bn-PO_3H_2-Vio]-modified TiO_2 films

The feasibility of obtaining colorless-to-blue ECDs based on **[Bn-PO_3H_2-Vio]**-modified TiO_2 nanostructured plastic electrodes prepared at low temperatures was evaluated. ECDs comprising TiO_2-coated ITO/PET substrates equally modified with **[Bn-PO_3H_2-Vio]** (5 mmol L^{-1} aqueous solution for 5 h) employed as WE and bare ITO/PET as the CE were assembled with liquid electrolyte. The devices properly switched between a colorless off state and a blue colored state at -2.5 V (Figure 3.11) demonstrating the viability of this layered ECDs to be employed with plastic substrates (ITO/PET).

Figure 3.11. Colorless-to-blue switching of an ECD based on **[Bn-PO_3H_2-Vio]**-modified TiO_2 electrodes on ITO/PET cured at 120 °C.

3.3.3. ECD performance

3.3.3.1. Cyclability

The stability upon redox cycling of ECDs comprising **[Bn-PO_3H_2-Vio]**-modified TiO_2 films was assessed. As the employment of liquid electrolyte while using flexible electrodes hinders the manipulation and measurement process, this cyclability study and other optimization procedures were carried out with rigid substrates (FTO/glass) avoiding these concerns. Hence, TiO_2-coated FTO/glass electrodes were initially modified with 5 mmol L^{-1} water solution of **[Bn-PO_3H_2-Vio]** for 20 h and the ECDs obtained after assembling with liquid electrolyte were tested.

Cyclability tests were performed by switching the devices between -1.8V (50 s) and +1.8V (90 s), thus requiring lower operating voltage than in the ITO/PET devices due to the higher conductivity of the former. The % of transmittance was registered versus time every 100 cycles at 600 nm, being this value approximately the maximum absorbance wavelength (λ_{max}) for blue colored materials as also deduced from Figure 3.5 . As shown by Figure 3.12, the initial transmittance in the colored state (T_c = 30%) remained constant during the first 100 cycles and then started to decrease gradually but the coloration was still intense (T_c = 38%) and homogeneous after 1000 cycles. The switching speed for the coloration step did not vary due to cycling whereas the bleaching became slower.

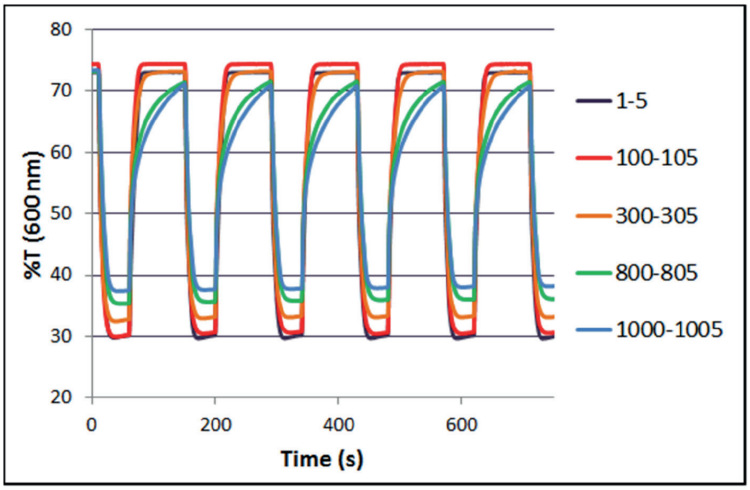

Figure 3.12. Evolution of the transmittance changes (at 600 nm) vs time of EDCs based on **[Bn-PO_3H_2-Vio]**-TiO_2 on FTO/glass electrodes after 100, 300, 800 and 1000 cycles while square wave potential-steps between bleached (+1.8 V for 90 s) and colored state (-1.8V for 50s) were being applied.

With the aim of enhancing the device performance in terms of transmittance change, the effect of the thickness of the TiO_2 film as well as the viologen grafting time were investigated. The results are described in the following sections.

3.3.3.2. Thickness effect

Mesoporous TiO_2 films of four different thickness (named TH1-TH4) and similar open porosity (34% as proven in published work)[13] were studied. These films, obtained by changing the drawing rate during dip-coating, exhibited thicknesses of approx. 700, 1300, 1800 and 2300 nm, for TH1-, TH2-, TH3-, and TH4-type respectively, as confirmed by cross-sectional SEM investigations (ZEISS Ultra-55) performed in Fraunhofer ISC (Figure 3.13).

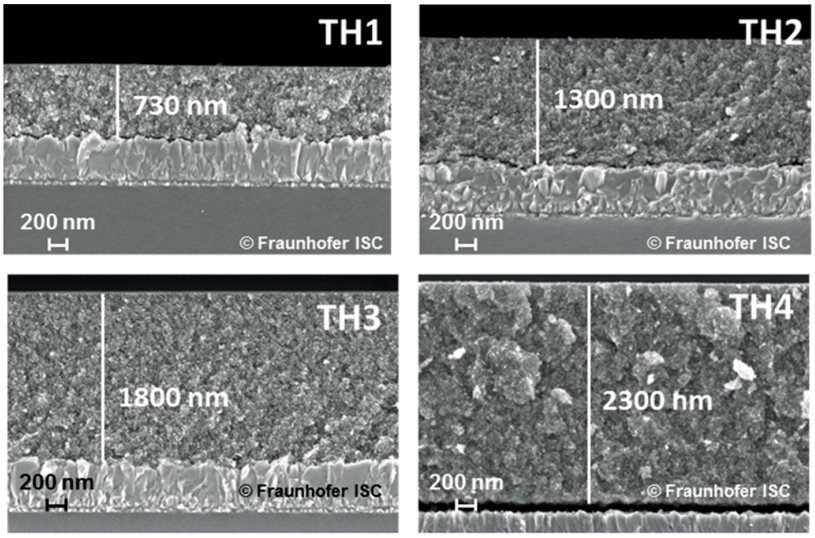

Figure 3.13. Cross-sectional SEM images of the mesoporous TiO_2 films (TH1 to TH4-type) on FTO/glass.

To evaluate the effect of TiO_2 film thickness on the transmittance change, films of the four different thicknesses were modified in IK4-CIDETEC with **[Bn-PO_3H_2-Vio]** (5 mmol L^{-1} solution for 20 h), and assembled using FTO/glass as counter electrode and liquid electrolyte. The most suitable reduction voltage and concentration of complementary redox species (HQ) to achieve the maximum steady-state coloration was figured out for each film thickness. To this end, the % of transmittance at 600 nm was registered over time for different HQ contents at different applied potentials. As an example, Figure 3.14a shows the measurements registered to select the most favorable switching voltage for TH1 thickness (with the optimal HQ content previously adjusted).[13]

Once the most satisfactory HQ content (0.005 mmol L^{-1} for TH1 thickness and 0.0075 mmol L^{-1} for the rest) and voltage (between -1.8 and -2.2 V) were found for each thickness, these four optimized systems were compared (Figure 3.14b).

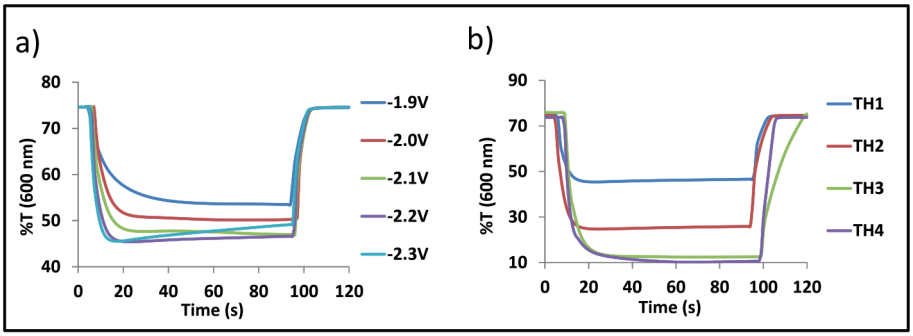

Figure 3.14. %T at 600 nm vs time upon application of coloring and bleaching steps (induced by reversed bias). a) Selection of the most favorable switching voltage for TH1 thickness (with the optimal HQ content previously adjusted at 0.005 mmol L^{-1}); b) Comparison between transmittance response registered for different thickness at suitable voltage for each case (TH1: -2.2V; TH2: -1.8V; TH3: -1.9V and TH4: -2.0V).

As expected,[4j] the change in transmittance D%T resulted to be highly dependent on the TiO_2 film thickness, ascribed to the higher amount of viologen anchored inside the thicker nanoparticle networks. Thus, while the bleached state presented a similar % of transmittance (around 75 %), the level of coloration drastically grew when increasing the thickness up to 1800 nm (TH3). In particular, 700 nm (TH1) and 1300 nm (TH2) thick layers provided D%T values of 28.5 % and 49.2 %, respectively. However, increasing the thickness from 1800 nm (TH3) to 2300 nm (TH4) did not result in a higher coloration level, being D%T approx. 63.5 % in both cases. This saturation may be attributed to the increasing difficulty for the viologen and electrolyte species to penetrate the small pores in thick films throughout their entire thickness. Additionally, it was observed that TH4-type films tended to crack, and as this effect might be aggravated on flexible ITO/PET substrates, TH3-type films were selected for the fabrication of small area plastic devices.

3.3.3.3. Grafting time effect

The dependence of the transmittance change on the grafting time was investigated in order to find out the minimum immersion time in viologen solution required to achieve the maximum level of coloration. TH3-type TiO_2 layers on ITO/PET were treated with 5 mmol L^{-1} **[Bn-PO_3H_2-Vio]** solution for 15 min, 30 min, 1 h, 3 h, 5 h and 20 h. Four ECDs for each grafting time were assembled using bare ITO/PET as the counter electrode and liquid electrolyte comprising 0.0075 mol L^{-1} of hydroquinone. The % of transmittance at bleached state and upon applying a suitable reduction voltage (-2.4 V) were registered at λ_{max} (600 nm). According to the results summarized in Table 3.1, the viologen **[Bn-PO_3H_2-Vio]** presents a very high affinity to attach to the TiO_2 surface, as the maximum D%T was accomplished in films immersed for only 30 min and even 15 min was enough to achieve a transmittance change very close to the maximum. Surprisingly, a slight decrease in the level of coloration was observed for longer grafting times which could be attributed to a slight damage of the TiO_2 layers that might be occurring when they are kept in the grafting solution for extended periods of time.

This fast grafting process (i.e., 15 – 30 min) strengthens the convenience of using **[Bn-PO_3H_2-Vio]** versus **[Et-PO_3H_2-Vio]** viologen in conjunction with plastic substrates. The bonding moiety of the **[Bn-PO_3H_2-Vio]** can be considered to be the *benzylphosphonic acid* due to the strong influence of the aromatic ring on the grafting time of the phosphonic acid group, as opposite to **[Et-PO_3H_2-Vio]** wherein *ethylphosphonic acid* can be considered the anchoring moiety. Therefore, it proves the more suitability of the *benzylphosphonic acid* in comparison with the most widely employed *ethylphosphonic acid*, to be rapidly anchored to TiO_2 nanostructured electrodes.

Table 3.1. Plastic ECDs (TH3): dependence of the device performance on the grafting time of **[Bn-PO_3H_2-Vio]** (average values of four samples).

Grafting time (h)	%Tb	%Tc	Δ%T	Contrast ratio
0,25	75.8	18.1	57.7 ± 2.9	4.2 ± 0.5
0,5	76.8	16.5	60.3 ± 1.7	4.6 ± 0.2
1	72.3	21.2	51.1 ± 3.7	3.5 ± 0.5
3	73.1	22.4	50.7 ± 4.5	3.2 ± 0.5
5	77.1	26.8	50.3 ± 3.4	2.9 ± 1.2
20	75.5	26.9	48.6 ± 1.7	2.8 ± 0.2

The electrochromic properties of a plastic device based on a TH3-type TiO_2-coated ITO/PET film modified for 15 min with **[Bn-PO_3H_2-Vio]** (5 mmol L^{-1}) were assessed. The results are summarized in Figure 3.15 and Table 3.2. As shown by Figure 3.15 and by color coordinates, the device switches from colorless off state to deep blue colored state upon application of -2.4 V.

Moreover, the device offers very good performance not only in terms of transmittance change but also in terms of switching speed reaching the 90% of the total transmittance change in 8 s with a coloration efficiency of 226 cm^2 C^{-1}, and even faster transition (6 s) and higher efficiency (708 cm^2 C^{-1}) was observed for the bleaching process.

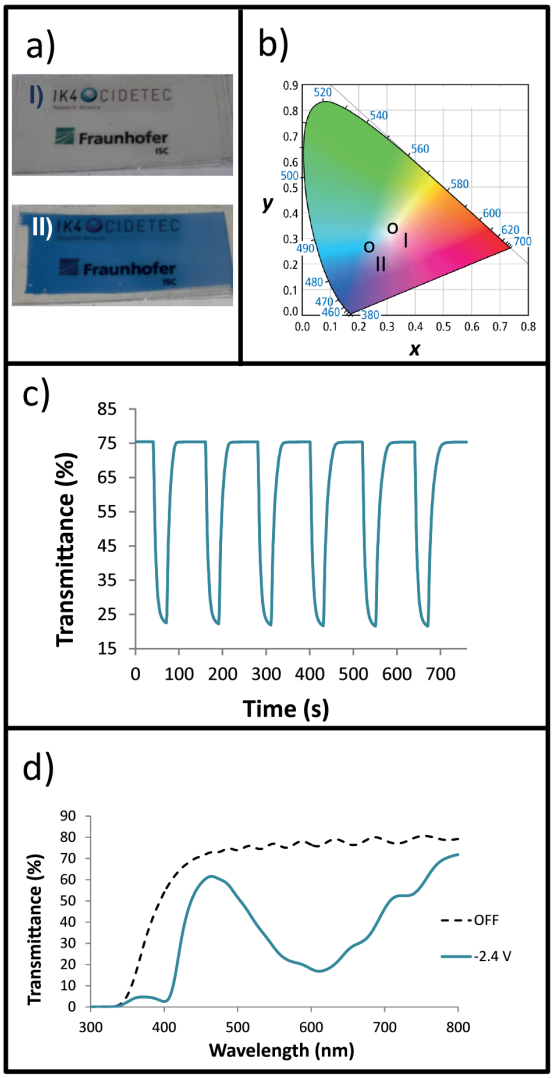

Figure 3.15. Plastic ECD based on a [**Bn-PO$_3$H$_2$-Vio**]-modified TiO$_2$ film (TH3-type; grafting time: 15 min); a) Photographs of the ECD in its bleached (I) and colored state upon applying switching voltage of -2.4 V (II); b) *xy* chromaticity diagram representing color coordinates obtained at bleached (I) and colored state at -2.4 V (II); c) Transmittance changes at the maximum D%T wavelength (600 nm) plotted against time while voltage steps between colored (-2.4 V, 30 s) and

bleached state (+2.4 V, 90 s) were applied; and d) the corresponding transmittance profiles in both states.

Table 3.2. Electrochromic properties and color coordinates (D65) of plastic ECDs (TH3-type; 15 minutes of grafting time of **[Bn-PO_3H_2-Vio]**):

State	%T[a]	t (s) [b]	CE (cm^2 C^{-1}) [c]	x[d]	y[d]	Y[d]	L*[e]	a*[e]	b*[e]	Color[f]
Bleached (0 V)	75	6	708	0.320	0.338	73.0	88	-1	4	
Colored (-2.4V)	22	8	226	0.240	0.266	30.6	62	-6	-26	

[a] %T = % of Transmittance at the maximum contrast wavelength (600 nm); [b] Switching times; [c] Color efficiencies; [d], [e] Color coordinates (D65): [d] xyY 1931 and [e] L*a^*b^* 1976;[f] Color interpretation of the corresponding color coordinates (L*a^*b).

3.3.3.5. Dual-type ECDs

As expounded in the chapter 1, ECDs can also be constructed by incorporating additional chromophore with complementary EC behavior on the counter electrode substrate to obtain simultaneously the coloration of both EC materials upon applying an appropriate external voltage. Thus, these "dual-type" ECDs can lead to high optical contrast through the suitable combination of a cathodically coloring layer such as viologen-coated TiO_2 films[4e, 4f, 4j, 5] with anodically coloring materials including Prussian Blue (PB),[4j] among others.[4e, 5]

Taking advantage of this strategy and with the aim of going a step further towards the achievement of high performance devices based on the low-temperature technology described in the present chapter, PB-coated ITO/PET film having a charge capacity of 2 mC cm^{-2} was used as the counter electrode. TH4-type films on FTO/glass was employed as the working electrode after modification with **[Bn-PO_3H_2-Vio]** for 15 min and both electrodes were assembled using hydroquinone-free liquid electrolyte. As

shown in Figure 3.16, a very competitive performance (71 % of transmittance change at 600 nm) with a transmittance of only 9 % in the colored state was achieved along with short switching times (7 s for coloring and 3 s for bleaching). It is worth noting that this should be considered a proof-of-concept experiment and an accurate balancing of the electrode charge capacities may further enhance the device performance.[14]

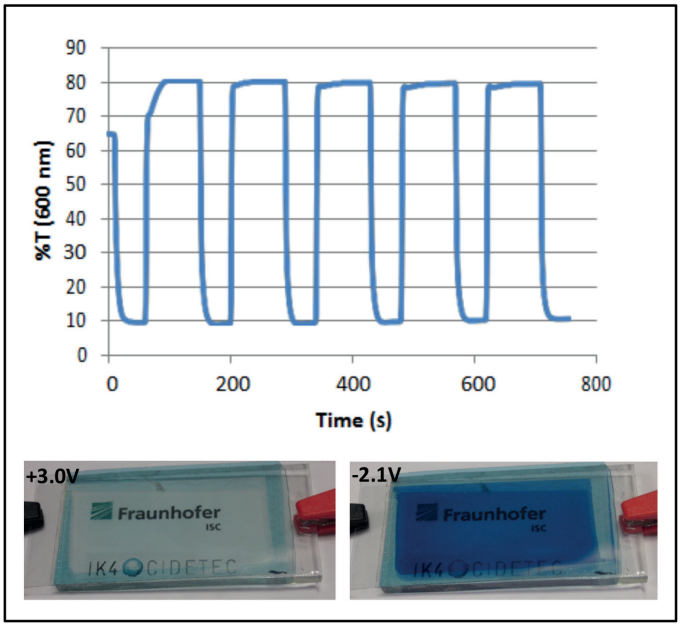

Figure 3.16. Dynamic transmittance response at 600 nm (top) and corresponding photographs in the bleached and colored states (bottom) of a ECD based on a [**Bn-PO$_3$H$_2$-Vio**]-modified TiO$_2$ film (TH4-type; grafting time: 15 min) on FTO/glass using PB on ITO/PET as the counter electrode.

3.3.4. Fabrication of large-area flexible all-solid ECDs

The feasibility of scaling-up the fabrication of [**Bn-PO$_3$H$_2$-Vio**]-TiO$_2$ films on ITO/PET and the subsequent assembly of operational large area ECDs was explored.

Despite the extended use of liquid electrolytes, they are less suitable for flexible and large area devices since the risk of leakage and of presence of bubbles increases. Additionally, the difficulty of preserving a regular distribution (thickness) of electrolyte throughout the device area may cause inhomogeneous coloration or even short-circuit between the WE and CE. With the aim to avoid all mentioned concerns and some solvent-related safety issues which hinder industrialization,[15] a transparent solid electrolyte was used for the assembly of the large area devices of the present work. This electrolyte which was viscous in its non-cross-linked form but a rubbery consistency when cross-linked after assembling by UV-radiation (FUSION UV lamp) was provided by IREQ.

The large area ECDs (30 cm x 40 cm) comprised PB-coated ITO/PET substrates as a CE and **[Bn-PO_3H_2-Vio]**-modified TiO_2-coated ITO/PET substrates as a WE. PB-coated ITO/PET films provided by Fraunhofer ISC were performed using a Schrems potentiostat/galvanostat model PGU 20V-5A-E, while TiO_2 films deposited on ITO/PET also provided by the latter were performed on a Click-and-Coat™ roll-to-roll (R2R) pilot coater (COATEMA Coating Machinery GmbH, Germany). In this occasion, TiO_2 films of TH2 thickness (1300 nm) were chosen to avoid the risk of cracking present in thicker films of large size, and were modified with **[Bn-PO_3H_2-Vio]** viologen (30 min) before device assembly.

Figure 3.17 shows the resulting large-area (30 cm x 40 cm) all-solid device switching properly between a colorless bleached state and a deep blue and homogeneous colored state, providing a transmittance change close to 32%. A completely colorless bleached state with a % of transmittance of 75.4% was achieved upon oxidation, decreasing to 43.8% (at 600 nm) upon reduction. This preliminary result demonstrates the feasibility of the ECDs reported in the present chapter to produce flexible all-solid ECDs of large-area, based on viologen-modified TiO_2 films obtained at low-temperature process.

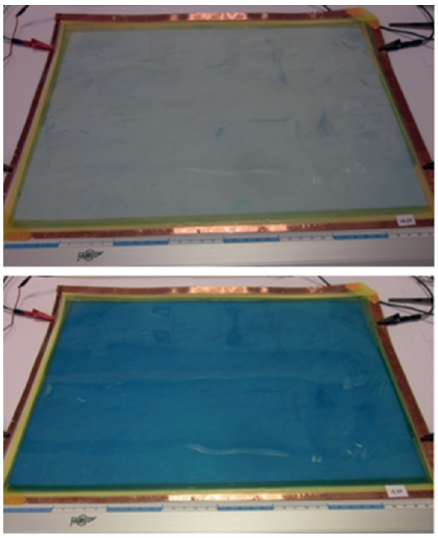

Figure 3.17. Flexible all-solid ECD with a size of 30 cm x 40 cm in the oxidized-bleached state (top) and in the reduced-colored state (bottom).

3.4. Conclusions

The synthesis of a new benzyl-substituted viologen **[Bn-PO_3H_2-Vio]** which exhibit very fast grafting onto the TiO_2 surface, while providing colorless-to-blue switching was demonstrated. The higher compatibility of this viologen with plastic electrode substrates (i.e., ITO/PET avoiding the ITO delamination) than the well-known ethyl viologen (**[Et-PO_3H_2-Vio]**), was also proven.

Additionally, the successful integration of **[Bn-PO_3H_2-Vio]** in flexible plastic ECDs based on viologen-modified nanostructured TiO_2 layers treated at only 120 ºC was demonstrated. The device performance was enhanced by establishing the best combination of TiO_2 layer thickness (1800 nm) and grafting time for the viologen (15 min), leading to plastic ECDs with a transmittance change as high as 60% and fast bleaching and

coloring response (i.e., 6 - 8 s). Furthermore, dual-type ECDs providing a very competitive transmittance change (71%) and the successful fabrication of large area (40 cm x 30 cm) plastic ECDs using a transparent solid electrolyte were also demonstrated, validating the viability of the present low-temperature methodology for scaling-up.

Moreover, the bonding moiety of the viologen described in this chapter, (hereafter considered to be *benzylphosphonic acid* due to the crucial influence of the aryl group on the grafting time), may open new avenues for the synthesis of other viologens provided with substituents of different nature, thus showing different colored states while maintaining the excellent bonding affinity towards TiO_2 nanostructured layers.

3.5. References

[1] P. M. S. Monk, *J. Electroanal. Chem.* **1997**, *432*, 175-179.

[2] D. C. Bookbinder, M. S. Wrighton, *J. Electrochem. Soc.* **1983**, *130*, 1080-1087.

[3] a) T. Gerfin, M. Grätzel, L. Walder, in *Progress in Inorganic Chemistry*, John Wiley & Sons, Inc., **2007**, pp. 345-393; b) Y. J. Kim, H. K. Jeong, J. K. Seo, S. Y. Chai, Y. S. Kim, G. I. Lim, M. H. Cho, I.-M. Lee, Y. S. Choi, W. I. Lee, *Journal of Nanoscience and Nanotechnology* **2007**, *7*, 4106-4110; c) S. Y. Choi, M. Mamak, N. Coombs, N. Chopra, G. A. Ozin, *Nano Letters* **2004**, *4*, 1231-1235.

[4] a) R. Cinnsealach, G. Boschloo, S. Nagaraja Rao, D. Fitzmaurice, *Sol. Energy Mater. Sol. Cells* **1999**, *57*, 107-125; b) R. Cinnsealach, G. Boschloo, S. Nagaraja Rao, D. Fitzmaurice, *Sol. Energy Mater. Sol. Cells* **1998**, *55*, 215-223; c) U. Bach, D. Corr, D. Lupo, F. Pichot, M. Ryan, *Adv. Mater.* **2002**, *14*, 845-848; d) M. Möller, S. Asaftei, D. Corr, M. Ryan, L. Walder, *Adv. Mater.* **2004**, *16*, 1558-1562; e) N. Vlachopoulos, J. Nissfolk, M. Möller, A. Briançon, D. Corr, C. Grave, N. Leyland, R. Mesmer, F. Pichot, M. Ryan, G. Boschloo, A. Hagfeldt, *Electrochim. Acta* **2008**, *53*, 4065-4071; f) H. J. Kim, J. K. Seo, Y. J. Kim, H. K. Jeong, G. I. Lim, Y. S. Choi, W. I. Lee, *Sol. Energy Mater. Sol. Cells* **2009**, *93*, 2108-2112; g) S. Bhandari, M. Deepa, A. K. Srivastava, S. T. Lakshmikumar, RamaKant, *Solid State Ionics* **2009**, *180*, 41-49; h) P. Pechy, F. P. Rotzinger, M. K. Nazeeruddin, O. Kohle, S. M. Zakeeruddin, R. Humphry-Baker, M. Gratzel, *Journal of the Chemical Society, Chemical Communications* **1995**, 65-66; i) S. M. Zakeeruddin, M. K. Nazeeruddin, P. Pechy, F. P. Rotzinger, R. Humphry-Baker, K. Kalyanasundaram, M. Grätzel, V. Shklover, T. Haibach, *Inorganic Chemistry* **1997**,

36, 5937-5946; j) F. Campus, P. Bonhôte, M. Grätzel, S. Heinen, L. Walder, *Sol. Energy Mater. Sol. Cells* **1999**, *56*, 281-297.

[5] D. Cummins, G. Boschloo, M. Ryan, D. Corr, S. N. Rao, D. Fitzmaurice, *J. Phys. Chem. B* **2000**, *104*, 11449-11459.

[6] a) A. Hagfeldt, L. Walder, M. Graetzel*, Vol. 2531*, **1995**, pp. 60-69; b) M. K. Nazeeruddin, P. Liska, J. Moser, N. Vlachopoulos, M. Grätzel, *Helv. Chim. Acta* **1990**, *73*, 1788-1803; cA) . Hagfeldt, N. Vlachopoulos, S. Gilbert, M. Graetzel*, Vol. 2255* (Eds.: V. Wittwer, C. G. Granqvist, C. M. Lampert), **1994**, pp. 297-304.

[7] a) X. Marguerettaz, R. O'Neill, D. Fitzmaurice, *J. Am. Chem. Soc.* **1994**, *116*, 2629-2630; b) A. Hagfeldt, N. Vlachopoulos, M. Grätzel, *J. Electrochem. Soc.* **1994**, *141*, L82-L84.

[8] N. G. Park, K. M. Kim, M. G. Kang, K. S. Ryu, S. H. Chang, Y. J. Shin, *Adv. Mater.* **2005**, *17*, 2349-2353.

[9] Z. Tebby, O. Babot, T. Toupance, D.-H. Park, G. Campet, M.-H. Delville, *Chem. Mater.* **2008**, *20*, 7260-7267.

[10] J.-H. Ryu, J.-H. Lee, S.-J. Han, K.-D. Suh, *Macromolecular Rapid Communications* **2006**, *27*, 1156-1161.

[11] V. V. Ragulin, *Russian Journal of General Chemistry* **2012**, *82*, 1928-1937.

[12] D. Biskupski, B. Herbig, G. Schottner, R. Moos, *Sensors and Actuators B: Chemical* **2011**, *153*, 329-334.

[13] Y. Alesanco, J. Palenzuela, R. Tena-Zaera, G. Cabañero, H. Grande, B. Herbig, A. Schmitt, M. Schott, U. Posset, A. Guerfi, M. Dontigny, K. Zaghib, A. Viñuales, *Sol. Energy Mater. Sol. Cells* **2016**, *157*, 624-635.

[14] K.-C. Ho, *Sol. Energy Mater. Sol. Cells* **1999**, *56*, 271-280.

[15] a) Å. Stefan, *J. New Mater. Electrochem. Syst.* **2001**, *4*, 173-179; b) L. Su, Z. Xiao, Z. Lu, *Mater. Chem. Phys.* **1998**, *52*, 180-183; c) L. Su, H. Wang, Z. Lu, *Mater. Chem. Phys.* **1998**, *56*, 266-270; d) S. Lianyong, W. Hong, L. Zuhong, *Supramolecular Science* **1998**, *5*, 657-659; e) L. Su, Z. Xiao, Z. Lu, *Thin Solid Films* **1998**, *320*, 285-289.

CHAPTER 4

PLASTIC ELECTROCHROMIC DEVIPOLYVINYL ALCOHOL-BORAX GEL AS A PROMISING POLYELECTROLYTE FOR HIGH-PERFORMANCE, EASY-TO-MAKE ELECTROCHROMIC DEVICES

4.1. Introduction

The EC behavior of the ECDs lies to a large degree in the electrolyte. As mentioned in chapter 1, to achieve high-performance ECDs, a model electrolyte has to exhibit high ionic conductivity (i.e., between $1e^{-4}$ and $1e^{-3}$ S cm^{-1}),[1] ideal zero electronic conductivity,[2] high thermal (i.e., up to +60 ºC)[1a] and electrochemical stability,[3] along with high transmission in the visible region.[1b] In addition, other requirements are desirable such as certain stickiness and adhesion[2-3] which translate into good interaction with the electrode and/or electrochromic layer, and elasticity[2] to relieve mechanical stress which may arise from the manipulation or from thermal variations, therefore extending the durability of the ECDs.

Electrolytes for ECDs are conventionally based on organic polar solvents with high dielectric constant and low viscosity to ease the ion migration,[4] wherein the electroactive components can be dissolved.[5] Despite their extended use, liquid electrolytes exhibit several disadvantages, such as risk of solvent leaking[6] and presence of bubbles, low chemical stability, or a complicated industrialization due to solvent-related safety issues.[2, 7] These drawbacks become more noticeable in the large area flexible ECDs as pointed out in the previous chapter. Solid electrolytes, similarly exhibit some limitations such as less transparency, and poorer performance of the resulting ECDs, due to the lower mobility of the ionic species into the solid matrix.

As also mentioned in chapter 1, several strategies towards the development of ideal semi-solid electrolytes have been proposed in the literature throughout the last 20 years. Some attempts comprises polymeric matrix to achieve more solid-like mechanical properties (i.e., PMMA, [1, 3a] PVC, [7c, 7d] PEO, [7b, 8] PAN[9]) dispersed in a conventional solvent (i.e., PC, EC, γ-butyrolactone), whereas others employed animal protein-derived gels in an aqueous media[10] or in organic solvents.[11] However, the large gelation times (i.e., between 3[7-8] and 5[1a] days) or the presence of bubbles difficult to avoid in the ones which exhibited rapid gelation process, make them less suitable for ECDs.

In other approaches, the ionic liquids (ILs) have replaced the current solvent in the electrolytes[12] combined with conventional polymers (e.g., PVA),[13] with gelatin,[14] or with poly(ionic liquids) (PILs).[12a, 15]

Other explored strategies aimed to obtain solid or semi-solid electrolytes employed irreversible chemical cross-linked polymers cured by UV-radiation[16] or thermal treatments,[12b] before[16a, 16d] or after being assembled,[16b] although they were not exempted from some non-desirable effects such as the risk of bubbles.

Therefore, despite the big efforts carried out aimed to achieve the ideal electrolyte, the performance of ECDs based on solid electrolytes is still poorer than that achieved with liquid ones and the development of electrolytes which ensure good interfacing with the electrodes and/or the EC layer remains an aspect to be improved.[17]

As outlined in the chapter 2, an interesting approach employed in the present thesis to overcome these problems has been the use of electrolyte mixtures which may be cured by dynamic covalent chemistries,[18] exhibiting rheological behavior about midway between the solid and liquid materials, hence non-Newtonian behavior. Specifically, the electrolytic matrix selected for the present thesis has been the PVA-

borax gel obtained by complexation of hydroxyl groups of the PVA chain with borate ions.

These PVA-borax gels,[19] with a similar chemistry to the well-known "Slime" developed by the Mattel Toy Corporation in the 1970s,[19i, 20] has been reported to be non-Newtonian, shear thickening and viscoelastic fluid.

Although the mechanism of the alcohol-borax complexation seems to be unsettled,[19h] the non-Newtonian character of the PVA-borax gel combines the advantages of both liquid and solid electrolytes while being easy to apply and offering excellent contact to both electrodes. Additionally, despite its rapid gelation process,[19h, 21] completely bubble-free material is obtained after allowing it to settle for a few minutes, due to its ability to flow.

4.1.1. Objective

The overall aim of the work reported in this chapter was the assessment of a new concept of semi-solid polyelectrolyte based on a non-Newtonian viscoelastic fluid, which combines the advantages of both liquid and solid electrolytes, while enabling the easy fabrication of high-performance ECDs.

The assessment of this PVA-borax gel as electrolyte in layered ECDs had to be initially proven.

Afterwards, the successful incorporation of the required electroactive materials into the PVA-borax gel to obtain all-in-one ECDs while maintaining the rheological properties of the gel was a major challenge to reach.

The optimization of EC formulations employed in all-in-one ECDs in terms of transmittance change and switching times was also required, along with the study of ionic conductivity and cyclability of the enhanced formulations.

4.2. Materials and methods

4.2.1. Materials

Poly(vinyl alcohol) (PVA, M_w 61 000), sodium tetraborate decahydrate (borax, 99.5%), 4,4'-bipyridyl (98%), %), ethyl bromide (98%), potassium ferrocyanide (98.5%) and potassium ferricyanide (99%), were purchased from Sigma-Aldrich. Required solvents such as acetone and acetonitrile were supplied by Scharlab. All these products were used without further purification. Fluorine-doped tin oxide (FTO) coated glass substrates (TEC7, Rs 6-8 Ω sq^{-1}) were supplied by Solems. Titanium dioxide dispersion (Ti-Nanoxide T, transparent) was purchased from Solaronix.

4.2.1.1. Synthesis and characterization of viologens

Synthesis of 1,1'-diethyl-4,4'-bipyridinium dibromide ***[EtVio]***

Viologen [**EtVio**] was synthesized according to previously reported procedure with minor modifications.[22] In brief, a mixture of 4,4'-bipyridyl (10 mmol) and ethyl bromide (80 mmol) was refluxed in acetonitrile (15 mL) for 16 hours. After cooling, the resulting yellowish solid was filtered and washed with acetonitrile and acetone. (Yield = 92%). ^{1}H NMR (500 MHz, DMSO-*d6*, δ): 9.44 ppm (d, 4H, *J* = 6.75 Hz), 8.82 ppm (d, 4H, *J* = 6.55 Hz), 4.75 ppm (q, 4H), 1.61 ppm (t, 6H).IR (bulk ATR): ν (cm^{-1}) = 3031 (C-H olefin st), 2977 (C-H alkyl st), 1638 (C=N st), 1511 (C=C), 1439,

(C-H alkyl δ) 853 (o-phenylene H); IC: % Br^- calculated for $C_{14}H_{18}N_2Br_2$: 42.7%, found 42.2%.

Synthesis of Bis(phosphonomethyl-4-benzyl)-4,4'-bipyridilium dichloride ***[Bn-PO$_3$H$_2$-Vio]*** has been described in the chapter 3.

4.2.2. Methods

4.2.2.1. Preparation of gel formulations

All gel formulations were prepared following the general procedure described in the section 2.2.2 of the chapter 2. Detailed information regarding the specific composition of the gels assessed in this chapter (i.e., concentration of complementary redox pair and viologen) are described below.

Preparation of ***Gel 1***

This formulation corresponds to the bare gel, that is to say PVA-borax gel without adding neither viologen nor potassium ferrocyanide/ferricyanide salts.

Preparation of ***Gels 2a-b***

These viologen-free gels were fabricated keeping the final concentration of the ferro/ferricyanide potassium pair at 1 and 6 $mmolL^{-1}$ values for **Gel 2a** and **b**, respectively.

Preparation of EC ***Gels 3a-h*** *with varying concentration of* ***[EtVio]*** *viologen*

The electrochromic **Gels 3a-h**, containing both viologen and potassium ferrocyanide/ferricyanide salts, were prepared by varying concentrations

of **[EtVio]** from 2.5 to 25.0 mmol L^{-1} while keeping the concentration of ferro/ferricyanide potassium pair at a constant value of 0.8 mmol L^{-1}. The final concentrations of viologen for **Gel 3a**, **Gel 3b**, **Gel 3c**, **Gel 3d**, **Gel 3e**, **Gel 3f**, **Gel 3g** and **Gel 3h** were 2.5, 5.0, 7.5, 10.0, 15.0, 17.5, 20.0 and 25.0 mmol L^{-1}, respectively (Table 4.1).

Table 4.1. Concentration [mmol L^{-1}] of **[EtVio]** and ferrocyanide/ferricyanide redox salts (Fe^{II}/Fe^{III}) in **Gels 3a-h**.

Gel	[Ethyl viologen dibromide] (mmol L^{-1})	[Fe(II)/Fe(III)](mmol L^{-1})
Gel 3a	2.5	0.8
Gel 3b	5.0	0.8
Gel 3c	7.5	0.8
Gel 3d	10.0	0.8
Gel 3e	15.0	0.8
Gel 3f	17.5	0.8
Gel 3g	20.0	0.8
Gel 3h	25.0	0.8

Preparation of EC **Gels $3g_{1-9}$** *with varying concentration of potassium ferrocyanide/ferricyanide salts*

The electrochromic **Gels $3g_{1-9}$**, containing both viologen and potassium ferrocyanide/ferricyanide salts, were prepared by varying concentrations of ferro/ferricyanide potassium pair from 0.4 to 6.0 mmol L^{-1} while keeping the concentration of **[EtVio]** at a constant value of 20.0 mmol L^{-1}. The final concentrations of redox salts for **Gel $3g_1$**, **Gel $3g_2$**, **Gel $3g_3$**, **Gel $3g_4$**, **Gel $3g_5$**, **Gel $3g_6$**, **Gel $3g_7$**, **Gel $3g_8$** and **Gel $3g_9$** were 0.4, 0.8, 1.2, 1.6, 2.0, 3.0, 4.0, 5.0 and 6.0 mmol L^{-1}, respectively. (Table 4.2).

Table 4.2. Concentration [mmol L^{-1}] of **[EtVio]** and ferrocyanide/ferrycyanide redox salts (Fe^{II}/Fe^{III}) in **Gels $3g_{1-9}$**

Gel	[Ethyl viologen dibromide] (mmol L^{-1})	[Fe(II)/Fe(III)](mmol L^{-1})
Gel $3g_1$	20.0	0.4
Gel 3 g_2	20.0	0.8
Gel 3 g_3	20.0	1.2
Gel 3 g_4	20.0	1.6
Gel 3 g_5	20.0	2.0
Gel 3 g_6	20.0	3.0
Gel 3 g_7	20.0	4.0
Gel 3 g_8	20.0	5.0
Gel 3 g_9	20.0	6.0

4.2.2.2. Fabrication of electrochromic devices

All-in-one and layered ECDs having an approximate active area of 4 cm^2 were assembled following the procedure described in the chapter 2 section 2.5.1. for two-electrode ECD using gel EC mixtures.

4.3. Results and discussion

With the aim of overcoming the above-mentioned problems associated with solid and liquid polyelectrolytes, PVA-borax gel (Figure 4.1a) was assessed as a polyelectrolytic matrix.

As shown by Figure 4.1b this non-Newtonian fluid exhibited quite attractive properties, behaving like a liquid under low stress (can flow and stretch) but conversely, behaving more like a solid under high stress.

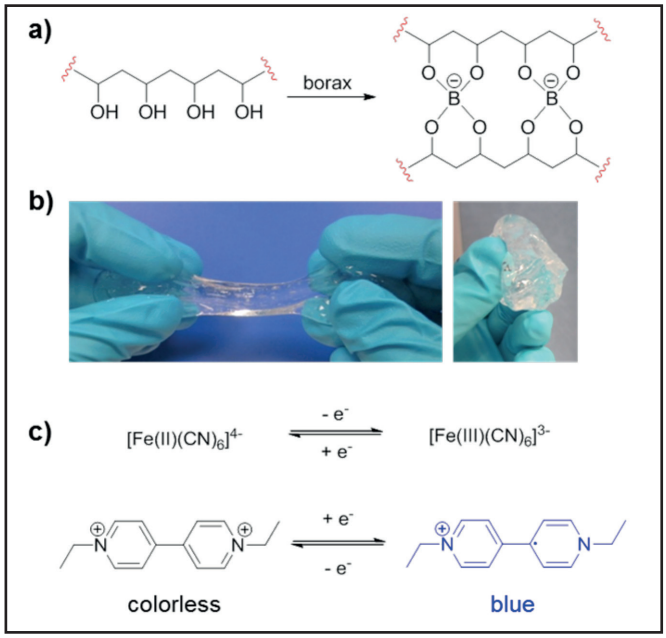

Figure 4.1. a) Synthesis and chemical structure of the PVA-borax gel; b) photographs showing the physical aspect and texture of the gel; c) ferrocyanide/ferricyanide complementary redox species used for the viologen electrochromic reaction and chemical structure of ethyl viologen in its oxidized state (left) and its reduced state (right).

This PVA-borax gel was initially tested in layered ECDs using nanostructured TiO_2 electrodes provided with viologen molecules chemically absorbed. In a second stage, this gel was tested in all-in-one ECDs, thus incorporating the electroactive materials (Figure 4.1c) into PVA-borax gel.

4.3.1. PVA-borax gel as electrolyte in layered-electrodes (proof of concept)

With the aim of evaluating the PVA-borax gel as potential electrolyte in layered ECDs, PVA-borax gel electrolyte was formulated and tested in TiO_2 nanostructured ECDs wherein the viologen molecules were previously chemisorbed.

To this end, nanostructured TiO_2 electrodes were fabricated from commercially available titanium dioxide dispersion by doctor blade technique using a wire wound rod of 100 μm groove depth. TiO_2 sintered layers exhibited a thickness of 4.5 μm according to cross-sectional SEM micrographs (Figure 4.2a), and anatase crystalline phase as confirmed by XRD (Figure 4.2b).[23] Afterwards, resulting films were conveniently modified with a viologen provided with anchoring group.

Taking advance of the great affinity towards TiO_2 nanostructured layers proven for *Bis*(phosphonomethyl-4-benzyl)-4,4'-bipyridilium dichloride [**Bn-PO_3H_2-Vio**] described in the previous chapter, this viologen was selected for this study.

The grafting conditions were fixed at 15 min of immersion time into 5 mmol L^{-1} solution of the viologen, followed by rinsing with water and ethanol and then dried overnight at 50 °C under vacuum.

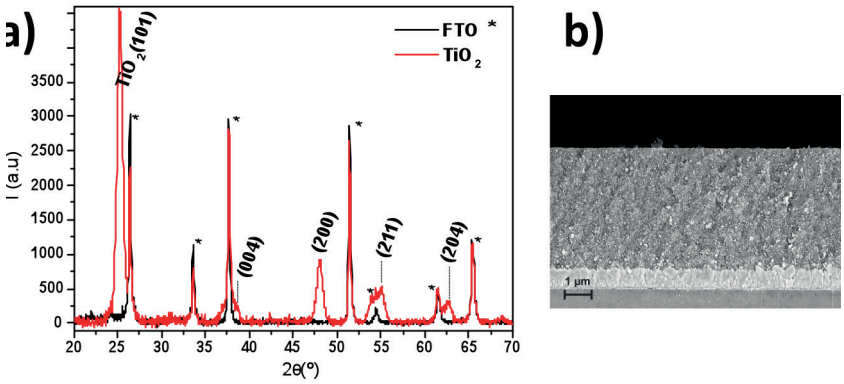

Figure 4.2. Characterization of nanostructured TiO_2 layers on FTO/glass: a) XRD of pattern of a representative sample showing Miller indices (hkl) representative of anatase crysralline phase (* FTO); b) Cross-sectional SEM micrographs.

Thus obtained films were conveniently assembled with a PVA-borax gel electrolyte comprising 1 mmol L^{-1} of potassium ferrocyanide and ferricyanide salts (**Gel 2a**) and the electrochromic behavior of the resulting ECDs was evaluated. It is worth to mention that concentration of ferro/ferricyanide salts as high as 5 mmol L^{-1} entailed perceptible bleaching of the ECDs even while reducing potential was being applied and accordingly, it was fixed at a lower value of 1 mmol L^{-1}.

As illustrated in Figure 4.3 the fabrication of devices was very easy, it only being necessary to spread the gel on the viologen-modified TiO_2-coated substrates and then covering it with the other electrode substrate. As mentioned above, if the PVA-borax gel was left to settle on its own for a few minutes before covering with the second electrode, a completely bubble-free device could be obtained.

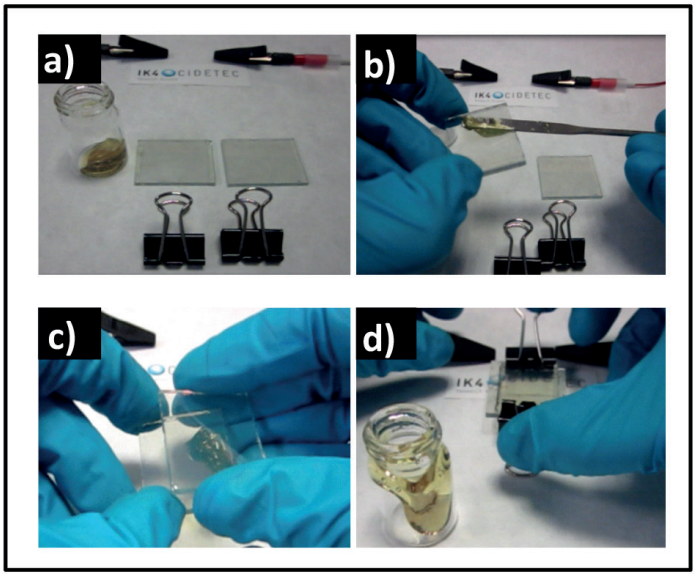

Figure 4.3. Assembly of electrochromic device. a) FTO glass electrodes, and electrochromic gel; b) "jelly-on-toast" application of electrochromic gel on the electrode; c) sandwiching with the second electrode; d) clipping the electrodes.

As shown by Figure 4.4a-b, the devices properly switched between colorless off state and purple color upon suitable applied potentials (between -2.0 and -2.6V).

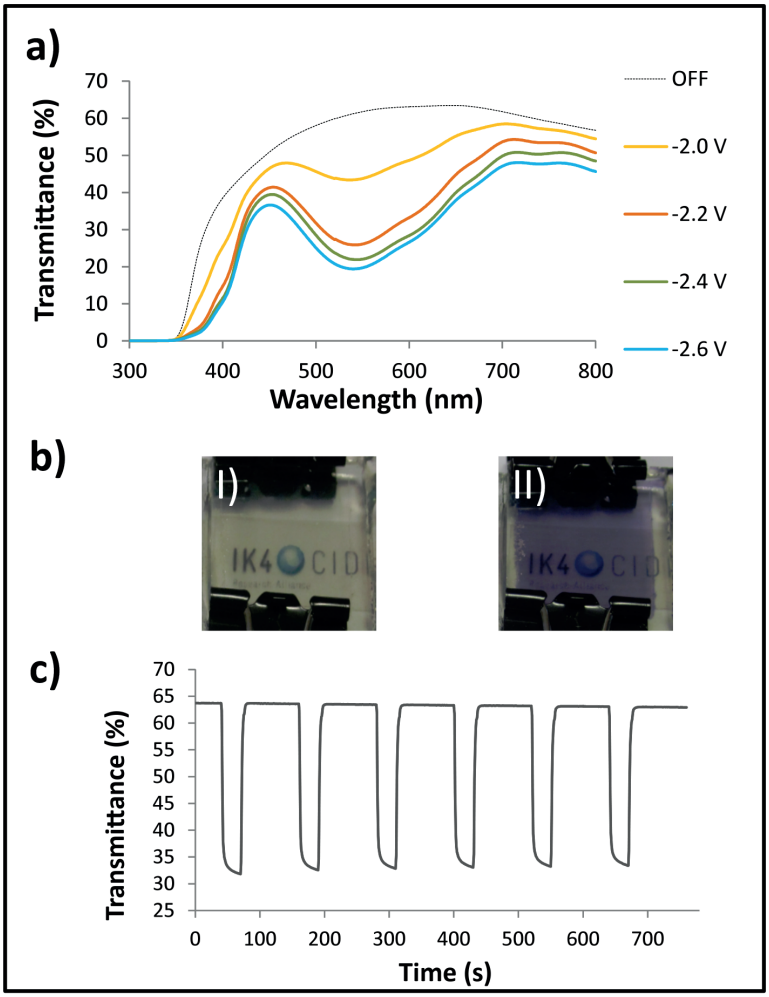

Figure 4.4. Layered ECD comprising **[Bn-PO_3H_2-Vio]** adsorbed on the TiO_2 coated electrode assembled with **Gel 2b** electrolyte: a) UV-vis transmittance response at off state and at different reduction potentials; b) observed colorations in bleached state (I) and while -2.4 V (II) were being applied; c) Transmittance changes registered at 550 nm plotted against time while voltage-steps between colored (-2.4 V for 50 s) and bleached state (0 V for 90 s) were being applied.

The switching performance of the layered ECD was also evaluated by registering the transmittance changes at maximum contrast wavelength (λ_{max} = 550 nm) while potential steps between colored (-2.4 V for 50 s) and bleached state (0 V for 90 s) were being applied. As deduced from the Figure 4.4c and summarized in the Table 4.3, layered ECDs comprising **Gel 2a** electrolyte exhibited excellent switching times (i.e., 3 and 4 s for the bleaching and coloring processes, respectively). Although the origins of the coloration will be discussed latter and in the following chapters, color coordinates were measured (Table 4.3) revealing purple colored state.

It is worth to mention that this assay should be considered a proof-of-concept experiment and an accurate optimization may lead to enhanced performance. Therefore, on the basis of these preliminary results it can be concluded that the PVA-borax may be used as electrolyte in layered ECDs.

Table 4.3. Electrochromic properties and color coordinates (D65) of layered ECD comprising **[Bn-PO_3H_2-Vio]** adsorbed on TiO_2 coated electrode assembled with **Gel 2b** electrolyte.

State	%T[(a)]	t (s) [(b)]	CE ($cm^2 C^{-1}$) [(c)]	x[(d)]	y[(d)]	Y[(d)]	L*[(e)]	a*[(e)]	b*[(e)]	Color[(f)]
Bleached (0 V)	63	3	108	0.329	0.351	61.3	83	-2	10	
Colored (-2.4V)	33	4	83	0.305	0.279	26.0	58	15	-14	

[a)] %T = % of Transmittance at the maximum contrast wavelength (600 nm); [b)] Switching times; [c)] Color efficiencies; [d), e)] Color coordinates (D65): [(d)] xyY 1931 and [(e)] L**a***b** 1976;[f)] Color interpretation of the corresponding color coordinates (L**a***b*).

Once PVA-borax gel had been demonstrated as a suitable polyelectrolyte in layered ECDs, it was also assessed in all-in-one ECDs, thus incorporating all the electroactive materials required to obtain an EC mixture. To this end, polyelectrolyte blends comprising PVA-borax gel in combination with

ferrocyanide/ferricyanide complementary redox pair and ethyl viologen [**EtVio**] were evaluated in ECDs.

4.3.2. All-in-one ECDs: Optimization of EC mixture

Optimization of the final amounts of the electrochromic and redox species is crucial for assuring a good performance of the resulting ECD. The systematic procedure followed to find out the most suitable formulations to achieve high levels of coloration and fast switching times is described above.

4.3.2.1. Optimization of viologen concentration

Aiming at achieving the highest possible level of coloration, a series of PVA-borax gel formulations comprising varying concentrations of [**EtVio**] from 2.5 to 25.0 mmol L^{-1} while keeping the concentration of ferro/ferricyanide potassium pair at a constant value of 0.8 mmol L^{-1}, were evaluated (**Gels 3a-h**).

The electrochemical window found for these gel-based two-electrode devices ranged from -2.8 V to +2.8 V. Beyond these values, gas generation was observed due to the water electrochemical decomposition.

After studying the variation in transmittance (%T) as a function of wavelength for different applied voltages in the operational range (from -2 V to -2.4 V) it was concluded that -2.3 V was the most suitable voltage to achieve the highest transmittance change. At this voltage, the ECDs provided bluish coloration attributed to the first reduced form of the [**EtVio**] (radical-cationic form ($bipm^{+\bullet}$)). Hereafter, the transmittance responses of the **Gels 3a-h** were registered at this cathodic potential.

Figure 4.5 shows transmittances vs wavelength plots obtained for the eight devices with different viologen concentrations (**Gels 3a-h**). The transparency at the off-bleached state was similar for all the concentrations, indicating that, for this system, the initial transmittance is not related to the

viologen concentrations, at least not in the studied concentration range. In the colored state, the transmittance kept decreasing as the viologen concentration increased, arriving to full absorbance between 500 and 600 nm at a concentration of 20 mmol L^{-1}, with a transmittance change of 68% at 550 nm. This high level of coloration was expected due to the high amount of chromophores distributed all over the electrolytic layer.

From the results obtained it was concluded that the most suitable concentration of **[EtVio]** to be employed in further experimentation would be 20 mmol L^{-1} (**Gel 3g**).

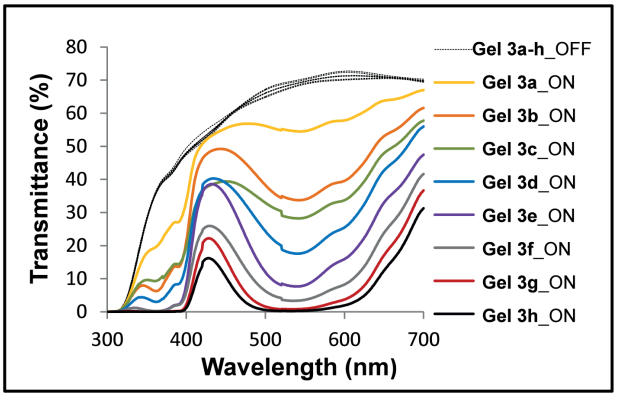

Figure 4.5. UV-Visible transmittance responses of different ECDs comprising **Gels 3a-h** at off state and upon applying -2.3 V.

4.3.2.2. Optimization of redox species concentration

The following step consisted in optimizing the device in terms of response time, by adjusting the appropriate amount of the complementary redox salts. A series of nine formulations with varying concentrations of ferro/ferricyanide potassium pair, and a constant concentration of ethyl viologen of 20 mmol L^{-1} (**Gels $3g_{1-9}$**) were evaluated.

The transmittance at maximum contrast wavelength (λ_{max} = 550 nm) was measured for corresponding ECDs and plotted against the time while square-wave potential-steps were being applied. The switching potentials and times for this study were set at -2.3 V at colored state for 30 s and 0 V at bleached state for 90 s (Figure 4.6). In the light of these results it can be concluded that a fast response can be obtained even for a relatively high transmittance change (~ 60%). Additionally, the response time could be easily customized, by adjusting the amount of ferro/ferricyanide potassium salts. This result can be of special interest in the field of electrochromic windows, as the pane could be kept in the colored state with little or no input of electric power (i.e., using **Gel 3g$_1$**).

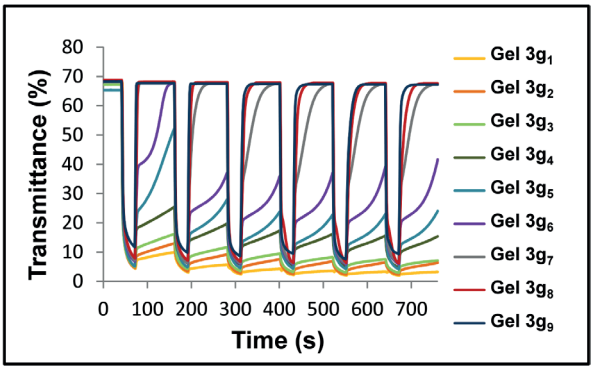

Figure 4.6. Transmittance changes registered at 550 nm for ECDs comprising **Gels 3g$_{1-9}$** while potential-steps between colored (-2.3 V for 30 s) and bleached state (0 V for 90 s) were being applied.

The ECD showing the fastest switching response was the one comprising **Gel 3g$_9$**, as a result of the higher amount of ferro/ferricyanide potassium salts. The latter undergoes the complementary redox process easing the bleaching of viologen, due to its close redox potentials to that of the viologen compounds.[24]

As shown in the Figure 4.7 the device based on **Gel 3g$_9$** provided total transparent and colorless-off state and deep colored state upon applying convenient reduction potential.

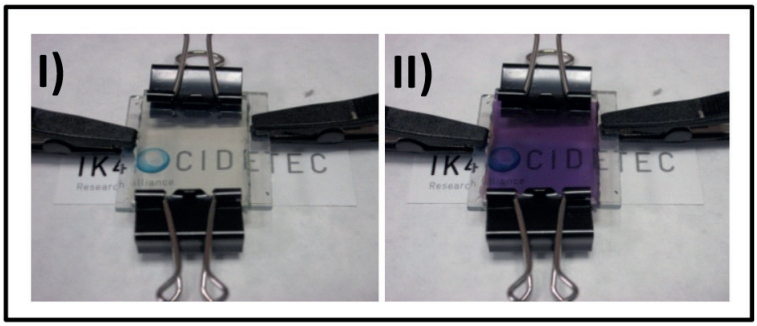

Figure 4.7. ECD comprising **Gel 3g$_9$**, in the off-bleached (I) and colored state after applying a voltage of -2.3 V (II).

This system (**Gel 3g$_9$**) was selected for the further characterizations as detailed in the following sections.

4.3.3. Electrochromic properties

The electrochromic performance of ECDs comprising **Gel 3g$_9$** was characterized in terms of transmittance change (Δ%T), switching times for coloration and bleaching processes (t_c and t_b), color coordinates (CIE *L*a*b*) and coloration efficiencies (η). As summarized in the Table 4.4, the **Gel 3g$_9$** exhibited great transmittance changes of 58% at 550 nm, and excellent switching times of 4 - 5 s for the bleaching and coloring processes, respectively. These low switching times, in the range of the ones reported for ECDs having gel or liquid electrolytes (1-8 s)[25] and overrunning some solid-state organic ECDs (4-60 s),[8b, 11b, 26] may be attributed to the dynamic character of the PVA-borax gel which might ease the transport of material and therefore the switching response.

Table 4.4. Electrochromic properties and color coordinates (D65) of **Gel 3g$_9$**.

State	%T[a]	t (s) [b]	CE (cm^2 C^{-1}) [c]	x[d]	y[d]	Y[d]	L*[e]	a*[e]	b*[e]	Color[f]
Bleached (0 V)	67	4	149	0.328	0.349	67.8	86	-2	9	
Colored (-2.3V)	9	5	75	0.319	0.226	14.4	45	37	-24	

[a] %T = % of Transmittance at the maximum contrast wavelength (550 nm); [b] Switching times; [c] Color efficiencies; [d], [e] Color coordinates obtained by spectrophotometric method (D65): [d] xyY 1931 and [e] *L*a*b** 1976; [f] Color interpretation of the corresponding color coordinates (L**a*b*).

The higher color efficiency obtained during the bleaching process for 4 cm^2-sized devices comprising **Gel 3g$_9$** could be ascribed to the ferricyanide mediator, which causes a very rapid chemical oxidation of the radical-cationic form (bipm$^{+\bullet}$), to reform the dication (bipm^{2+}). [27] Possible entry of oxygen in the device could also lead to the same effect.

The color coordinates obtained by spectrophotometric method, (Table 4.4) revealed the contribution of both red (+*a**) and blue (-*b**) colors at the reduced state leading to the purple coloration observed. This perceived hue is related to the color mixing of the blue ethyl viologen radical cation (bipm$^{+\bullet}$) in equilibrium with the red ethyl viologen radical cation dimer ((bipm)$_2^{2+}$) that is likely to be formed in the aqueous electrolyte solution.[28]

*L*a*b* color coordinates of the same ECD comprising **Gel 3g$_9$** were additionally measured by colorimetric method for comparative purposes. The coordinates obtained at colored state, (i.e., $L^\star$ = 7.12, $a^\star$ = 18.08 and $b^\star$ = -21.02) also confirmed the influence of red and blue colorations, although they translate into darker colorations as deduced form the lower value of $L^\star$. This difference may be ascribed to the required opaque background while using colorimetric method. As the results obtained by spectrophotometric

method were in better agreement with the observed colorations, it was selected for the further characterization.

It should be noted that despite the slight absorption of the ferro/ferricyanide pair at the bleached state (~ 420 nm), its contribution to the overall color of the device is negligible at the chosen concentration. It was equally confirmed by the very similar color coordinates obtained at bleached state for bare PVA-borax gel exempted from **[EtVio]** and redox pair (**Gel 1**) (i.e., L^* = 87, a^* = -2 and b^* = 9) and for **Gel 2b** comprising 6 mmol L^{-1} of redox pair (i.e., L^* = 87, a^* = -4 and b^* = 12).

The rheological behavior and the conductivity of the electrochromic **Gel 3g$_9$** was also evaluated. These characterizations are described in the following sections.

4.3.4. Rheological behavior

The rheological behavior of bare PVA-borax gel without neither viologen nor potassium ferrocyanide/ferricyanide salts (**Gel 1**) was first studied and compared with that obtained for optimized **Gel 3g$_9$**.

As shown in Figure 4.8, **Gel 1** presented a liquid-like behavior at low frequencies with storage modulus lower than loss modulus (G' < G"). Then, a liquid-to-gel transition (G' = G") was observed at a frequency of 2 Hz, and at higher frequencies, **Gel 1** exhibited solid-like behavior, with G' > G". This rheological behavior was as expected for a viscoelastic fluid, also in agreement with previous studies dealing with PVA-borax gels.[19l, 29]

For the fully formulated **Gel 3g$_9$** (Figure 4.8), although the liquid-to-gel transition was shifted to lower frequencies (0.4 Hz) indicating a more solid-like character, similar viscoelastic response was observed. Therefore, despite the addition of electroactive materials required to achieve high-performance EC formulation, the gel remains a viscoelastic fluid. Indeed, such particular rheological behavior permits the facile manipulation of this electrolyte mixtures during the device assembling process.

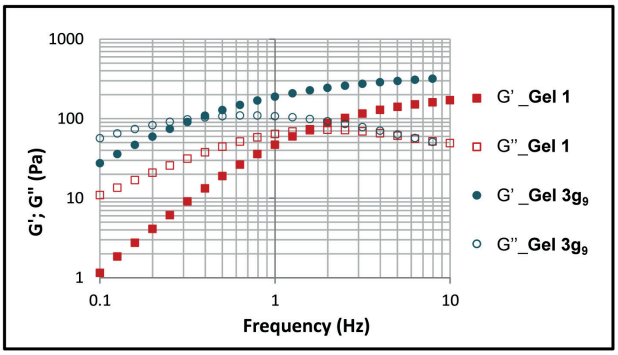

Figure 4.8. Dynamic rheological behaviors of **Gel 1** and **Gel 3g$_9$**. Filled and empty symbols correspond to storage (G') and loss (G") modulus, respectively.

4.3.5. Conductivity

It would be expected that the labile bonding between the PVA hydroxyl groups and the negatively charged central boron atoms could offer some ionic conductivity,[19f] also enhancing the flow of the electroactive materials through the polymer network. The variation of the ionic conductivity of different PVA-borax gels is presented as a function of 1 000 T^{-1} in Figure 4.9. As expected, the conductivity of the electrolyte gels was highly dependent on the content of ionic species and also on the temperature. In order to evaluate the contribution of the different ionic species present in the final ECDs, the conductivities of neat PVA-borax gel (**Gel 1**), the gel containing just the redox pair (**Gel 2b**) and the fully formulated Gel (**Gel 3g$_9$**) were compared. As anticipated, the conductivity increased with the presence of redox pair and viologen, in the following order: **Gel 1** < **Gel 2b** < **Gel 3g$_9$**. The ionic conductivity also increased with the temperature in a similar manner to that reported for other gel and highly viscous electrolytes.[1b, 3a, 30]

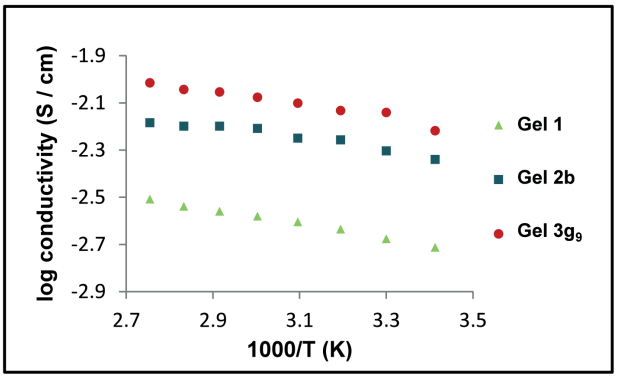

Figure 4.9. Variation in the conductivity of **Gel 1** (bare gel), **Gel 2b** (6 mmol L^{-1} of 1:1 mixture of ferro/ferricyanide potassium salts) and **Gel 3g$_9$** (6 mmol L^{-1} of 1:1 mixture of ferro/ferricyanide potassium salts and 20 mmol L^{-1} of ethyl viologen) as a function of temperature.

4.3.6. Cyclability

Cyclability of ECDs is a very important issue as far as their industrial applicability is concerned. In order to analyze the cyclability of the ECDs described in this chapter, three identical ECDs were fabricated from **Gel 3g$_9$**. These ECDs were hermetically sealed using a UV-curable adhesive and switched between colored (-2.3 V for 20 s) and bleached states (0 V for 180 s).

The results indicated that these ECDs maintained their switching response and transmittance change (Δ%T) up to 10 000 cycles (Figure 4.10). Above these cycles, the bleached state started showing a slightly pink coloration, leading to a decrease in the transmittance change. Thus, the Δ%T was 58% up to 10 000 cycles, being diminished to 50% after 15 000 cycles and to 33% after 25 000 cycles.

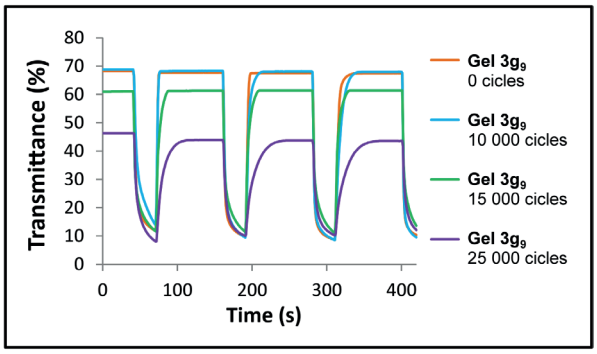

Figure 4.10. Evolution of the cycling performance of ECDs comprising **Gel 3g9** after 10 000, 15 000 and 25 000 cycles. Transmittance changes registered at 550 nm while potential-steps between colored (-2.3 V for 30 s) and bleached state (0 V for 90 s) were being applied.

It is worth pointing out that some previously published studies affirmed that the all-in-one configurations (substrate/TCO/EC formulation/TCO/substrate) were unsuitable for most applications since the dimerization, comproportionation, and aging process present in these kind of devices reduce their durability.[31] Furthermore, although it has been repeatedly published that the redox reversibility of the viologens in aqueous solution was poor,[24, 32] PVA-borax electrolytic matrix seems to offer greater reversibility and therefore more competitive cyclability than other water-based electrolytes.

4.4. Conclusions

The successful employment of a new concept of semi-solid polyelectrolyte based on a non-Newtonian viscoelastic fluid which combines the advantages of both liquid and solid electrolytes while easing the device assembly was demonstrated.

The effective integration of the PVA-borax gel as electrolyte in layered ECDs wherein the viologen molecules were previously anchored was equally verified at a proof of concept stage.

The successful incorporation of electroactive materials into PVA-borax electrolytic matrix while maintaining the rheological properties of the gel was also proven, thus expanding the potential applicability of these gel electrolyte in all-in-on ECDs.

The performance of the all-in-one ECDs was enhanced by establishing the best concentration of electrochromic material (**[EtVio]** 20 mmol L^{-1}) and complementary redox pair (ferro/ferricyanide potassium salts 6 mmol L^{-1}), leading to ECDs with a transmittance change of around 60% and fast bleaching and coloring response (i.e., 4 - 5 s). The rheological behavior, ionic conductivity and cyclability (up to 25 000 cycles) of the enhanced formulations were also evaluated. Additionally, the easy adaptability of the formulations to achieve tailored levels of coloration and switching times of the resulting ECDs was confirmed.

The competitive performance obtained in terms of transmittance, response time, conductivity and cyclability suggest that the PVA-borax gel could have a very promising potential for the fabrication of high-performance, easy-to-make inexpensive ECDs. Accordingly, this PVA-borax gel will be employed in the following chapters as polyelectrolyte in both all-in-one and layered ECDs.

4.5. References

[1] a) M. Kucharski, T. Lukaszewicz, P. Mrozek, *Opto-Electronics Review* **2004**, *12*, 175-180 ; b) S. S. Sekhon, Deepa, S. A. Agnihotry, *Solid State Ionics* **2000**, *136–137*, 1189-1192.

[2] Å. Stefan, *J. New Mater. Electrochem. Syst.* **2001**, *4*, 173-179.

[3] a) S. A. Agnihotry, Nidhi, Pradeep, S. S. Sekhon, *Solid State Ionics* **2000**, *136–137*, 573-576; b) R. J. Mortimer, *Annu. Rev. Mater. Res.* **2011**, *41*, 241-268.

[4] P. Bonhôte, E. Gogniat, F. Campus, L. Walder, M. Grätzel, *Displays* **1999**, *20*, 137-144.

[5] a) C. Pozo-Gonzalo, M. Salsamendi, A. Viñuales, J. A. Pomposo, H.-J. Grande, *Sol. Energy Mater. Sol. Cells* **2009**, *93*, 2093-2097; b) C. P. Gonzalo, R. M. Garcia, M. S. Telleria, J. A. P. Alonso, H. J. G. Telleria, **2011**; c) G. C. Pozo, G. R. Marcilla, T. M. Salsamendi, A. J. A. POMPOSO, T. H. J. GRANDE, **2012**.

[6] R. Cinnsealach, G. Boschloo, S. Nagaraja Rao, D. Fitzmaurice, *Sol. Energy Mater. Sol. Cells* **1998**, *55*, 215-223.

[7] a) L. Su, Z. Xiao, Z. Lu, *Mater. Chem. Phys.* **1998**, *52*, 180-183; b) L. Su, H. Wang, Z. Lu, *Mater. Chem. Phys.* **1998**, *56*, 266-270; c) S. Lianyong, W. Hong, L. Zuhong, *Supramolecular Science* **1998**, *5*, 657-659; d) L. Su, Z. Xiao, Z. Lu, *Thin Solid Films* **1998**, *320*, 285-289.

[8] a) S. Lianyong, F. Jinghuai, L. Zuhong, *Jpn. J. Appl. Phys.* **1997**, *36*, 5747-5750; b) D. Mecerreyes, R. Marcilla, E. Ochoteco, H. Grande, J. A. Pomposo, R. Vergaz, J. M. Sánchez Pena, *Electrochim. Acta* **2004**, *49*, 3555-3559.

[9] S. S. Sekhon, N. Arora, S. A. Agnihotry, *Solid State Ionics* **2000**, *136–137*, 1201-1204.

[10] a) M. M. Silva, P. C. Barbosa, L. C. Rodrigues, A. Gonçalves, C. Costa, E. Fortunato, *Optical Materials* **2010**, *32*, 719-722; b) S. C. de Oliveira, L. C. de Morais, A. A. da Silva Curvelo, R. M. Torresib, *J. Electrochem. Soc.* **2003**, *150*, E578-E583.

[11] a) C. O. Avellaneda, D. F. Vieira, A. Al-Kahlout, E. R. Leite, A. Pawlicka, M. A. Aegerter, *Electrochim. Acta* **2007**, *53*, 1648-1654; b) C. O. Avellaneda, D. F. Vieira, A. Al-Kahlout, S. Heusing, E. R. Leite, A. Pawlicka, M. A. Aegerter, *Sol. Energy Mater. Sol. Cells* **2008**, *92*, 228-233.

[12] a) Q. Du, X. Fu, S. Liu, L. Niu, *Polymer International* **2012**, *61*, 222-227; b) S.-Y. Kao, C.-W. Kung, H.-W. Chen, C.-W. Hu, K.-C. Ho, *Sol. Energy Mater. Sol. Cells* **2016**, *145, Part 1*, 61-68.

[13] a) Y.-S. Ye, J. Rick, B.-J. Hwang, *Journal of Materials Chemistry A* **2013**, *1*, 2719-2743; b) A. L. Saroj, R. K. Singh, *Journal of Physics and Chemistry of Solids* **2012**, *73*, 162-168.

[14] P. Vidinha, N. M. T. Lourenco, C. Pinheiro, A. R. Bras, T. Carvalho, T. Santos-Silva, A. Mukhopadhyay, M. J. Romao, J. Parola, M. Dionisio, J. M. S. Cabral, C. A. M. Afonso, S. Barreiros, *Chemical Communications* **2008**, 5842-5844.

[15] a) H.-C. Lu, S.-Y. Kao, H.-F. Yu, T.-H. Chang, C.-W. Kung, K.-C. Ho, *ACS Appl. Mater. Interfaces* **2016**, *8*, 30351-30361; b) R. Marcilla, F. Alcaide, H. Sardon, J. A. Pomposo, C. Pozo-Gonzalo, D. Mecerreyes, *Electrochemistry Communications* **2006**, *8*, 482-488.

[16] a) T.-H. Chang, C.-W. Hu, R. Vittal, K.-C. Ho, *Sol. Energy Mater. Sol. Cells* **2014**, *126*, 213-218; b) H.-C. Lu, S.-Y. Kao, T.-H. Chang, C.-W. Kung, K.-C. Ho, *Sol. Energy Mater. Sol. Cells* **2016**, *147*, 75-84; c) A. M. Soutar, D. R. Rosseinsky, W. Freeman, X. Zhang, X. How, H. Jiang, X. Zeng, X. Miao, *Sol. Energy Mater. Sol. Cells* **2012**, *100*, 268-270; d) G. Chidichimo, B. C. De Simone, D. Imbardelli, M. De Benedittis, M. Barberio, L. Ricciardi, A. Beneduci, *The Journal of Physical Chemistry C* **2014**, *118*, 13484-13492.

[17] C. A. Nguyen, A. A. Argun, P. T. Hammond, X. Lu, P. S. Lee, *Chem. Mater.* **2011**, *23*, 2142-2149.

[18] a) S. J. Rowan, S. J. Cantrill, G. R. L. Cousins, J. K. M. Sanders, J. F. Stoddart, *Angewandte Chemie International Edition* **2002**, *41*, 898-952; b) Y. Jin, C. Yu, R. J. Denman, W. Zhang, *Chem. Soc. Rev.* **2013**, *42*, 6634-6654.

[19] a) E. Z. Casassa, A. M. Sarquis, C. H. Van Dyke, *J. Chem. Educ.* **1986**, *63*, 57; b) *Vol. Jan. 18, 2017*, RSC Advancing the Chemical Sciences, http://www.rsc.org/learn-chemistry/resource/res00000756/; c) K. W. McLaughlin, N. K. Wyffels, A. B. Jentz, M. V. Keenan, *J. Chem. Educ.* **1997**, *74*, 97; d) E. T. Wise, S. G. Weber, *Macromolecules* **1995**, *28*, 8321-8327; e) H.-L. Lin, Y.-F. Liu, T. L. Yu, W.-H. Liu, S.-P. Rwei, *Polymer* **2005**, *46*, 5541-5549; f) H. Ochiai, Y. Fujino, Y. Tadokoro, I. Murakami, *Polym J* **1982**, *14*, 423-426; gR. K. Schultz, R. R. Myers, *Macromolecules* **1969**, *2*, 281-285; h) V. de Zea Bermudez, P. P. de Almeida, J. F. Seita, *J. Chem. Educ.* **1998**, *75*, 1410; i) D. A. Katz., *Vol. Jan. 18, 2017*, http://www.chymist.com/PVA%20Slime.pdf, **2005**; j*) Vol. Jan. 18, 2017*, https://projects.ncsu.edu/project/chemistrydemos/Organic/Slime.pdf; k) G. A. Hurst, M. Bella, C. G. Salzmann, *J. Chem. Educ.* **2015**, *92*, 940-945; l) A. Koike, N. Nemoto, T. Inoue, K. Osaki, *Macromolecules* **1995**, *28*, 2339-2344; m) G. G. Stroebel, J. A. Whitesell, R. M. Kriegel, *J. Chem. Educ.* **1993**, *70*, 893.

[20] D. A. Katz, *J. Chem. Educ.* **1994**, *71*, 891.

[21] H. Ochiai, S. Fukushima, M. Fujikawa, H. Yamamura, *Polym J* **1976**, *8*, 131-133.

[22] J. Bruinink, C. G. A. Kregting, J. J. Ponjeé, *J. Electrochem. Soc.* **1977**, *124*, 1854-1858.

[23] S. Bhandari, M. Deepa, A. K. Srivastava, S. T. Lakshmikumar, RamaKant, *Solid State Ionics* **2009**, *180*, 41-49.

[24] J. Mizuguchi, H. Karfunkel, *Ber. Bunsen-Ges. Phys. Chem.* **1993**, *97*, 1466-1472.

[25] a) R. D. Rauh, F. Wang, J. R. Reynolds, D. L. Meeker, *Electrochim. Acta* **2001**, *46*, 2023-2029; b) P.-H. Aubert, A. A. Argun, A. Cirpan, D. B. Tanner, J. R. Reynolds, *Chem. Mater.* **2004**, *16*, 2386-2393.

[26] a) M. A. De Paoli, G. Casalbore-Miceli, E. M. Girotto, W. A. Gazotti, *Electrochim. Acta* **1999**, *44*, 2983-2991; b) F. Tran-Van, L. Beouch, F. Vidal, P. Yammine, D. Teyssié, C. Chevrot, *Electrochim. Acta* **2008**, *53*, 4336-4343.

[27] G. Levey, T. W. Ebbesen, *The Journal of Physical Chemistry* **1983**, *87*, 829-832.

[28] a) P. M. S. Monk, *Dyes Pigm.* **1998**, *39*, 125-128; b) R. J. Mortimer, T. S. Varley, *Chem. Mater.* **2011**, *23*, 4077-4082.

[29] T. Inoue, K. Osaki, *Rheologica Acta* **1993**, *32*, 550-555.

[30] S. A. Agnihotry, P. Pradeep, S. S. Sekhon, *Electrochim. Acta* **1999**, *44*, 3121-3126.

[31] J.-H. Ryu, M.-S. Park, K.-D. Suh, *Colloid Polym. Sci.* **2007**, *285*, 1675-1681.

[32] C. L. Bird, A. T. Kuhn, *Chem. Soc. Rev.* **1981**, *10*, 49-82.

CHAPTER 5

COLORLESS TO NEUTRAL-COLOR ALL-IN-ONE ELECTROCHROMIC DEVICES BASED ON ASYMMETRIC VIOLOGENS

5.1. Introduction

To expand the potential of the electrochromic technology, researches have conducted a large amount of inquiry in the last years on generating full-color devices and diversifying the colors of the EC materials.[1] However, among all palette of colors, ECDs that provide more neutral (i. e., grayish) colorations remain a field to be explored.[2] Neutral-tones such as gray not only adapt better aesthetically to the surrounding environment easing their implementation in different applications, but also absorb in the most of the visible range, making them excellent candidates for effective light filtering.

The reported strategies to achieve colorless to neutral-color electrochromic devices comprise different color chromophores through coupling their absorption profiles. These approaches include EC formulations based on 3 viologens,[3] or more complex device configurations such as ECDs containing one of the electrodes doubly layered (i. e., blue and green viologen-modified nanostructured films successively deposited on the working electrode),[4] devices with both electrodes bilayered (one of them with two cathodically colored polymers and the other with anodically colored polymers),[5] or even devices including four electrodes (two working electrodes and two counter electrodes).[6]

An interesting approach to achieve neutral-color ECDs while avoiding the complexity in the device architecture comprises the design and synthesis of new molecules which incorporate two different chromophores.[7] In this regard, some "black-to-transmissive" EC polymers have been synthesized through random copolymerization of two different monomers.[8] The

parallelism of this concept in the field of viologens might be the synthesis of asymmetric violgens. The viologens exhibit different colors in their reduced state depending on the nature of the substituents bonded to the nitrogen atoms. Hence, as pointed out in the introductory chapters, 1,1'-alkyl substituted viologens provide blue/violet color,[9] whereas 1,1'-aryl substituted viologens usually exhibit green colorations upon applying a suitable reduction potential.[9-10] The most wide studied viologens are symmetrically 1,1'- alkyl or 1,1'-aryl substituted, thus provide pure colors in their reduced states. However, asymmetrically 1-alkyl-1'-aryl substituted viologens might show more neutral colors about midway between alkyl and aryl-substituted viologens due to the contribution of both groups. Nevertheless, although some asymmetric viologens have been reported for other purposes as explained in section 2.2.1,[11] they were not specifically designed for neutral color electrochromics. Therefore, the design and synthesis of asymmetric viologens aiming at achieving colorless-to-neutral color (gray) electrochromism was addressed in the present chapter. Moreover, facing the challenge of maintaining very simple device architecture, all-in-one ECDs were developed in this section. Taking into account the successful results obtained in the previous chapter, PVA-borax gel was chosen as electrolytic media.

5.1.1. Objective

The main goal of the research study described in this chapter was to develop all-in-one ECDs which switched from colorless-off state to neutral colored state, while offering high performance.

To achieve this objective, the synthesis of 1-alkyl-1'-aryl substituted viologens exempted from anchoring group and their successful incorporation in the PVA-borax gel electrolytic matrix was required.

The spectroelectrochemical study of these new colorless-to- neutral color EC systems based on 1-alkyl-1'-aryl asymmetric viologens and their

comparison with the corresponding symmetric viologens was equally necessary to assess their intermediate EC behavior.

Studying the response of the devices including switching time and cycling performance as well as finding out more about the effect of the solvent in the observed coloration were important issues to be explored.

5.2. Materials and methods

5.2.1. Materials

Poly(vinyl alcohol) (PVA, Mw 61 000), sodium tetraborate decahydrate (borax, 99.5%), potassium ferrocyanide (98.5%) potassium ferricyanide (99%), 4,4'-bipyridyl (98%), 2,4-dinitrochlorobenzene (99%), *p*-cyanoaniline (98%), ethyl bromide (98%), benzyl bromide (98%), hydroquinone (≥ 99%) and 1-butyl-3-methylimidazolium tetrafluoroborate (98%), were purchased from Sigma-Aldrich and used without further purification. Charcoal activated powder and required solvents such as acetone, ethanol, THF, acetonitrile, methanol, diethyl ether and propylene carbonate were supplied by Scharlab and used as received. Fluorine-doped tin oxide and indium tin oxide coated glass substrates (R_s 6-8 and 25-35 Ωsq^{-1}, respectively) were provided by Solems and cleaned with warm acetone prior to use.

5.2.1.1. Synthesis and characterization of viologens

Asymmetric viologens were synthesized as follows:

1-(2,4-Dinitrophenyl)-4,4'-bipyridinium Monochloride (intermediate [**I**]) was synthesized by Zincke reaction according to previously reported procedure.[12] In brief, a mixture of 4,4'-bipyridyl (50 mmol) and 2,4-dinitrochlorobenzene (50 mmol) was refluxed in ethanol (125 mL) for 16 h. The ethanol was removed by rotary evaporation *in vacuo*, acetone was added (150 mL) and the solution was stirred for 2 h. The resulting brownish

appearance solid was filtered and recrystallized from ethanol and acetone followed by drying in vacuo. (yield = 40%). ^{1}H NMR (500 MHz, D_2O, δ): 9.42 ppm (s, 1H), 9.28 ppm (d, 2H, *J* = 6.76 Hz), 8.97 and 8.95 ppm (d of d, 1H, J = 2.42 and 2.43 Hz), 8.87 ppm (d, 2H, *J* = 6.15 Hz), 8.72 ppm (d, 2H, *J* = 6.78 Hz), 8.30 ppm (d, 1H, *J* = 8.69 Hz), 8.06 ppm (d, 2H, *J* = 6.19 Hz).

1-(p-Cyanophenyl)-4,4'-bipyridinium Monochloride (intermediate [**II**]) was synthesized as follows: a mixture of 1-(2,4-dinitrophenyl)-4,4'-bipyridinium monochloride [**I**] (15 mmol) and *p*-cyanoaniline (30 mmol) was refluxed in deionized water (30 mL) for 48 h. After cooling, the resulting solid was filtered. The solid residue was removed and the filtrate was decolorized with charcoal activated powder for 16 h. The water of the filtrate was removed by rotary evaporation *in vacuo*, THF was added (150 mL), and the solid was filtered followed by drying under vacuum. (Yield = 79%). ^{1}H NMR (500 MHz, D_2O, δ): 9.32 ppm (d, 2H, *J* = 6.95 Hz), 8.86 ppm (d, 2H, *J* = 6.11 Hz), 8.68 ppm (d, 2H, *J* = 6.93 Hz), 8.20 ppm (d, 2H, *J* = 8.75 Hz), 8.05 ppm (m, 4H). IR (bulk ATR): ν (cm^{-1}) = 3104 (C-H olefin st), 2233 (-CN st), 1632 (C=N st), 1594, 1502 (C=C), 815 (*o*-phenylene H); IC: % Cl^- calculated for $C_{17}H_{12}N_3Cl$, 12.1%; found, 11.8%.

1-Ethyl-1'-(p-cyanophenyl)-4,4'-bipyridinium dibromide [**Et-pCNVio**] was synthesized as follows: a mixture of 1-(*p*-cyanophenyl)-4,4'-bipyridinium monochloride [**II**] (3.5 mmol) and ethyl bromide (18 mmol) was refluxed in acetonitrile (20 mL) for 48 hours. The cooled solution was filtered and the resulting yellowish powder was washed with acetonitrile and acetone. (Yield = 87%). Elemental analysis data: Anal. Calcd for $C_{19}H_{17}N_3Br_2$: C, 51.03; H, 3.83; N, 9.40. Found: C, 48.47; H, 4.17; N, 9.35. ^{1}H NMR (500 MHz, DMSO-*d6*, δ): 9.70 ppm (d, 2H, *J* = 6.90 Hz), 9.45 ppm (d, 2H, *J* = 6.79 Hz), 8.99 ppm (d, 2H, *J* = 6.91 Hz), 8.92 ppm (d, 2H, *J* = 6.61 Hz), 8.32 ppm (d, 2H, *J* = 8.67 Hz), 8.18 ppm (d, 2H, *J* = 8.69 Hz), 4.75 ppm (q, 2H), 1.61 ppm (t, 3H) (Figure 5.1). ^{13}C NMR (500 MHz, D_2O, δ ppm): 154.3, 152.1, 148.1, 147.6, 137.5, 129.8, 128.0, 120.4, 117.6, 60.5, 18.2 (Figure 5.2). IR (bulk ATR): ν (cm^{-1}) = 3098 (C-H olefin st), 2990 (C-H alkyl st), 2227 (-CN st), 1635 (C=N st), 1600, 1495 (C=C), 1435 (C-H alkyl δ), 824 cm^{-1}

(*o*-phenylene H); IC: % Br^- calculated for $C_{19}H_{17}N_3Br_2$, 35.7%; found, 33.5% (Figure 5.3).

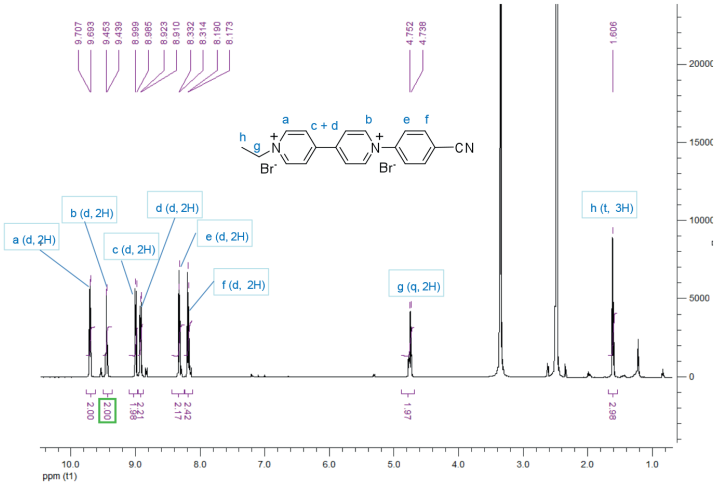

Figure 5.1. ^{1}H NMR spectra of **[Et-pCNVio]**.

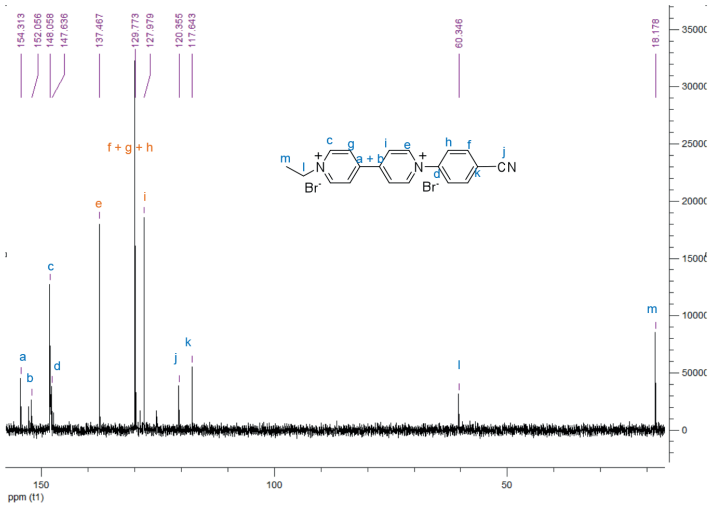

Figure 5.2. ^{13}C NMR spectra of **[Et-pCNVio]**. Estimation quality is indicated by color: good, rough.

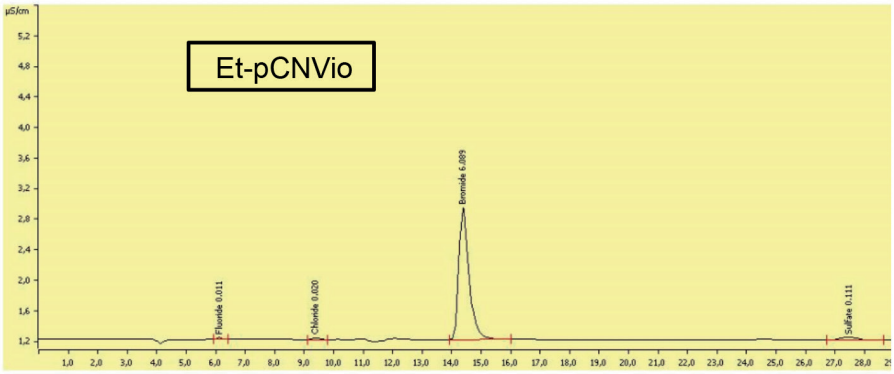

Figure 5.3. Anion chromatogram of [**Et-pCNVio**].

1-Benzyl-1'-(p-cyanophenyl)-4,4'-bipyridinium dibromide [**Bn-pCNVio**] was synthesized following the same procedure described above for the [**Et-pCNVio**], using benzyl bromide as alkyl substituent instead (Yield = 89%). Elemental analysis data: Anal. Calcd for $C_{24}H_{19}N_3Br_2$: C, 56.60; H, 3.76; N, 8.25. Found: C, 56.01; H, 4.18; N, 8.51. ^{1}H NMR (500 MHz, D_2O, δ): 9.47 ppm (d, 2H, J = 6.96 Hz), 9.25 ppm (d, 2H, J = 6.85 Hz), 8.79 ppm (d, 2H, J = 6.96 Hz), 8.68 ppm (d, 2H, J = 6.80 Hz), 8.21 ppm (d, 2H, J = 8.78 Hz), 8.07 ppm (d, 2H, J = 8.79 Hz), 7.58 ppm (s, 5H), 6.00 ppm (s, 2H) (Figure 5.4). ^{13}C NMR (500 MHz, D_2O, δ ppm): 154.2, 152.6, 148.3, 148.2, 147.7, 137.6, 134.8, 132.9, 132.4, 132.0, 130.0, 129.9, 128.1, 120.4, 117.8, 67.6 (Figure 5.5). IR (bulk ATR): ν (cm^{-1}) = 3101, 3025 (C-H olefin st), 2987 (C-H alkyl st), 2227 (-CN st), 1635 (C=N st), 1495 (C=C), 1435 (C-H alkyl δ), 827 (*o*-phenylene H); IC: % Br^- calculated for $C_{24}H_{19}N_3Br_2$, 31.4%; found, 30.1% (Figure 5.6).

Information regarding the synthesis procedures followed to obtain symmetric viologens employed for comparative purposes is detailed below.

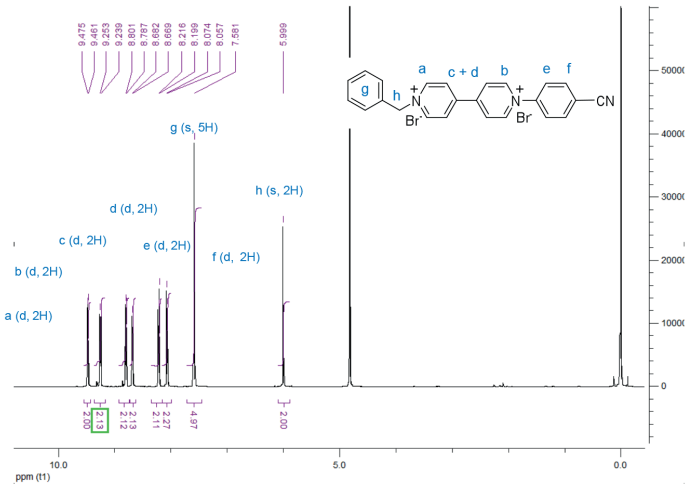

Figure 5.4. [1]H NMR spectra of **[Bn-pCNVio]**.

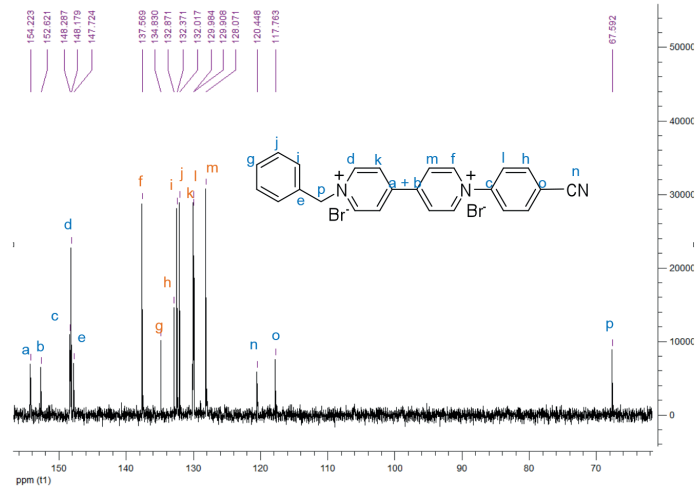

Figure 5.5. [13]C NMR spectra of **[Bn-pCNVio]**. Estimation quality is indicated by color: good, rough.

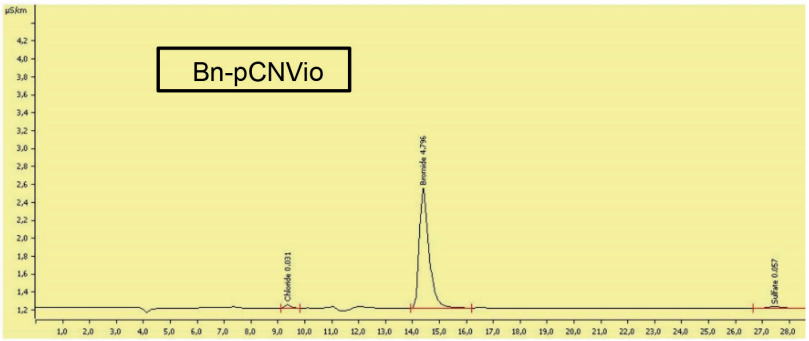

Figure 5.6. Anion chromatogram of [**Et-pCNVio**].

1,1'-Bis-(p-cyanophenyl)-4,4'-bipyridilium dichloride [**pCNVio**] was synthesized as follows: 4,4'-bipyridyl (98%) (40 mmol) and 2,4-dinitrochlorobenzene (100 mmol) were refluxed in ethanol (250 ml) for 16 hours. After cooling, the precipitate was filtered and washed with acetone to obtain 1,1'-bis-(2,4-dinitrophenyl)-4,4'-bipyridilium dichloride. (Yield = 95%). 7 mmol of this intermediate product were dissolved with *p*-cyanoaniline (20 mmol) in 100 ml of water and refluxed very strongly for 48 hours. The water was removed by rotary evaporation *in vacuo* and the dark solid residue extracted with hot methanol (150 ml, 3 h), to which ether was added (after reducing the volume to 30 ml aprox.) to effect precipitation of a crude product. Recrystallization of this powder from methanol and ether, followed by drying *in vacuo* produced a brownish appearance powder. (Yield = 75 %). ^{1}H NMR (500 MHz, DMSO-*d6*, δ): 9.77 and 9.18 ppm (d of d, 4H*J* = 4.00 Hz and 4H*J* = 3.84 Hz, Ar H), 8.35 and 8.23 ppm (d of d, 4H *J* = 7.56 Hz and 4H*J* = 7.26 Hz, bipyridine); IR (bulk ATR): ν (cm^{-1}) = 3091 (C-H olefin st), 2227 (-CNst), 1629(C=N st), 1603, 1508 (C=C), 831 (*o*-phenylene H); IC: % Cl^- calculated for $C_{24}H_{16}N_4Cl_2$: 16.4%, found 15.0%.

1,1'-Dibenzyl-4,4'-bipyridinium dibromide [**BnVio**] was synthesized as follows: a mixture of 4,4'-bipyridyl (10 mmol) and benzyl bromide (40 mmol) was refluxed in acetonitrile (15 mL) for 16 hours. After cooling, the resulting yellowish solid was filtered and washed with acetonitrile and

acetone. (Yield = 93%).^{1}H NMR (500 MHz, D_2O, δ): 9.18 ppm (d, 4H, *J* = 6.85 Hz), 8.55 ppm (d, 4H, *J* = 6.78 Hz), 7.55 ppm (s, 10H), 5.55 ppm (s, 4H); IR (bulk ATR): ν (cm^{-1}) = 3025 (C-H olefin st), 2994, 2946 (C-H alkyl st), 1629 (C=N st), 1492 (C=C), 1448, (C-H alkyl δ) 729 (*o*-phenylene H); IC: % Br^- calculated for $C_{24}H_{22}N_2Br_2$: 32.1%, found 32.4%.

Synthesis 1,1'-Diethyl-4,4'-bipyridinium dibromide **[EtVio]** has been described in the chapter 4.

5.2.2. Methods

5.2.2.1. Preparation of gel formulations

All gel formulations were prepared following the general procedure described in the section 2.2.2.1 of the chapter 2. Detailed information regarding the specific composition of the gels assessed in this chapter (i.e., concentration of complementary redox pair and viologen) are described below.

*Preparation of **pCNVio**, **EtVio** and **BnVio gels**:*

These electrochromic gels were prepared keeping the final concentration of corresponding symmetric viologens 1,1'-bis-(*p*-cyanophenyl)-4,4'-bipyridilium dichloride **[pCNVio]**, 1,1'-diethyl-4,4'-bipyridinium dibromide **[EtVio]** or 1,1'-dibenzyl-4,4'-bipyridinium dibromide **[BnVio]** at 10 mmol L^{-1} and the concentration of the ferro/ferricyanide potassium pair at 5 mmol L^{-1}.

*Preparation of **Et-pCNVio** and **Bn-pCNVio gels:***

These electrochromic gels were prepared keeping the final concentration of corresponding asymmetric viologens 1-ethyl-1'-(*p*-cyanophenyl)-4,4'-bipyridinium dibromide **[Et-pCNVio]** or 1-benzyl-1'-(*p*-cyanophenyl)-4,4'-bipyridinium dibromide **[Bn-pCNVio]** at 20 mmol L^{-1} and the concentration of the ferro/ferricyanide potassium pair at 5 mmol L^{-1}.

*Preparation of **EtVio + pCNVio gel***:

This electrochromic gel was prepared keeping the final concentration of both **[EtVio]** and **[pCNVio]** at 10 mmol L^{-1} and the concentration of the ferro/ferricyanide potassium pair at 5 mmol L^{-1}.

*Preparation of **BnVio + pCNVio gel***:

This electrochromic gel was prepared keeping the final concentration of both **[BnVio]** and **[pCNVio]** at 10 mmol L^{-1} and the concentration of the ferro/ferricyanide potassium pair at 5 mmol L^{-1}.

*Preparation of **Gel electrolyte***:

This viologen-free gel was prepared keeping the final concentration of the ferro/ferricyanide potassium pair at 5 mmol L^{-1}**.**

5.2.2.2. Preparation of anhydrous formulations

*Preparation of **anhydrous EC systems** (general procedure)*:

All liquid systems were prepared according to a procedure previously reported by our group.[13] Briefly, a mixture of the corresponding viologen (0.12 mmol), hydroquinone (0.14 mmol) and 1-Butyl-3-methylimidazolium tetrafluoroborate (18 mmol) was dissolved in 5 g of propylene carbonate and stirred until homogeneous solution was obtained.

*Preparation of **anhydrous electrolyte**:*

The procedure was similar to the one described above for ***anhydrous EC systems*** without adding any viologen.

5.2.2.3. Fabrication of electrochromic devices

All-in-one ECDs based on two-electrode (2-E) and three-electrode (3-E) configuration were assembled following the procedure described in the chapter 2 section 2.5.1. and 2.5.2., respectively.

5.3. Results and discussion

Two asymmetrically 1-alkyl-1'-aryl substituted viologens, specifically 1-ethyl-1'-(*p*-cyanophenyl)-4,4'-bipyridinium dibromide [**Et-pCNVio**] and 1-benzyl-1'-(*p*-cyanophenyl)-4,4'-bipyridinium dibromide [**Bn-pCNVio**] were synthesized following the synthetic route shown in the Scheme 5.1.

Scheme 5.1. Synthetic Route for Asymmetric Viologens [**Et-pCNVio**] and [**Bn-pCNVio**].

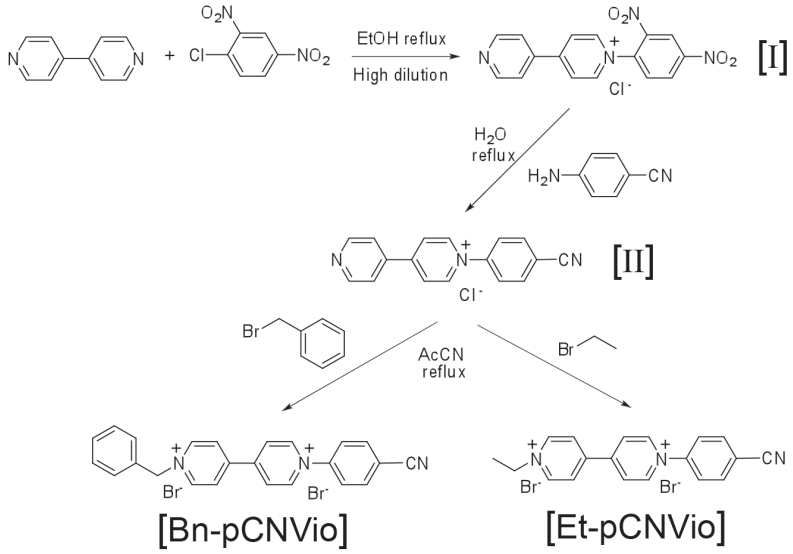

This procedure consists of three-steps wherein the aryl substituent was first attached by the well-known two-step Zincke reaction, while the alkyl group was second bonded through the corresponding alkyl halide. It is worth noting that the attachment of the alkyl chain in the first step is also possible through the employment of an adequate nonpolar solvent in which the monoalkyl substituted intermediate precipitates.[9] Regardless of the synthetic route, it is essential to ensure the formation of the pure monosubstituted intermediate, molecule [**I**] in the present case.

Corresponding symmetric viologens **[EtVio]**, **[BnVio]** and **[pCNVio]** were also synthesized for comparative purposes (Figure 5.7).

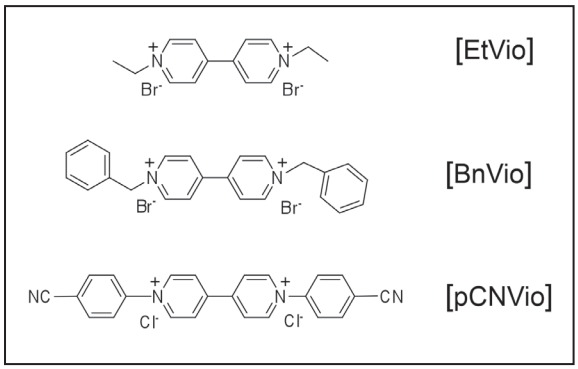

Figure 5.7. Chemical structures of **[EtVio]**, **[BnVio]** and **[pCNVio]** symmetric viologens.

5.3.1. Spectroelectrochemical Study of [Et-pCNVio] and [Bn-pCNVio] Asymmetric Viologens.

The electrochemical behavior of **[Et-pCNVio]** and **[Bn-pCNVio]** asymmetric viologens was investigated using three-electrode (3-E) ECD configuration provided with a pseudoreference electrode which enables the in situ spectroelectrochemical study of these EC materials. To this end, after systematic optimization study, EC formulations containing PVA-borax gel polyelectrolyte, **[Et-pCNVio]** and **[Bn-pCNVio]** as electrochromic materials (20 mmol L^{-1}) and potassium ferrocyanide/ferricyanide salts as complementary redox species (5 mmol L^{-1}) were formulated and the resulting **Et-pCNVio** and **Bn-pCNVio gels** were evaluated.

As proven in the previous chapter, this new concept of viscoelastic polyelectrolyte enables the easy fabrication of high-performance ECDs. Additionally, the non-electrochromic character of the viologen-free **Gel electrolyte** (5 mmol L^{-1} of ferro/ferricyanide potassium pair) at the

potential range employed was proven by spectroelectrochemical study using 3-E configuration (Figure 5.8).

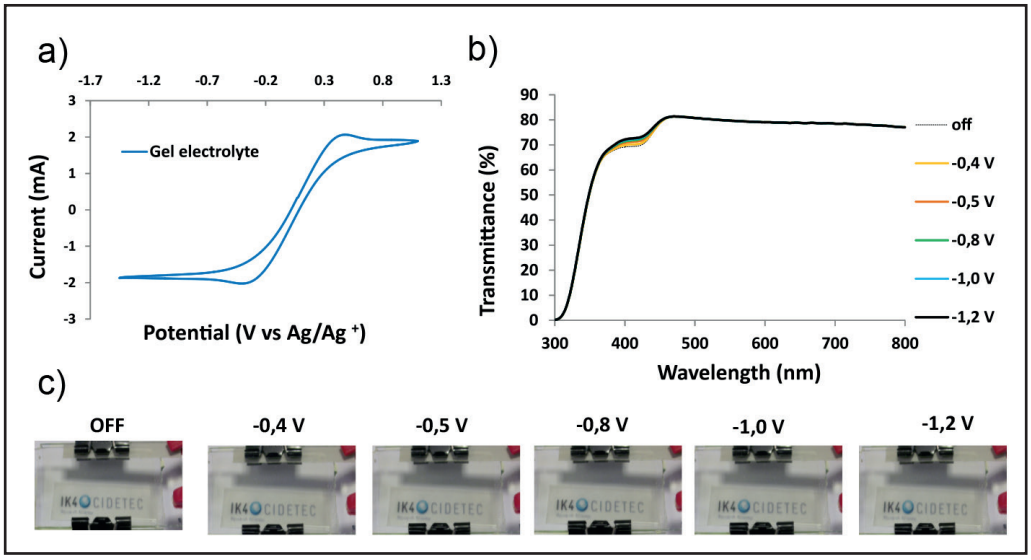

Figure 5.8. Spectroelectrochemical study of 3-E ECD containing **Gel electrolyte** for comparative purposes. a) Cyclic voltammetry (CV); b) UV/vis transmittance responses as a function of wavelength and (c) photograph of the device for different applied potentials from -0.4 to -1.2 V.

Figure 5.9a shows the cyclic voltammetry (CV) registered for **Et-pCNVio gel** while using 3-E configuration. Aside from the one which appears closer to 0 V assigned to the uncolored redox process of ferricyanide ion, two well-defined peaks were observed on the cathodic branche of the CV. The reduction peak observed at -0.7 V (vs Ag/Ag^{+}) (1) can be related to the radical-cation ($bipm^{+\bullet}$) obtained through the first reduction of the most stable dicationic form ($bipm^{2+}$), whereas the reduction peak registered at -1.2 V (vs Ag/Ag^{+}) (2) can be correlated with the neutral state ($bipm^{0}$), formed as a result of the second reduction of the dicationic form. The electrochemical behavior of **[Et-pCNVio]** asymmetric viologen, was compared to the ones exhibited by the corresponding symmetric viologens **[pCNVio]**, **[EtVio]** (Figure 5.9a inset), and it was found that the reduction

potentials of the [**Et-pCNVio**] asymmetric viologen were about midway between the values registered for the corresponding symmetric viologens, showing intermediate electrochemical character. A similar study was carried out with [**Bn-pCNVio**] asymmetric viologen and their corresponding symmetric viologens, [**Bn-pCNVio**] and [**pCNVio**], leading to the same conclusion (Figure 5.9b).

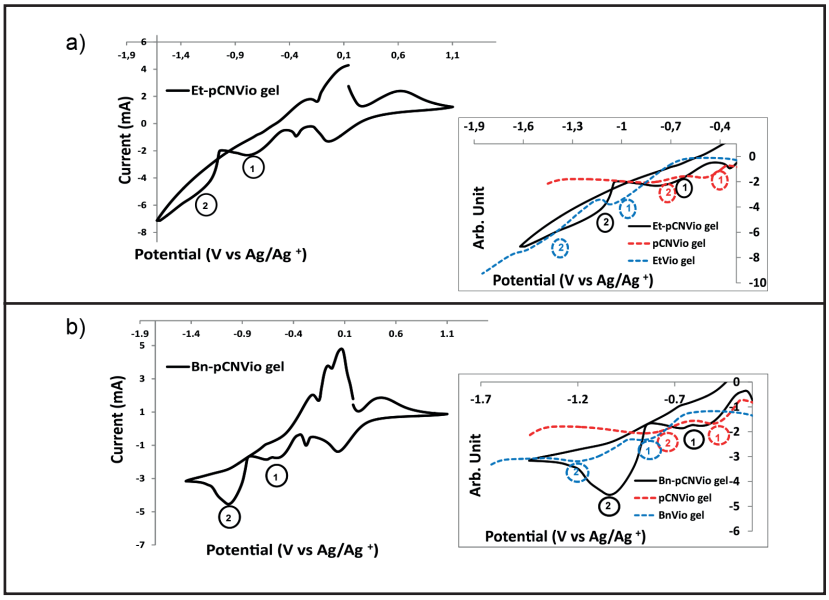

Figure 5.9. 3-E ECD of (a) **Et-pCNVio** and (b) **Bn-pCNVio gels**: cyclic voltammetry (CV) and the superposition of them (cathodic sweep) with voltammograms of the corresponding symmetric viologens separately (inset) (**pCNVio** and **EtVio gels** in a) and **pCNVio** and **BnVio gels** in b)). Electrochemical studies of the symmetric viologens carried out in standard electrochemical cells can be found in the literature. [10-11, 14]

The electrochromic behavior of the **Et-pCNVio** and **Bn-pCNVio gels** was also studied using the same 3-E configuration. As shown by the UV-vis transmittance responses of **Et-pCNVio** and **Bn-pCNVio gels** under different applied potentials (Figure 5.10a and b respectively) both asymmetric viologens exhibited different transmittance profiles. **Bn-**

pCNVio gel showed well-defined transmittance valleys at around 600 and 420 nm, meaning high absorption at these regions, whereas **Et-pCNVio gel**, on the contrary, absorbed more equally along most of the visible wavelength range.

Accordingly, observed colorations upon applying the first reduction potentials in each case revealed more neutral colored state for **Et-pCNVio gel** than the one observed for **Bn-pCNVio gel**.

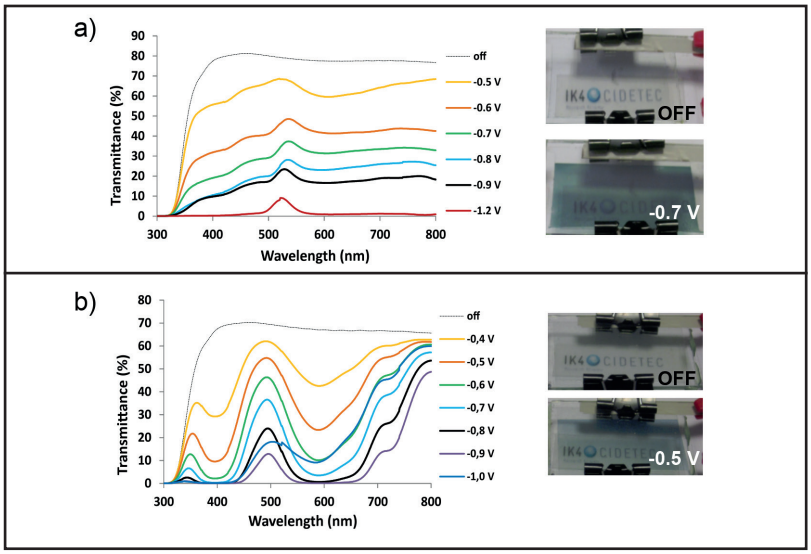

Figure 5.10. 3-E ECDs containing (a) **Et-pCNVio** and (b) **Bn-pCNVio gels**. UV-vis transmittance response at different applied potentials and observed coloration in their off state and while an appropriate reduction potential was being applied.

Color coordinates obtained by spectrophotometric method, also revealed more gray-EC behavior for the **Et-pCNVio gel** (Table 5.1), as the chromaticity values for both a^* and b^* were closer to 0 than the ones obtained for the **Bn-pCNVio gel** (Table 5.2). Indeed, the former exhibited more grayish coloration at low reduction potentials up to -0.9 V ($bipm^{+\bullet}$) being a^* and $b^* \leq |15|$, turning into more green color upon applying a reduction potential of -1.2 V ($bipm^0$), as confirmed by the more negative value of a^* component at this potential.

Table 5.1. % Transmittance, transmittance changes (Δ%T) and color coordinates of 3-E ECDs containing **Et-pCNVio gel**.

V	%T	Δ%T [a]	x [b]	y [b]	Y [b]	L^* [c]	a^* [c]	b^* [c]	Color [d]
off	77.5	-	0.309	0.326	78.4	91	0	-2	
-0.5	59.7	17.9	0.307	0.337	64.0	84	-6	2	
-0.6	41.5	36.0	0.317	0.353	44.1	72	-7	8	
-0.7	31.4	46.1	0.326	0.366	33.1	64	-7	11	
-0.8	23.1	54.4	0.335	0.380	24.2	56	-8	15	
-0.9	16.6	60.9	0.316	0.370	18.8	50	-10	9	
-1.2	0.9	76.6	0.234	0.559	3.3	21	-38	19	

[a] Transmittance change at λ = 600 nm. [b], [c] Color coordinates (D65): [b] xyY 1931 and [c] $L^*a^*b^*$ 1976. [d] Color interpretation of the corresponding color coordinates (L^*a^*b).

In the case of **Bn-pCNVio gel**, b^* components registered at different reduction potentials were negative up to -0.9 V showing more blue character, and acquired positive value upon applying -1.0 V, which corresponds to yellowish color.

The grayish EC behavior achieved with the **Et-pCNVio gel** (a^* and b^* < |15|) while maintaining highly-transmissive and colorless bleached state (%Tb ~ 77 %), along with competitive transmittance changes (i.e., ~ 60 %) is especially noteworthy. This system improves the performance of several polymer-based ECDs previously described in the literature even if providing gray color in their neutral state,[15] partially doped state,[16] or full-doped oxidized state,[17] did not exhibit a colorless bleached state.

Table 5.2. % Transmittance, transmittance changes (Δ%T) and color coordinates of 3-E ECDs containing **Bn-pCNVio gel**.

V	%T	Δ%T [a]	x [b]	y [b]	Y [b]	*L**[c]	*a** [c]	*b** [c]	Color [d]
off	67.1	-	0.309	0.326	67.9	86	0	-2	
-0.4	42.9	24.2	0.294	0.331	49.9	76	-9	-2	
-0.5	24.0	43.0	0.269	0.329	34.5	65	-17	-5	
-0.6	10.6	56.4	0.233	0.325	21.8	54	-27	-9	
-0.7	3.8	63.3	0.195	0.321	12.8	43	-35	-12	
-0.8	0.7	66.4	0.150	0.327	6.1	30	-43	-11	
-0.9	0.1	67.0	0.116	0.341	2.5	18	-42	-8	
-1.0	10.2	56.9	0.342	0.418	13.2	43	-12	20	

[a] Transmittance change at λ = 600 nm. [b], [c] Color coordinates (D65): [b] xyY 1931 and [c] $L^*a^*b^*$ 1976. [d] Color interpretation of the corresponding color coordinates (L^*a^*b).

Transmittance changes (Δ%T) and %T registered at the maximum contrast wavelength for different applied potentials along with the corresponding color interpretation of the L^*a^*b color coordinates are also summarized in Table 5.1 and 5.2 for **Et-pCNVio** and **Bn-pCNVio gels**, respectively.

5.3.2. Comparative Color Performance Study: Asymmetric vs Symmetric Viologens

With the aim of assessing the more neutral color provided by the asymmetric viologens, their electrochromic behavior was compared to the one exhibited by symmetric viologens and the mixture of them. To this end, PVA-borax gel formulations comprising a mixture of the corresponding symmetric viologens (10 mmol L^{-1} of each), **EtVio + pCNVio gel** in the case of **Et-pCNVio** and **BnVio + pCNVio gel** in the case of **Bn-pCNVio**, were also formulated. In this occasion, two-electrode (2-E) configuration

was used requiring higher operational voltages than the ones needed when 3-E configuration is being used.[18]

Additionally, while comparing ECDs based on different viologens, the cathodic potential required to form the radical-cation ($bipm^{+\bullet}$) differ from one viologen to another, as confirmed above, not allowing to select one specific reduction potential for all the studied systems. Consequently, the systematic procedure followed in this thesis to perform these comparative studies consisted on choosing in each case the potential required to achieve comparative values of Δ%T at the maximum contrast wavelength. To this end, the transmittance profiles of each EC system are previously registered independently at different applied potentials. As an example, Figure 5.11 shows the transmittance response obtained for 2-E ECDs comprising **Et-pCNVio** and **Bn-pCNVio gel** (a and b, respectively). The responses registered for ECDs based on symmetric viologens (**EtVio**, **BnVio** and **pCNVio gels**) and the mixtures of them (**EtVio + pCNVio** and **BnVio + pCNVio gels**) at different applied potentials are provided as Annex 5.1.

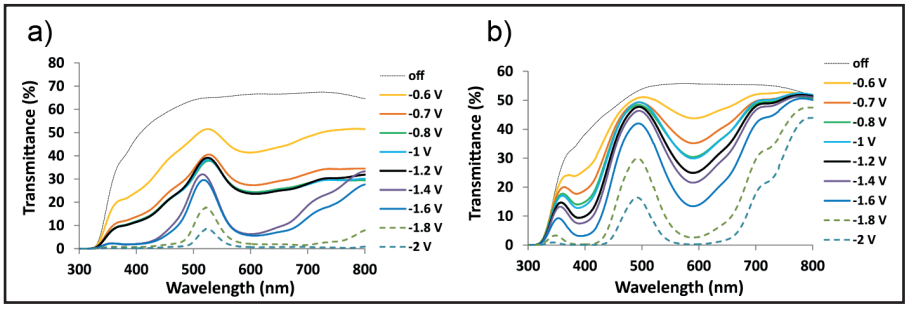

Figure 5.11. UV/Vis transmittance profiles of 2-E ECDs containing (a) **Et-pCNVio** and (b) **Bn-pCNVio gels**.

The final comparisons for each asymmetric viologen are summarized in the Figure 5.12. Figure 5.12a shows the transmittance profiles of four different 2-E ECDs containing **Et-pCNVio gel**, formulations comprising the corresponding symmetric viologens **EtVio** and **pCNVio gels**, as well as a composition including the mixture of them **EtVio + pCNVio gel**. In a

similar way, Figure 5.12b depicts the transmittance spectra of **Bn-pCNVio gel**, along with **BnVio**, **pCNVio** and **BnVio + pCNVio gels**.

The maximum absorption wavelength for the ECDs containing 1,1'-alkyl symmetric viologens, (**EtVio** and **BnVio gels**), was registered at around 550 nm, whereas the ones exhibited by **pCNVio gel** were found at 600 and 420 nm, as expected for violet and green materials respectively. Gels containing the mixture of the symmetric viologens, **EtVio + pCNVio** and **BnVio + pCNVio gels**, also displayed their maximum absorbance wavelengths at 600 and 420 nm, showing mainly the contribution of the 1,1'-aryl viologen. On the contrary, the ECDs comprising the asymmetric viologens, **Et-pCNVio** and **Bn-pCNVio gels**, exhibited a hypsochromic shift respect to **pCNVio** and mixed gels, but bathochromic shift respect to the **EtVio** and **BnVio gels**. This effect was less noticeable in the case of **Et-pCNVio gel**, being ascribed to the more equal absorption of this viologen along the most of the visible wavelength range, as mentioned above.

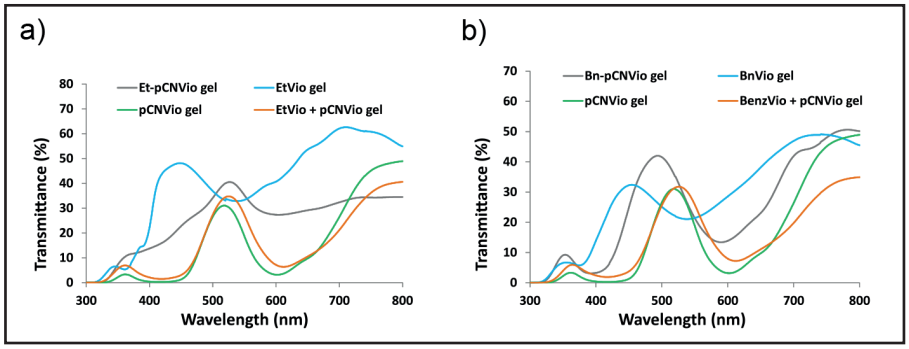

Figure 5.12. UV-vis transmittance response of 2-E ECDs containing (a) **Et-pCNVio** and (b) **Bn-pCNVio gels** vs corresponding symmetric viologens and the mixtures of them.

The visual appearance and the CIE color space plots (Figure 5.13a) obtained for **Et-pCNVio gel** (1) at colored state, also showed more neutral-gray color than the ones exhibited by the corresponding symmetric systems **EtVio** (2) and **pCNVio gels** (3), and the mixture of them **EtVio + pCNVio**

gel (4). Similar comparison performed for the **Bn-pCNVio gel** and their corresponding symmetric viologens and the mixture of them (Figure 5.13b) also led to the same results.

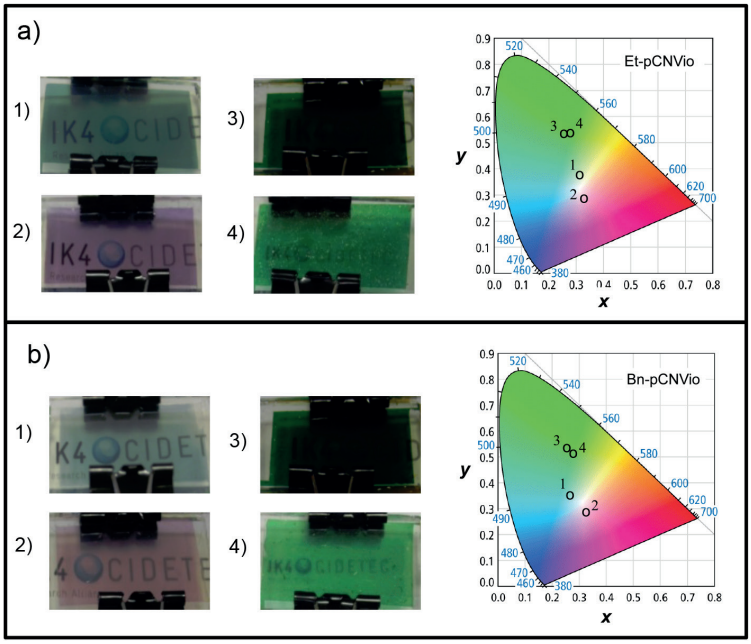

Figure 5.13. a) Photographs of 2-E ECDs containing **Et-pCNVio gel** (1) vs corresponding symmetric viologens **EtVio** (2) and **pCNVio** (3) and the mixture of them (**EtVio + pCNVio gel**) (4) along with corresponding color coordinates represented in the chromaticity diagram. b) similar comparison carried out with **Bn-pCNVio gel** (1) vs corresponding symmetric viologens **BnVio** (2) and **pCNVio** (3), and the mixture of them (**BnVio + pCNVio gel**) (4).

Color coordinates of each gel (Table 5.3), similarly revealed highly negative values of a^* component for the **pCNVio**, **EtVio + pCNVio,** and **BnVio + pCNVio gels**. Conversely, the asymmetric systems **Et-pCNVio** and **Bn-pCNVio gels** exhibited less negative values of a^* than **pCNVio gel**, and less negative value of b^* than **EtVio** and **BnVio gels**. These results confirmed that the studied EC-gels containing **[Et-pCNVio]** and **[Bn-pCNVio]** asymmetric viologens exhibit more neutral-color EC behavior

than their corresponding symmetric ones. Besides that, the symmetric mixture formulations showed the presence of precipitates, which were also appreciable in the ECDs.

Table 5.3. Transmittance, Δ%T and color coordinates of 2-E ECDs containing different gels.

EC-gel	λ_{max}	$\%T_b$	$\%T_c$	Δ%T[a]	x [b]	y [b]	Y [b]	L^*[c]	a^* [c]	b^* [c]	Color [d]
Et-pCNVio	600	66.5	27.4	39.2	0.314	0.384	32.8	64	-17	14	
Bn-pCNVio	600	55.7	13.9	41.8	0.255	0.335	23.4	55	-22	-5	
EtVio	550	70.3	33.4	37.0	0.316	0.295	37.4	68	14	-9	
BnVio	550	60.7	21.4	39.3	0.321	0.295	24.9	57	14	-8	
pCNVio	600	48.6	3.2	45.4	0.244	0.545	15.7	47	-60	31	
EtVio + pCNVio	600	54.7	7.3	47.4	0.278	0.531	20.7	53	-53	37	
BnVio + pCNVio	600	48.8	9.1	39.7	0.291	0.501	20.7	53	-45	33	

[a] Transmittance change at λ = 600 nm. [b], [c] Color coordinates (D65): [b] xyY 1931 and [c] $L^*a^*b^*$ 1976. [d] Color interpretation of the corresponding color coordinates (L^*a^*b).

5.3.3. EC Properties and cyclability

Switching responses of the 2-E ECDs containing **Et-pCNVio** and **Bn-pCNVio gels** were also studied for two different applied potentials. As discussed before, less negative reduction potentials provided more neutral-grayish colorations, whereas more cathodic ones led to more green and blue colors for **Et-pCNVio** and **Bn-pCNVio gels**, respectively.

To evaluate both colorations, transmittance changes of ECDs containing **Et-pCNVio** and **Bn-pCNVio gels** were recorded at 600 nm vs time (Figure 5.14a, and b respectively), while square-wave potential-steps between bleached (0 V for 90 s) and colored states (-0.8 or -1.6 V for 30 s) were being applied.

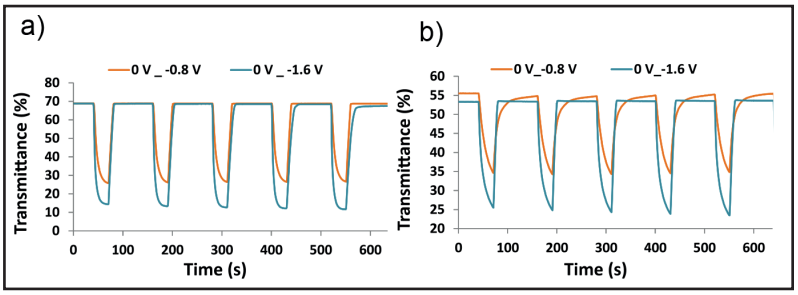

Figure 5.14. Transmittance changes (600 nm) vs time of ECDs containing (a) **Et-pCNVio** and (b) **Bn-pCNVio gels** while square-wave potential-steps between bleached (0 V for 90 s) and colored state (-0.8 or -1.6 V for 30 s) were being applied.

At the two studied potentials, ECDs containing **Et-pCNVio gel** exhibited faster coloring times and higher transmittance changes than the ones obtained for **Bn-pCNVio gel** (Table 5.4). This difference could be expected, because of the lower volume of the alkyl substituent the former presents, allowing faster mobility of the molecules within the PVA-gel matrix. It is worth to mention that switching times achieved by **Et-pCNVio gel** are comparable to ECDs comprising solid or gel electrolytic matrix.[19] In addition, these switching responses overrun those registered for some gray-black to colorless inorganic EC materials, such as nickel, molybdenum or iridium metal oxides,[2] which habitually display long coloration and bleaching times even in the range of minutes.[8a, 20]

Table 5.4. Electrochromic properties of 2-E ECDs containing **Et-pCNVio** and **Bn-pCNVio gels**.

EC-Gel	Potential (V)	Δ %T[a]	t_c (s) [b]	t_b (s) [b]	η_c (cm² C⁻¹) [c]	η_b (cm² C⁻¹) [c]
Et-pCNVio	-0.8	42	14	7	118	188
	-1,6	56	11	15	157	243
Bn-pCNVio	-0.8	20	22	24	180	255
	-1,6	30	19	8	152	341

[a] Transmittance change at λ = 600 nm. [b] Switching times. [c] Color efficiencies

As demonstrated in the previous chapter, PVA-borax gel offers better reversibility than other water-based electrolytes.[11a, 21] In order to assess the cycling performance of these systems, 2-E ECDs containing **Et-pCNVio** and **Bn-pCNVio gels** were exposed to square-wave potential-steps between bleached and colored states (Figure 5.15). This cyclability study revealed that ECDs containing **Et-pCNVio gel** (Figure 5.15a) maintained their switching response and Δ%T up to 15 000 cycles (with a slight decrease of 3% of the %T at bleached state after 7 500 cycles, and 6% after 15 000) while preserving satisfactory the neutral-color. In the case of ECDs comprising **Bn-pCNVio gel** (Figure 5.15b), they acquired more bluish EC character and more heterogeneous aspect during the cycles but equally preserved their switching performance up to 15 000 cycles.

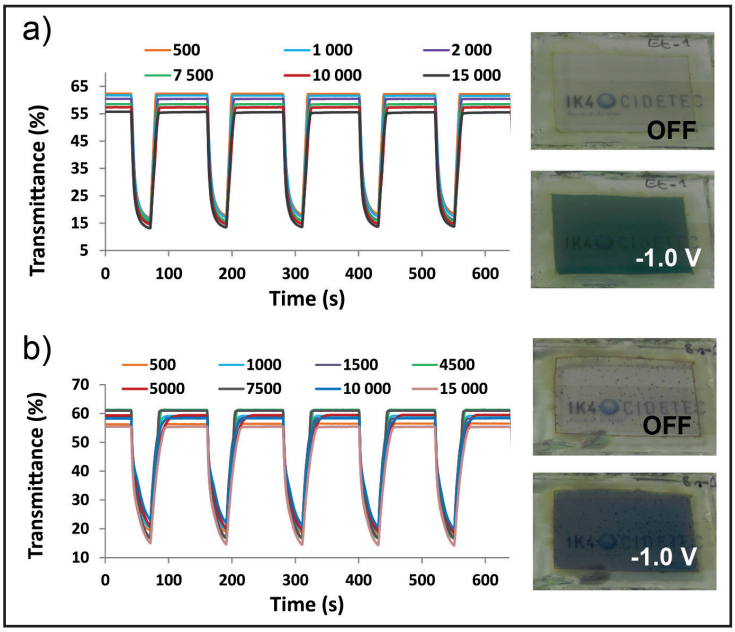

Figure 5.15. Evolution of the switching performance of ECDs containing (a) **Et-pCNVio** and (b) **Bn-pCNVio gels** up to 15 000 cycles while square-wave potential-steps between bleached (0 V for 90 s) and colored state (-1.0 V for 30 s) were being applied. Photographs of the ECDs at bleached (off) and at colored state after 15 000 cycles (inset).

Therefore, even though these systems comprise a water-based gel electrolyte and simple device architecture, they showed very good reversibility, most notably in the case of **Et-pCNVio gel**. These results could be ascribed to the presence of ferrocyanide within it, as the latter may ease the dissociation of the dimer through stabilizing radical cation moieties hindering the overlap of the parallel π-clouds of them.[22]

5.3.4. Dependence of Electrochromic Behavior on the Solvent

The effect of the solvent on the electrochromic behavior of the **[Et-pCNVio]** and **[Bn-pCNVio]** asymmetric viologens has also been investigated, as the nature of the electrolyte may play a crucial role in the observed coloration of the ECDs. Since the PVA-borax based gels employed so far in this chapter contained water as single solvent, alternative anhydrous electrolyte was used for comparative purposes.

To this end, propylene carbonate (PC) based formulations comprising **[Et-pCNVio]** and **[Bn-pCNVio]** as electrochromic materials and hydroquinone as complementary redox species were formulated, and their electrochromic behavior was studied for different applied potentials (Annex 5.2). Interestingly, **Et-pCNVio** and **Bn-pCNVio anhydrous solutions** displayed mainly green coloration at the studied potentials showing their maximum absorbance wavelengths at around 650 and 420 nm. By comparing the UV-vis spectra of these anhydrous solutions and the **Et-pCNVio** and **Bn-pCNVio gels** (Figure 5.16) a hypsochromic shift of the maximum absorbance wavelength was observed for ECDs containing gel electrolytes. It is worth noting that the spectroelectrochemical performance of **anhydrous electrolyte** in the absence of any viologen was also studied in a 3-E configuration to confirm that no coloration was observed due to the electrolyte by itself (Annex 5.3).

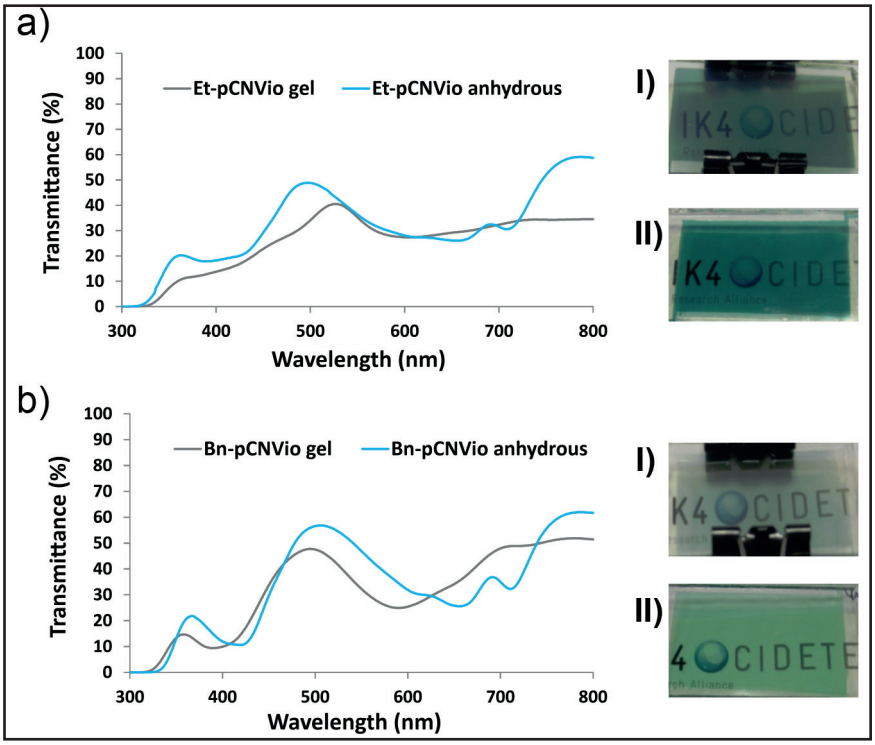

Figure 5.16. Transmittance profiles of 2-E ECDs containing (a) **Et-pCNVio** and (b) **Bn-pCNVio gels** vs corresponding anhydrous formulations in their colored states. Photographs of the devices based on gel formulation (I) and anhydrous formulation (II) in their colored states (inset).

To gain further insights into the more neutral-gray color observed in the case of **Et-pCNVio** and **Bn-pCNVio gels**, similar study was carried out employing ECDs based on symmetric alkyl viologens, ([**EtVio**] and [**BnVio**]) in the same anhydrous electrolyte (Annex 5.2 for different applied potentials). Curiously, analogous hypsochromic shift was observed in the **EtVio** and **BnVio gels** when comparing to anhydrous solutions (Figure 5.17), due to the more bluish character of the latter.

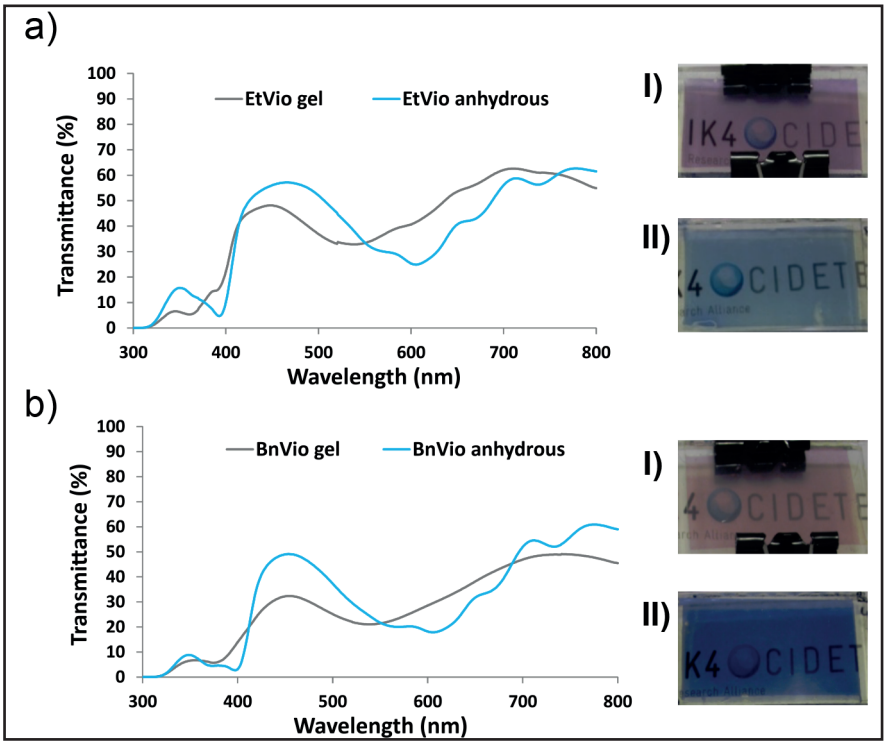

Figure 5.17. Transmittance profiles of 2-E ECDs containing (a) **EtVio** and (b) **BnVio gels** vs corresponding anhydrous formulations in their colored states. Photographs of the devices based on gel formulation (I) and anhydrous formulation (II) in their colored states (inset).

In this regard, several studies based on symmetric 1-1'-alkyl viologens demonstrated the formation of radical-cation as a dimer form ($(bipm)_2^{2+}$) in ECDs containing aqueous electrolytes. In fact, it is well documented that the violet coloration observed when symmetric alkyl-substituted viologens are tested within a water-based electrolytes, is the result of both the blue monomer and the red dimer contributions.[23] Previous studies related the formation of these dimers to a hypsochromic shift and the presence of new

absorption bands at higher wavelengths in their absorption profiles.[9, 24] Actually, the formation of radical-cation dimers have been demonstrated by ESR technique, for methyl and heptyl viologens within a PVA polymeric matrix, wherein the hypsochromic shift was also observed.[11a] In contrast, the dimer formation is hindered in some organic solvents such as propylene carbonate (PC).[25]

Hence, the reduced alkyl-symmetric viologen derivatives are blue in anhydrous solvents and purple in aqueous electrolytes due to the well-documented contribution of the both radical cation monomer and dimer formation. In a similar manner, the more neutral-gray colorations and the characteristic hypsochromic shift of the absorption profiles observed in ECDs containing **Et-pCNVio** and **Bn-pCNVio gels** and not observed in anhydrous electrolytes can be ascribed to the presence of their radical-cation dimer. This fact explains the transmittance profile obtained for the **Et-pCNVio gel**, which absorbed quite equally along the most visible wavelength, presumably due to both the monomer and dimer contributions by coupling their absorbance profiles.

This is also in agreement with the mainly dark green coloration observed in the scarcely reported ECDs based on asymmetrically substituted 1-alkyl-1'-aryl viologens covalently bonded to a nanostructured electrode.[11b] In that case, the dimerization is less likely to occur due to the non-aqueous electrolytes usually employed and to the poor mobility of the viologen molecules attached to the coated electrode. Hence the dimerization would only be allowed in concentrated systems wherein the viologen molecules are very close together.

Consequently, this kind of asymmetric viologens conveniently assembled within the PVA-borax gel polyelectrolytes provide colorless to neutral-gray electrochromic behavior enhanced by the dimerization phenomenon, while allowing very competitive performance and cyclability (up to 15 000 cycles).

5.4. Conclusions

Colorless to neutral-grayish color ECDs based on a single 1-alkyl-1'-aryl asymmetric viologen and using a very simple all-in-one device architecture (glass/TCO/EC gel/TCO/glass) were successfully developed.

The synthesis of asymmetrically 1-alkyl-1'-aryl substituted viologens, specifically, 1-ethyl-1'-(p-cyanophenyl)-4,4'-bipyridinium dibromide **[Et-pCNVio]** and 1-benzyl-1'-(p-cyanophenyl)-4,4'-bipyridinium dibromide **[Bn-pCNVio]** and their incorporation in PVA-borax gel polyelectrolytes was equally proven.

The more neutral coloration and intermediate electrochemical behavior of **Et-pCNVio** and **Bn-pCNVio gels**, in comparison with those comprising corresponding symmetric viologens was also confirmed.

The effect of the solvent was also investigated, further noting that a hypsochromic shift was occurring in the absorption profiles of **Et-pCNVio** and **Bn-pCNVio gels** when comparing to anhydrous solutions. This was ascribed to the presence of the radical-cation as a dimmer form in the **Et-pCNVio** and **Bn-pCNVio gels** which translates into more neutral-color observed.

The viability of the ECDs based on **Et-pCNVio** and **Bn-pCNVio gels** to achieve high-performance neutral-color ECDs was demonstrated. Thus, chromaticity coordinates very close to gray color (a^* and $b^* \leq |15|$), satisfactory colorless bleached state (%Tb ~ 77 %), transmittance changes (i.e., ~ 60 %), switching times (≤ 15s) and cyclability (i.e., ~ 15 000 cycles), were achieved with ECDs comprising **Et-pCNVio gel**.

Neutral-grayish color ECDs reported in this chapter offer many advantages over other neutral-color ECDs previously reported, such as significantly easier manufacturing process, competitive switching times, good cyclability and a colorless off state. Moreover, this colorless-to-neutral color ECDs

may significantly extend the potential of the electrochromic technology, as they adapt better aesthetically to the surrounding environment easing their implementation in different applications.

5.5. References

[1] a) A. L. Dyer, E. J. Thompson, J. R. Reynolds, *ACS Appl. Mater. Interfaces* **2011**, *3*, 1787-1795; b) R. H. Bulloch, J. A. Kerszulis, A. L. Dyer, J. R. Reynolds, *ACS Appl. Mater. Interfaces* **2015**, *7*, 1406-1412.

[2] R. J. Mortimer, *Annu. Rev. Mater. Res.* **2011**, *41*, 241-268.

[3] P.-Y. Chen, C.-S. Chen, T.-H. Yeh, *J. Appl. Polym. Sci.* **2014**, *131*, n/a-n/a.

[4] C. S. Ah, J. Song, S. M. Cho, T.-Y. Kim, H. N. Kim, J. Y. Oh, H. Y. Chu, H. Ryu, *Bull. Korean Chem. Soc.* **2015**, *36*, 548-552.

[5] H. Shin, Y. Kim, T. Bhuvana, J. Lee, X. Yang, C. Park, E. Kim, *ACS Appl. Mater. Interfaces* **2012**, *4*, 185-191.

[6] E. Unur, P. M. Beaujuge, S. Ellinger, J.-H. Jung, J. R. Reynolds, *Chem. Mater.* **2009**, *21*, 5145-5153.

[7] M. Sassi, M. M. Salamone, R. Ruffo, C. M. Mari, G. A. Pagani, L. Beverina, *Adv. Mater.* **2012**, *24*, 2004-2008.

[8] a) P. M. Beaujuge, S. Ellinger, J. R. Reynolds, *Nat. Mater.* **2008**, *7*, 795-799; b) P. Shi, C. M. Amb, E. P. Knott, E. J. Thompson, D. Y. Liu, J. Mei, A. L. Dyer, J. R. Reynolds, *Adv. Mater.* **2010**, *22*, 4949-4953.

[9] P. M. S. Monk, *The viologens: physicochemical properties, synthesis, and applications of the salts of 4,4'-bipyridine*, Wiley, **1998**.

[10] M. Hiroshi, M. Jin, *Jpn. J. Appl. Phys.* **1987**, *26*, 1356-1360.

[11] a) C. L. Bird, A. T. Kuhn, *Chem. Soc. Rev.* **1981**, *10*, 49-82; b) J.-H. Ryu, Y.-H. Lee, K.-D. Suh, *J. Appl. Polym. Sci.* **2008**, *107*, 102-108; c) J.-H. Ryu, J.-H. Lee, S.-J. Han, K.-D. Suh, *Colloids and Surfaces A: Physicochemical and Engineering Aspects* **2008**, *315*, 31-37.

[12] a) T. Zincke, W. Würker, *Justus Liebigs Ann. Chem.* **1904**, *330*, 361-374; b) D. Bongard, M. Möller, S. N. Rao, D. Corr, L. Walder, *Helv. Chim. Acta* **2005**, *88*, 3200-3209.

[13] a) C. P. Gonzalo, R. M. Garcia, M. S. Telleria, J. A. P. Alonso, H. J. G. Telleria, **2011**; b) G. C. Pozo, G. R. Marcilla, T. M. Salsamendi, A. J. A. POMPOSO, T. H. J. GRANDE, **2012**.

[14] J. Palenzuela, A. Viñuales, I. Odriozola, G. Cabañero, H. J. Grande, V. Ruiz, *ACS Appl. Mater. Interfaces* **2014**, *6*, 14562-14567.

[15] a) G. Wang, X. Fu, J. Huang, L. Wu, Q. Du, *Electrochim. Acta* **2010**, *55*, 6933-6940; b) D. Chao, X. Jia, H. Liu, L. He, L. Cui, C. Wang, E. B. Berda, *J. Polym. Sci., Part A: Polym. Chem.* **2011**, *49*, 1605-1614; c) Y. A. Udum, C. G. Hızlıateş, Y. Ergün, L. Toppare, *Thin Solid Films* **2015**, *595, Part A*, 61-67; d) K. Lin, Y. Zhao, S. Ming, H. Liu, S. Zhen, J. Xu, B. Lu, *J. Polym. Sci., Part A: Polym. Chem.* **2016**, *54*, 1468-1478; e) W. T. Neo, C. M. Cho, Z. Shi, S.-J. Chua, J. Xu, *J. Mater. Chem. C* **2016**, *4*, 28-32.

[16] a) G. Xu, J. Zhao, J. Liu, C. Cui, Y. Hou, Y. Kong, *J. Electrochem. Soc.* **2013**, *160*, G149-G155; b) T. Yi-Jie, C. Hai-Feng, Z. Wen-Wei, Z. Zhao-Yang, *J. Appl. Polym. Sci.* **2013**, *127*, 636-642; c) W. Yang, J. Zhao, C. Cui, Y. Kong, X. Zhang, P. Li, *J. Solid State Electrochem.* **2012**, *16*, 3805-3815.

[17] a) S. Cogal, M. Kiristi, K. Ocakoglu, L. Oksuz, A. U. Oksuz, *Mater. Sci. Semicond. Process.* **2015**, *31*, 551-560; b) E. N. Esmer, S. Tarkuc, Y. A. Udum, L. Toppare, *Mater. Chem. Phys.* **2011**, *131*, 519-524; c) B. Kim, J. Kim, E. Kim, *Macromolecules* **2011**, *44*, 8791-8797; d) B. Yigitsoy, S. M. A. Karim, A. Balan, D. Baran, L. Toppare, *Synth. Met.* **2010**, *160*, 2534-2539; e) H. Zhao, Y. Wei, J. Zhao, M. Wang, *Electrochim. Acta* **2014**, *146*, 231-241.

[18] C. Xu, L. Liu, S. E. Legenski, D. Ning, M. Taya, *J. Mater. Res.* **2004**, *19*, 2072-2080.

[19] a) D. Navarathne, W. G. Skene, *J. Mater. Chem. C* **2013**, *1*, 6743-6747; b) F. Tran-Van, L. Beouch, F. Vidal, P. Yammine, D. Teyssié, C. Chevrot, *Electrochim. Acta* **2008**, *53*, 4336-4343.

[20] P. Monk, Roger Mortimer,, D. Rosseinsky., *Electrochromism and Electrochromic Devices*, Cambridge University Press, **2007**.

[21] J. Mizuguchi, H. Karfunkel, *Ber. Bunsen-Ges. Phys. Chem.* **1993**, *97*, 1466-1472.

[22] P. M. S. Monk, *J. Electroanal. Chem.* **1997**, *432*, 175-179.

[23] a) P. M. S. Monk, *Dyes Pigm.* **1998**, *39*, 125-128; b) R. J. Mortimer, T. S. Varley, *Chem. Mater.* **2011**, *23*, 4077-4082.

[24] E. M. Kosower, J. L. Cotter, *J. Am. Chem. Soc.* **1964**, *86*, 5524-5527.

[25] Y.-C. Hsu, K.-C. Ho, *J. New Mater. Electrochem. Syst.* **2005**, *8*, 49-57.

CHAPTER 6

CONSECUTIVE ANCHORING OF SYMMETRIC VIOLOGENS: MONOLAYERED ELECTROCHROMIC DEVICES PROVIDING COLORLESS TO NEUTRAL-COLOR SWITCHING

6.1. Introduction

As commented in the previous chapter, the development of high-performance neutral-color electrochromic devices (ECDs) may significantly extend the applicability of the electrochromic technology.[1] However, most common EC materials, exhibit a lack of intrinsic neutral colorations whereas the ones proved to show gray-black colored state, exhibited very slow switching responses or were not colorless in the bleached state. To overcome these limitations little reported strategy comprises the synthesis of new molecules which incorporate different chromophores,[2] as also demonstrated in the previous chapter for all-in-one ECDs comprising single asymmetric viologen.[3]

On the other hand, most studied procedures to achieve neutral-color ECDs are based on color mixing approach,[4] often entailing complex device architectures.[5] In this regard, double-layered TiO_2-based working electrodes in which blue and green viologens were successively immobilized in the bottom and top layers of the stacked electrode, have been confirmed to provide neutral-color electrochromism.[6] However, apart from the additional steps necessary in the fabrication of the double-layered ECDs, the specific processing conditions required for the second TiO_2 film may limit the final device performance. Therefore, the controlled co-anchoring of different viologens in the same TiO_2 layer appears to be an appealing approach.

Accordingly, aiming at exploring the color mixing strategy while easing the fabrication process and the device architecture, this chapter dealt with the

sequential anchoring of two symmetric viologens in a single nanostructured TiO_2 layer.

To this end, taking into account the strong binding affinity towards TiO_2 nanostructured layer of **[Bn-PO_3H_2-Vio]** blue switching viologen developed in the chapter 3,[7] it was combined with an aryl-substituted green-switching viologen by means of sequential bonding on the same TiO_2 layer.

Additionally, applying the knowledge acquired in the previous chapter, the use of PVA-borax gel electrolyte was also studied aiming at enhancing the neutral-coloration of the ECDs.

6.1.1. Objective

The overall purpose of the research work reported in this chapter was to assess the color mixing approach to achieve neutral-color ECDs while maintaining TiO_2-monolayered device architecture.

To accomplish this goal, blue and green switching symmetric viologens (1,1'-alkyl and 1,1'-aryl, respectively) provided with an anchoring group which ensured rapid grafting process were required.

The optimization of the device performance involved the study of different parameters including the thickness of the TiO_2 monolayer and viologen grafting conditions such as time, anchoring order and concentration of viologen.

With the purpose of assessing the more neutral-colored state of the sequential anchoring strategy, the comparison of the resulting ECDs with the ones based on single viologen was equally necessary.

Additionally, aiming at enhancing the neutral-coloration of the ECDs the employment of PVA-borax gel electrolyte was also studied.

6.2. Materials and methods

6.2.1. Materials

4,4'-dipyridyl (98%), 2,4-dinitrochlorobenzene (98%), Poly(vinyl alcohol) (PVA, Mw 61 000), sodium tetraborate decahydrate (borax, 99.5%), potassium ferrocyanide (98.5%) potassium ferricyanide (99%), lithium perchlorate trihydrate and hydroquinone (HQ) (≥ 99%) were provided by Aldrich, whereas diethyl 4-aminobenzylphosphonate (98%) and γ-butyrolactone were supplied by Acros Organics. Hydrochloric acid (37%) and required organic solvents such as 2-propanol, acetone, ethanol were purchased from Scharlab. Titanium dioxide dispersion (Ti-Nanoxide T) was supplied by Solaronix. All these reagents were used without further purification except for γ-butyrolactone which was degassed for 15 min with N_2 prior to use.

Fluorine-doped tin oxide (FTO) coated glass substrates provided by Solems (Rs 6-8 Ωsq^{-1}) were washed with heated acetone before being used.

6.2.1.1. Synthesis and characterization of viologens

1,1'-Bis(phosphonomethyl-4-phenyl)-4,4'-bipyridilium dichloride ***[Ph-PO$_3$H$_2$-Vio]*** was synthesized as previously reported.[8] (79% yield). ^{1}H NMR (D_2O, δ, ppm): 9.42 (unresolved dd, 4H, J = 6.83 Hz), 8.79 (unresolved dd, 4H, J = 6.85 Hz), 7.66 (dd, 4H, J = 8.54, Hz) 2C_6H_4, 7.77 (unresolved dd, 4H, J = 8.33 Hz) and 3.18 (d, 4H, 2CH_2P, J = 20.9 Hz). ^{13}C NMR (D_2O, δ, ppm): 153.11, 148.14, 143.31, 142.21, 134.27, 129.76, 126.75, 38.63 and 37.62. ^{31}P NMR (D_2O, δ, ppm): 18.4. IR (bulk ATR): v (cm^{-1}) = 3028 (C-H), 2800-2413 (PO-H st), 2340-2250 (PO-H comb), 1631, 1596 (C=C, C=N), 1207, 1169 (P=O st), 1050-969, 928 (P-OH st) and 827 (*o*-phenylene H).

Synthesis of Bis(phosphonomethyl-4-benzyl)-4,4'-bipyridilium dichloride ***[Bn-PO$_3$H$_2$-Vio]*** has been described in the chapter 3.

6.2.2. Methods

6.2.2.1. Preparation of electrolytes

Anhydrous electrolytes were prepared by varying concentrations of redox mediator hydroquinone from 0.0075 to 2.0 mmol L^{-1} while keeping the concentration of $LiClO_4$ at a constant value of 0.2 molL^{-1}, in γ-butyrolactone.

Gel electrolyte comprising 2 mmol L^{-1} of potassium ferrocyanide and ferricyanide was prepared following the general procedure described in the section 2.2.2.1 of the chapter 2.

6.2.2.2. Fabrication of layered electrochromic devices

Layered ECDs based on two-electrode (2-E) and three-electrode (3-E) configurations were prepared and assembled following the procedure described in the chapter 2 section 2.5.1. and 2.5.2., respectively.

Preparation of viologen-modified TiO_2 electrodes

Transparent nanostructured TiO_2 films were modified by anchoring the viologen as follows: TiO_2-coated FTO/glass substrates were dipped into a beaker containing water solution of the viologen for a suitable grafting time. In the case of 1,1'-*Bis*(phosphonomethyl-4-benzyl)-4,4'-bipyridilium dichloride **[Bn-PO_3H_2-Vio]** (also referred to herein as **B** from blue color) the concentration was fixed at 5 mmol L^{-1} and the immersion time at 15 min. The same procedure was followed for the modification with 1,1'-*Bis*(phosphonomethyl-4-phenyl)-4,4'-bipyridilium dichloride **[Ph-PO_3H_2-Vio]** (also referred to herein as **G** from green color), with the concentration of it being 1 mmol L^{-1} and with variable grafting times (0.33, 1, 5, 7 and 10 min). Then, the viologen-modified TiO_2 electrodes were removed from the beaker, afterwards washed with water and ethanol and left drying overnight at 50 ºC under vacuum. When the sequential anchoring was carried out, the films were dried at 50 ºC for 3 hours prior to the adsorption of the second viologen.

6.3. Results and discussion

Electrochromic devices (ECDs) comprising a single nanostructured TiO_2 film and two different symmetric viologens provided with phosphonic acid groups that exhibited strong grafting affinity, were investigated. To this end, symmetrically substituted 1,1'-alkyl and 1,1'-aryl viologens, specifically 1,1'-*Bis*(phosphonomethyl-4-benzyl)-4,4'-bipyridilium dichloride **[Bn-PO_3H_2-Vio]** *(*blue viologen or **B** developed in the chapter 3) and 1,1'-*Bis*(phosphonomethyl-4-phenyl)-4,4'-bipyridilium dichloride **[Ph-PO_3H_2-Vio]** *(*green viologen or **G**) respectively, were synthesized and studied independently in a two-electrode (2-E) configuration using liquid anhydrous electrolyte (Figure 6.1).

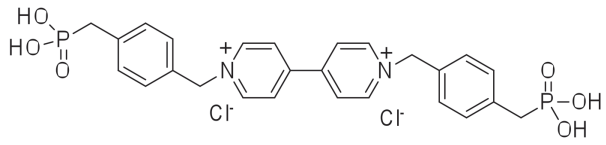

[*Bn-PO$_3$H$_2$-Vio*] (B)

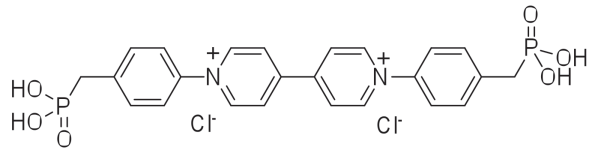

[*Ph-PO$_3$H$_2$-Vio*] (G)

Figure 6.1. Chemical structures of the viologens.

6.3.1. Optimization of the nanostructured TiO_2 layer

The effect of the thickness of the TiO_2 layer on the performance of the devices was studied for ECDs containing a single viologen **[Bn-PO_3H_2-Vio]** *(***B**) and **[Ph-PO_3H_2-Vio]** *(***G**) separately. The thickness of the TiO_2 films was tailored by varying the groove depths of the doctor-blade

applicators employed, encompassing 12, 50 and 100 µm (leading to TH1, TH2 and TH3 thicknesses respectively). The sintered films exhibited very homogeneous thicknesses and according to the cross-sectional SEM images (Figure 6.2a) they resulted to be of 1.9, 2.6 and 4.3 µm for TH1, TH2 and TH3 respectively, being constituted by anatase crystalline phase in all the cases (Figure 6.2b).[9]

In order to evaluate the effect of the thickness on the transmittance change of the ECDs, nanostructured TiO_2 films of these three different thicknesses were modified by anchoring **B** and **G** viologens separately. The grafting conditions such as immersion times and concentrations of viologens required to achieve optimal transmittance changes, were studied for each viologen. As proven in the chapter 3, viologen **[Bn-PO_3H_2-Vio]** (**B**) shows significantly faster grafting speed than other alkyl-substituted symmetric viologens reported in the literature also provided with phosphonate anchoring group (i.e., 1,1'-*Bis*(2-phosphonoethyl)-4,4'-bipyridilium dichloride **[Et-PO_3H_2-Vio]**).[7] In particular, after grafting time study it was found that 15 min of immersion time in a 5 mmol L^{-1} solution of **B** viologen, and 10 min in a 1 mmol L^{-1} solution of **G** viologen, were enough to complete the binding. It is worth noting that higher grafting times or concentrations of **G** viologen may result in a noticeable decrease of transmittance at the bleached state due to the initial yellowish color of this viologen by itself.

In order to find out the electrolyte composition which provided steady-state colorations while the ECDs were being colored, the concentration of complementary redox promoter (HQ) was studied and set at 7.5 mmol L^{-1} and 0.2 mol L^{-1} for devices containing **B** and **G** viologens respectively (Figure 6.2c). Equally, the reduction potentials were fixed at ~ -1.5 and -2.0 V for **B** and **G** viologen based ECDs, respectively.

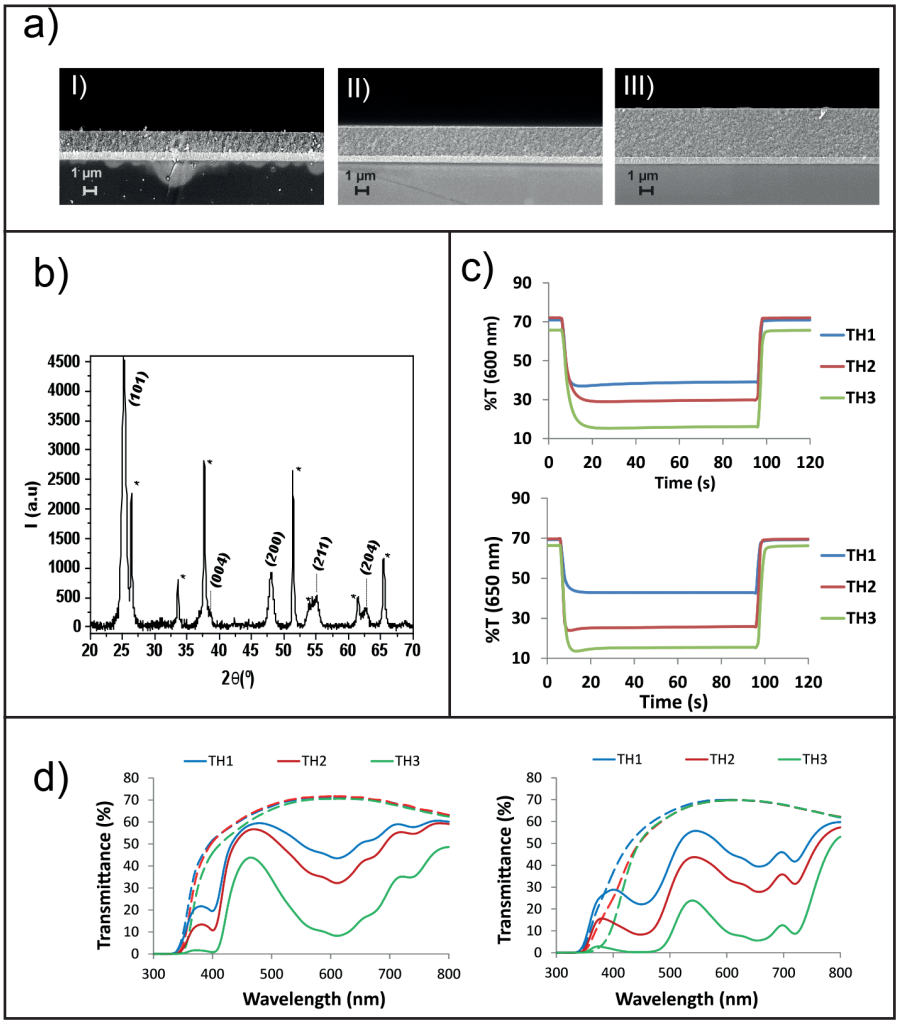

Figure 6.2. Effect of the thickness of the nanostructured TiO_2 layer. a) Cross-sectional SEM micrographs of TiO_2 films on FTO/glass (TH1 (I), TH2 (II) and TH3 (III)); b) XRD of pattern of a representative glass/FTO TiO_2 sample showing Miller indices (hkl) representative of anatase crysralline phase (* FTO); c) Transmittance versus time upon applying suitable reduction potential of 2-E ECDs containing **B** (top) and **G** (bottom) viologens-modified TiO_2 films of different thicknesses. Data registered at maximum contrast wavelength (600 and 650 nm) with optimum concentration of complementary redox promoter, 7.5 mmol L^{-1} and 0.2 mol L^{-1} for devices containing **B** and **G** viologens respectively; d) UV-vis transmittance response of 2-E ECDs containing **B** (left) and **G** (right) viologen-modified TiO_2 films of different thicknesses in their bleached and colored states (dashed and solid lines respectively).

As shown by UV/Vis transmittance spectra of ECDs comprising viologen-modified TiO_2 films of different thicknesses (Figure 6.2d and Table 6.1), the transmittance change increased with the thickness of the nanostructured film, more significantly when it raised from 2.6 to 4.3 μm. Thus, the thickest provided Δ%T of 61.6% and 63.8% for ECDs containing **B** and **G** viologens respectively.

Table 6.1. Transmittance, transmittance changes (Δ%T) and color coordinates of two electrode ECDs based on **B** and **G** viologen-modified TiO_2 films of different thickness (TH).

Viologen	TH (μm)	$\%T_b$	$\%T_c$	Δ%T [a]	x [b]	y [b]	Y [b]	L^*[c]	a^* [c]	b^* [c]	Color [d]
B	1.9	71.4	44.2	27.2	0.294	0.323	50.2	76	-6	-5	
	2.6	71.7	33.1	38.6	0.276	0.306	41.0	70	-6	-12	
	4.3	70.5	8.9	61.6	0.212	0.241	17.5	49	-7	-31	
G	1.9	69.4	39.7	29.7	0.349	0.416	49.6	76	-16	31	
	2.6	69.4	28.1	41.3	0.373	0.469	37.3	68	-21	47	
	4.3	69.5	5.6	63.8	0.367	0.581	15.7	47	-34	61	

[a] ΔT% at maximum contrast wavelength (650 nm for the G devices and 600 nm for the B devices). [b], [c] Color coordinates (D65) registered for xyY (CIE 1931) ([b]) and L^*a^*b (CIE 1976) ([c]) quantitative scales.[d] Color swatches representing L^*a^*b color coordinates.

The color coordinates obtained for each device at colored states (Table 1) also revealed that the blue EC-behavior of the ECDs containing **B** viologen increased with the thickness of the TiO_2 film, since the b^* component became more negative as the thickness of the films increased. Similarly the a^* component of the ECDs containing **G** viologen became more negative with the thickness of the film showing increasingly green EC-behavior. Moreover, in both cases the L^* value decreased with the thickness

indicating higher levels of coloration. These results also in agreement with that observed in the chapter 3, could be explained by the higher amount of viologen anchored within the thicker nanostructured networks.[7]

On the basis of the results, 4.3 μm was considered to be thick enough to provide competitive transmittance changes and it was selected for the sequential anchoring study employed to obtain more neutral colorations.

6.3.2. Optimization of the sequential grafting conditions

With the aim of obtaining the most neutral-color ECDs, different grafting conditions were evaluated. Series of ECDs based on 4.3 μm thickness TiO_2 films were fabricated by varying the grafting times and the order in which the blue and green viologens were anchored. The grafting time for **B** viologen was set at 15 min, whereas the one for **G** viologen was modified from 20 seconds to 10 min. The hydroquinone (HQ) content in the liquid anhydrous electrolyte was set at 0.1 mol L^{-1}, as a tradeoff between the suitable amounts for both **G** and **B** viologen based ECDs.

Following the same procedure explained in the previous chapter, the comparison was carried out between spectra which provided similar transmittance change (i.e., $\Delta\%T \geq 45$ %) at maximum contrast wavelength. UV-vis spectra of each ECD at different applied potentials is available as Annex 6.1.

Figure 6.3 shows the transmittance response in bleached (dashed lines) and colored states (solid lines) for ECDs obtained by **B** + **G** (Figure 6.3a) and **G** + **B** (Figure 6.3b) sequential grafting, along with the ones registered for the ECDs containing a single viologen (**B** and **G**) for comparative purposes. In both cases (**B** + **G** and **G** + **B** devices), the absorption profiles were in-between the ones obtained for the single viologens, showing more neutral behavior of the formers. Thus, the **B** + **G** and **G** + **B** devices exhibited higher absorption levels (i. e., transmittance decay in the Figure 6.3) from 420 to 520 nm than the **B** device, but lower than **G** device at the colored states. The

absorptions registered between 650 and 800 nm for the **B** + **G** and **G** + **B** devices were also higher than the ones obtained for **B** device, due to the **G** viologen contribution.

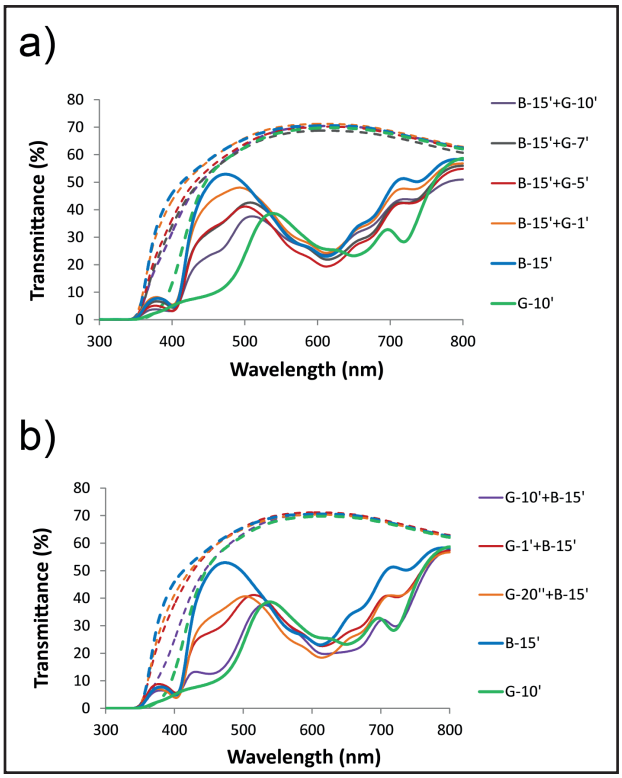

Figure 6.3. UV-vis spectra of two-electrode ECDs based on **B** + **G** (a) and **G** + **B** (b) sequential grafting procedures and those obtained for the **B** and **G** devices independently in their bleached and colored states (dashed and solid lines respectively).

This effect was also confirmed by color coordinates registered for each device (Table 6.2). Thus, as the grafting time of the **G** viologen decreased, the b^* component became more negative, in particular from 10 to -8 for the **B** + **G** series and from 27 to -4 in the case of **G** + **B** series, reaching the minimum value of -15 for the **B** device. This influence was less noticeable

in the case of *a** component, which increased only slightly in most cases as the anchoring time of G viologen decreased. It is also noteworthy the strong binding affinity of the **B** viologen towards nanostructured TiO_2 layer, evidenced by the presence of it in the **G** + **B** series, thus after the **G** viologen having occupied most of the accessible active centers of the nanostructured film.

Table 6.2. Transmittance changes (Δ%T) and color coordinates of 2-E ECDs based on **B** + **G** and **G** + **B** sequential grafting strategies and those obtained for the **B** and **G** devices independently.

Sequence	Device	Δ%T [a]	x [b]	y [b]	Y [b]	*L** [c]	*a** [c]	*b** [c]
B+G	B-15′+G-10′	46.1	0.307	0.373	30.2	62	-16	10
	B-15′+G-7′	45.3	0.281	0.348	32.3	64	-18	1
	B-15′+G-5′	49.6	0.272	0.335	29.4	61	-17	-3
	B-15′+G-1′	45.7	0.271	0.320	34.8	66	-13	-8
G+B	G-10′+B-15′	48.5	0.325	0.437	29.4	61	-26	27
	G-1′+B-15′	46.9	0.292	0.365	32.5	64	-19	7
	G-20″+B-15′	50.4	0.268	0.334	29.2	61	-18	-4
-	B-15′	46.2	0.260	0.299	34.0	65	-11	-15
	G-10′	46.2	0.359	0.464	31.3	63	-23	40

[a] ΔT% at maximum contrast wavelength (650 nm for the G device and 600 nm for the rest).
[b], [c] Color coordinates (D65) registered for xyY (CIE 1931) ([b]) and *L***a***b* (CIE 1976) ([c]) quantitative scales.

The sequential combination consisting in 15 min grafting time of the **B** viologen followed by 7 min grafting time of the **G** viologen (**B**-15' + **G**-7'), offered the closest to 0 *b** component, which is about midway between blue and yellow. Since yellow color can be considered the contribution from green viologen, this sequential combination was considered to provide more neutral-color EC behavior and selected for the further investigations.

6.3.3. EC properties and cyclability

Switching responses of 2-E ECDs consisting of **B**-15' + **G**-7' sequential combination were also studied for the selected potential. Transmittance changes registered *vs* time at 600 nm while the devices were being exposed to coloring (-1.6 V for 50 s) and bleaching (0 V for 90 s) potential-steps (Figure 6.4a), revealed good cycling performance for the sequential ECDs. Additionally, the device reached the 90% of the total ΔT% in 6 s for the coloring process exhibiting a coloration efficiency of 134 cm^2 C^{-1}, and even quicker conversion of 3 s and higher color efficiency of 263 cm^2 C^{-1} was obtained for the bleaching process.

The stability over redox cycles of **B**-15' + **G**-7' sequential combination was equally evaluated by switching the devices between the colored and bleached processes (-1.6 V for 50 s and 0 V for 90 s, respectively) and recording the %T after 100, 300, 500, 700 and 1 000 cycles while the same potential steps were being applied.

The transmittance changes remained practically permanent during the initial 700 cycles as they were higher than 40% in all cases (Figure 6.4b). Above these cycles, even though the bleached state still showed similar transmittance values, the coloration level decreased leading to diminution of the transmittance change. Regarding the switching speed, both coloration and bleaching processes were still comparable to the ones observed for the freshly prepared device, as can be deduced from the Figure 6.4b.

It is worth to mention that the stability and cycling performances of these systems can be affected by the cathodic potential and the amount of complementary redox promoter employed, since each viologen (**B** and **G**) require certain values of these parameters which differ from one another. However, the number of cycles registered may be adequate for some disposable systems such as smart labels or smart cards among others.

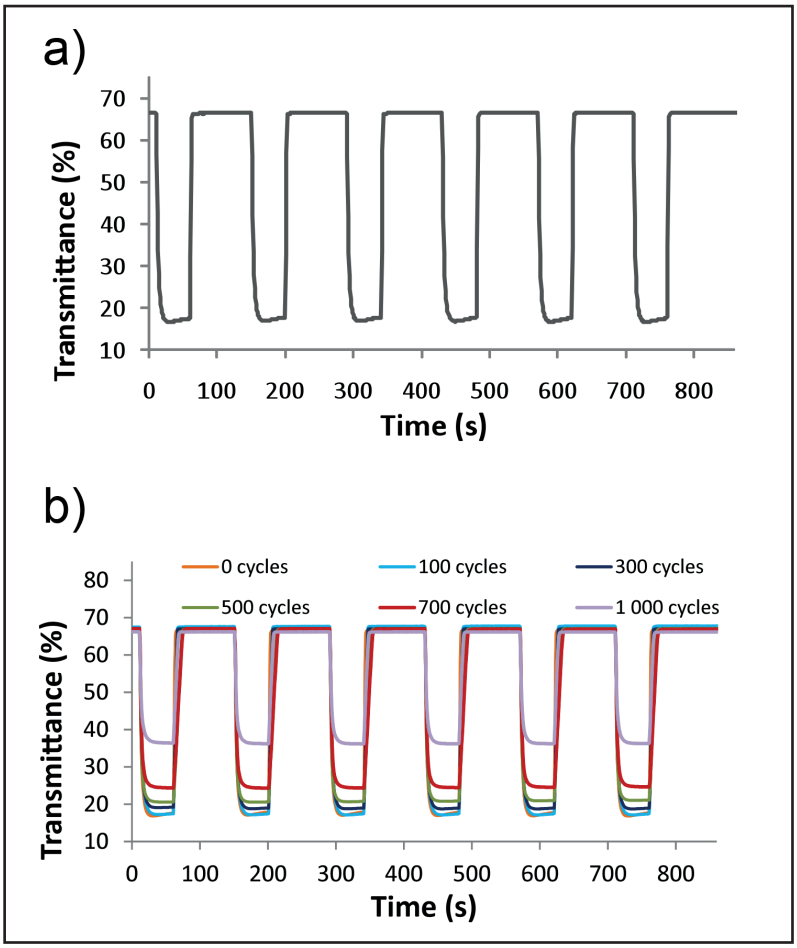

Figure 6.4. Two electrode ECDs based on **B**-15' + **G**-7' sequential grafting strategy. a) Transmittance changes registered at 600 nm plotted against time while voltage steps between colored (-1.6 V, 50 s) and bleached state (0 V, 90 s) were being applied, for freshly prepared device and b) its evolution after 100, 300, 500 700 and 1 000 cycles.

6.3.4. Spectroelectrochemical study

The spectroelectrochemical behavior of ECDs based on **B**-15' + **G**-7' sequential combination was investigated and compared with that obtained for **G** and **B** viologens separately. As shown in the schematic sequence of the fabrication process (Figure 6.5a), three-electrode (3-E) ECDs employed to this end also included a TiO_2 layer (~ 4.3 μm).

First, the spectroelectrochemical behavior of bare TiO_2 film (viologen free film) was studied in a similar 3-E configuration (Annex 6.2.I) proving that no coloration was observed in the potential window selected due to the nanostructured TiO_2 film by itself. Additionally, some peaks ascribed to the electrochemical activity of TiO_2 layer were detected.[9]

The CV of the 3-E ECD containing **B** viologen (Annex 6.2.II) exhibited two reduction process at around -0.85 V and -1.3 V (*vs* Ag/Ag^+) attributed to the formation of the radical-cation ($bipm^{+\bullet}$) and the di-reduced neutral state ($bipm^0$), respectively, apart from the uncolored process close to -0.6 V associated to the TiO_2-electrolyte activity.

Similarly, CV of **G** viologen (Annex 6.2.III) showed two cathodic peaks at around -0.6 V and -0.9 V (*vs* Ag/Ag^+) accompanied by green and yellowish coloration, being the former presumably overlapped with a redox peak assigned to the TiO_2-electrolyte activity.

Cyclic voltammetry (CV) registered for **B**-15' + **G**-7' 3-E ECD (Figure 6.5b) revealed two recognizable peaks on the cathodic span of the scan at approx. -0.7 and -1.0 V (*vs* Ag/Ag^+), and an uncertain one at around -1.4 V, although no significant coloration was observed until the potential reached -1.0 V (Annex 6.3 and Table 6.3). Then, a growing green and blue contribution was observed as potential increased up to ~ -1.4 V, whereas the device turned into yellowish upon applying more negative potentials.

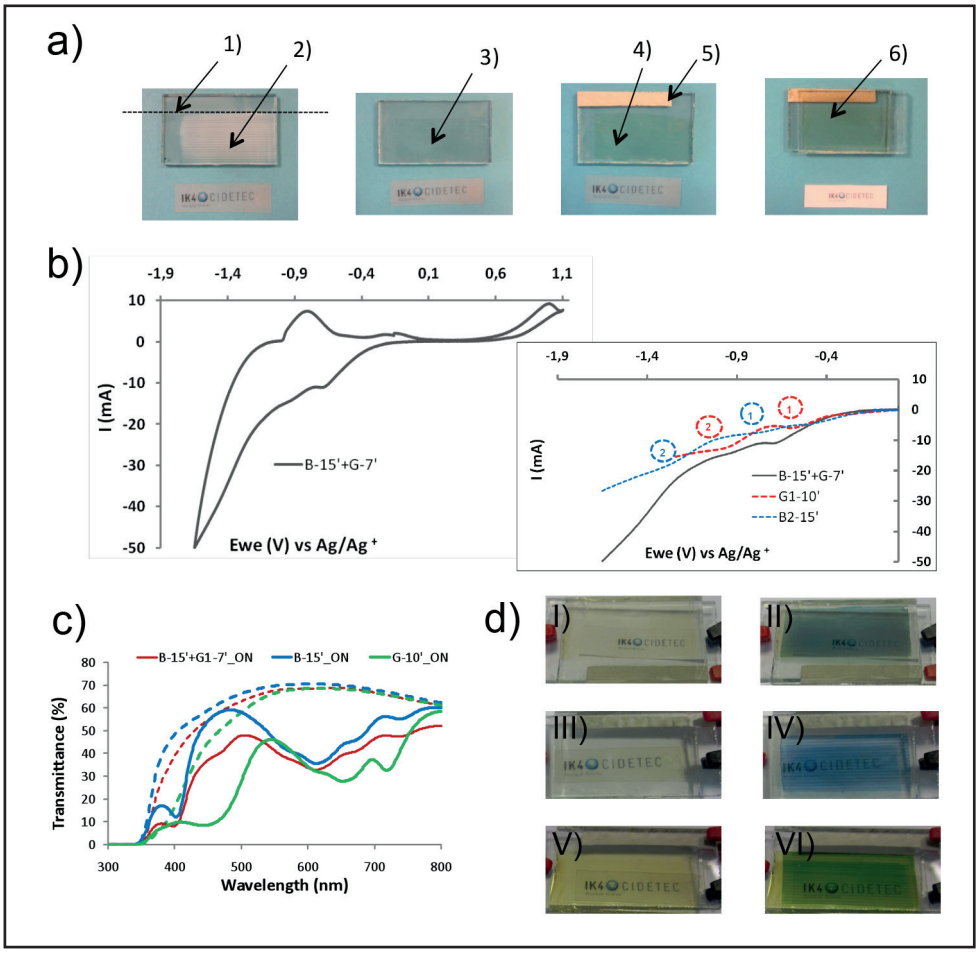

Figure 6.5. 3-E EDCs provided with nanostructured TiO_2 film. a) Photographs showing the fabrication steps and components (laser scribing (1), nanostructured TiO_2 layer before (2) and after heating treatment (3), viologen-modified TiO_2 layer (4), pseudoreference electrode (5) and resulting device after being assembled and filled with the electrolyte; b) CV of **B**-15' + **G**-7' sequential combination device and its comparison (inset, cathodic sweep) with devices comprising **B** and **G** viologens separately; c) their UV-vis transmittance responses at bleached and colored states (dashed and solid lines respectively); d) photographs at bleached (left) and colored state (right) (**B**-15' + **G**-7' (I and II), **B** (III and IV), and **G** devices (V and VI)).

Table 6.3. Transmittance changes (Δ%T) and color coordinates of 3-E ECD based on **B**-15' + **G**-7' sequential combination at different applied potentials.

V	%T	Δ%T [a]	x [b]	y [b]	Y [b]	L^* [c]	a^* [c]	b^* [c]	Color [d]
OFF	68.5	-	0.329	0.353	66.8	85	-3	11	
-0.8 V	68.3	0.1	0.329	0.353	66.6	85	-3	11	
-1.0 V	55.3	13.2	0.320	0.355	57.7	81	-7	9	
-1.1 V	49.3	19.2	0.312	0.351	53.7	78	-9	7	
-1.2 V	38.1	30.4	0.299	0.346	45.2	73	-12	3	
-1.4 V	33.5	34.9	0.300	0.350	40.3	70	-13	4	
-1.6 V	51.2	17.3	0.337	0.378	51.3	77	-8	19	

[a] ΔT% at maximum contrast wavelength (600 nm).
[b], [c] Color coordinates (D65) registered for xyY (CIE 1931) ([b]) and L^*a^*b (CIE 1976) ([c]) quantitative scales.
[d] Color swatches representing L^*a^*b color coordinates.

On the basis of the results obtained for these three systems (**B**, **G** and **B** + **G**) (Figure 6.5b (inset)) it can be suggested that when the **B**-15' + **G**-7' sequential combination system is displaying neutral colored state (from -1.0 to -1.4 V), the **B** viologen may be exhibiting the radical-cationic form, while part of the **G** viologen molecules may be present as neutral form (yellowish). This can also explain the no significant changes in the a^* coordinate while the grafting time of the G viologen was being diminished, since the lower contribution of the latter would have more impact in the b^* component (dropping it due to the less yellow character influence) than in the a^* component (rinsing it because of the less green character contribution).

By comparing the absorption profiles (Figure 6.5c), the observed colorations (Figure 6.5d) and the color coordinates of **B**, **G** and **B** + **G** systems at similar Δ%T (Table 6.4), it was proved that **B**-15' + **G**-7' sequential combination showed more neutral character than single-viologen-containing ECDs, as also detected for 2-E ECDs.

Table 6.4. Transmittance changes (Δ%T) and color coordinates of 3-E ECDs based on the **B**-15' + **G**-7' sequential combination strategy and those obtained for the 3-E ECDs containing **B** and **G** viologens independently.

Device	Δ%T [a]	x [b]	y [b]	Y [b]	L^* [c]	a^* [c]	b^* [c]	Color [d]
B-15'+ G1-7'	34.9	0.300	0.350	40.3	70	-13	4	
B-15'	33.4	0.281	0.321	46.1	74	-11	-7	
G-10'	34.4	0.371	0.473	38.4	68	-23	48	

[a] ΔT% at maximum contrast wavelength (650 nm for the G devices and 600 nm for the rest).
[b], [c] Color coordinates (D65) registered for xyY (CIE 1931) ([b]) and L^*a^*b (CIE 1976) ([c]) quantitative scales.
[d] Color swatches representing L^*a^*b color coordinates.

6.3.5. Dependence of electrochromic behavior on the electrolyte

The influence of the electrolyte on the electrochromic behavior of ECDs based on **B**-15' + **G**-7' sequential combination was explored in 2-E configuration. As proven in the previous chapter, polyvinyl alcohol-borax (PVA-borax) polyelectrolytic matrix may enhance the neutral EC character of some devices. In that section, viologens were dissolved into electrolytic matrix in all-in-one architecture (i., e., glass/TCO/EC gel/TCO/glass). [3] With the aim of investigating monolayered sequential combination strategy with the PVA-borax electrolyte, **B**-15' + **G**-7' (TH3) 2-E ECDs were assembled with this gel electrolyte and studied in terms of transmittance profiles (Figure 6.6a) and switching response (Figure 6.6b).

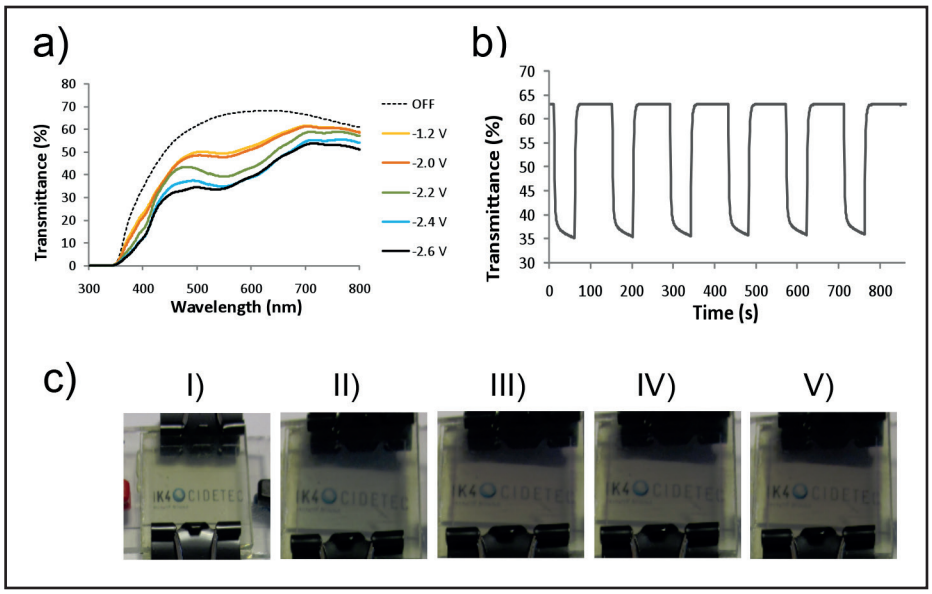

Figure 6.6. 2-E EDCs based on **B**-15' + **G**-7' sequential combination containing PVA-borax gel electrolyte: a) UV-vis transmittance responses for different applied potentials; b) Transmittance changes registered at 550 nm plotted against time while voltage steps between colored (-2.2 V, 50 s) and bleached state (0 V, 90 s) were being applied; c) Observed colorations in bleached state (I) and while -1.2 V (II), -2.0 V (III), -2.2 V (IV) and -2.4 V (V) were being applied.

Interestingly, these ECDs exhibited great gray color in their colored states upon applying suitable external voltages (Figure 6.6c). Color coordinates and corresponding color interpretations (Table 6.5) also confirmed the more gray EC character of these devices, showing a^* and b^* coordinates closer to 0 for similar value of L^* (i.e., 70) than the ones registered while testing with liquid anhydrous electrolyte. Conversely, transmittance changes (Table 6.5) and switching times were poorer than those obtained for liquid electrolyte. Thus, the gel-based ECDs required 8 and 6 seconds to reach the 90% of the total transmittance change for coloration and bleaching processes, showing color efficiencies of 125 and 143 $cm^2\ C^{-1}$ respectively.

Table 6.5. Transmittance changes (Δ%T) and color coordinates of 2-E EDCs based on **B**-15' + **G**-7' sequential combination containing PVA-borax gel electrolyte at different applied potentials.

Potential (V)	%T	Δ%T [a]	x [b]	y [b]	Y [b]	L^* [c]	a^* [c]	b^* [c]	Color [d]
OFF	66.1	-	0.331	0.355	65.6	85	-3	12	
-1.2 V	49.4	16.8	0.331	0.351	50.6	76	-1	10	
-2.0 V	47.7	18.5	0.331	0.349	49.0	75	0	9	
-2.2 V	39.0	27.1	0.325	0.334	41.3	70	3	3	
-2.4 V	34.8	31.3	0.329	0.338	36.9	67	3	5	
-2.6 V	33.9	32.3	0.338	0.344	35.9	66	4	7	

[a] ΔT% at maximum contrast wavelength (550 nm).
[b], [c] Color coordinates (D65) registered for xyY (CIE 1931) ([b]) and L^*a^*b (CIE 1976) ([c]) quantitative scales.
[d] Color swatches representing L^*a^*b color coordinates.

As mentioned above, the enhancement of the neutral character when employing PVA-borax gel electrolyte was equally observed in the previous chapter while all-in-one device configurations were being used. The latter approach allowed greater mobility of the viologen molecules,[3] and the more neutral-colored state was attributed to the formation of radical-cation dimmer due to its similarity to that observed in well-studied alky-substituted symmetric viologens (characteristic hypsochromic shift of the absorption profiles).[10] By comparing the UV-vis spectra of the sequential ECDs (**B**-15' + **G**-7') containing anhydrous electrolyte with the one registered when the PVA-borax gel electrolyte was being employed (Figure 6.7 and Table 6.6) a hypsochromic shift was similarly observed for ECDs containing gel electrolyte accompanied by less green character (less negative value of a^* component observed for the latter).

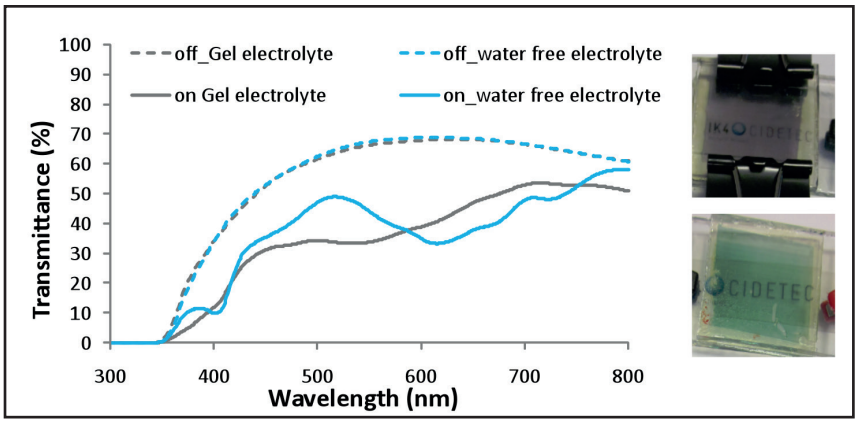

Figure 6.7. Transmittance spectra of 2-E EDCs based on **B**-15' + **G**-7' sequential combination containing PVA-borax gel electrolyte *vs* anhydrous formulation in their bleached and colored states. Photographs of the device based on gel electrolyte (top) and anhydrous electrolyte (bottom) in their colored states for similar transmittance changes (inset).

Similarly, **B** and **G** viologen-modified-TiO_2 electrodes were studied with the same gel electrolyte separately, and the hypsochromic shift was also noticed while comparing to anhydrous electrolyte (Annex 6.4). This change in the absorption profile was equally accompanied by a modification in the observed colored state and color coordinates (Annex 6.4), more noteworthy in the case of **B** viologen based devices. The latter exhibited purple color in its colored state while employing PVA-borax gel electrolyte, which as described for other alkyl-substituted symmetric viologens and also mentioned in previous chapters, is attributed to the presence of the radical-cation monomer (blue, b* (-)) and dimer (red, a* (+)).[11]

Therefore, even though the formation of radical-cation dimers may be hindered in this kind of configurations (glass/TCO/Viologens-modified-TiO_2/electrolyte/TCO/glass) due to the poor mobility of the viologen molecules covalently bonded to the coated electrode, the dimer appears to be forming when appropriate electrolytic matrix such as PVA-borax gel is being employed. Actually, it can be assumed that in concentrate systems

wherein the molecules are near enough to allow the formation of the dimer, the chemisorption of the viologen molecules may promote de dimerization as reported for some non-anchored viologens (i.e., methyl and heptyl viologen) adsorbed on a matrix of paper[12] or on a TiO_2 particles.[13]

Table 6.6. Transmittance changes (Δ%T) and color coordinates of 2-E EDCs based on **B**-15' + **G**-7' sequential combination containing PVA-borax gel electrolyte *vs* anhydrous formulation.

Electrolyte	$\lambda_{max\ abs\ (nm)}$	Δ%T	x [(a)]	y [(a)]	Y [(a)]	L^* [(b)]	a^* [(b)]	b^* [(b)]	Color [(c)]
Gel	550	32.3	0.338	0.344	35.9	66	4	7	
Anhydrous	600	33.7	0.303	0.360	42.0	71	-15	7	

[a), b)] Color coordinates (D65) registered for xyY (CIE 1931) ([(b)]) and L^*a^*b (CIE 1976) ([(c)]) quantitative scales.
[c)] Color swatches representing L^*a^*b color coordinates acquired through a color converter software.

On the other hand, although the poor reversibility of the radical-cation dimer has been repeatedly reported,[10b, 14] the great reversibility of the PVA-borax electrolytic matrix was widely proven in the previous chapters (4 and 5). Thus, EC systems comprising single viologen dissolved in PVA-borax gel electrolyte were cycled up to 15 000 cycles despite the formation of the radical-cation dimer in the colored state.[3, 15] However, as shown in Figure 6.8 and also noticed for ECDs comprising liquid electrolyte, this cycling performance may be limited herein by the incorporation of two viologens and the consequent need to choose a tradeoff between the requirements of each viologen (i.e., amount of complementary redox promoter and cathodic potential).

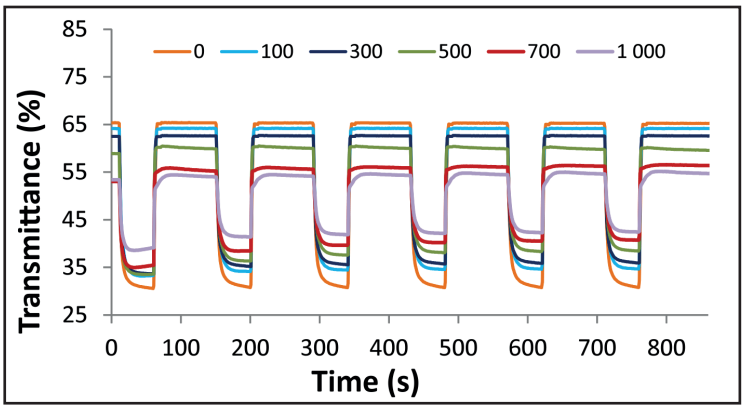

Figure 6.8. Evolution of switching performances over cycling of 2-E ECD based on **B**-15' + **G**-7' sequential combination containing PVA-borax gel electrolyte. Transmittance changes registered at 550 nm plotted against time while voltage steps between colored (-2.2 V, 50 s) and bleached state (0 V, 90 s) were being applied.

In any case, universality to the findings developed in the previous chapter in non-anchored viologens is equally demonstrated for bonded viologens. Therefore, the formation and use of the radical-cation dimer may open a new path in the field of ECDs based on viologen-modified nanostructured films, as it can afford new colorations at its reduced states.

6.4. Conclusions

The achievement of colorless to neutral-grayish color ECDs based on color mixing approach by means of the sequential anchoring of alkyl-substituted and aryl-substituted symmetric viologens (offering blue and green switching respectively) was proven.

The successful integration of a 1,1'-alkyl (**[Bn-PO_3H_2-Vio]** developed in the chapter 3), and 1,1'-aryl symmetric viologens (**[Pn-PO_3H_2-Vio]**) in a monolayered device architecture (glass/TCO/viologens-modified-TiO_2/TCO/glass) while requiring very short grafting times (≤ 15 min), was equally demonstrated.

The device performance was enhanced by establishing the best combination of nanostructured TiO_2 layer thickness (4.3 μm), sequential grafting conditions (**B** + **G** viologens) and grafting time for each viologen (15 and 7 min. respectively), leading to competitive switching times (i.e., 6 s for the colored and 3 s for the bleached steps) and good cycling performance up to 700 cycles.

The more neutral-colored state of the optimized ECDs was equally confirmed showing both absorption profiles and color coordinates about midway between that obtained for the both viologens separately.

Last but not least, the proof-of-concept of the employment of PVA-borax gel as electrolyte to enhance the neutral-grayish switching performance (a^* and $b^* \leq |10|$), was also demonstrated in these monolayered ECDs.

All in all, the reported results offer many advantages over other neutral-color ECDs previously reported, such as competitive switching times and a colorless off state (i.e., $T_b \sim 70\%$) as well as an easier manufacturing process which only requires a single nanostructured layer.

Moreover, the finding of the radical-cation dimer formation in this PVA-borax gel based ECDs wherein viologens are covalently bonded to the coated electrode may be extrapolated to other anchored viologens, thus significantly contributing to diversify the provided colorations of the ECDs and expanding the potential of the EC technology.

6.5. References

[1] R. J. Mortimer, *Annu. Rev. Mater. Res.* **2011**, *41*, 241-268.

[2] M. Sassi, M. M. Salamone, R. Ruffo, C. M. Mari, G. A. Pagani, L. Beverina, *Adv. Mater.* **2012**, *24*, 2004-2008.

[3] Y. Alesanco, A. Viñuales, G. Cabañero, J. Rodriguez, R. Tena-Zaera, *ACS Appl. Mater. Interfaces* **2016**, *8*, 29619-29627.

[4] P.-Y. Chen, C.-S. Chen, T.-H. Yeh, *J. Appl. Polym. Sci.* **2014**, *131*, n/a-n/a.

[5] a) H. Shin, Y. Kim, T. Bhuvana, J. Lee, X. Yang, C. Park, E. Kim, *ACS Appl. Mater. Interfaces* **2012**, *4*, 185-191; b) E. Unur, P. M. Beaujuge, S. Ellinger, J.-H. Jung, J. R. Reynolds, *Chem. Mater.* **2009**, *21*, 5145-5153.

[6] C. S. Ah, J. Song, S. M. Cho, T.-Y. Kim, H. N. Kim, J. Y. Oh, H. Y. Chu, H. Ryu, *Bull. Korean Chem. Soc.* **2015**, *36*, 548-552.

[7] Y. Alesanco, J. Palenzuela, R. Tena-Zaera, G. Cabañero, H. Grande, B. Herbig, A. Schmitt, M. Schott, U. Posset, A. Guerfi, M. Dontigny, K. Zaghib, A. Viñuales, *Sol. Energy Mater. Sol. Cells* **2016**, *157*, 624-635.

[8] R. Cinnsealach, G. Boschloo, S. Nagaraja Rao, D. Fitzmaurice, *Sol. Energy Mater. Sol. Cells* **1999**, *57*, 107-125.

[9] S. Bhandari, M. Deepa, A. K. Srivastava, S. T. Lakshmikumar, RamaKant, *Solid State Ionics* **2009**, *180*, 41-49.

[10] a) P. M. S. Monk, *The viologens: physicochemical properties, synthesis, and applications of the salts of 4,4'-bipyridine*, Wiley, **1998**; b) C. L. Bird, A. T. Kuhn, *Chem. Soc. Rev.* **1981**, *10*, 49-82; c) E. M. Kosower, J. L. Cotter, *J. Am. Chem. Soc.* **1964**, *86*, 5524-5527.

[11] R. J. Mortimer, T. S. Varley, *Chem. Mater.* **2011**, *23*, 4077-4082.

[12] P. M. S. Monk, C. Turner, S. P. Akhtar, *Electrochim. Acta* **1999**, *44*, 4817-4826.

[13] E. Borgarello, E. Pelizzetti, W. A. Mulac, D. Meisel, *Journal of the Chemical Society, Faraday Transactions 1: Physical Chemistry in Condensed Phases* **1985**, *81*, 143-159.

[14] J. Mizuguchi, H. Karfunkel, *Ber. Bunsen-Ges. Phys. Chem.* **1993**, *97*, 1466-1472.

[15] Y. Alesanco, J. Palenzuela, A. Viñuales, G. Cabañero, H. J. Grande, I. Odriozola, *ChemElectroChem* **2015**, *2*, 218-223.

CHAPTER 7

COLORLESS-TO-BLACK/GRAY ELECTROCHROMIC DEVICES BASED ON A SINGLE 1-ALKYL-1′-ARYL ASYMMETRIC VIOLOGEN-MODIFIED MONOLAYERED ELECTRODES

7.1. Introduction

Among emerging neutral electrochromic systems,[1] prominent attention is recently being paid to the colorless-to-black electrochromism.[2] Apart from the general core strengths of neutral-color electrochromism pointed out in the previous sections (i.e., better aesthetic adaptation to any chromaticity surfaces and effective light filtering), black electrochromism may open up new opportunities. Thus, black EC materials can be incorporated in displays (e.g., e-paper applications),[3] as well as in transparent-to-black panes to ensure privacy while changing at will from total transmissive state to almost opaque under suitable applied potential. However, the achievement of high performance EC materials which provide colorless-to-black electrochromism by themselves remains a strategic challenge.[4]

The most widely employed strategy to achieve black electrochromism has been based on the "color mixing" principle by combining two,[2b, 5] three,[6] or even four[7] EC materials of different colored states in diverse device architectures including blends,[6] multilayered devices (i.e., monolayered both working electrode (WE) and counter electrode (CE),[2b] bilayered WEs[5b] and bilayered WEs and CEs[7]) or even multielectrodes[5a]. Nevertheless, apart from the complexity of these systems, the larger number of layers and/or electrodes may lead to some operational problems such as the loss of transparency or the increment of the electrical resistivity which might limit the size of the ECDs and the response time.

In the previous chapters the development of viologen-based colorless-to-gray EC systems was proven for different device architectures following

different approaches. However, the colorless-to-black electrochromism was not achieved.

The gray EC behavior obtained in the previous chapter by color mixing of blue and green switching symmetric viologens on monolayered ECDs was enhanced by employing PVA-borax gel electrolyte, ascribed to the radical-cation dimer formation.[8] However, the presence of two different viologens and the consequent need to choose a tradeoff between the requirements of each viologen (i.e., amount of complementary redox promoter and cathodic potential), may limit device performance and ciclability as noticed in that section.

This inadequacy may be addressed by using a single EC material which integrate different chromophores in its molecular structure,[9] such as the 1-alkyl-1'-aryl asymmetrically substituted viologens reported in the chapter 5.[10] The latter strategy equally provided satisfactorily colorless-to-gray switching when tested in all-in-one configuration dissolved into PVA-borax gel electrolytic matrix, ascribed to the contribution of both alkyl and aryl substituents. However, the potential window wherein gray coloration was observed was quite narrow and furthermore, the black colored state was not achieved due to the limited solubility of these asymmetric viologens into electrolytic matrix.

Accordingly, aiming at overcoming the above-mentioned limitations and considering the knowledge acquired in the chapters 5 and 6, the design of 1-alkyl-1'-aryl asymmetric viologens functionalized with anchoring groups and their integration in nanostructured ECDs of tailored thickness with PVA-borax gel electrolyte, was the next strategy to be explored. To this end and taking into account successful results obtained in the chapter 3, benzylphosphonic acid was also employed as bonding moiety due to its excellent grafting affinity towards TiO_2 nanostructured layers.

7.1.1. Objective

The main goal of the research work reported in this chapter was to develop monolayered ECDs comprising a single viologen which switched from colorless-off state to neutral colored state including black, while maintaining high performance and fast grafting process.

To achieve this goal, the synthesis of new 1-alkyl-1'-aryl asymmetric viologens conveniently functionalized with phosphonic acid anchoring groups in both alkyl and aryl substituents were required.

Their successful grafting on TiO_2 nanostructured films, subsequent assembly with PVA-borax gel electrolyte using simple device architecture (i.e., glass/TCO/Viologen-modified-TiO_2/PVA-borax gel electrolyte/TCO/glass), and their comparison with the corresponding symmetric viologens had to be proven to assess their more neutral EC behavior.

The optimization of some parameters such as thickness of the nanostructured TiO_2 layer and the grafting conditions, as well as the subsequent evaluation of the resulting device performance was also required.

Furthermore, the assessment of these 1-alkyl-1'-aryl asymmetric viologens in non-transparent (scattering or opaque) electrodes was equally a requisite to extend their field of application.

7.2. Materials and methods

7.2.1. Materials

4,4'-dipyridyl (98%), 2,4-dinitrochlorobenzene (98%), diethyl-2-bromoethylphosphonate (97%), Poly(vinyl alcohol) (PVA, Mw 61 000), sodium tetraborate decahydrate (borax, 99.5%), potassium ferrocyanide (98.5%) potassium ferricyanide (99%), lithium perchlorate trihydrate, hydroquinone (HQ) (≥ 99%), Poly(ethylene glycol) (PEG, Mw 20 000) and Triton X-100, were provided by Aldrich, whereas diethyl

4-aminobenzylphosphonate (98%) and γ-butyrolactone were supplied by Acros Organics. Hydrochloric acid (37%), charcoal activated powder and required organic solvents such as 2-propanol, THF, acetone, and ethanol were purchased from Scharlab. Titanium oxide powder (15 nm, Anatasa) was provided by Nanostructured & Amorphous Materials. Titanium dioxide dispersion (Ti-Nanoxide T, transparent) was supplied by Solaronix. All these reagents were used without further purification except for γ-butyrolactone which was degassed for 15 min with N_2 prior to use.

Fluorine-doped tin oxide (FTO) coated glass substrates provided by Solems (Rs 6-8 Ωsq^{-1}) were washed with heated acetone before being used.

7.2.2. Synthesis and characterization of viologens

Asymmetric viologens were synthesized as follows:

1-(2,4-Dinitrophenyl)-4,4'-bipyridinium monochloride (intermediate [**I**]) was synthesized in the chapter 5.[10]

1-(phosphonomethyl-4-phenyl)-4,4'-bipyridinium monochloride (intermediate [**II**]) was synthesized as follows: a mixture of intermediate [**I**] (40 mmol) and diethyl 4-aminobenzylphosphonate (45 mmol) was refluxed in ethanol (300 mL) for 24 h. The solvent was removed by rotary evaporation *in vacuo*, deionized water was added (200 mL) and the solution was stirred for 2 hours. The solid residue was removed and the filtrate was decolorized with charcoal activated powder for 24h. The water of the filtrate was removed by rotary evaporation *in vacuo*, THF was added (150 mL) and the solid was filtered followed by drying under vacuum. (Yield = 81%). (81% yield). ^{1}H NMR (500MHz, DMSO-*d6*, δ): 9.53 (d, *J* = 6.86 Hz, 2H,), 8.91 (d, *J* = 6.05 Hz, 2H,), 8.80 (d, *J* = 6.83 Hz, 2H,), 8.17 (d, *J* = 6.08 Hz, 2H,), 7.91 (d, *J* = 8.29 Hz, 2H,), 7.65 (d, *J* = 6.36 Hz, 2H,), 4.02 (m, 4H, $2OCH_2$), 3.49 (overlapped, 2H, CH_2P), 1.22 (t, 6H, $2CH_3$).

1-(2-phosphonoethyl)1'-(phosphonomethyl-4-phenyl)-4,4'-bipyridilium dichloride **[Et-Ph-PO_3H_2-Vio]** was obtained as follows: to a stirred solution of intermediate [**II**] (5 mmol) in deionized water (10 mL), diethyl-2-bromoethylphosphonate (20 mmol) was added and refluxed for 48 h. Then, reaction mixture was concentrated and 20 mL of HCl were added and refluxed for further 24h. The solvent was removed by rotary evaporation in vacuo and the resulting solid was washed with ethanol followed by drying under vacuum. (67% yield). Elemental analysis data: Anal. Calcd for $C_{19}H_{22}N_2O_6P_2Cl_2$: C, 44.99; H, 4.37; N, 5.52. Found: C, 43.97; H, 4.23; N, 5.33. ^{1}H NMR (500MHz, D_2O, δ): 9.39 (d, *J* = 6.83 Hz, 2H), 9.22 (d, *J* = 6.72 Hz, 2H), 8.73 (d, *J* = 6.82 Hz, 2H), 8.65 (d, *J* = 6.67 Hz, 2H), 7.78 (d, *J* = 8.28 Hz, 2H), 7.67 (d, *J* = 6.43 Hz, 2H), 4.98 (m, 2H, NCH_2), 3.31 (d, *J* = 21.06 Hz, 2H, $PhCH_2P$), 2.51 (m, 2H, CH_2P) (Figure 7.1). ^{13}C NMR (500MHz, D_2O, δ): 153.27, 152.88, 148.42, 148.05, 143.41, 141.30, 134.25, 129.74, 129.67, 126.78, 60.47, 37.10, 32.66 (Figure 7.2). ^{31}P NMR (500MHz, D_2O, δ): 18.67, 14.75 (Figure 7.3).

IR (bulk ATR): *ν* (cm^{-1}) = 3113, 3028 (C-H), 2700 - 2540 (PO-H st), 2330-2180 (PO-H comb), 1632, 1543 (C=C, C=N), 1248, 1128 (P=O st), 910 (P-OH st), 816 (*o*-phenylene H).

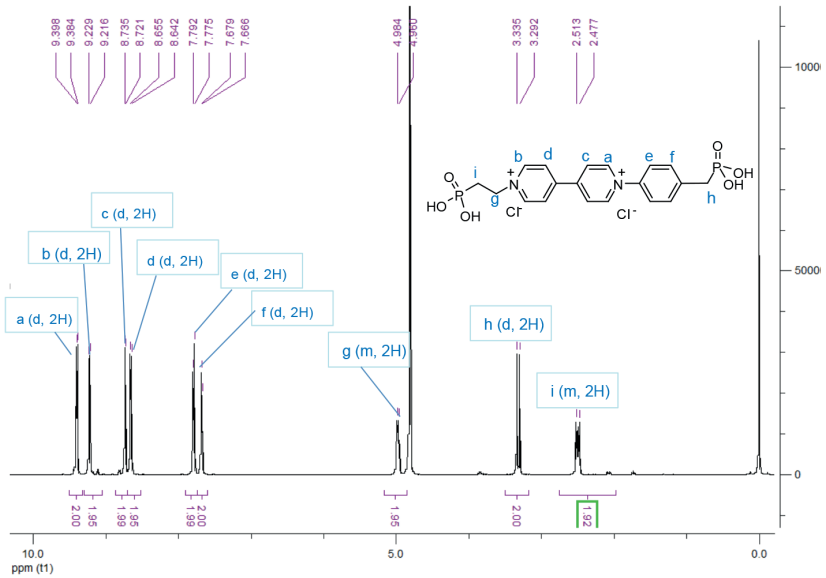

Figure 7.1. ^{1}H NMR spectra of [**Et-Ph-PO$_3$H$_2$-Vio**].

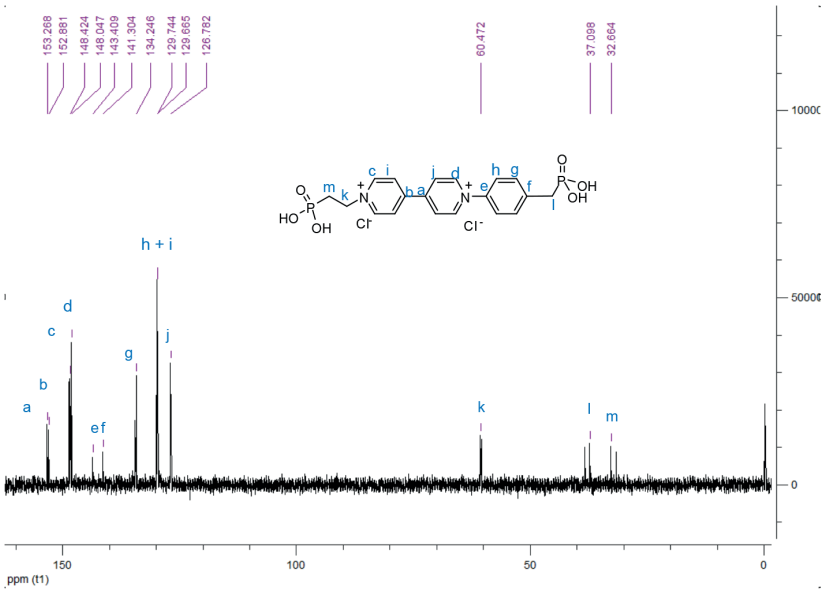

Figure 7.2. ^{13}C NMR spectra of [**Et-Ph-PO$_3$H$_2$-Vio**].

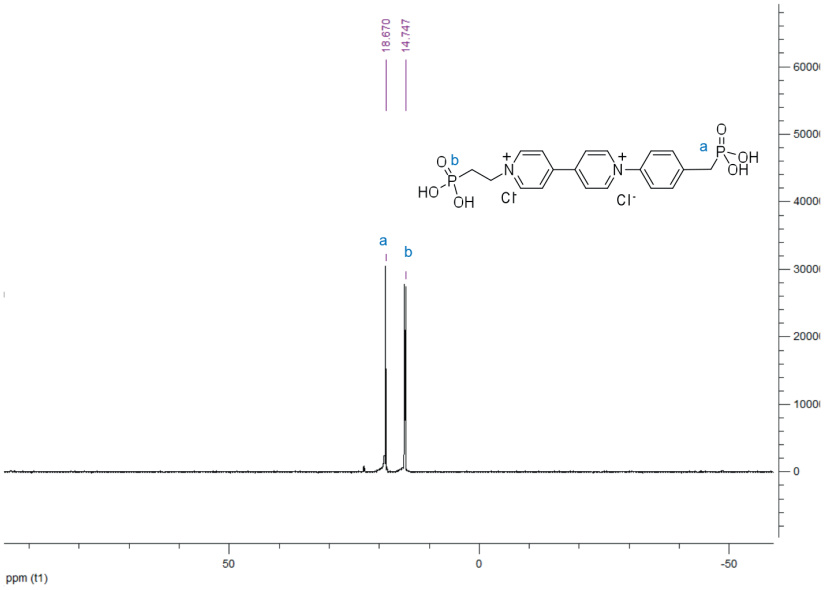

Figure 7.3. ^{31}P NMR spectra of [**Et-Ph-PO$_3$H$_2$-Vio**].

Synthesis of *1-(phosphonomethyl-4-benzyl)1'-(phosphonomethyl-4-phenyl)-4,4'-bipyridilium dichloride* [**Bn-Ph-PO$_3$H$_2$-Vio**].

Diethyl(4-chloromethyl)benzylphosphonate was synthesized in the chapter 3.[11] Synthesis of *1-(phosphonomethyl-4-benzyl)1'-(phosphonomethyl-4-phenyl)-4,4'-bipyridilium dichloride* [**Bn-Ph-PO$_3$H$_2$-Vio**] was carried out as follows:

To a stirred solution of intermediate [**II**] (5 mmol) in ethanol (10 mL), *diethyl(4-chloromethyl)benzylphosphonate* (20 mmol) was added and refluxed for 48 h. Then, reaction mixture was concentrated and added dropwise to beaker provided with 2-propanol stirring on ice bath. The resulting solid was washed with 2-propanol and dried under vacuum to obtain the intermediate [**III**] (51% yield). ^{1}H NMR (500MHz, D_2O, δ): 9.39 (d, J = 5.34 Hz, 2H), 9.19 (d, J = 6.56 Hz, 2H), 8.70 (d, J = 5.75 Hz, 2H), 8.61 (d, J = 6.44 Hz, 2H), 7.74 – 7.66 (dd, J = 39.43 Hz, 4H), 7.48 – 7.45 (dd, J = 17.14 Hz, 4H), 5.94 (s, 2H), 3.88 (m, ~ 8H), 3.20 (m, 2H) 3.08 (m, 2H), 1.18 (m, 12H).

Intermediate [**III**] (3 mmol) was mixed with 15 mL of concentrated HCl and refluxed for further 24h. The solvent was removed by rotary evaporation in vacuo and the resulting solid was washed with ethanol followed by drying under vacuum. (99% yield). Elemental analysis data: Anal. Calcd for $C_{25}H_{26}N_2O_6P_2Cl_2$: C, 51.47; H, 4.49; N, 4.80. Found: C, 49.04; H, 4.61; N, 4.42. ^{1}H NMR (500MHz, D_2O, δ): 9.37 (d, *J* = 6.83 Hz, 2H), 9.18 (d, *J* = 6.75 Hz, 2H), 8.69 (d, *J* = 6.87 Hz, 2H), 8.61 (d, *J* = 6.74 Hz, 2H), 7.75 (d, *J* = 8.35 Hz, 2H), 7.66 (d, *J* = 2.09 Hz, 2H), 7.49 (d, *J* = 8.03 Hz, 2H), 7.45 (d, *J* = 1.99 Hz, 2H), 5.93 (s, 2H, NCH_2), 3.26 (d, 2H, *J* = 21.06 Hz, CH_2P), 3.15 (d, *J* = 20.95 Hz, 2H, $PhCH_2P$) (Figure 7.4). ^{13}C NMR (500MHz, D_2O, δ): 153.37, 153.15, 148.46, 148.30, 143.45, 142.55, 139.89, 134.48, 133.67, 133.05, 132.51, 130.07, 129.88, 126.92, 67.58, 38.94, 37.93 (Figure 7.5). ^{31}P NMR (500MHz, D_2O, δ): 18.30, 16.97 (Figure 7.6).

IR (bulk ATR): *ν* (cm^{-1}) = 3116, 3034 (C-H), 2700-2450 (PO-H st), 2340-2160 (PO-H comb), 1632, 1543 (C=C, C=N), 1239, 1128 (P=O st), 917 (P-OH st), 820 (*o*-phenylene H).

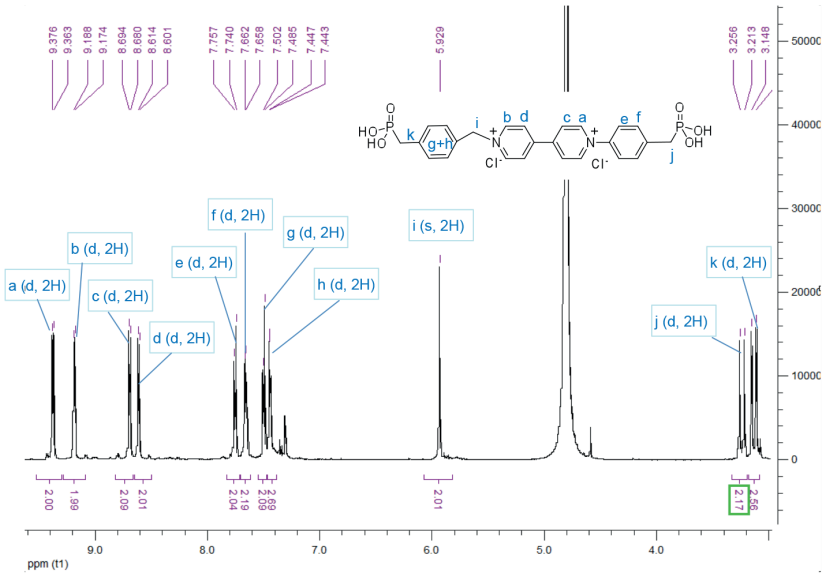

Figure 7.4. ^{1}H NMR spectra of [**Bn-Ph-PO_3H_2-Vio**].

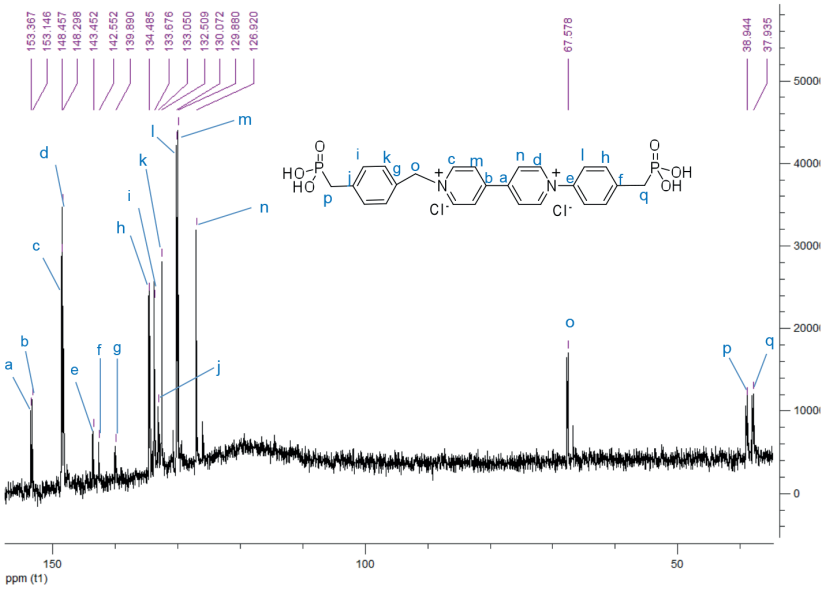

Figure 7.5. ^{13}C NMR spectra of [**Bn-Ph-PO$_3$H$_2$-Vio**].

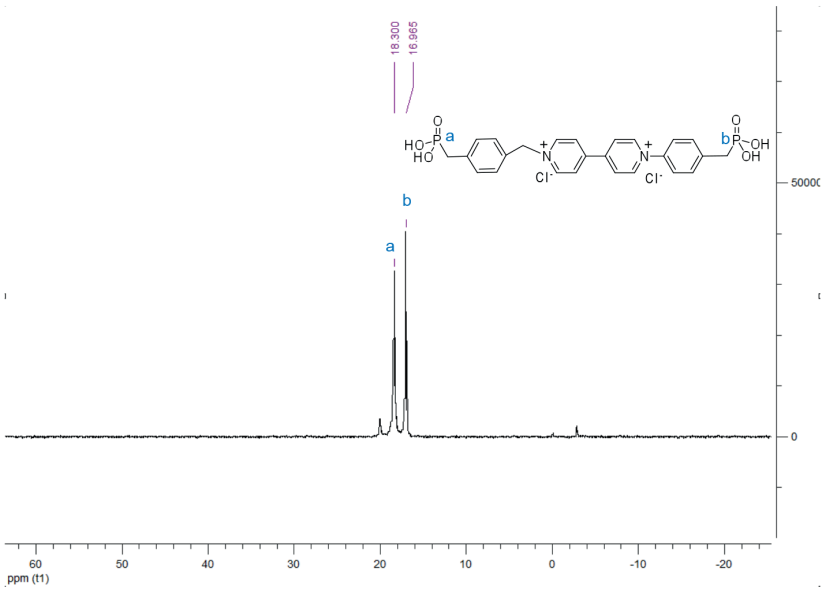

Figure 7.6. ^{31}P NMR spectra of [**Bn-Ph-PO$_3$H$_2$-Vio**].

Information regarding the synthesis procedures followed to obtain symmetric viologens employed for comparative purposes were included in previous chapters. Thus, *1,1'-Bis(2-phosphonoethyl)-4,4'-bipyridilium dichloride* **[Et-PO_3H_2-Vio]** and *1,1'-Bis(phosphonomethyl-4-benzyl)-4,4'-bipyridilium dichloride* **[Bn-PO_3H_2-Vio]** were synthesized in chapter 3,[11] whereas *1,1'-Bis(phosphonomethyl-4-phenyl)-4,4'-bipyridilium dichloride* **[Ph-PO_3H_2-Vio]** was synthesized in chapter 6.[8]

7.2.3. Methods

7.2.3.1. Preparation of electrolytes

PVA-borax gel electrolytes were prepared by varying concentrations of potassium ferrocyanide and ferricyanide salts employed as redox mediator from 1.0 to 3.5 mmol L^{-1} following the general procedure described in the section 2.2.2.1. of the chapter 2.

Anhydrous liquid electrolyte prepared for comparative purposes consisted of γ-butyrolactone solution containing 0.1 mol L^{-1} of hydroquinone redox mediator and 0.2 mol L^{-1} of $LiClO_4$.

7.2.3.2. Fabrication of layered electrochromic devices

Layered ECDs based on two-electrode (2-E) and three-electrode (3-E) configuratios were prepared and assembled following the procedure described in the chapter 2 section 2.5.1. and 2.5.2., respectively.

The dispersion employed to obtain opaque electrodes was prepared following previously reported procedure.[12]

Preparation of viologen-modified TiO_2 electrodes

Transparent nanostructured TiO_2 films were modified by anchoring the viologen as follows: TiO_2-coated FTO/glass substrates were dipped into a beaker containing water solution of the viologen for a suitable grafting time. In the case of **[Et-Ph-PO_3H_2-Vio]** and **[Bn-Ph-PO_3H_2-Vio]** asymmetric

viologens, concentration was fixed at 5 mmol L^{-1} and the immersion time at 15 min, except from the devices employed for the grafting time study wherein different immersion times in a 20 mmol L^{-1} solution were evaluated. The same procedure was followed for the modification with **[Et-PO_3H_2-Vio]**, **[Bn-PO_3H_2-Vio]** and **[Ph-PO_3H_2-Vio]** symmetric viologens, being concentrations and grafting times of 20 mmol L^{-1} for 48 hours, 5 mmol L^{-1} for 15 min and 1 mmol L^{-1} for 10 min, respectively. Afterwards, the viologen-modified TiO_2 electrodes were washed with water and ethanol and left drying for at least 5 hours at 50 °C.

7.3. Results and discussion

Asymmetric 1-alkyl-1'-aryl viologens provided with phosphonic acid anchoring groups in both substituents were synthesized following the synthetic route shown in the Scheme 7.1. Specifically 1-(2-phosphonoethyl)-1'-(phosphonomethyl-4-phenyl)-4,4'-bipyridilium dichloride **[Et-Ph-PO_3H_2-Vio]** and 1-(phosphonomethyl-4-benzyl)-1'-(phosphonomethyl-4-phenyl)-4,4'-bipyridilium dichloride **[Bn-Ph-PO_3H_2-Vio]** were selected for this study.

As shown in the Scheme 7.1, this synthetic route involved four different phases. Two steps were required to attach the aryl substituent through the Zincke reaction, another one for the bonding of the alkyl substituent and the last one corresponding to the hydrolysis of ethoxy groups of both alkyl and aryl chains leading to phosphonic acid anchoring groups. Even though the aryl chain has been first bonded to the bypiridine herein, it is similarly possible to attach the alkyl substituent in the first step providing that the hydrolysis is always carried out at the last stage.

Scheme 7.1. Synthetic route for [**Bn-Ph-PO_3H_2-Vio**] and [**Et-Ph-PO_3H_2-Vio**] asymmetric viologens provided with anchoring group.

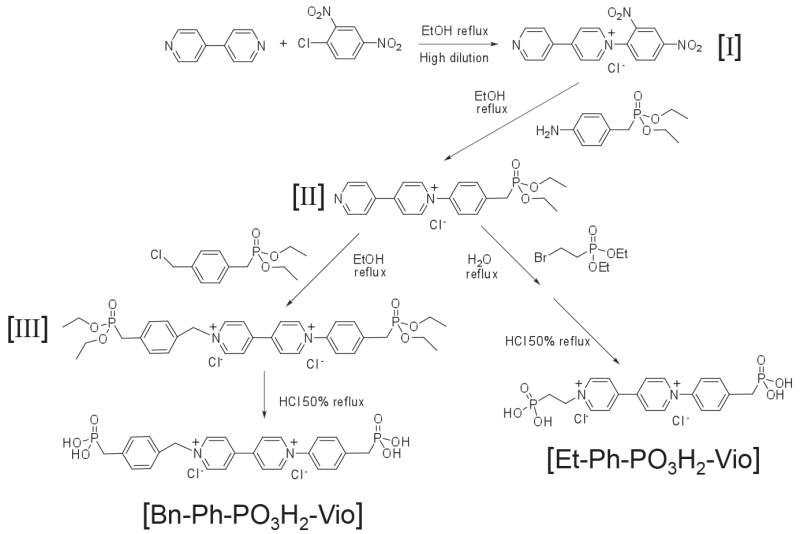

The isolation of the intermediate [**III**] was found to ease the purification of the [**Bn-Ph-PO_3H_2-Vio**], whereas in the case of [**Et-Ph-PO_3H_2-Vio**], the hydrolysis was carried out without prior purification of its precursor.

7.3.1. Assessment of [Et-Ph-PO_3H_2-Vio] and [Bn-Ph-PO_3H_2-Vio] Asymmetric viologens

The electrochromic and electrochemical behavior of [**Et-Ph-PO_3H_2-Vio**] and [**Bn-Ph-PO_3H_2-Vio**] asymmetric viologens was studied using both two-electrode (2-E) and three electrode (3-E) configuration.

7.3.1.1. Electrochromic Behavior of [Et-Ph-PO_3H_2-Vio] and [Bn-Ph-PO_3H_2-Vio] Asymmetric viologens

The electrochromic behavior of [**Et-Ph-PO_3H_2-Vio**] and [**Bn-Ph-PO_3H_2-Vio**] asymmetric viologens was assessed using 2-E electrochromic devices (ECDs) provided with transparent nanostructured TiO_2 films on FTO/glass substrates.

To this end, doctor-blade processed (100 µm applicator) TiO_2 sintered layers with a thickness of 4,3 – 4,6 µm according to cross-sectional SEM micrographs (Figure 7.7a-I), were employed. Thus, this thickness similar to that selected in the previous chapter, was also in the range of those reported for viologen modified-TiO_2 electrodes.[13] The grafting conditions were fixed for each viologen at 15 min of immersion time into 5 mmol L^{-1} solution of the viologen, being this concentration the maximum water solubility of **[Bn-Ph-PO_3H_2-Vio]** asymmetric viologen.

Thus obtained films were conveniently assembled with a PVA-borax gel electrolyte comprising 2 mmol L^{-1} of potassium ferrocyanide and ferricyanide salts and the electrochromic behavior of the resulting ECDs was evaluated. As confirmed by visual appearance (Figure 7.7a) and through spectrophotometric method (Figure 7.7b-c and Table 7.1), both **[Et-Ph-PO_3H_2-Vio]** and **[Bn-Ph-PO_3H_2-Vio]** used as single chromophore provided great gray colorations upon a wide range of reduction potentials from -1.2 to -2.2 V. Above this value the transmittance changes at the maximum contrast wavelength decreased. Regarding the bleached state, [**Et-Ph-PO_3H_2-Vio**] exhibited excellent colorless-off state whereas [**Bn-Ph-PO_3H_2-Vio**] showed slight yellowish coloration leading to a more noteworthy decrease of the %T between 420 and 480 nm. This underlying coloration was also manifested in the colored state as confirmed by the corresponding color coordinates (Table 7.1). Thus, the values of b^* component registered for ECDs based on **[Bn-Ph-PO_3H_2-Vio]** were higher than the ones registered for **[Et-Ph-PO_3H_2-Vio]** in both bleached and colored states. Therefore, ECDs comprising **[Et-Ph-PO_3H_2-Vio]** as a single asymmetric viologen exhibited excellent colorless-off state and more gray EC behavior with both chromaticity coordinates (a^* and b^*) closer to 0 value.

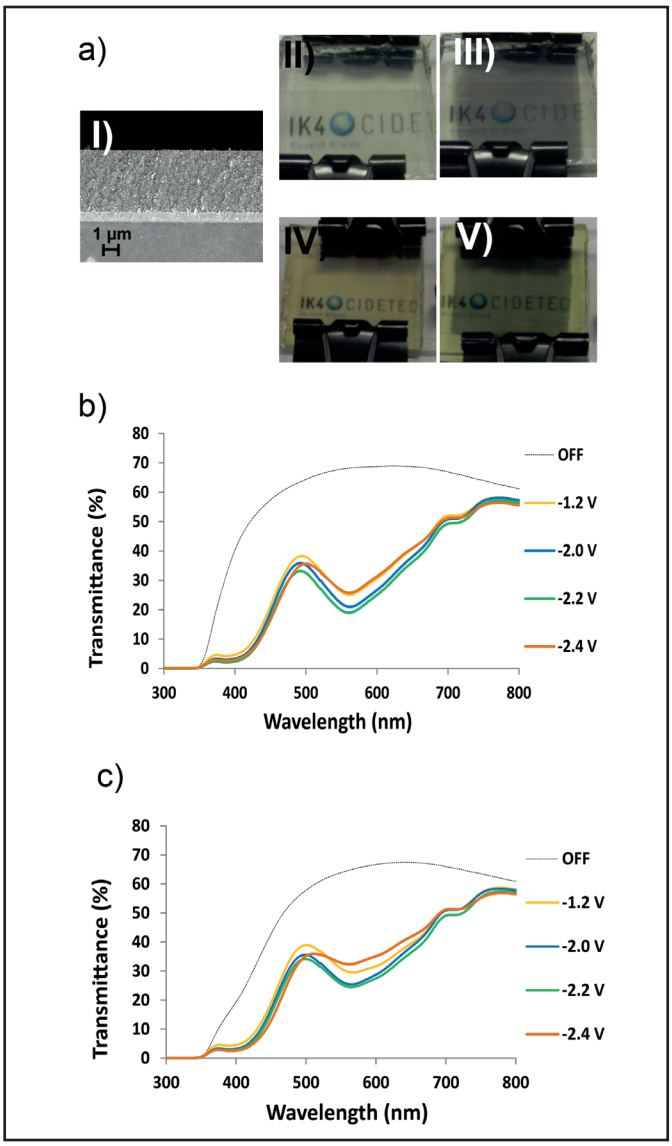

Figure 7.7. a) Cross-sectional SEM micrograph of TiO_2 film (4.5 µm) on FTO/glass (I), and photographs of 2-E ECDs based on similar nanostructured films comprising **[Et-Ph-PO_3H_2-Vio]** (II and III) and **[Bn-Ph-PO_3H_2-Vio]** (IV and V) at bleached state (II and IV) and upon applying -2.2V (III and V); UV-vis transmittance responses of ECDs comprising (b) **Et-Ph-PO_3H_2-Vio]** and (c) **[Bn-Ph-PO_3H_2-Vio]** at different applied potentials.

It is also noteworthy the wider range of cathodic potentials in which **[Et-Ph-PO_3H_2-Vio]** and **[Bn-Ph-PO_3H_2-Vio]** offer gray coloration (from -1.2 to -2.2 V) in comparison to that achieved with asymmetrically substituted viologens without anchoring group, developed in the chapter 5,[10] therefore denoting a significant progress. The latter exhibited neutral-gray colorations within a more limited range of potentials (i.e., from -0.8 to -1.3 V), and outside this limits they offered green or bluish colored states.

Table 7.1. Transmittance changes (Δ%T) and color coordinates of 2-E ECDs based on nanostructured TiO_2 films (4.5 μm) comprising [**Et-Ph-PO_3H_2-Vio**] and [**Bn-Ph-PO_3H_2-Vio**] viologens at different applied potentials.

	V	%T	Δ%T [a]	x [b]	y [b]	Y [b]	L^* [c]	a^* [c]	b^* [c]	Color [d]
Et-Ph-PO_3H_2-Vio	OFF	68.3	-	0.326	0.349	67.3	86	-2	9	
	-1.2 V	25.1	43.2	0.332	0.362	30.2	62	-4	11	
	-2.0 V	21.0	47.3	0.330	0.357	26.5	59	-3	9	
	-2.2 V	19.0	49.2	0.334	0.358	24.3	56	-2	9	
	-2.4 V	25.8	42.5	0.349	0.384	30.1	62	-5	18	
Bn-Ph-PO_3H_2-Vio	OFF	64.8	-	0.344	0.374	63.3	84	-4	20	
	-1.2 V	29.6	35.3	0.336	0.384	32.9	64	-10	17	
	-2.0 V	25.4	39.5	0.339	0.381	29.2	61	-7	16	
	-2.2 V	24.5	40.4	0.340	0.386	28.0	60	-8	17	
	-2.4 V	32.3	32.5	0.365	0.415	34.0	65	-9	30	

[a] ΔT% at λ_{max} = 562 nm

[b], [c] Color coordinates (D65) registered for xyY (CIE 1931) ([b]) and L^*a^*b (CIE 1976) ([c]) quantitative scales.

[d] Color swatches representing L^*a^*b color coordinates.

It is worth remarking that **[Et-Ph-PO$_3$H$_2$-Vio]** and **[Bn-Ph-PO$_3$H$_2$-Vio]** asymmetric viologens revealed both absorption profiles (Figure 7.8a-b) and color coordinates (Figure 7.8c and Table 7.2) about midway between the ones acquired for the corresponding symmetric viologens.

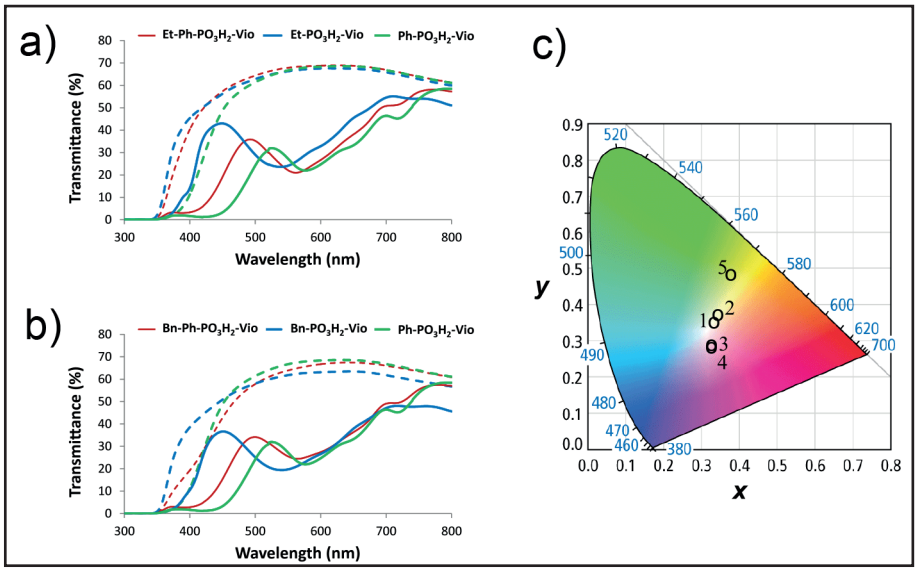

Figure 7.8. UV-vis spectra of 2-E ECDs based on (a) **[Et-Ph-PO$_3$H$_2$-Vio]** and (b) **[Bn-Ph-PO$_3$H$_2$-Vio]** asymmetric viologens and those obtained for corresponding symmetric viologens **[Et-PO$_3$H$_2$-Vio], [Bn-PO$_3$H$_2$-Vio]** and **[Ph-PO$_3$H$_2$-Vio]** in their bleached and colored states (dashed and solid lines respectively); c) corresponding color coordinates represented in the chromaticity diagram, being (1) **[Et-Ph-PO$_3$H$_2$-Vio]**, (2) **[Bn-Ph-PO$_3$H$_2$-Vio]**, (3) **[Et-PO$_3$H$_2$-Vio]**, (4) **[Bn-PO$_3$H$_2$-Vio]** and (5) **[Ph- PO$_3$H$_2$-Vio]** at colored state.

Hence, 1,1'-aryl symmetric viologen, **[Ph-PO$_3$H$_2$-Vio]** provided greater green and yellow colored states than the asymmetric viologens, as confirmed by the more negative value of a^* and more positive value of b^* components, respectively. Equally, 1,1'-alkyl symmetric viologens, **[Et-PO$_3$H$_2$-Vio]** and **[Bn-PO$_3$H$_2$-Vio]**, exhibited lower values of b^* (blue) and higher of a^* components (red) due to the presence of the radical-cation monomer and dimer respectively.[14]

Table 7.2. Color coordinates of 2-E ECD based on [**Et-Ph-PO_3H_2-Vio**] and [**Bn-Ph-PO_3H_2-Vio**] viologens and corresponding symmetric viologens registered for comparable transmittance changes (Δ%T = 40 – 46 % at λ_{max}).

Device	$\lambda_{max.}$ Abs. (nm)	Δ%T	x [(a)]	y [(a)]	Y [(a)]	L^* [(b)]	a^* [(b)]	b^* [(b)]	Color [(c)]
Et-Ph-PO_3H_2-Vio	562	43.2	0.332	0.362	30.2	62	-4	11	
Bn-Ph-PO_3H_2-Vio	565	40.5	0.340	0.386	28.0	60	-8	17	
Et-PO_3H_2-Vio	539	42.2	0.312	0.277	28.8	61	19	-14	
Bn-PO_3H_2-Vio	540	41.8	0.308	0.275	23.7	56	17	-14	
Ph-PO_3H_2-Vio	577	46.0	0.389	0.476	26.1	58	-15	46	

[a), b)] Color coordinates (D65) registered for xyY (CIE 1931) ([(a)]) and L^*a^*b (CIE 1976) ([(b)]) quantitative scales.
[c)] Color swatches representing L^*a^*b color coordinates acquired through a color converter software.

The formation of the dimer was confirmed in the previous chapters for alkyl substituted viologens when being tested in PVA-borax gel, by their characteristic purple coloration and hypsochromic shift of the absorption profiles.[8, 10] Actually, similar blue shift and more neutral colorations were found when 1-alkyl-1'-aryl asymmetric viologens exempted from anchoring group developed in the chapter 5 were evaluated dissolved into PVA-borax gel electrolyte in comparison to those tested with anhydrous electrolytes.[10] Interestingly, analogous hypsochromic shift was observed for the ECDs developed in the present chapter comprising asymmetric viologens attached to the coated electrode (Annex 7.1), when being tested with PVA-borax gel, equally leading to more neutral-gray colorations.

7.3.1.2. Spectroelectrochemical Study of [Et-Ph-PO_3H_2-Vio] *and* [Bn-Ph-PO_3H_2-Vio] Asymmetric Viologens.

The in situ spectroelectrochemical behavior of **[Et-Ph-PO_3H_2-Vio]** and **[Bn-Ph-PO_3H_2-Vio]** viologen-modified TiO_2 films was studied in a 3-E configuration using ECDs provided with pseudo-reference electrode and assembled with the same gel electrolyte.

Apart from additional cathodic peaks attributed to other uncolored redox process, (i.e., the reduction of the ferricyanide ion ~ -0.1V vs Ag/Ag^+ or the electrochemical activity of TiO_2 layer),[15] cyclic voltammograms (CVs) of both systems revealed two distinct peaks on the cathodic span of the scan. The latter, habitually correlated to the well-known first and second reduction processes of the viologens, provided gray (~ -0.9V vs Ag/Ag^+) and yellowish coloration (~ -1.3V vs Ag/Ag^+), respectively, as shown by Figure 7.9 for **[Bn-Ph-PO_3H_2-Vio]** comprising ECD. Therefore, it can be concluded that the radical-cationic form ($bipm^{+\bullet}$) of these asymmetric viologens offers neutral-gray colors, whereas devices turn into yellow coloration when the applied potentials are sufficiently negative to form the neutral state ($bipm^0$).

In addition, the first and second reduction potentials of the asymmetric viologens provided with anchoring group described herein, seem to appear in-between the ones recorded for the corresponding symmetric viologens. This fact confirms the transitional electrochemical behavior of the formers, also detected for asymmetric viologens exempted from anchoring group and dissolved into electrolytic matrix developed in the chapter 5.[10]

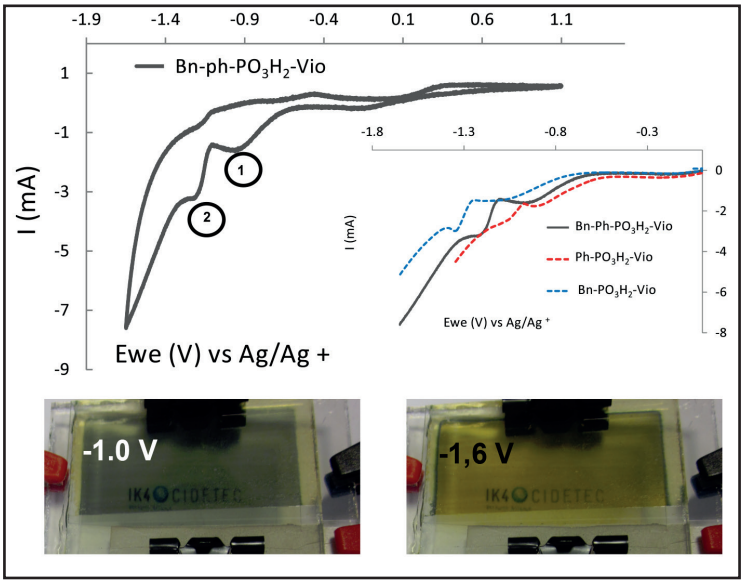

Figure 7.9. 3-E ECD based on nanostructured TiO_2 film comprising **[Bn-Ph-PO_3H_2-Vio]** asymmetric viologen: cyclic voltammetry (CV), photograph at first and second reduced states and CVs (cathodic sweep) of this asymmetric viologen vs corresponding symmetric viologens [**Bn-** PO_3H_2-V^{2+}] and [**Ph-**PO_3H_2-V^{2+}] (inset).

7.3.1.3. White-to-Gray ECDs

With the aim of extending the applicability of the asymmetric viologens reported herein, they were also tested in opaque electrodes providing a white background to prove their compatibility with these non-transparent surfaces. To this end, sintered nanostructured layer of 12 μm of thickness (Figure 7.10 I) conveniently modified with **[Et-Ph-PO_3H_2-Vio]** asymmetric viologen was assembled with gel electrolyte. Thus obtained ECDs switched between a white opaque off state to a neutral-gray colored opaque state (Figure 7.10 II-III) upon applying suitable external voltage (from -1.6 to -2.3V). For more cathodic potentials applied, the devices turned into yellowish colored state (correlated to the di-reduced form as detected for transparent electrodes). Additionally, the more gray-colored state in

comparison to that observed when tested with anhydrous liquid electrolytes was also proved for these reflective ECDs.

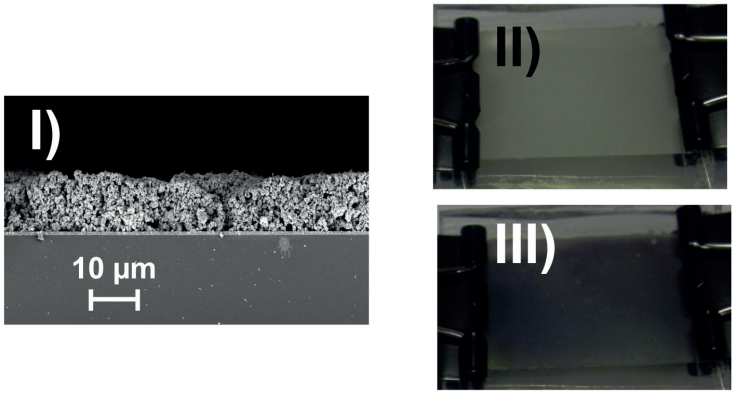

Figure 7.10. Cross-sectional SEM micrograph of scattering TiO_2 film (12 µm) on FTO/glass (I), and photographs of the 2-E ECDs based on similar nanostructured films comprising **[Et-Ph-PO_3H_2-Vio]** at bleached state (II) and upon applying -2.2V (III).

Therefore, the new asymmetric viologens reported herein may also be employed in diverse applications wherein non-transparent surfaces might be required, including displays and smart cards among others.

7.3.2. Colorless-to-Black ECDs

With the aim of achieving the lowest possible transmittance at colored state while keeping the simple device configuration, the thickness of the nanostructured TiO_2 layer was adjusted. As pointed out in the chapter 3, thicker nanostructured networks may somewhat accommodate higher amount of viologen molecules, thus providing highly colored states.[11]

After systematic study with a series of doctor-blade applicators of diverse groove depths, sintered films of 8 µm thickness (200 µm applicator) were selected (Figure 7.11a-I) since thicker films led to the formation of cracks on the surface of the nanostructured films.

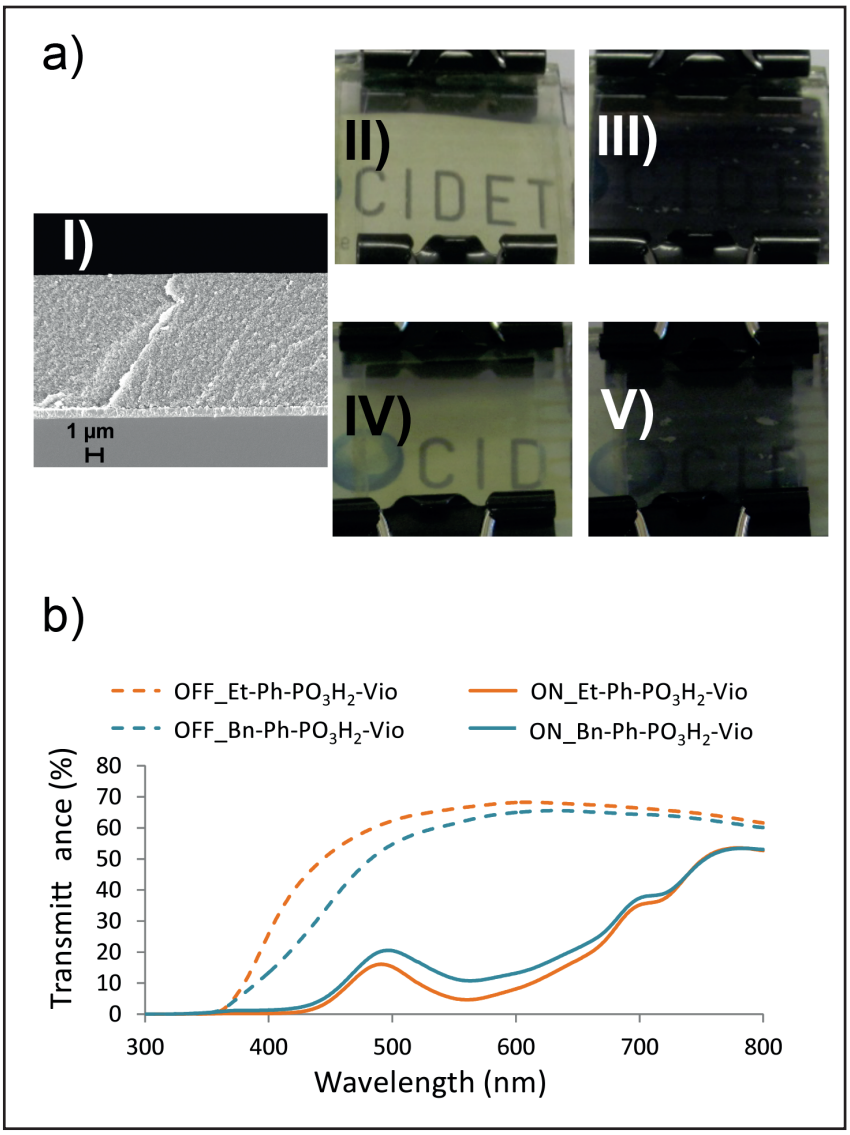

Figure 7.11. a) Cross-sectional SEM micrograph of TiO_2 film (8 µm) on FTO/glass (I), and photographs of 2-E ECDs based on similar nanostructured films comprising **[Et-Ph-PO_3H_2-Vio]** (II and III) and **[Bn-Ph-PO_3H_2-Vio]** (IV and V) at bleached state (II and IV) and upon applying -2.2V (III and V); b) UV-vis transmittance responses of ECDs comprising **[Et-Ph-PO_3H_2-Vio]** and **[Bn-Ph-PO_3H_2-Vio]** at bleached and colored states.

Thus obtained nanostructured TiO_2 electrodes were modified by anchoring **[Et-Ph-PO_3H_2-Vio]** and **[Bn-Ph-PO_3H_2-Vio]** asymmetric viologens using similar grafting conditions (15 min immersed in 5 mmol L^{-1} water solution of viologen) and the EC properties of the resulting 2-E ECDs were evaluated. Surprisingly, these ECDs based on a single asymmetric viologen exhibited colorless-to-black EC behavior, more spectacularly for **[Et-Ph-PO_3H_2-Vio]** due to its more transparent colorless-off state (Figure 7.11a). The absorption profiles of these ECDs were registered for different applied potentials (Table 7.3) reaching %T at colored state lower than 5% for **[Et-Ph-PO_3H_2-Vio]** and as low as 10% for **[Bn-Ph-PO_3H_2-Vio]**.

Table 7.3. Transmittance changes (Δ%T) and color coordinates of 2-E ECDs based on nanostructured TiO_2 films (8.0 μm) comprising **[Et-Ph-PO_3H_2-Vio]** and **[Bn-Ph-PO_3H_2-Vio]** viologens at different applied potentials.

	V	%T	Δ%T [a]	x [b]	y [b]	Y [b]	L^* [c]	a^* [c]	b^* [c]	Color [d]
Et-Ph-PO_3H_2-Vio	OFF	66.8	-	0.332	0.358	65.8	85	-3	13	
	-1.0V	10.2	56.6	0.335	0.364	15.1	46	-3	9	
	-1.4 V	7.7	59.1	0.331	0.361	12.0	41	-3	8	
	-2.0 V	8.0	58.8	0.333	0.358	12.7	42	-2	7	
	-2.2 V	5.5	61.3	0.329	0.355	9.4	37	-2	6	
	-2.3 V	4.7	62.1	0.334	0.352	8.3	35	0	6	
Bn-Ph-PO_3H_2-Vio	OFF	62.7	-	0.353	0.386	60.9	82	-5	25	
	-1.4 V	12.8	49.9	0.332	0.394	16.1	47	-11	15	
	-2.2 V	12.2	50.5	0.335	0.389	15.6	46	-9	14	
	-2.3V	10.8	51.9	0.339	0.387	14.0	44	-7	14	
	-2.4 V	12.1	50.6	0.361	0.402	14.9	45	-5	20	

[a] ΔT% at λ_{max} = 562 nm.
[b], [c] Color coordinates (D65) registered for xyY (CIE 1931) ([b]) and L^*a^*b (CIE 1976) ([c]) quantitative scales.
[d] Color swatches representing L^*a^*b color coordinates.

By comparing the transmittance responses of these two viologens (Figure 7.11b) at off state and at -2.3 V, it is once again evident the better EC performance of **[Et-Ph-PO_3H_2-Vio]** due to its higher transparency at off state and the higher level of coloration reached.

Color coordinates (a^* and b^*) for these ECDs at different potentials (Table 7.3) remained as close to 0 as the ones registered for thinner films (4.5 μm) but with lower values of L^* due to the higher level of coloration, proving the excellent neutral-black electrochromic behavior of the ECDs reported in the present chapter.

7.3.2.1. EC performance and cyclability

EC performance in terms of switching time and optical contrast of 2-E colorless-to-black ECDs comprising **[Et-Ph-PO_3H_2-Vio]** and **[Bn-Ph-PO_3H_2-Vio]** modified TiO_2 films were assessed. With the aim of achieving suitable switching times between the off-bleached state and the reduced-black state, the optimal concentration of redox mediator in the PVA-Borax electrolytic gel was searched and finally set at 3.5 mmol L^{-1}. Thereafter, switching performance of thus obtained ECDs were studied by recording the transmittance changes at maximum contrast wavelength (562 nm) while the devices were being exposed to coloring (-2.2 V for 50 s) and bleaching (+2.2 V for 10 s and then 0 V for 80 s) steps (Figure 7.12). The coloring process resulted to be faster (≤ 6 s) than the bleaching step (≤ 10 s) for both devices, being the required times as short as 5 s to reach the 90% the total transmittance change (i.e., Δ%T 60%) in the case of the ECDs comprising **[Et-Ph-PO_3H_2-Vio]**. It is remarkable that in spite of the simple device configuration, these values of transmittance change are similar to the maximum values reported for black-to-transmissive ECDs with rather complex architectures and/or using multimaterials.[2b]

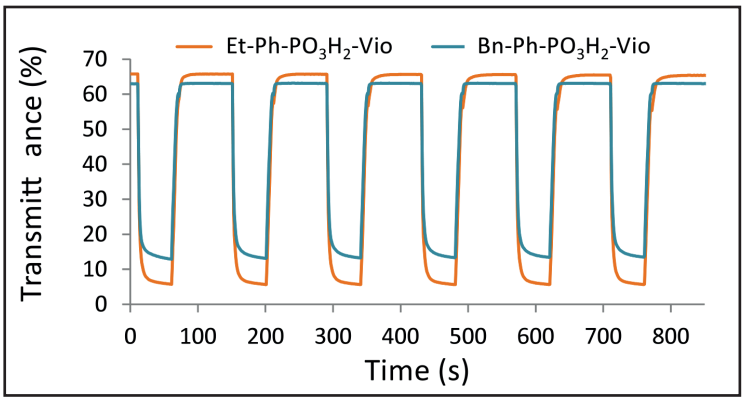

Figure 7.12. Transmittance changes registered at 562 nm plotted against time for ECDs comprising [**Et-Ph-PO_3H_2-Vio**] and [**Bn-Ph-PO_3H_2-Vio**] while voltage steps between colored (-2.2 V for 50 s) and bleached steps (+2.2 V for 10 s and 0 V for 80 s) were being applied.

On the basis of the results, although both devices revealed reversible and suitable switching along with satisfactory color efficiencies (Table 7.4), the ECD comprising [**Et-Ph-PO_3H_2-Vio**] offered better overall performances than the [**Bn-Ph-PO_3H_2-Vio**].

Table 7.4. Switching times and color efficiencies of [**Et-Ph-PO_3H_2-Vio**] and [**Bn-Ph-PO_3H_2-Vio**] viologens containing ECDs.

Device	T_b	T_c	Δ %T[a]	t_c (s) [b]	t_b (s) [b]	η_c (cm^2 C^{-1}) [c]	η_b (cm^2 C^{-1}) [c]
Et-Ph-PO_3H_2-Vio	65.5	5.6	60	5	10	246	177
Bn-Ph-PO_3H_2-Vio	63.1	13.4	49.7	6	8	229	210

[a] $\Delta T\%$ at λ_{max} = 562 nm. [b] Switching times. [c] Color efficiencies.

The cyclability was equally evaluated by switching the devices between the bleached (-1.4 V for 50 s) and colored states (+1.4 V for 10 s and 0 V for 80 s) up to 10 000 cycles (Figure 7.13). Thus, the %T was recorded every certain number of cycles while the same potential steps were being applied. In this regard, the slight difference in transmittance change detected between

-1.4 V and the maximum contrast voltage (~ 2 – 3 %) was considered to be undetectable for the naked eye, but may play a significant role in the device durability. ECDs based on **[Et-Ph-PO_3H_2-Vio]** (Figure 7.13a) showed satisfactory cycling performances as more than 70% of the initial transmittance change was preserved after 7 000 cycles (~ 100 operating hours at colored state) while still providing transmittance changes of 40 %. Additionally, a minor diminution of 7% was observed for the transmittance at off state after 10 000 cycles (~ 140 operating hours at colored state).

With regard to ECDs comprising **[Bn-Ph-PO_3H_2-V^{2+}]** (Figure13b), the transmittance changes after 6 000 cycles were of 34 % and a diminution of 12% was detected for transmittance at bleached state after 10 000 cycles.

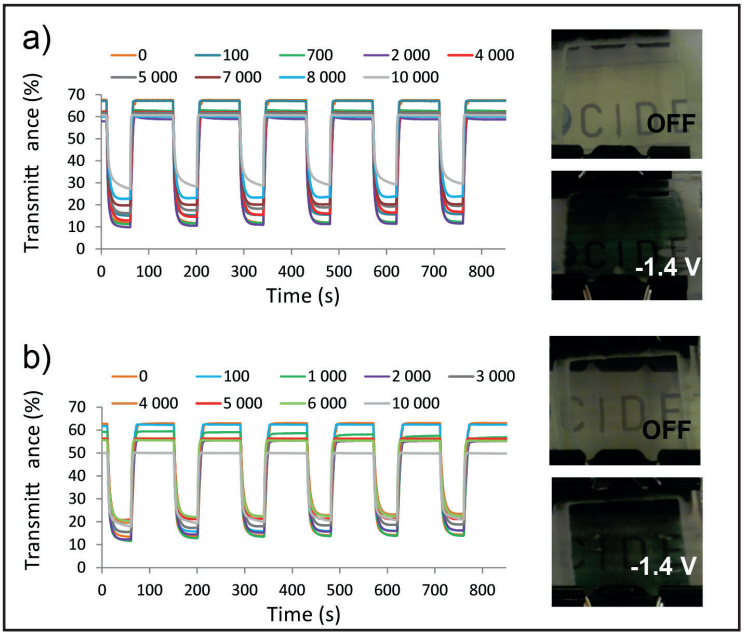

Figure 7.13. Evolution of the switching performance of ECDs containing (a) **[Et-Ph-PO_3H_2-Vio]** and (b) **[Bn-Ph-PO_3H_2-Vio]** up to 10 000 cycles while square-wave potential-steps between colored (-1.4 V for 50 s) and bleached steps (+1.4 V for 10 s and 0 V for 80 s) were being applied. Photographs of the ECDs at bleached (off) and at colored state after 10 000 cycles (inset).

The results achieved with **[Et-Ph-PO_3H_2-Vio]** are comparable to those reported for common symmetric viologens equally adsorbed on TiO_2 nanostructured layer, exposed to the same number of operating hours,[13c] and significantly higher than the ones showed by recently reported black ECDs based on a single small molecule.[2a] Furthermore, the number of cycles reported herein prove the suitability of these ECDs for some applications such as smart labels, smart cards or other disposable systems.

7.3.2.2. Grafting Conditions of the [Et-Ph-PO_3H_2-Vio] Asymmetric Viologen

Aiming at finding out the minimum grafting time required to reach the highest level of coloration, anchoring conditions of the asymmetric viologen were readjusted. For this study **[Et-Ph-PO_3H_2-Vio]** was chosen due to its better overall performance and colorless bleached state. Taking advantage of its high water solubility, the concentration was increased up to 20 mmol L^{-1}, while different immersion times were evaluated. It is worth to mention that despite the high concentration of viologen employed for the bonding, no degradation was observed in the modified TiO_2 films, as deduced from FE-SEM characterization performed before and after the anchoring step (Figure 7.14a).

Based on the observed colorations and absorption profiles (Figure 7.14b), it can be concluded that times just as low as 1 min were enough to accomplish colorless-to-black electrochromic behavior, while maintaining high transmittance change ($\Delta\%T \geq 60\%$) (Table 7.5), and fast switching times as shown by the video S0 included as Supporting Information in the published work.[16]

Color coordinates equally revealed the neutral-black EC character of this device (a^* and $b^* \leq |5|$ at colored state), and a great variation of the level of coloration between bleached and colored state ($\Delta L^* = 53$), similar to that previously reported for black ECDs based on a single EC layer,[9a] or overrunning them.[17]

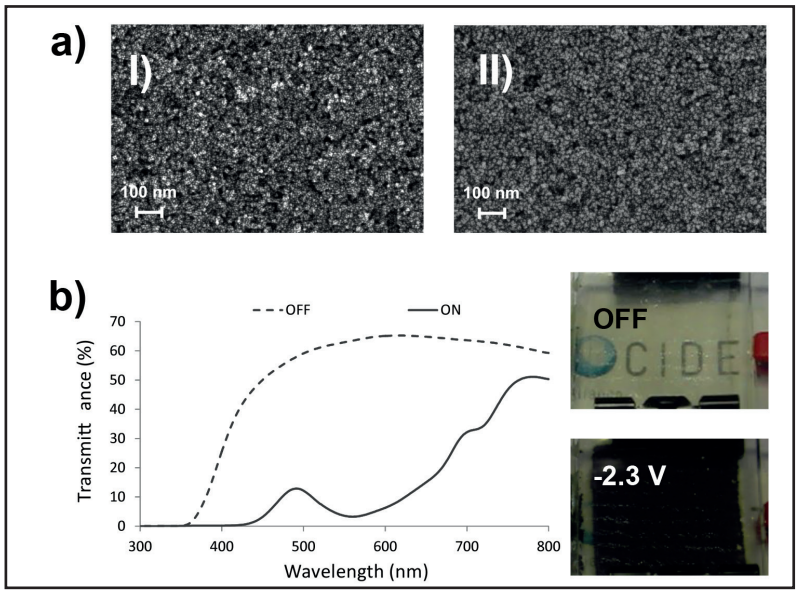

Figure 7.14. a) SEM images of the TiO_2 electrode (I) before and (II) after being modified with 20 mmol L^{-1} water solution of **[Et-Ph-PO_3H_2-V^{2+}]** for 15 min; b) UV-vis transmittance responses and photographs (inset) of 2-E ECD comprising **[Et-Ph-PO_3H_2-Vio]** after 1 min of grafting time, at bleached and colored states.

Table 7.5. Transmittance change (Δ%T) and color coordinates of 2-E ECD based on nanostructured TiO_2 film (8.0 μm) after 1 min grafting time into [**Et-Ph-PO_3H_2-Vio]** viologen solution at bleached and colored state.

State	%T	Δ%T [a]	x [b]	y [b]	Y [b]	L^* [c]	a^* [c]	b^* [c]	Color [d]
OFF	63.5	-	0.332	0.356	62.7	83	-3	12	
ON	3.2	60.3	0.341	0.350	6.3	30	2	5	

[a] $\Delta T\%\ \lambda_{max} = 562$ nm.
[b], [c] Color coordinates (D65) registered for xyY (CIE 1931) ([b]) and L^*a^*b (CIE 1976) ([c]) quantitative scales.
[d] Color swatches representing L^*a^*b color coordinates.

This rapid grafting rate can be ascribed to the presence of anchoring groups in both alkyl and aryl substituents of the molecule, and mainly to the presence of benzylphosphonic acid moiety. In this regard, in the little reported asymmetric viologens the asymmetry was basically used as a strategy to provide the molecule with an appropriate anchoring group,[18] being these viologens provided with a single bonding group in one of the substituents. Additionally, in most of them, ethylphosphonic acid was employed as anchoring moiety,[2b] which as demonstrated for corresponding symmetric viologen (i.e., 1,1'-*Bis*(2-phosphonoethyl)-4,4'-bipyridilium dichloride), required long grafting times to ensure complete chemisorption.[13a, 13c] Unlike these last, the asymmetric viologens reported in the this chapter are provided with anchoring groups in both substituents bonded to the nitrogen atoms, wherein at least one of them contains aromatic rings in the adjacent carbons of the phosphonic acid group (β). As proven in the chapter 3, benzylphosphonic acid moiety allows the rapid chemisorption of the viologen onto the nanostructured TiO_2 coated electrode.[11]

The short grafting times required, the high levels of coloration achieved and the excellent EC performances exhibited by the 1-alkyl-1'-aryl asymmetric viologens reported in the present chapter result in a unique combination and significant progress beyond of the state of the art, which place the anchored asymmetric viologens as very promising candidates for the production of colorless-to-black ECDs. In this regard, it is highlighted that the short grafting times required to ensure the chemisorption of these new asymmetric viologen, makes them compatible with any coating or printing technology required for up-scaling such as slot-die, gravure, slide-bead, dip-coating or ink-jet including roll-to-roll processing.

7.4. Conclusions

The development of monolayered ECDs comprising a single asymmetric viologen which switched from colorless-off state to neutral colored state including black was proven.

The synthesis of new 1-alkyl-1'-aryl asymmetric viologens conveniently functionalized with phosphonic acid anchoring groups in both alkyl and aryl substituents which exhibited fast grafting speeds (1 min) was equally demonstrated.

The successfull incorportion of these new viologens in a simple device configuration with PVA-borax gel electrolyte (glass/TCO/Viologen-modified-TiO_2/PVA-borax gel electrolyte/TCO/glass) was proven to provide excellent colorless-to-neutral color EC behavior in both transparent and opaque electrodes. The assesment of the more neutral colored state was confirmed by comparinson with their corresponding symmetric violgens.

The optimization of some parameters such as thickness of the nanostructured TiO_2 layer and the grafting conditions was also carried out and the overall performances of the resulting ECDs were also evaluated. Thus, the extraordinary black colored state (a^* and $b^* \leq |5|$), great variation of the level of coloration ($\Delta L^* = 53$) and transmittance change between the off-bleached and on-colored states ($\Delta\%T \geq 60$), was confirmed for **[Et-Ph-PO_3H_2-Vio]** based ECDs, after 1 min of grafting time. The fast switching times (5 – 10 s) and good cyclability (~ 10 000 cycles) were also proved for these asymmetric viologen based ECDs.

To sum up, the EC systems described herein offer many advantages over previously reported black ECDs including the simplicity in the device configuration and competitive performances while being compatible with any coating process required for up-scaling. Therefore, the colorless-to-black and gray ECDs based on a single 1-alkyl-1'-aryl asymmetric viologen

anchored to a nanostructured electrode reported in the present chapter may meaningfully expand the applicability of the EC technology.

7.5. References

[1] a) M. Sassi, M. M. Salamone, R. Ruffo, G. E. Patriarca, C. M. Mari, G. A. Pagani, U. Posset, L. Beverina, *Advanced Functional Materials* **2016**, *26*, 5240-5246; b) M. Sassi, M. M. Salamone, R. Ruffo, C. M. Mari, G. A. Pagani, L. Beverina, *Adv. Mater.* **2012**, *24*, 2004-2008.

[2] a) W. H. Nguyen, C. J. Barile, M. D. McGehee, *The Journal of Physical Chemistry C* **2016**, *120*, 26336-26341; b) D. Weng, Y. Shi, J. Zheng, C. Xu, *Organic Electronics* **2016**, *34*, 139-145.

[3] P. M. Beaujuge, J. R. Reynolds, *Chem. Rev.* **2010**, *110*, 268-320.

[4] R. J. Mortimer, *Annu. Rev. Mater. Res.* **2011**, *41*, 241-268.

[5] a) E. Unur, P. M. Beaujuge, S. Ellinger, J.-H. Jung, J. R. Reynolds, *Chem. Mater.* **2009**, *21*, 5145-5153; b) C. S. Ah, J. Song, S. M. Cho, T.-Y. Kim, H. N. Kim, J. Y. Oh, H. Y. Chu, H. Ryu, *Bull. Korean Chem. Soc.* **2015**, *36*, 548-552.

[6] P.-Y. Chen, C.-S. Chen, T.-H. Yeh, *J. Appl. Polym. Sci.* **2014**, *131*, 40485.

[7] H. Shin, Y. Kim, T. Bhuvana, J. Lee, X. Yang, C. Park, E. Kim, *ACS Appl. Mater. Interfaces* **2012**, *4*, 185-191.

[8] Y. Alesanco, A. Viñuales, J. Ugalde, E. Azaceta, G. Cabañero, J. Rodriguez, R. Tena-Zaera, *Sol. Energy Mater. Sol. Cells* **2017**.

[9] a) P. M. Beaujuge, S. Ellinger, J. R. Reynolds, *Nat. Mater.* **2008**, *7*, 795-799; b) P. Shi, C. M. Amb, E. P. Knott, E. J. Thompson, D. Y. Liu, J. Mei, A. L. Dyer, J. R. Reynolds, *Adv. Mater.* **2010**, *22*, 4949-4953.

[10] Y. Alesanco, A. Viñuales, G. Cabañero, J. Rodriguez, R. Tena-Zaera, *ACS Appl. Mater. Interfaces* **2016**, *8*, 29619-29627.

[11] Y. Alesanco, J. Palenzuela, R. Tena-Zaera, G. Cabañero, H. Grande, B. Herbig, A. Schmitt, M. Schott, U. Posset, A. Guerfi, M. Dontigny, K. Zaghib, A. Viñuales, *Sol. Energy Mater. Sol. Cells* **2016**, *157*, 624-635.

[12] Y. J. Kim, H. K. Jeong, J. K. Seo, S. Y. Chai, Y. S. Kim, G. I. Lim, M. H. Cho, I.-M. Lee, Y. S. Choi, W. I. Lee, *Journal of Nanoscience and Nanotechnology* **2007**, *7*, 4106-4110.

[13] a) R. Cinnsealach, G. Boschloo, S. Nagaraja Rao, D. Fitzmaurice, *Sol. Energy Mater. Sol. Cells* **1998**, *55*, 215-223; b) P. Bonhôte, E. Gogniat, F. Campus, L. Walder, M.

Grätzel, *Displays* **1999**, *20*, 137-144; c) D. Cummins, G. Boschloo, M. Ryan, D. Corr, S. N. Rao, D. Fitzmaurice, *J. Phys. Chem. B* **2000**, *104*, 11449-11459; d) H. J. Kim, J. K. Seo, Y. J. Kim, H. K. Jeong, G. I. Lim, Y. S. Choi, W. I. Lee, *Sol. Energy Mater. Sol. Cells* **2009**, *93*, 2108-2112.

[14] R. J. Mortimer, T. S. Varley, *Chem. Mater.* **2011**, *23*, 4077-4082.

[15] S. Bhandari, M. Deepa, A. K. Srivastava, S. T. Lakshmikumar, RamaKant, *Solid State Ionics* **2009**, *180*, 41-49.

[16] Y. Alesanco, A. Viñuales, G. Cabañero, J. Rodriguez, R. Tena-Zaera, *Advanced Optical Materials* **2017**.

[17] M. İçli, M. Pamuk, F. Algı, A. M. Önal, A. Cihaner, *Organic Electronics* **2010**, *11*, 1255-1260.

[18] J.-H. Ryu, Y.-H. Lee, K.-D. Suh, *J. Appl. Polym. Sci.* **2008**, *107*, 102-108.

CHAPTER 8

MULTICOLOR ELECTROCHROMICS: ALL-IN-ONE RAINBOW-LIKE DEVICES

8.1. Introduction

Despite the significant improvements achieved in the last 30 years with regard to the EC systems, a further challenge was to find ECDs that exhibit multielectrochromic behavior. Multi-electrochromism may significantly extend the market opportunities in different fields such as displays, smart windows and climate adaptive building shell (CABS),[1] due to their aesthetic properties providing diverse colorations over time under different applied potentials.

There are many reports dealing with the multi-electrochromism principle and preliminary proof-of-concept systems.[2] However, most of the proposed multielectrochromic devices do not show sufficiently diversified colors in their different colored states which may limit their practical use in the above-described applications.[2a, 2b, 3] The most performed strategies to obtain multi-electrochromic devices are based on the integration of different electrochromic materials.[3-4] Fabrication strategies include different device architectures such as dual-type (i.e. complementary anodic and cathodic EC materials[5]) and patterned-based devices[5a, 6] (e.g. pixel configuration: Nanochromics TM displays developed by NTERA, Ltd[6a]). However, in addition to the complexity in the device preparation (e.g. larger number of layers,[3, 5] multielectrode configurations,[4d, 7] or the need of complex patterned electrodes), the color versatility of these ECDs may be significantly limited by the single coloration of the monoelectrochromic materials generally used.[8] Many approaches have also been developed with the aim of diversifying the colors of a single EC material. In this context, ambipolar materials[9] and the conjugated polymers have been widely

studied as promising multi-electrochromic materials through their band gap control by structural modification.[4a, 5a, 6b, 10] However, EC polymers often exhibit a lack of a sufficiently colorless bleached state and slow response time in comparison to several single-molecular materials, such as viologens.[2c] When using the latter, the colorless and highly colored states of dication and radical-cation forms respectively, are commonly exploited in monoelectrochromic devices.[11] Nevertheless, the consideration of di-reduced species, whose behavior and stability are relatively un-known, may open wide avenues for developing viologen-based multielectrochromic materials. In this regard, the employment of polyelectrolyte systems which could stabilize such species could offer new opportunities.

8.1.1. Objective

The overall purpose of the research work described in this chapter was to develop easy-to-make all-in-one multi-electrochromic devices avoiding complex device architectures.

To accomplish this goal, the different redox states of some viologens and their stabilization in the electrolytic media had to be considered.

The development of ECDs based on zoning design approach which allows the adjustment of the color independently in each zone while maintaining the all-in-one configuration was equally required to expand the potential of this technology.

8.2. Materials and methods

8.2.1. Materials

Poly(vinyl alcohol) (PVA, Mw 61 000), sodium tetraborate decahydrate (borax, 99.5%), potassium ferrocyanide (98.5%) and potassium ferricyanide (99%) were purchased from Sigma-Aldrich and used without further purification. Fluorine-doped tin oxide (FTO) coated glass substrates (TEC,

Rs 6-8 Ωsq^{-1}) and tin-doped indium oxide glass substrates (ITO Sol 30/1.1, Rs 25-35 Ωsq^{-1}) were supplied by Solems and cleaned with warm acetone prior to use.

8.2.1.1. Synthesis and characterization of viologens

Information regarding the synthesis procedures followed to obtain symmetric viologens employed were included in previous chapters. Thus, 1,1'-diethyl-4,4'-bipyridinium dibromide (ethyl viologen dibromide, [**EtVio**]) was synthesized in the chapter 4, whereas 1,1'-Bis-(*p*-cyanophenyl)-4,4'-bipyridilium dichloride (*p*-cyanophenylviologen dichloride, [**pCNVio**]) was synthesized in chapter 5.

8.2.2. Methods

8.2.2.1. Preparation of gel formulations

All gel formulations were prepared following the general procedure described in the section 2.2.2.1 of the chapter 2. Detailed information regarding the specific composition of the gels assessed in this chapter (i.e., concentration of complementary redox pair and viologen) are described below.

*Preparation of EC gels with varying concentration of **[pCNVio]** viologen:* A series of nine electrochromic gels was prepared by varying concentrations of [**pCNVio**] from 0.25 to 4.0 mmol L^{-1} (0.25, 0.5, 1.0, 1.5, 2.0, 2.5, 3.0, 3.5 and 4.0 mmol L^{-1}) while keeping the concentration of ferro/ferricyanide potassium pair at a constant value of 0.4 mmol L^{-1}.

Preparation of EC gels with varying concentration of ferro/ferricyanide potassium salts: A series of 10 electrochromic gels was prepared by varying concentrations of ferro/ferricyanide potassium pair from 0.2 to 5.0 mmol L^{-1} (0.2, 0.4, 0.6, 0.8, 1.0, 1.5, 2.0, 3.0, 4.0 and 5.0 mmol L^{-1}) while keeping the concentration of [**pCNVio**] at a constant value of 3.5 mmol L^{-1}.

*Preparation of **pCNVio gel**:* This electrochromic gel was prepared keeping the final concentration of [**pCNVio**] at 3.5 mmol L^{-1} and the concentration of the ferro/ferricyanide potassium pair at 4 mmol L^{-1} value.

*Preparation of **EtVio gel***: This electrochromic gel was prepared keeping the final concentration of [**EtVio**] at 20 mmol L^{-1} and the concentration of the ferro/ferricyanide potassium pair at 6 mmol L^{-1} value.

*Preparation of **Blend gel** and **Blend gel 2*****:*** These electrochromic gels were prepared by mixing **EtVio gel** and ***p*CNVio gel** in 2:1 and 1:1 weight ratios respectively, followed by vigorous stirring with spatula. The formulations were left to settle on its own until a completely bubble-free materials were obtained.

8.2.2.2. Fabrication of electrochromic devices

All-in-one ECDs based on two-electrode (2-E) and three-electrode (3-E) configurations were prepared and assembled following the procedure described in the chapter 2 section 2.5.1. and 2.5.2., respectively.

Fabrication of Rainbow-like Electrochromic Devices

The all-in-one rainbow-like electrochromic devices were prepared as follows: 5 cm x 5 cm ITO-coated glass substrate was electrically insulated by laser scribing into different sections having all of them an approximate active area of 5 cm x 1 cm. Each section was employed as stand-alone working electrode (WE) for rainbow-like electrochromic device. Similarly laser scribed substrate was employed as counter electrode (CE). The following steps required for device assembling were similar to those indicated for 2-E electrochromic devices.

8.3. Results and discussion

8.3.1. Bichromic devices

PVA-borax gel-based ECDs with a single viologen, 1,1'-bis-(*p*-cyanophenyl)-4,4'-bipyridilium dichloride (**[pCNVio]**, Figure 8.1a) and potassium ferrocyanide and ferricyanide salts as complementary redox species were investigated using a conventional two-electrode (2-E) configuration.

In order to achieve optimized formulations in terms of transmittance change and switching times, PVA-borax gels comprising diverse amount of viologen (from 0.25 to 4.0 mmol L^{-1}) and redox pair (from 0.2 to 5.0 mmol L^{-1}) were evaluated. As proven in the chapter 4[12] and also reported for other viologen-based devices (i.e., aqueous liquid systems),[13] faster switching times were obtained as the amount of the complementary redox species increased. After systematic optimization study of the gel formulations (Annex 8.1), the EC gel comprising 3.5 mmol L^{-1} of viologen and 4.0 mmol L^{-1} of redox species, hereafter named **pCNVio gel**, was selected for the entire study and characterization.

As pointed out in the introductory chapters, green color is expected for the radical-cation form of this type of aryl substituted viologen. Surprisingly, in addition to the green color shown by **[pCNVio]** and observed upon applying -1.4 V voltage (Figure 8.1b-II), red coloration occurred as a result of applying more cathodic potential of -1,8 V (Figure 8.1b-III). Although the second reduction of **[pCNVio]** was previously discussed in aqueous liquid systems,[13-14] no red coloration was reported. Furthermore, limited electrochemical reversibility and insolubility in water was suggested for the di-reduced (i.e, neutral state) form of **[pCNVio]**.[13-14]

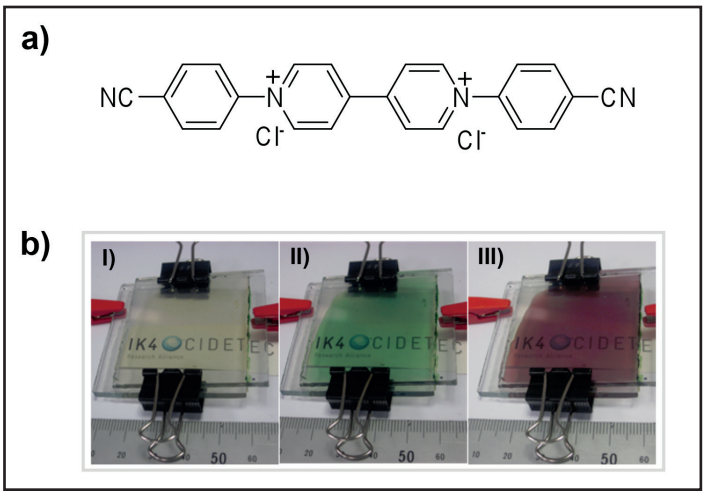

Figure 8.1. a) Chemical structure of **[pCNVio]** viologen; b) Photographs of an electrochromic device containing **[pCNVio]** viologen in its bleached state (I) and colored states at switching voltages of −1.4 V (II) and −1.8 V (III).

8.3.1.1. Spectroelectrochemical study

In order to evaluate the electrochemical behavior of the **pCNVio gel** and gain further insights into the origin of the unexpected red coloration, three-electrode (3-E) configuration was used to correlate the electrochemical behavior with color variation.

Figure 8.2a shows the cyclic voltammetry of 3-E ECDs containing **pCNVio gel**, as well as a water solution containing the same amount of viologen (**[pCNVio]**) and redox pair for comparative purposes. In the potential range from 1.10 to -1.45 V, two well-defined peaks could be distinguished on the cathodic sweep of the scan of both systems, apart from the uncolored reduction peak of ferricyanide ion (~ -0.2 V). The first reduction peak (~ -0.5 V) was correlated with the green radical-cation ($bipm^{+\bullet}$) formed by one-electron reduction of the dication ($bipm^{2+}$), while the second reduction peak (~ -0.9 V) was related to the di-reduced form ($bipm^{0}$) obtained by one-electron reduction of the radical-cation. Figure 8.2b and c display the visual

appearance and UV-Vis transmittance spectra of devices under different potentials (i.e., 0, -0.5 and -0.9 V), respectively. The color coordinates obtained for devices based on both systems at two applied potentials are represented in the chromaticity diagram (Figure 8.2d).

As shown in Figure 8.2b and d, the ECD containing **pCNVio gel** exhibited green coloration when the external voltage was set at ~ -0.5 V, and the color turned reddish upon applying external voltage of ~-0.9 V. By comparing the UV-Vis spectra (Figure 8.2c), different absorption profiles were observed in the case of **pCNVio gel**. Thus, when the applied potential was set at ~ -0.5 V, the ECD exhibited two strong absorption bands (i.e., transmittance valleys in Figure 8.2c) at around 420 and 600 nm, characteristic of the green materials. When a more cathodic potential of ~ -0.9 V was applied, the transmittance was quenched (indicating very significant absorption) around 500 nm and the ECD color turned into the red. After the potential was set again to 0 V, the ECD turned back to its original colorless form, showing reversible response.

Nevertheless, in the case of reference aqueous liquid systems (without PVA-borax), the results revealed that upon applying a switching voltage of ~ -0.9V, the device showed mainly dark green coloration (Figure 8.2b and d) and the corresponding transmittance profiles (Figure 8.2c). These results, also detected in the 2-E configuration (Annex 8.2), showed that even though the applied potential was sufficiently negative for di-reduction to occur, the red coloration was not observed in the aqueous liquid system. As cathodic potential increased, the absorption profiles registered corresponded to the green color with varying degrees of coloration intensities. Besides that, aqueous solutions were unstable since the formation of precipitate was observed, as reported by other groups and mentioned above.

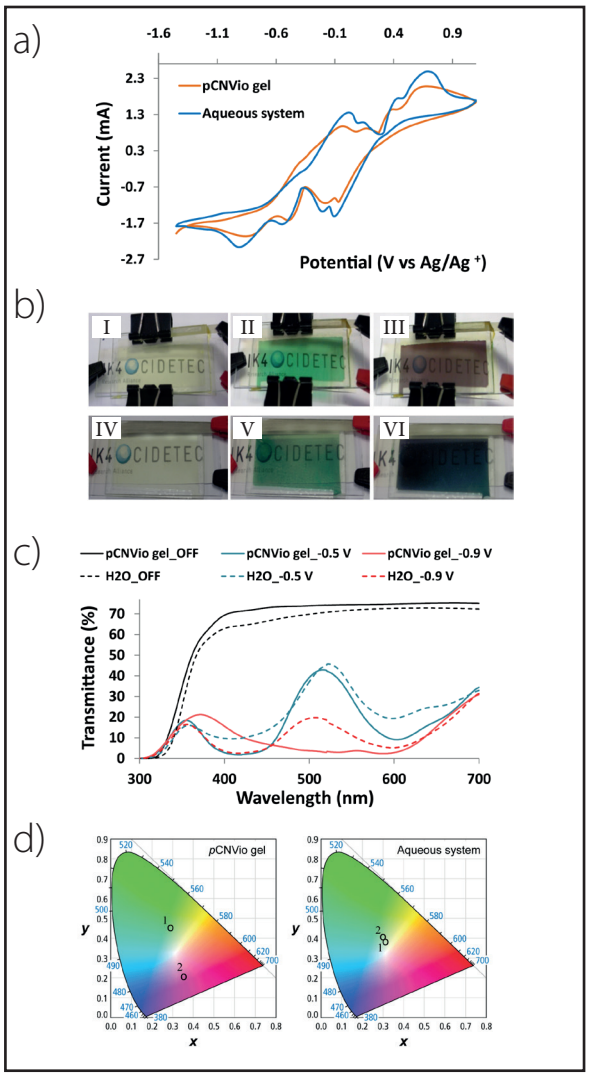

Figure 8.2. pCNVio gel vs reference aqueous liquid system in 3-E ECD configuration. a) Cyclic voltammogram. b) Photograph of the devices in their bleached state (left), colored state after applying switching voltages of -0,5V (middle) and -0,9V (right) of **pCNVio gel** (I – III) and aqueous liquid system (IV – VI); c) UV/Vis transmittance response in bleached state and upon applying -0.5V and -0.9 V voltages; d) *xy* chromaticity diagram representing the color coordinates of devices containing **pCNVio gel** (left) and aqueous system (right) upon applying a -0.5 V (1) and -0.9 V (2).

The lack of red colored state in the aqueous liquid system can be attributed to the comproportionation mechanism, which is more likely to happen in this aqueous media. The electron transfer interaction between the red di-reduced species ($bipm^{0}$) and the dication ($bipm^{2+}$) would result in the generation of the radical-cations ($bipm^{+\bullet}$) and consequently the green color observed in the device.

The comproportionation has been demonstrated to take place in other systems through electron spin resonance (ESR) techniques,[15] frequently followed by the formation of the electro-inactive radical-cation dimers ($(bipm)_2^{2+}$).[16] It has been scarcely reported that di-reduced bipirydilium species with aryl substituents can provide scarlet-red colors, and moreover they appear to be very unstable owing to their powerful reducing properties.[11] Related to these matters, it has been proposed that one way of preventing this issue could be the inclusion of the viologen within the cavity of a cyclodextrin sugar or polymeric matrix.[11, 14] In a similar manner, the viscosity of the present PVA gel-based polyelectrolyte seemed to avoid the di-reduced species and the dications to meet, preventing the comproportionation process and consequently making possible the observation of the red di-reduced species upon applying suitable voltage of -0.9 V (in 3-E configuration). For further investigations, aqueous formulation containing the same amount of viologen ([**pCNVio**]), redox pair, and PVA as **pCNVio gel** without borax, and therefore with much lower viscosity, were studied (Annex 8.3) and the red coloration was not observed. Interestingly, when higher concentrations (i.e., 10 mmol) of viologen were used in the PVA-borax gel while maintaining the rest of the components at the same concentrations, red coloration was not detected. This fact was equally consistent with the comproportionation mechanism proposed, since the direduced species and the dications were too close together in the more concentrated systems. These results revealed that the presence of the PVA gel polyelectrolyte acts as a stabilizer enabling

for the first time bichromic devices based on this viologen while greatly simplifying the assembly process.

8.3.1.2. EC performance and cyclability

Electrochromic properties of **pCNVio gel** such as optical contrast (Δ%T), switching time for the colored and bleached steps (t_c and t_b), coloration efficiencies (η), as well as color coordinates were determined for both applied potentials (-1.4 V and -1.8 V) and are summarized in Table 8.1. Additionally to the competitive optical contrast (i.e. ~ 60 %), it is worth noting that switching times were in the range of ECDs based on gel or solid electrolytes.[17] Color efficiencies obtained for the coloring processes were in the range of those registered for PVA-borax gel comprising **[EtVio]** viologen developed in the chapter 4.

Table 8.1. Electrochromic properties and color coordinates (D65) CIE *L*a*b* of 2-E ECD comprising **pCNVio gel**.

Potential (V)	$\%T_b$	$\%T_c$	Δ %T[a]	t_c (s)[b]	t_b (s)[b]	η_c (cm² C⁻¹)[c]	*L**[d]	*a**[d]	*b**[d]	Color[e]
-1.4	68	7	61	16	8	78	62	-44	27	
-1.8	61	2	59	14	4	83	29	38	-15	

[a] ΔT% at fixed λ = 600 and 500 nm for -1.4 and -1.8 V, respectively. [b] Switching times. [c] Color efficiency of the coloring process. [d] Color coordinates (D65) registered for *L*a*b* (CIE 1976) quantitative scales. [e] Color swatches representing *L*a*b* color coordinates.

Additionally, the cycling performance of ECDs comprising **pCNVio gel** was equally evaluated in 2-E configuration up to 10 000 cycles. Aiming at assessing the cyclability at both colored states, some ECDs were exposed to green-switching and others to red-switching potential steps (i.e., -1.4 and -1.8 V, respectively for 20 s) being all of them bleached at the same conditions (0 V for 90 s). The evolution of the cycling performance was evaluated by recording the %T after certain number of cycles at fixed wavelength (600

and 500 nm for -1.4 (green) and -1.8 V (red), respectively), while the same potential steps detailed above were being applied.

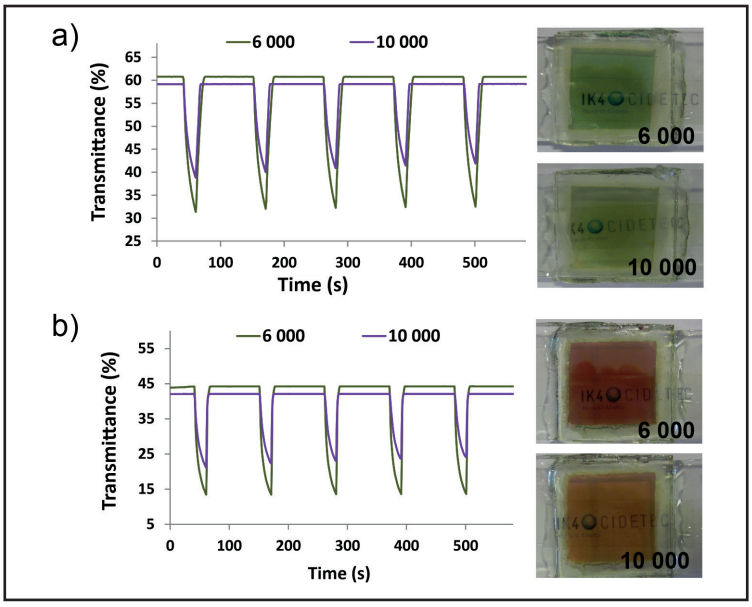

Figure 8.3. Evolution of the switching performance of 2-E ECDs containing **pCNVio gel** after 6 000 and 10 000 redox cycles. %T vs time at maximum contrast wavelengtht (600nm in a) and 500 nm in b)) while square-wave potential-steps between bleached (0 V for 90 s) and colored states (-1.4 V and -1.8 V in a) and b) respectively, for 90 s), were being applied.

Photographs of the ECDs at colored state after 6 000 and 10 000 cycles (inset).

As shown in Figure 8.3, the devices showed a transmittance change of around 30% after being cycled up to 6 000 cycles at both switching potentials. Despite the decay in Δ%T, the two different colorations were still noticeable at naked eye. After 10 000 cycles, the level of coloration diminished at both switching potentials, being the Δ%T of 20%. It is worth to mention that the diminution of the %T at bleached state of the devices which were exposed to green-switching potential steps was lower than

that observed for devices switched at red colored steps, ascribed to the less cathodic potential required for the former, thus less damaging conditions.

8.3.2. Multi-electrochromic behavior devices

Taking advantage of the bicolor electrochromic behavior observed in **pCNVio gel** and with the purpose of finding ECDs that exhibit multielectrochromic behavior, new PVA gel-based electrochromic formulations including two different kinds of viologens were investigated. These new formulations incorporated potassium ferrocyanide and ferricyanide salts as complementary redox species, and [**pCNVio**] and 1,1'-diethyl-4,4'-bipyridinium dibromide ([**EtVio**]) as electrochromic materials. As proven in the chapter 4, the latter provides purple colorations when tested within PVA-borax polymeric matrix upon suitable applied potentials.[12]

Two multigel formulations (**Blend gel** and **Blend gel-2**) were prepared by mixing appropriate amounts of previously prepared **pCNVio** and **EtVio gels**.

The electrochemical behavior of a 3-E ECD based on the **Blend gel** was investigated by cyclic voltammetry (CV) (Figure 8.4a). In the potential range from 0 to -1.7 V, four well-defined features were observed during the cathodic sweep, apart from the one attributed to the redox pair. As shown in the inset, there was good agreement between these features and the sum of those detected in devices based on the single gels **pCNVio** and **EtVio gels** separately. The first and second reduction peak (~ -0.6 V and ~ -0.8 V) were correlated with reduction processes of the [**pCNVio**], which is consistent with that observed in the Figure 8.2a for **pCNVio gel** and explained above. The third and fourth peaks observed (~ -1.2 and ~ -1.6 V) were related to the radical-cation of the [**EtVio**] formed by one-electron reduction of the dication and its di-reduced form obtained by one-electron

reduction of the radical-cation, respectively, also in agreement with that observed for **EtVio gel**.

As no significant overlap in the redox potentials of the [**pCNVio**] and [**EtVio**] was detected in the CV of the **Blend gel**-based ECD, the latter was expected to behave as a multi-electrochromic device or even provide new colorations when their absorption profiles are coupled due to a mixture of prereduced states. Thus, the multi-electrochromic behavior encompassing five different colorations, colorless (0 V), green (~ -0.7 V), pink-violet (~ -0.9 V), orange (~ -1.1 V) and purple (~ -1.7 V) was visually confirmed (Figure 8.4b). The absorbance spectrum (Figure 8.4c) of the 3-E ECD after applying a switching voltage of ~ -0.7 V was characteristic of green materials with two absorption bands at around 420 and 600 nm. As more cathodic potential of ~ -0.9 V was applied, the ECD exhibited a broader band with its maximum located at 520 nm, which is in good agreement with the observed violet coloration. For a more negative potential of -1.1 V the absorption band showed hypsochromic shift to give a maximum absorption band at 460 nm, characteristic of orange materials. When a more cathodic potential of -1.7 V was set, ECD exhibited a strong absorption band at around 520 nm and a new band grew up from 415 to 380 nm where the spectra ends. The color coordinates obtained at each potential are represented in the chromaticity diagram in Figure 8.4d.

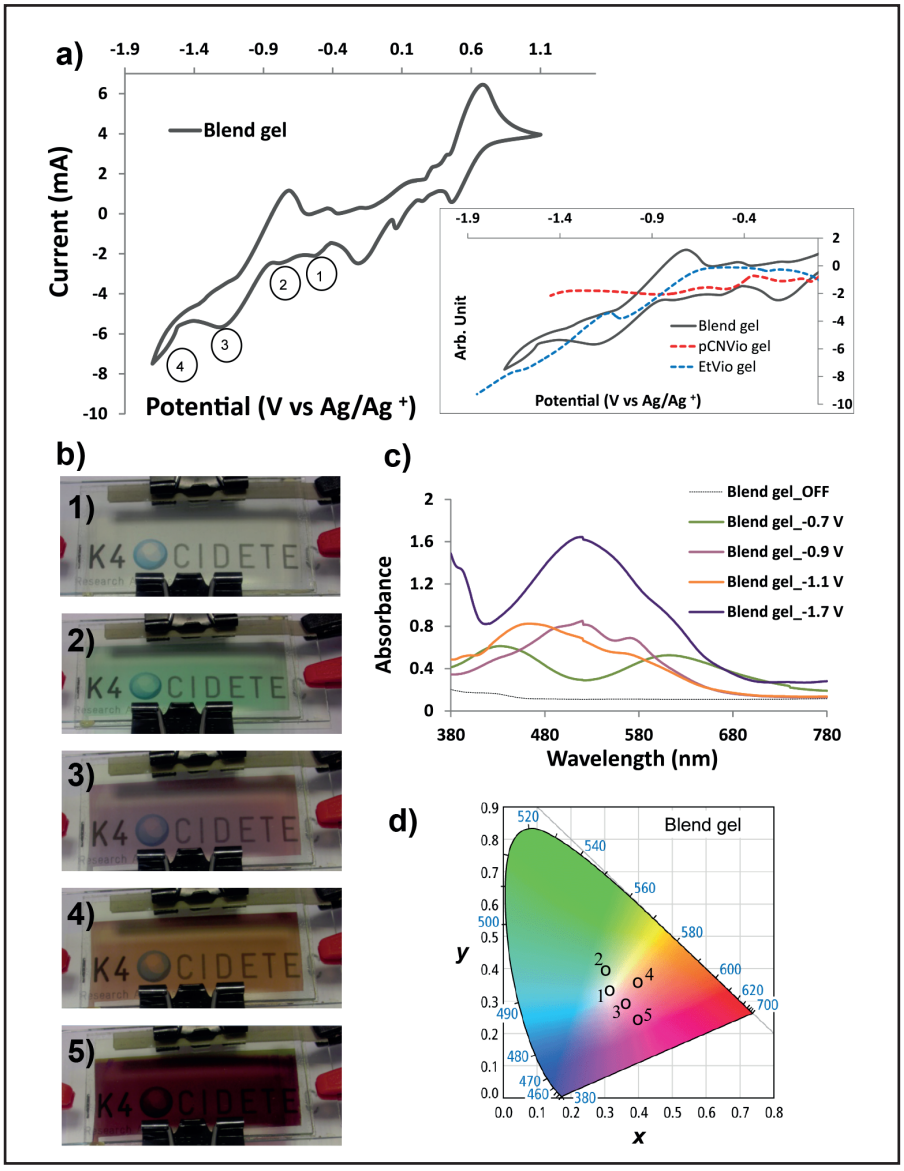

Figure 8.4. Multicolor 3-E electrochromic device containing **Blend gel**: a) Cyclic voltammetry (CV) of **Blend gel** and comparison with CVs of **pCNVio** and **EtVio gels** separately (cathodic sweep, inset). b) Observed coloration c) absorption profiles and d) *xy* chromaticity diagram at off state (**1**, colorless) and after applying a switching potential of -0.7 V (**2**, green), -0.9 V (**3**, pink-violet), -1.1 V (**4**, orange) and -1.7 V (**5**, purple) respectively.

The reproducibility and the electrochemical reversibility of **Blend gel** was assessed by measuring color coordinates of three ECDs at each potential (Table 8.2) and evolution of CV upon cycling (Figure 8.5). On the basis of the results, **Blend gel** system provides reproducible and electrochemically reversible multi-ECDs with four well-defined colorations from a colorless off state. Therefore, these multielectrochromic PVA gel systems contribute to address the above-mentioned shortcomings frequently present in the multi-EC systems, such as the device complexity or not distinct enough coloration in their different redox states, among others.

Table 8.2. Color coordinates of 3-E ECDs containing **Blend gel** at different applied potentials (n = 3).

Potential (V)	x [(a)]	y [(a)]	Y [(a)]	L^* [(b)]	a^* [(b)]	b^* [(b)]	Color [(c)]
-0.7	0.306 ± 0.002	0.392 ± 0.004	47.9 ± 9.1	74.5 ± 5.6	-24.6 ± 2.3	17.2 ± 2.4	
-0.9	0.355 ± 0.018	0.272 ± 0.015	22.6 ± 1.1	54.6 ± 1.2	31.8 ± 0.3	-15.7 ± 4.2	
-1.1	0.395 ± 0.007	0.353 ± 0.014	30.4 ± 1.0	62.0 ± 0.9	18.9 ± 5.0	17.6 ± 4.0	
-1.7	0.404 ± 0.003	0.260 ± 0.015	8.6 ± 2.4	34.8 ± 4.7	38.9 ± 1.5	-5.1 ± 2.8	

[a), b)] Color coordinates (D65): [(a)] xyY 1931 and [(b)] $L^*a^*b^*$ 1976. [c)] Color interpretation of the corresponding color coordinates (L^*a^*b).

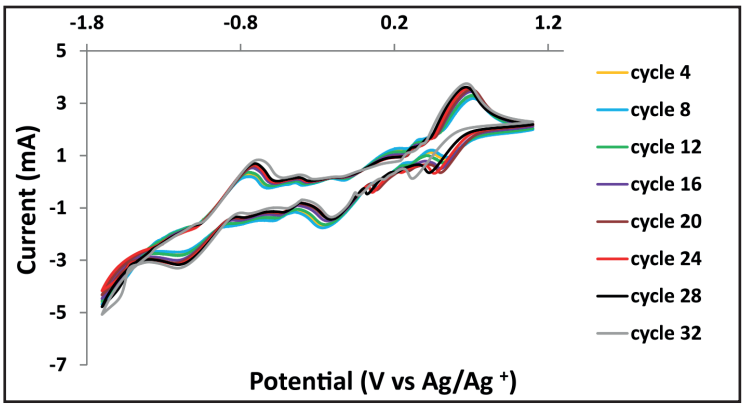

Figure 8.5. Cyclic voltammetry of 3-E ECD containing **Blend gel** and evolution upon cycling.

Additionally, apart from the application in multi-color devices, the developed two-viologen PVA-borax-based formulations may have significant impact in other electrochromic applications such as visible light filters. As an example, ECD with very low transmittance in most of the visible range (i.e., ≤ 3% between 555 - 300 nm and ≤ 6% between 600 – 300 nm) were also fabricated by using **Blend gel-2** (Figure 8.6). The reached transmittance was as low as that previously reported by using more complex approaches, therefore representing a significant advantage in the field of dynamic light filtering.[5b, 7a]

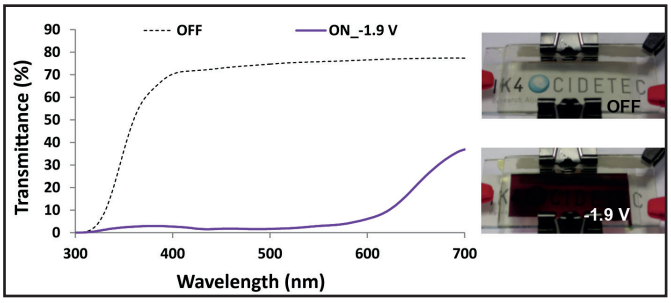

Figure 8.6. UV/Vis transmittance response and photograph of 3-E ECD containing **Blend gel-2** in bleached state and upon applying -1.9 V voltage.

8.3.3. Rainbow-like ECDs

Going one step further, an easy-to-make multi-electrochromic device based on zoned electrodes (hereafter named rainbow-like ECD) providing simultaneously different colorations was also developed. It should be noticed that the fabrication process of rainbow-like ECDs was relatively straightforward; it only was necessary to sandwich a single layer of **Blend gel** between two ITO-coated glass substrates previously zoned in rows by laser scribing. As shown in Figure 8.7 and Annex 8.4, each zone exhibits multielectrochromic behavior, enabling the adjustment of their color independently and changing over time under suitable applied potentials according to the needs. In addition, the rainbow-like ECD can be programmed to function in customized segments, improving the aesthetics while filtering different wavelengths of the visible region, as shown by the video S0 included as Supporting Information in the published work.[18]

This achievement could extend the market opportunities for electrochromics in different fields such as full-color displays, smart windows, and emerging climate adaptive building shell (CABS),[1] since the building sector is showing an increasing demand to develop highly energy-efficient and pleasant spaces, including adaptive system designs.

This represents significant novelty and performance enhancement versus the current state of the art smart windows which provide different intermediate tint levels, but always of the same bluish color.[19] Windows and zoning strategies made of this technology could enhance the aesthetics and enable users and operators to optimize light transmission and thermal and visual comfort, adjusting to location and needs of the occupants.

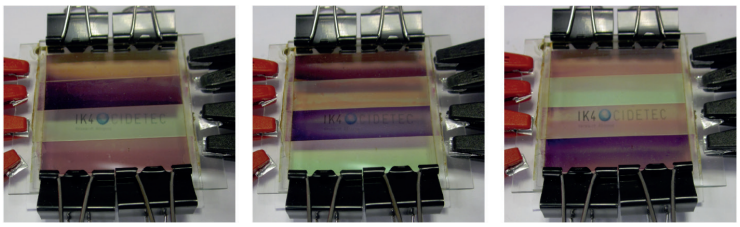

Figure 8.7. Photographs of a rainbow-like ECD containing **Blend gel**. Multi-electrochromic device provided with zoning design and colors observed in each row of the device while the suitable voltage is being applied.

8.4. Conclusions

The development of PVA-borax-based systems enabling the achievement of all-in-one easy-to-make multielectrochromic devices was demonstrated.

The accomplishment of single viologen-based electrochromic devices (**pCNVio gel**), providing two different and well-defined colored states (i.e. green and red in addition to the colorless state), was proven, by means of stabilizing the second redox state within the PVA-borax electrolyte. Equally, the crucial role of the PVA-borax gel was confirmed by comparing this EC system with similar EC aqueous liquid solutions in absence of the borax and PVA-borax gel. The finding of this PVA-borax gel electrolytic matrix which may stabilize the direduced species of the viologen molecules, might be extrapolated to other viologens which exhibit sufficiently diversified colors in their both reduced states, thus expanding the provided colorations.

Furthermore, the successful fabrication of all-in-one multi-electrochromic devices, based on a formulation containing two viologens (**Blend gel**), providing five well-defined colorations was demonstrated. The resulting devices showed multi-electrochromic behavior including colorless, green, pink-violet, orange and purple, involving just a single EC layer sandwiched between two electrodes following the next configuration: glass/TCO/**Blend gel**/TCO/glass.

The potential of these multi-EC devices to reach very low transmission in most of the visible wavelength range enabling an effective blocking of the whole visible radiation in smart windows was also shown.

The proof-of-concept of an all-in-one rainbow-like ECD, based on a simple zoning design which allows the adjustment of the color independently in each zone was demonstrated as well.

These results may have broad impact in the field of displays, smart windows and climate adaptive building shell (CABS) and clearly indicates that viologen-based EC gel offers many advantages over other multi-electrochromic devices previously reported. Thus, the multi-EC formulations described in the present chapter could be potential candidates for easy-to-make multi-electrochromic or full-color electrochromic devices, which bring us closer to rainbow-like windows.

8.5. References

[1] R. C. G. M. Loonen, M. Trčka, D. Cóstola, J. L. M. Hensen, *Renewable Sustainable Energy Rev.* **2013**, *25*, 483-493.

[2] a) G. Wang, X. Fu, J. Huang, C. Wu, L. Wu, Q. Du, *Organic Electronics* **2011**, *12*, 1216-1222; b) G. Wang, X. Fu, L. He, X. Huang, Q. Miao, *Organic Electronics* **2014**, *15*, 622-630; c) R. H. Bulloch, J. A. Kerszulis, A. L. Dyer, J. R. Reynolds, *ACS Appl. Mater. Interfaces* **2015**, *7*, 1406-1412.

[3] B. Xu, L. Xu, G. Gao, Y. Yang, W. Guo, S. Liu, Z. Sun, *Electrochim. Acta* **2009**, *54*, 2246-2252.

[4] a) H. C. Ko, S. Kim, H. Lee, B. Moon, *Advanced Functional Materials* **2005**, *15*, 905-909; b) C. Pozo-Gonzalo, M. Salsamendi, A. Viñuales, J. A. Pomposo, H.-J. Grande, *Sol. Energy Mater. Sol. Cells* **2009**, *93*, 2093-2097; c) G. Sonmez, H. B. Sonmez, C. K. F. Shen, F. Wudl, *Adv. Mater.* **2004**, *16*, 1905-1908; d) E. Unur, J.-H. Jung, R. J. Mortimer, J. R. Reynolds, *Chem. Mater.* **2008**, *20*, 2328-2334.

[5] a) A. A. Argun, P.-H. Aubert, B. C. Thompson, I. Schwendeman, C. L. Gaupp, J. Hwang, N. J. Pinto, D. B. Tanner, A. G. MacDiarmid, J. R. Reynolds, *Chem. Mater.*

2004, *16*, 4401-4412; b) H. Shin, Y. Kim, T. Bhuvana, J. Lee, X. Yang, C. Park, E. Kim, *ACS Appl. Mater. Interfaces* **2012**, *4*, 185-191.

[6] a) M. Möller, S. Asaftei, D. Corr, M. Ryan, L. Walder, *Adv. Mater.* **2004**, *16*, 1558-1562; b) J. A. Kerszulis, K. E. Johnson, M. Kuepfert, D. Khoshabo, A. L. Dyer, J. R. Reynolds, *J. Mater. Chem. C* **2015**, *3*, 3211-3218.

[7] a) E. Unur, P. M. Beaujuge, S. Ellinger, J.-H. Jung, J. R. Reynolds, *Chem. Mater.* **2009**, *21*, 5145-5153; b) Y.-M. Zhang, X. Wang, W. Zhang, W. Li, X. Fang, B. Yang, M. Li, S. X.-A. Zhang, *Light Sci Appl* **2015**, *4*, e249.

[8] G. Bar, N. Larina, L. Grinis, V. Lokshin, R. Gvishi, I. Kiryuschev, A. Zaban, V. Khodorkovsky, *Sol. Energy Mater. Sol. Cells* **2012**, *99*, 123-128.

[9] a) M. E. Mulholland, D. Navarathne, S. Khedri, W. G. Skene, *New Journal of Chemistry* **2014**, *38*, 1668-1674; b) H.-M. Wang, S.-H. Hsiao, *J. Mater. Chem. C* **2014**, *2*, 1553-1564.

[10] a) A. A. Argun, A. Cirpan, J. R. Reynolds, *Adv. Mater.* **2003**, *15*, 1338-1341; b) P. M. Beaujuge, J. R. Reynolds, *Chem. Rev.* **2010**, *110*, 268-320.

[11] P. M. S. Monk, *The viologens: physicochemical properties, synthesis, and applications of the salts of 4,4'-bipyridine*, Wiley, **1998**.

[12] Y. Alesanco, J. Palenzuela, A. Viñuales, G. Cabañero, H. J. Grande, I. Odriozola, *ChemElectroChem* **2015**, *2*, 218-223.

[13] J. Mizuguchi, H. Karfunkel, *Ber. Bunsen-Ges. Phys. Chem.* **1993**, *97*, 1466-1472.

[14] M. Hiroshi, M. Jin, *Jpn. J. Appl. Phys.* **1987**, *26*, 1356-1360.

[15] D. R. Rosseinsky, P. M. S. Monk, *Sol. Energy Mater. Sol. Cells* **1992**, *25*, 201-210.

[16] P. M. S. Monk, *J. Electroanal. Chem.* **1997**, *432*, 175-179.

[17] a) F. Tran-Van, L. Beouch, F. Vidal, P. Yammine, D. Teyssié, C. Chevrot, *Electrochim. Acta* **2008**, *53*, 4336-4343; b) D. Navarathne, W. G. Skene, *J. Mater. Chem. C* **2013**, *1*, 6743-6747.

[18] Y. Alesanco, A. Viñuales, J. Palenzuela, I. Odriozola, G. Cabañero, J. Rodriguez, R. Tena-Zaera, *ACS Appl. Mater. Interfaces* **2016**, *8*, 14795-14801.

[19] a*) Vol. Nov. 23, 2016*, http://sageglass.com; b) http://viewglass.com.

CHAPTER 9

CONCLUSIONS, FUTURE WORK AND CONTRIBUTIONS

9.1. Summary and conclusions

The most significant findings and conclusions drawn from the research work developed along this thesis are summarized below.

- Viologens comprising a suitable anchoring moiety (i.e., benzylphosphonic acid) which offer strong chemisorption towards TiO_2 nanostructured layers and rapid binding process (i.e., 1 - 15 min), therefore compatible with plastic substrates (i.e., ITO/PET) and with any fabrication process required for up-scaling, were successfully synthesized. The employment of this bonding moiety may open wide possibilities for the synthesis of other fast-grafting viologens beyond those synthesized in the present thesis, provided with substituents of different nature, thus showing different properties and colored states.
- New concept of semi-solid electrolyte consisting of PVA-borax viscoelastic gel which combines the advantages of both liquid and solid electrolytes while avoiding their weaknesses was developed. Thus, the PVA-borax polyelectrolyte exhibited high ionic conductivity, electrochemical stability and transmission in the visible region, as well as certain stickiness and elasticity which contribute not only to ease the fabrication of the ECDs but also to extend their durability while avoiding the risk of leaking and presence of bubbles.

  The suitability of this PVA-borax gel for being used not only as electrolyte in layered ECDs, but also in all-in-one configuration

comprising all the electroactive materials while maintaining the rheological properties and providing high-performance ECDs, was equally achieved.

The possibility of stabilizing the radical-cationic dimer form of the viologen in the PVA-borax medium while ensuring good reversibility may open new opportunities to extend the palette of colors of the viologen-based ECDs. It is also noteworthy the excellent cyclability (i.e. up to 15 000 cycles) and overall high performance achieved and not reported before for a water-based all-in-one ECDs consisting of non-anchored viologens.

- The development of neutral color (gray and black) ECDs which overcome the limitations of the previously reported ECDs, thus showing suitable switching times and colorless-off state while maintaining easy device configuration, were achieved following different approaches using PVA-borax gel electrolyte.

    - One strategy based on a color-mixing of two symmetric viologens anchored in a single nanostructured electrode (layered configuration) providing gray electrochromism.

    - A more innovative approach based on single asymmetric viologens provided with substituents of different nature (i.e., 1-alkyl-1'-aryl) without anchoring moiety (all-in-one configuration) also exhibiting gray colored state.

    - A third strategy that lead not only to gray but also to black electrochromism using novel asymmetric viologens (i.e., 1-alkyl-1'-aryl) functionalized with a suitable anchoring moiety in both substituents (layered configuration) exhibiting grafting times as fast as 1 min with simple device architecture and competitive overall performance. To the best of our knowledge, transparent colorless-off state ECDs

based on a single asymmetric viologen exhibiting so black colored state (a^* and $b^* \leq |5|$) had not been reported so far.

- All-in-one ECDs based on a single viologen and providing two well-defined colored states (green and red) by means of stabilizing its direduced form was achieved using PVA-borax electrolytic matrix which somehow avoids the comproportionation mechanism. This finding might be extrapolated to other viologens which exhibit sufficiently diversified colors in their both reduced states, thus expanding the provided colorations.
- The development of all-in-one ECDs exhibiting multielectrochromic behavior providing five well-defined colorations as well as the proof of concept of ECDs based on simple zoning design (rainbow-like) which allows the adjustment of the color independently in each zone was demonstrated as well. These results offer many advantages over other multi-electrochromic devices previously reported including the easy device configuration (glass/TCO/multi-EC gel/TCO/glass), the simple fabrication process and the significantly different colorations provided.

In the light of the achievements stated throughout these chapters and summarized above, it can be concluded that this thesis represents a significant contribution in the field of electrochromic materials and devices, addressing some weaknesses detected while diversifying the colorations obtained including the challenging gray and black as well as multicoloration. Moreover, some reported strategies (e.g., the employment of asymmetric viologens, the stabilization of the radical-cation dimer and direduced species of the viologens by means of using aqueous PVA-borax gel) can be the key to successfully develop new colorations using other single viologens and simple device architecture.

Therefore, these findings may contribute to expand the potential of the electrochromic technology, showing great potential to be implemented in different applications such as displays and disposable systems (e.g., labels or cards) as well as other smart systems for the automotive and building industries (i.e., rearview mirrors, helmet visors, smart windows or panes and climate adaptive building shell (CABS)), enabling contemporary man to adjust their environment in a reversible way according to the needs and opening wide avenues for the emerging creative industry.

9.2. On-going and future work

Some research lines which are already being investigated with the materials developed and described in the present thesis are listed below.

- Expanding the knowledge regarding the species present in the reduced states of some systems developed in this thesis (i.e., radical-cation dimer, direduced forms and the extent of them), especially in bi or multielectrochromic systems, matching them with the observed colorations. To this end, electron spin resonance (ESR) spectroelectrochemical measurements are already in progress in collaboration with Leibniz Institute for Solid State and Materials Research (IFW) (Dresden).
- Considering the knowledge acquired in the present thesis in the development of both all-in-one and layered ECDs, the subsequent step of combining both approaches in the same device may be an interesting technique to expand the provided colorations achieving multielectrochromic systems. This ongoing research which consists in incorporating at least one viologen provided with anchoring moiety covalently anchored onto nanostructured layer while one or more

viologens exempted from any anchoring group are incorporated dissolved into PVA-borax electrolytic matrix.

Some research lines which could be investigated following-up with the research work described in the present thesis are listed below.

- Considering other non-Newtonian viscoelastic fluids to be assessed as electrolytic matrix in ECDs. To this end, new formulations equally based on PVA-borax mixtures on different solvents and/or using different polyhydroxy polymers including PVA of different molecular weights among others, may be an interesting approach to be explored.
- Assessing the radical-cation dimer form of other symmetric and asymmetric viologens as a way to achieve new colorations.
- Exploring the direduced form of other viologens, especially those which comprise at least an aryl group in one of the substituents directly bonded to the nitrogen atom.

9.3. Intellectual property dissemination and protection: publications, congresses and patents

The results of the innovative research work developed along this thesis have been translated into 6 scientific papers (being one of them cover page), two oral communications in international congresses and two patents.

These intellectual property dissemination and protection activities related to the different chapters of this thesis are detailed below.

9.3.1. Publications

Plastic Electrochromic Devices Based on Viologen-Modified TiO_2 Films Prepared at Low Temperature. (***Chapter 3***)

Yolanda Alesanco, Jesús Palenzuela, Ramón Tena-Zaera, Germán Cabañero, Hans Grande, Bettina Herbig, Angelika Schmitt, Marco Schott, Uwe Posset, Abdelbast Guerfi, Martin Dontigny, Karim Zaghib.

Sol. Energy Mater. Sol. Cells **2016,** *157*, 624-635.

Impact factor: **4.732**

Polyvinyl Alcohol–Borax Slime as Promising Polyelectrolyte for High-Performance, Easy-to-Make Electrochromic Devices. *Cover page* (***Chapter 4***)

Yolanda Alesanco, Jesús Palenzuela, Ana Viñuales, Germán Cabañero, Hans-Jürgen Grande, Ibon Odriozola.

ChemElectroChem **2015,** *2*, 218-223.

Impact factor: **3.506**

Colorless to Neutral Color Electrochromic Devices Based on Asymmetric Viologens. (***Chapter 5***)

Yolanda Alesanco, Ana Viñuales, Germán Cabañero, Javier Rodriguez, Ramón Tena-Zaera.

ACS Appl. Mater. Interfaces **2016,** *8*, 29619-29627.

Impact factor: **7.145**

Consecutive Anchoring of Symmetric Viologens: Electrochromic Devices Providing Colorless to Neutral-Color Switching. (***Chapter 6***)

Yolanda Alesanco, Ana Viñuales, Joseba Ugalde, Eneko Azaceta, Germán Cabañero, Javier Rodriguez, Ramón Tena-Zaera.

Sol. Energy Mater. Sol. Cells **2017**. (vol, pages) DOI: 10.1016/j.solmat.2017.01.033

Impact factor: **4.732**

Colorless-to-Black/gray Electrochromic Devices Based on a Single 1-Alkyl-1'-Aryl Asymmetric Viologen-Modified Monolayered electrodes. (***Chapter 7***)

Yolanda Alesanco, Ana Viñuales, Germán Cabañero, Javier Rodriguez, Ramón Tena-Zaera.

Adv. Opt. Mater, **2017**. (vol, page)

Impact factor: **5.36**

Multicolor Electrochromics: Rainbow-Like Devices. (***Chapter 8***)

Yolanda Alesanco, Ana Viñuales, Jesús Palenzuela, Ibon Odriozola. Germán Cabañero, Javier Rodriguez, Ramón Tena-Zaera.

ACS Appl. Mater. Interfaces **2016,** *8*, 14795-14801.

Impact factor: **7.145**

9.3.2. Patents

Multichromic compositions and use thereof *(**chapter 8**)*

Javier Sobrado Aranguena, Ramón Tena Zaera, **Yolanda Alesanco**, Ana Viñuales, Ibon Odriozola, Francisco Javier Rodriguez Parra, Germán Cabañero.

Application Nº: EP15382656.5

Date: Dec. 22, 2015

Componentes de respuesta dinámica con propiedades estéticas *(**chapter 5 and 8**)*

Yolanda Alesanco, Ramón Tena Zaera, Ana Viñuales, Ibon Odriozola, Francisco Javier Rodriguez Parra, Germán Cabañero, Javier Sobrado Aranguena.

Application Nº: PCT/ES2016/070932

Date: Dec. 22, 2016

9.3.3. Congresses

Easy-to-make multielectrochromic devices based on viologen-containing polyvinyl alcohol-borax slime polyelectrolyte: toward rainbow-like smart systems. *(**chapter 4 and 8**)*

Yolanda Alesanco, Ramón Tena-Zaera, Jesús Palenzuela, Ibon Odriozola, Germán Cabañero, Javier Rodriguez and Ana Viñuales.

IME-12_The 12^{tH} International Meeting on Electrochromism. August 28 – September 1, 2016. Delft university of technology, delf, the Netherlands.

Oral communication

Plastic electrochromic windows based on viologen-modified TiO_2 films prepared at low temperature *(**chapter 3**)*

Ana Viñuales, **Yolanda Alesanco**, Jesús Palenzuela, Bettina Herbig and Uwe Posset.

65th Annual Meeting of the International Society of Electrochemistry. August 31 – September 5, 2014. International Society of Electrochemistry (ISE), Lausanne, Switzerland.

Oral communication

CHAPTER 10

ANNEX

[**ANNEX 5.1]:** Characterization of two-electrode (2-E) ECDs based on PVA-gel formulations comprising symmetric viologens (EtVio, BnVio and pCNVio gels) and the mixture of them (EtVio + pCNVio and BnVio + pCNVio gels).

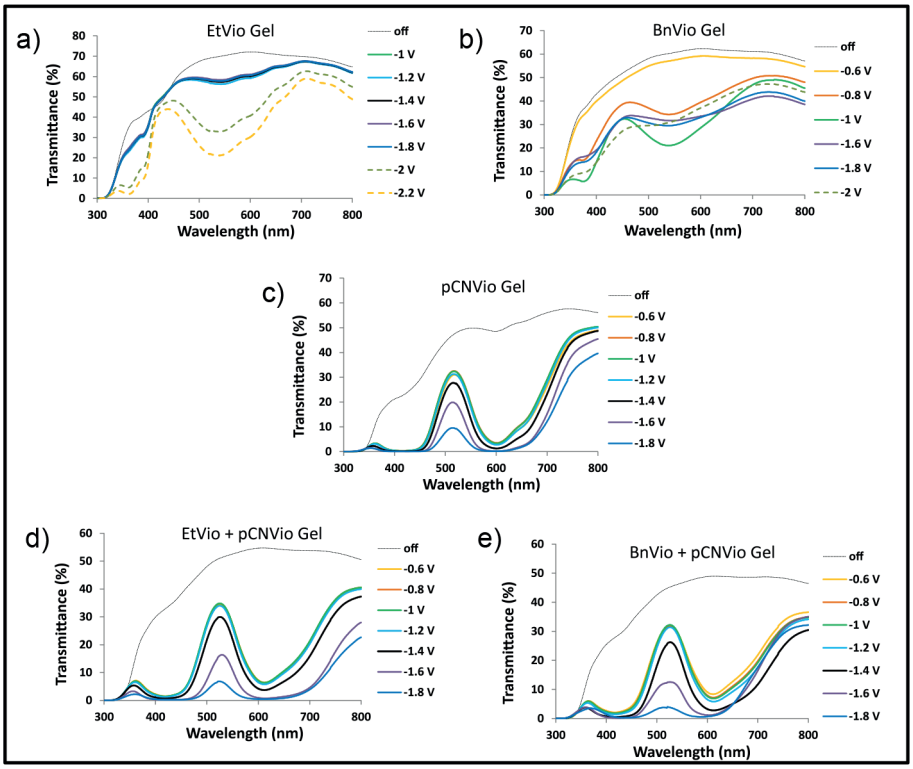

[**Figure Annex 5.1**]. UV/Vis transmittance profiles of 2-E ECDs containing (a) **EtVio**, (b) **BnVio** (c) **pCNVio**, (d) **EtVio + pCNVio** and (e) **BnVio +pCNVio gels**.

[**ANNEX 5.2**]: Characterization of two-electrode (2-E) ECDs based on anhydrous formulations comprising Et-pCNVio and Bn-pCNVio asymmetric viologens and EtVio and BnVio symmetric viologens.

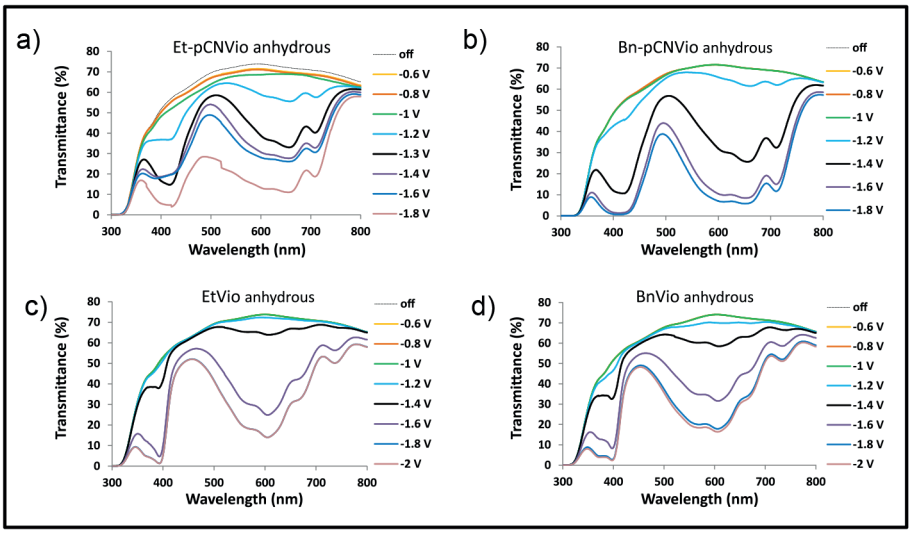

[**Figure Annex 5.2].** UV/Vis transmittance profiles of 2-E ECDs containing (a) **Et-pCNVio**, (b) **Bn-pCNVio** (c) **EtVio** and (d) **BnVio anhydrous EC systems**.

[**ANNEX 5.3**]: Spectroelectrochemical study of three-electrode ECD containing Anhydrous electrolyte for comparative purposes.

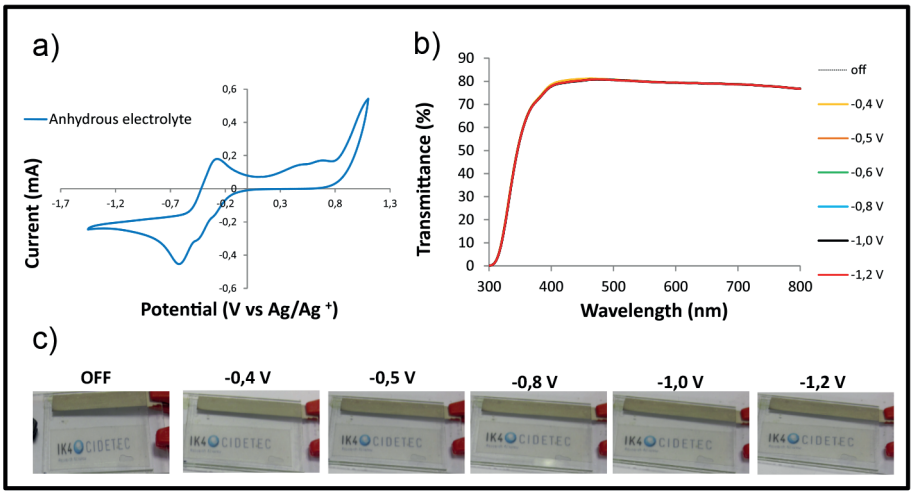

Potential (V)	%T off (λ = 600nm)	%T on (λ = 600nm)	Δ%T off-on (λ = 600nm)
off	79.5	-	-
-0.4		79.5	0.1
-0.5		79.4	0.1
-0.6		79.5	0.1
-0.8		79.4	0.1
-1.0		79.5	0.1
-1.2		79.4	0.1

[**Figure Annex 5.3**]. Spectroelectrochemical study of three-electrode (3-E) ECD containing anhydrous electrolyte for comparative purposes. a) Cyclic voltammetry (CV); b) UV-vis transmittance responses as a function of wavelength and (c) photograph of the device for different applied potentials from -0.4 to -1.2 V.

[**ANNEX 6.1**]. Electrochromic study of two-electrode (2-E) ECDs comprising **B** (a) and **G** viologens (b) along with **B** + **G** (c – f) and **G** + **B** sequential modification (g – i).

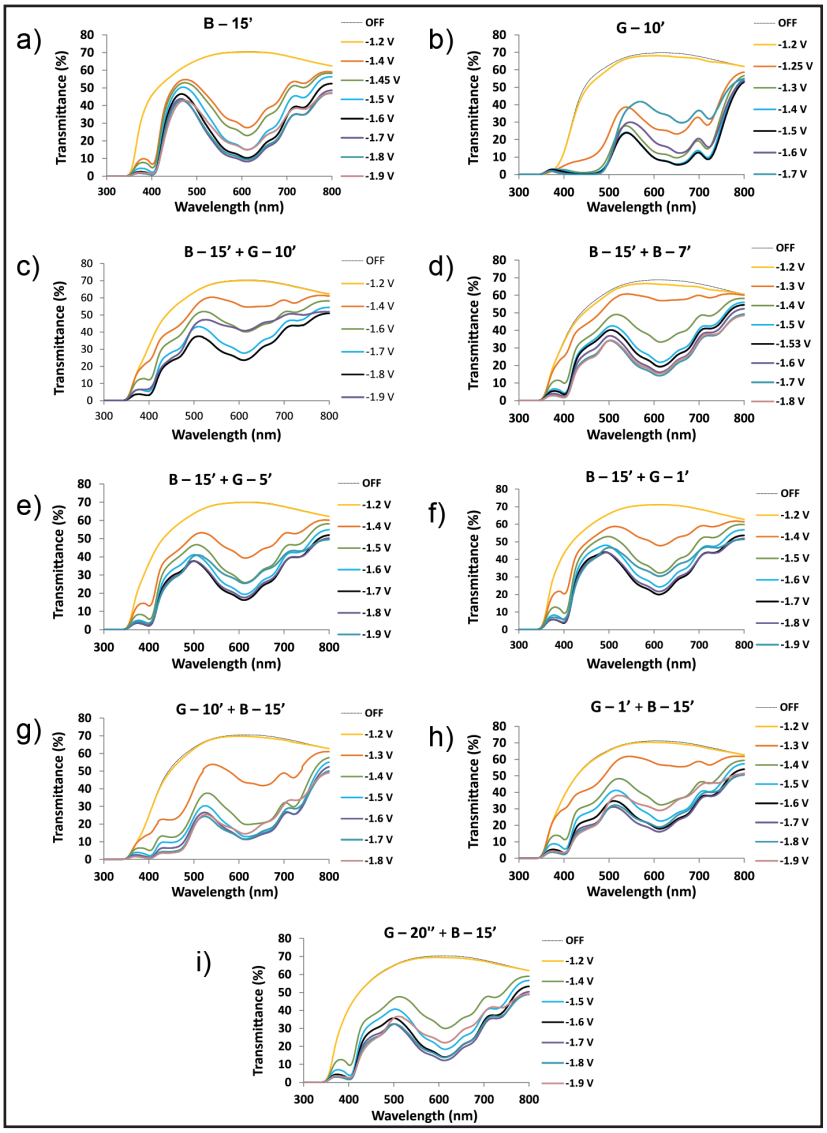

[**Figure Annex 6.1**].

[**ANNEX 6.2**]. Spectroelectrochemical study of three-electrode (3-E) ECD containing (I) bare TiO_2 film (II) B and (III) G viologen modified TiO_2 films.

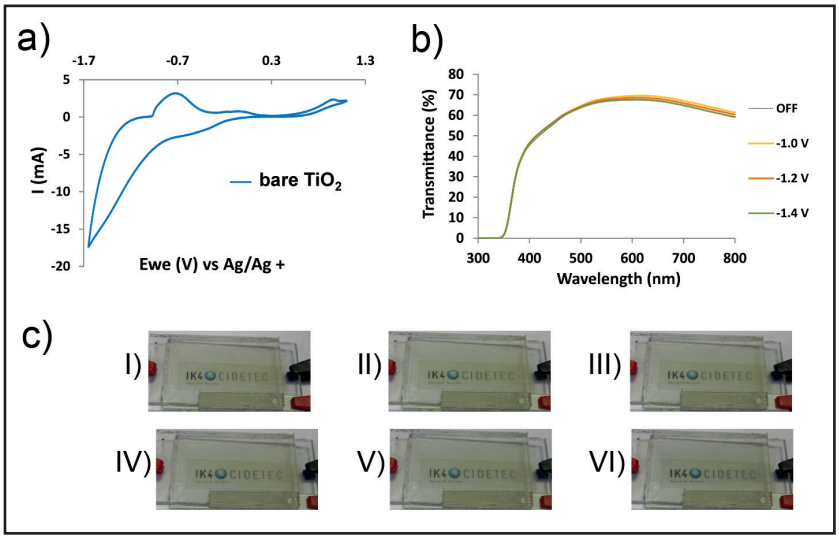

[**Figure Annex 6.2.I**]. Bare TiO_2 film: a) cyclic voltammetry, b) the UV-vis transmittance responses and c) photographs of the devices upon applying -0.0 (I), -0.5 (II), -0.8 (III), -1.0 (IV), -1.2 (V) and -1.4 V (VI).

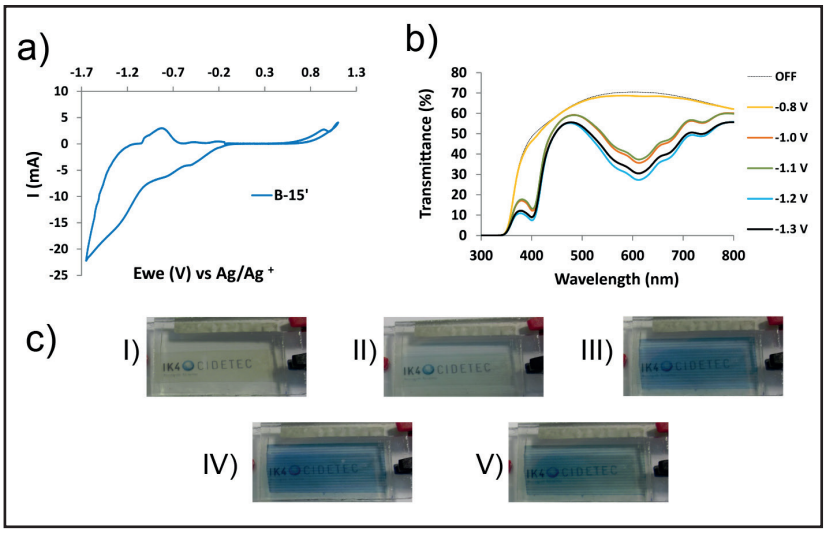

[**Figure Annex 6.2.II**]. **B** viologen modified TiO_2 film: a) cyclic voltammetry, b) the UV-vis transmittance responses and c) observed colorations at bleached state (I) and upon applying -1.0 (II), -1.1 (III), -1.4 (IV) and -1.5 V (V).

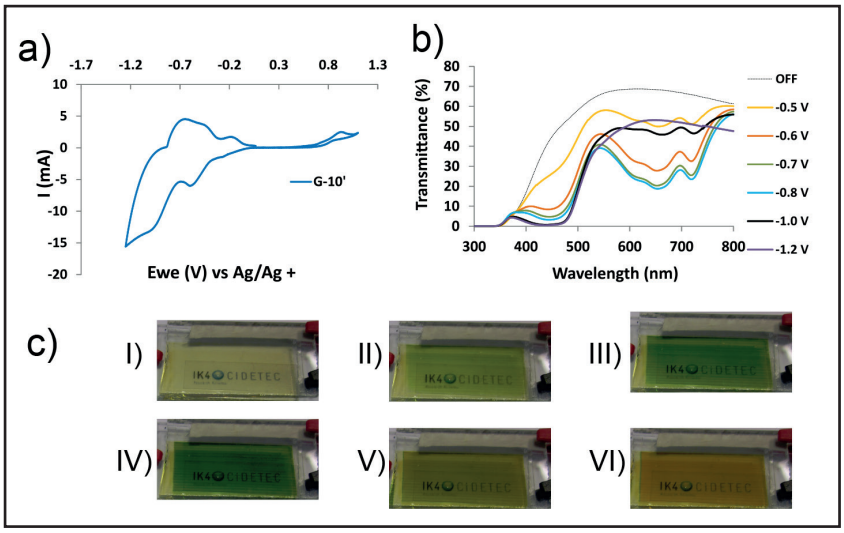

[**Figure Annex 6.2.III**]. **G** viologen modified TiO_2 film: a) cyclic voltammetry, b) the UV-vis transmittance responses and c) observed colorations at bleached state (I) and upon applying -0.5 (II), -0.6 (III), -0.8 (IV), -1.0 (V) and -1.2 V (VI).

[**ANNEX 6.3**]. Spectroelectrochemical study of 3-E ECD containing **B**-15' + **G**-7' sequential combination modified TiO_2 film.

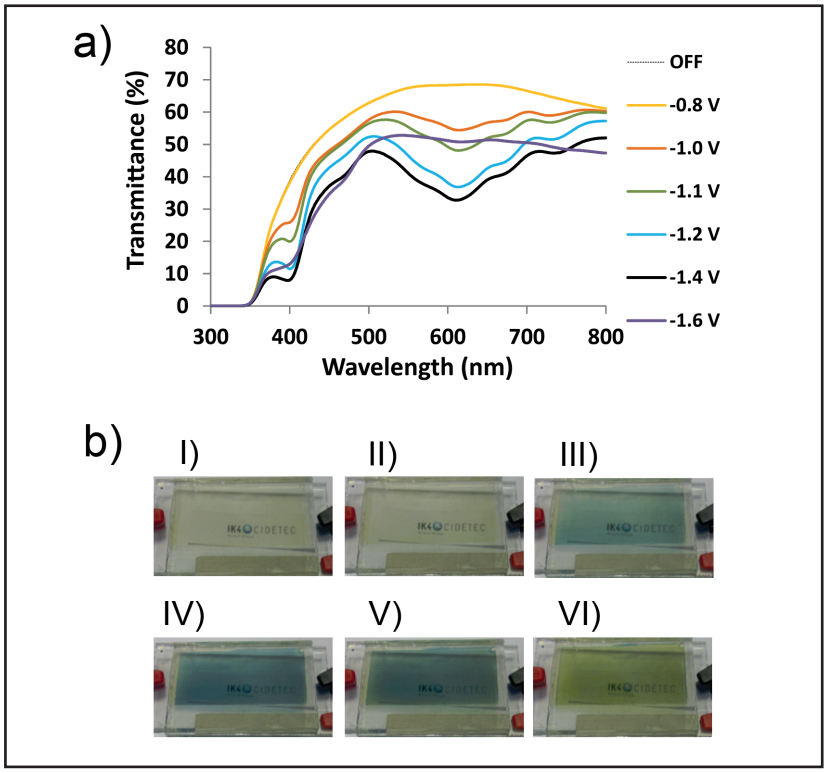

[**Figure Annex 6.3**]. 3-E EC based on **B**-15' + **G**-7' sequential combination: a) UV-vis transmittance responses and b) observed colorations for different applied potentials off (I),-0.8 (II), -1.0 (III), -1.2 (IV), -1.4 (V) and -1.6 V (VI).

[**ANNEX 6.4**]. Comparison between devices comprising gel electrolyte and anhydrous electrolyte.

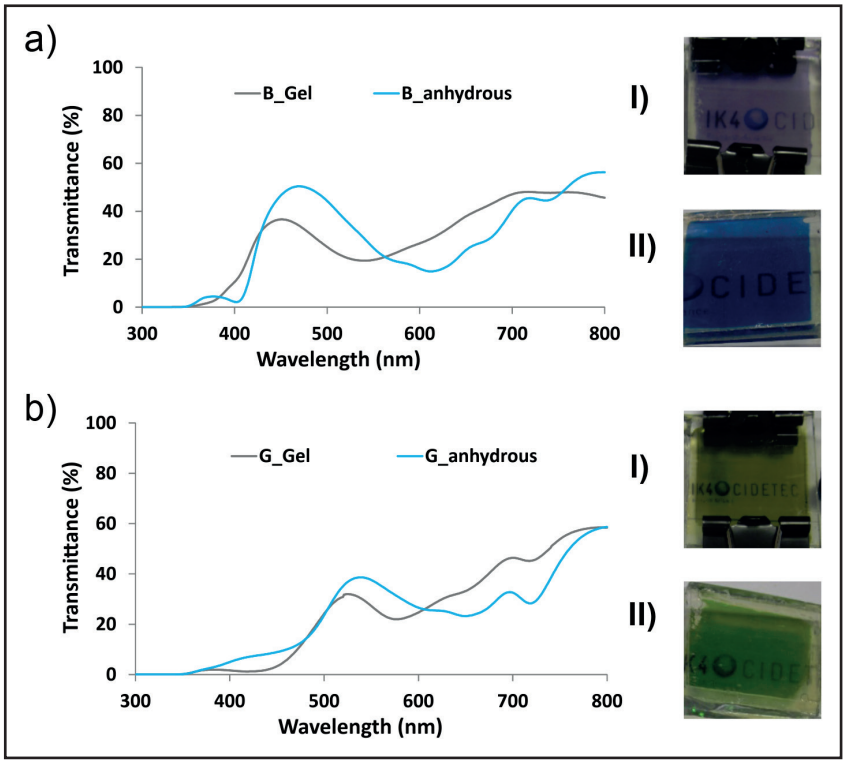

[**Figure Annex 6.4**]. Transmittance profiles of 2-E ECDs based on nanostructured TiO_2 layer containing (a) **B** and (b) **G** viologens in their colored states. Photographs of the devices comprising gel electrolyte (I) and anhydrous electrolyte (II) in their colored states (inset).

[Table Annex 6.4]. Comparison between devices comprising gel electrolyte and anhydrous electrolyte. Color coordinates obtained for 2-E ECDs based on nanostructured TiO_2 layer containing **B** and **G** viologens in their colored states.

Device	λ max. Abs. (nm)	Δ%T (a)	x (b)	y (b)	Y (b)	L*(c)	a* (c)	b* (c)	Color (d)
B- Anhydrous	600	41.8	0.269	0.307	37.8	68	-10	-12	
B- Gel	550	42.1	0.308	0.275	23.7	56	17	-14	
g- Anhydrous	650	46.2	0.359	0.464	31.3	63	-23	40	
G- Gel	577	46.0	0.389	0.476	26.1	58	-15	46	

[a)] ΔT% at maximum contrast wavelength.
[b), c)] Color coordinates (D65) registered for xyY (CIE 1931) ([(b)]) and *L*a*b* (CIE 1976) ([(c)]) quantitative scales.
[d)] Color swatches representing *L*a*b* color coordinates.

[**ANNEX 7.1**]. Comparison between devices comprising gel electrolyte and anhydrous electrolyte.

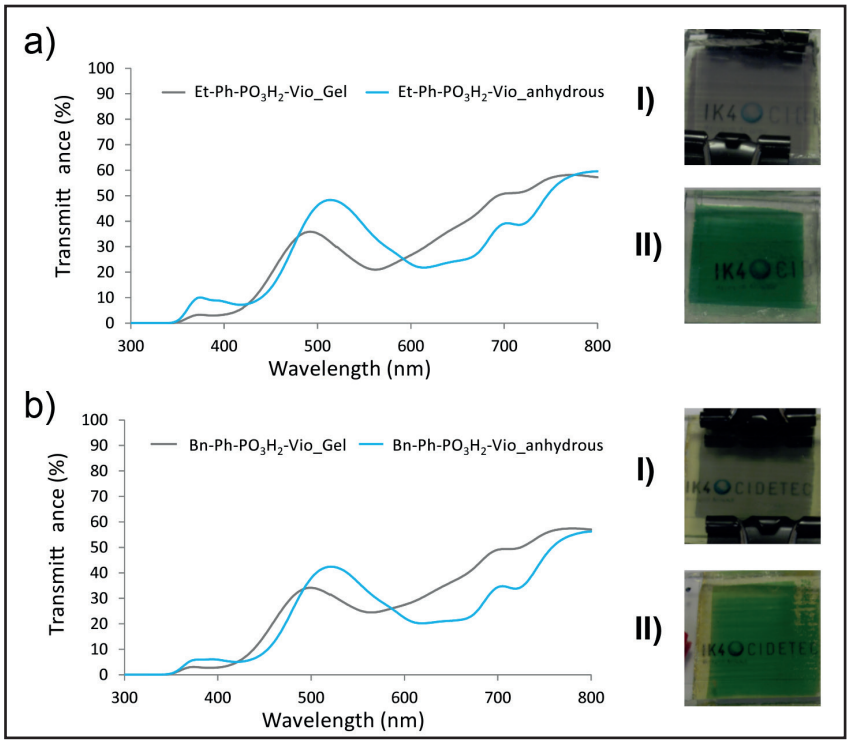

[**Figure Annex 7.1**]. Transmittance profiles of 2-E ECDs based on nanostructured TiO_2 layer containing (a) [**Et-Ph-PO_3H_2-Vio**] and (b) [**Bn-Ph-PO_3H_2-Vio**] viologens in their colored states. Photographs of the devices comprising gel electrolyte (I) and anhydrous electrolyte (II) in their colored states (inset).

[Table Annex 7.1]. Comparison between devices comprising gel electrolyte and anhydrous electrolyte. Color coordinates obtained for 2-E ECDs based on nanostructured TiO_2 layer containing **[Et-Ph-PO_3H_2-Vio]** and **[Bn-Ph-PO_3H_2-Vio]** viologens in their colored states for similar transmittance changes (Δ%T at λ_{max}).

Device	λ max. Abs. (nm)	Δ%T	x (a)	y (a)	Y (a)	L*(b)	a* (b)	b* (b)	Color (c)
Et-Ph-PO3H2-Vio - Anhydrous	600	47.2	0.302	0.435	35.0	66	-35	25	
Et-Ph-PO3H2-Vio- Gel	563	47.3	0.330	0.357	26.5	59	-3	9	
Bn-Ph-PO3H2-Vio- Anhydrous	600	44.4	0.319	0.463	32.0	63	-35	33	
Bn-Ph-PO3H2-Vio- Gel	563	40.4	0.340	0.386	28.0	60	-8	17	

[a), b)] Color coordinates (D65) registered for xyY (CIE 1931) ([(a)]) and L^*a^*b (CIE 1976) ([(b)]) quantitative scales.
[c)] Color swatches representing L^*a^*b color coordinates acquired through a color converter software.

[**ANNEX 8.1**]. Optimization study of the [**pCNVio**] based gel formulations.

[**Table Annex 8.1**]**.** Optimizing viologen concentration of the [**pCNVio**] based electrochromic gels: Transmittance percentages and corresponding transmittance changes of the ECDs based on formulations comprising different concentration of [**pCNVio**] viologen (constant amount of redox pair, 0.4 mmol L^{-1}), while -1.4 V and -1.8 V were being applied at fixed wavelengths (600 and 500 nm respectively).

[pCNVio] [mmol L-1]	%Tb	%Tc (-1.4 V)	Δ%T	%Tb	%Tc (-1.8 V)	Δ%T
0.25	71.3	60.9	10.4	66.1	50.9	15.2
0.5	69.4	53.2	16.2	64.2	35.2	29.0
1	75.5	40.4	35.1	69.8	29.2	40.6
1.5	71.8	33.2	38.6	65.6	17.7	47.9
2	72.6	25.1	47.5	65.9	13.8	52.1
2.5	70.8	20.4	50.4	64.1	9.8	54.3
3	69.9	10.9	59.0	63.2	4.4	58.7
3.5	68.3	7.3	61.0	60.9	2.1	58.8
4	69.4	7.2	62.2	62.6	1.4	61.2

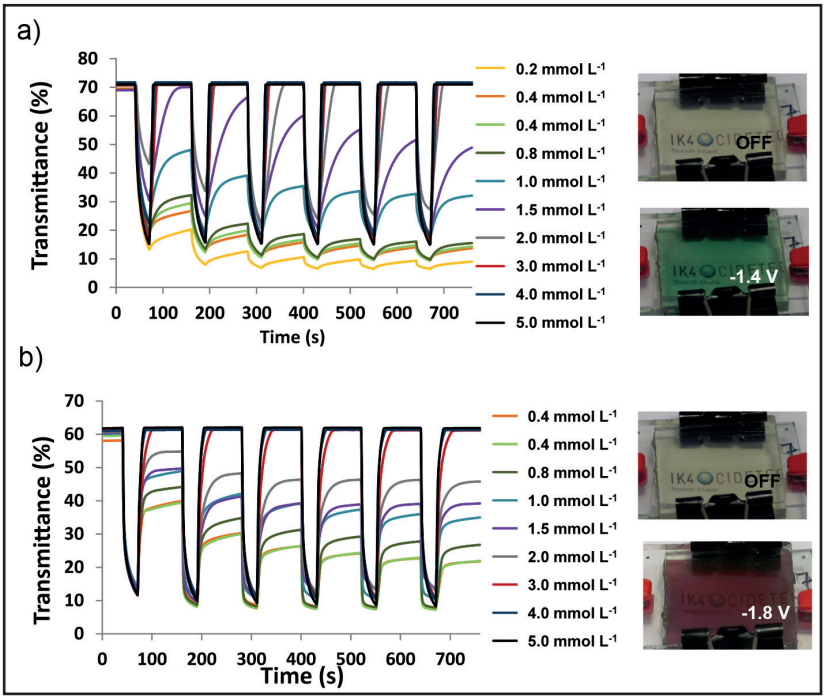

[**Figure Annex 8.1**]. Optimizing concentration of redox species of the [**pCNVio**] based electrochromic gels. Transmittance changes at fixed wavelength (600 and 500 nm in a) and b), respectively) of the ECDs containing different concentrations of ferro/ferricyanide potassium salts (constant amount of [**pCNVio**], 3.5 mmol L^{-1}), plotted against time while potential steps between colored (-1.4 and -1.8 V in a) and b), respectively for 20 s) and bleached state (0 V for 90 s) were being applied.

[**ANNEX 8.2**]. Electrochromic behavior of the two-electrode (2-E) ECD containing aqueous liquid system similar to **pCNVio gel** but without PVA-borax.

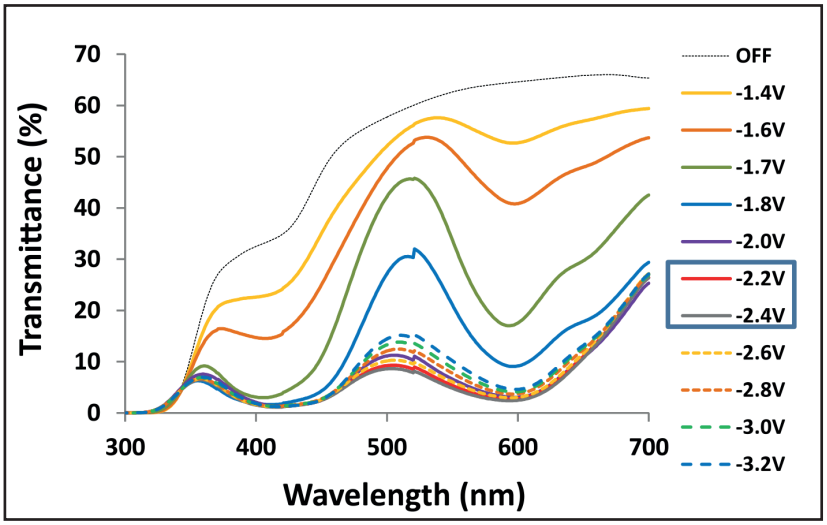

[**Figure Annex 8.2**]. UV/vis transmittance responses as a function of wavelength registered for aqueous liquid system (similar amount of vilogen and complementarly redox pair to **pCNVio gel**) for different applied potentials.

[**Table Annex 8.2**]. Tranmittance changes (λ = 600 nm) and color coordinates obtained with aqueous liquid system (similar amount of vilogen and complementarly redox pair to **pCNVio gel**) at different applied potentials.

Potential (V)	%Tc	Δ%T	x (a)	y (a)	Y (a)	L*(b)	a* (b)	b* (b)	Color (c)
-2.2	2.8	61.1	0.292	0.401	5.274	28	-16	8	
-2.4	2.5	60.8	0.292	0.409	5.757	29	-17	10	

[a), b)] Color coordinates (D65) registered for xyY (CIE 1931) ([(a)]) and *L*a*b* (CIE 1976) ([(b)]) quantitative scales.
[c)] Color swatches representing *L*a*b* color coordinates.

[**ANNEX 8.3**]. Electrochromic behavior of the 2-E ECD containing aqueous liquid system similar to **pCNVio gel** but without borax.

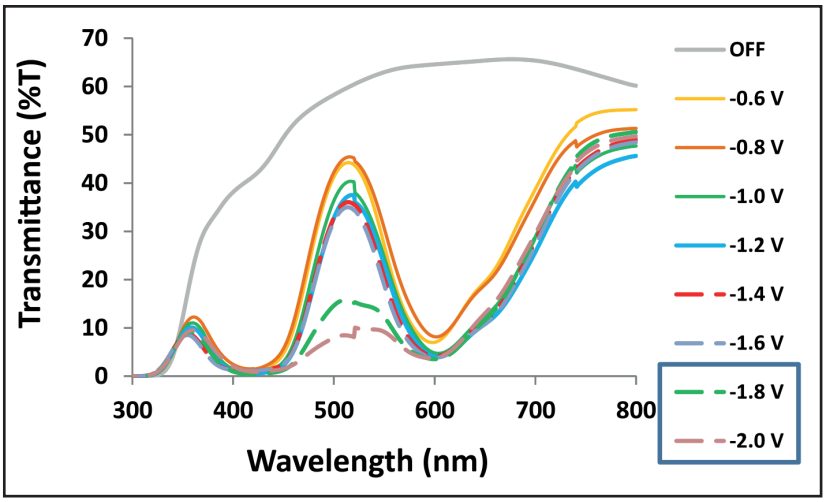

[**Figure Annex 8.3**]. UV/vis transmittance responses as a function of wavelength of aqueous liquid system similar to **pCNVio gel** but without borax (PVA-4%, [**pCNVio**] and redox pair) for different applied potentials.

[**Table Annex 8.3**]. Tranmittance changes (λ = 600 nm) and color coordinates obtained with aqueous liquid system similar to **pCNVio gel** but without borax (PVA-4%, [**pCNVio**] and redox pair) at different applied potentials.

Potential (V)	%Tc	Δ%T	x (a)	y (a)	Y (a)	L*(b)	a* (b)	b* (b)	Color (c)
-1.8	3.5	61.1	0.298	0.497	9.8	37	-33	25	
-2	3.8	60.8	0.349	0.460	7.3	32	-15	23	

[a), b)] Color coordinates (D65) registered for xyY (CIE 1931) ([(a)]) and *L*a*b* (CIE 1976) ([(b)]) quantitative scales.
[c)] Color swatches representing *L*a*b* color coordinates.

[**ANNEX 8.4**]. Rainbow-like ECD containing **Blend gel**.

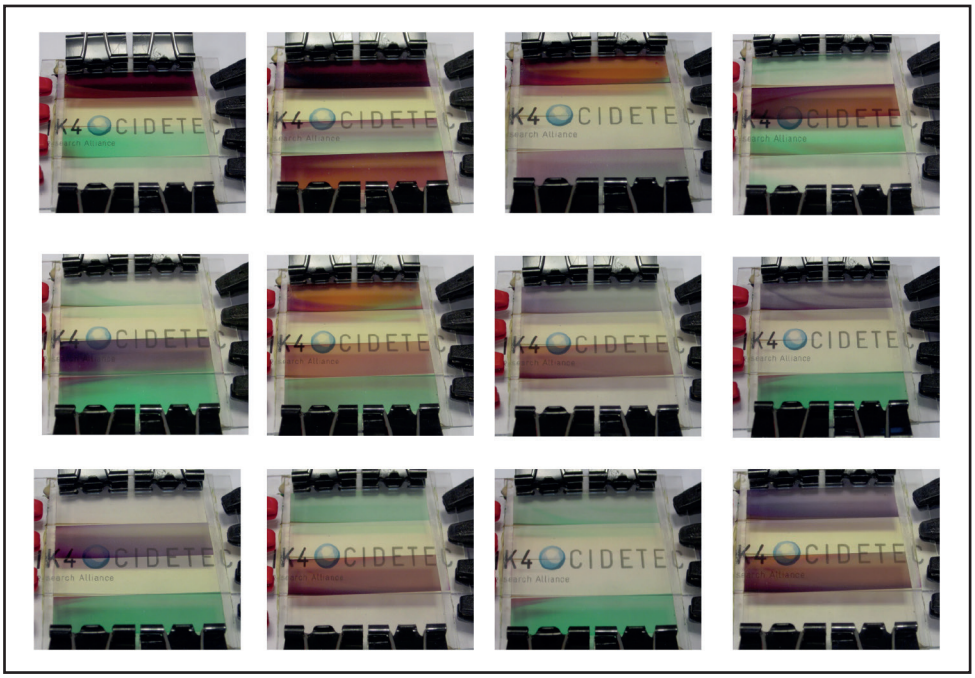

[**Figure Annex 8.4**]**.** Rainbow-like ECD containing **Blend gel** provided by zoning design and colors observed in each row of the device while the suitable voltage was being applied.